Methods in Molecular Biology™

VOLUME 164

Kinesin Protocols

Edited by

Isabelle Vernos

HUMANA PRESS

Kinesin Protocols

METHODS IN MOLECULAR BIOLOGY™

John M. Walker, SERIES EDITOR

176. **Steroid Receptor Methods:** *Protocols and Assays,* edited by *Benjamin A. Lieberman, 2001*
175. **Genomics Protocols**, edited by *Michael P. Starkey and Ramnath Elaswarapu, 2001*
174. **Epstein-Barr Virus Protocols,** edited by *Joanna B. Wilson and Gerhard H. W. May, 2001*
173. **Calcium-Binding Protein Protocols, Volume 2:** *Methods and Techniques,* edited by *Hans J. Vogel, 2001*
172. **Calcium-Binding Protein Protocols, Volume 1:** *Reviews and Case Histories,* edited by *Hans J. Vogel, 2001*
171. **Proteoglycan Protocols,** edited by *Renato V. Iozzo, 2001*
170. **DNA Arrays:** *Methods and Protocols,* edited by *Jang B. Rampal, 2001*
169. **Neurotrophin Protocols,** edited by *Robert A. Rush, 2001*
168. **Protein Structure, Stability, and Folding,** edited by *Kenneth P. Murphy, 2001*
167. **DNA Sequencing Protocols,** *Second Edition,* edited by *Colin A. Graham and Alison J. M. Hill, 2001*
166. **Immunotoxin Methods and Protocols**, edited by *Walter A. Hall, 2001*
165. **SV40 Protocols**, edited by *Leda Raptis, 2001*
164. **Kinesin Protocols,** edited by *Isabelle Vernos, 2001*
163. **Capillary Electrophoresis of Nucleic Acids, Volume 2:** *Practical Applications of Capillary Electrophoresis,* edited by *Keith R. Mitchelson and Jing Cheng, 2001*
162. **Capillary Electrophoresis of Nucleic Acids, Volume 1:** *The Capillary Electrophoresis System as an Analytical Tool,* edited by *Keith R. Mitchelson and Jing Cheng, 2001*
161. **Cytoskeleton Methods and Protocols**, edited by *Ray H. Gavin, 2001*
160. **Nuclease Methods and Protocols,** edited by *Catherine H. Schein, 2001*
159. **Amino Acid Analysis Protocols,** edited by *Catherine Cooper, Nicole Packer, and Keith Williams, 2001*
158. **Gene Knockoout Protocols,** edited by *Martin J. Tymms and Ismail Kola, 2001*
157. **Mycotoxin Protocols,** edited by *Mary W. Trucksess and Albert E. Pohland, 2001*
156. **Antigen Processing and Presentation Protocols,** edited by *Joyce C. Solheim, 2001*
155. **Adipose Tissue Protocols,** edited by *Gérard Ailhaud, 2000*
154. **Connexin Methods and Protocols,** edited by *Roberto Bruzzone and Christian Giaume, 2001*
153. **Neuropeptide Y Protocols**, edited by *Ambikaipakan Balasubramaniam, 2000*
152. **DNA Repair Protocols:** *Prokaryotic Systems*, edited by *Patrick Vaughan, 2000*
151. **Matrix Metalloproteinase Protocols,** edited by *Ian M. Clark, 2001*
150. **Complement Methods and Protocols,** edited by *B. Paul Morgan, 2000*
149. **The ELISA Guidebook**, edited by *John R. Crowther, 2000*
148. **DNA–Protein Interactions:** *Principles and Protocols* **(2nd ed.)**, edited by *Tom Moss, 2001*
147. **Affinity Chromatography:** *Methods and Protocols*, edited by *Pascal Bailon, George K. Ehrlich, Wen-Jian Fung, and Wolfgang Berthold, 2000*
146. **Mass Spectrometry of Proteins and Peptides,** edited by *John R. Chapman, 2000*
145. **Bacterial Toxins:** ***Methods and Protocols***, edited by *Otto Holst, 2000*
144. **Calpain Methods and Protocols**, edited by *John S. Elce, 2000*
143. **Protein Structure Prediction:** *Methods and Protocols*, edited by *David Webster, 2000*
142. **Transforming Growth Factor-Beta Protocols**, edited by *Philip H. Howe, 2000*
141. **Plant Hormone Protocols**, edited by *Gregory A. Tucker and Jeremy A. Roberts, 2000*
140. **Chaperonin Protocols**, edited by *Christine Schneider, 2000*
139. **Extracellular Matrix Protocols**, edited by *Charles Streuli and Michael Grant, 2000*
138. **Chemokine Protocols**, edited by *Amanda E. I. Proudfoot, Timothy N. C. Wells, and Christine Power, 2000*
137. **Developmental Biology Protocols, Volume III**, edited by *Rocky S. Tuan and Cecilia W. Lo, 2000*
136. **Developmental Biology Protocols, Volume II,** edited by *Rocky S. Tuan and Cecilia W. Lo, 2000*
135. **Developmental Biology Protocols, Volume I,** edited by *Rocky S. Tuan and Cecilia W. Lo, 2000*
134. **T Cell Protocols:** *Development and Activation*, edited by *Kelly P. Kearse, 2000*
133. **Gene Targeting Protocols,** edited by *Eric B. Kmiec, 2000*
132. **Bioinformatics Methods and Protocols,** edited by *Stephen Misener and Stephen A. Krawetz, 2000*
131. **Flavoprotein Protocols,** edited by *S. K. Chapman and G. A. Reid, 1999*
130. **Transcription Factor Protocols,** edited by *Martin J. Tymms, 2000*
129. **Integrin Protocols,** edited by *Anthony Howlett, 1999*
128. **NMDA Protocols,** edited by *Min Li, 1999*
127. **Molecular Methods in Developmental Biology:** Xenopus *and Zebrafish*, edited by *Matthew Guille, 1999*
126. **Adrenergic Receptor Protocols,** edited by *Curtis A. Machida, 2000*
125. **Glycoprotein Methods and Protocols:** *The Mucins,* edited by *Anthony P. Corfield, 2000*
124. **Protein Kinase Protocols,** edited by *Alastair D. Reith, 2001*
123. ***In Situ* Hybridization Protocols (2nd ed.),** edited by *Ian A. Darby, 2000*
122. **Confocal Microscopy Methods and Protocols,** edited by *Stephen W. Paddock, 1999*
121. **Natural Killer Cell Protocols:** *Cellular and Molecular Methods,* edited by *Kerry S. Campbell and Marco Colonna, 2000*
120. **Eicosanoid Protocols,** edited by *Elias A. Lianos, 1999*
119. **Chromatin Protocols,** edited by *Peter B. Becker, 1999*
118. **RNA–Protein Interaction Protocols,** edited by *Susan R. Haynes, 1999*
117. **Electron Microscopy Methods and Protocols,** edited by *M. A. Nasser Hajibagheri, 1999*
116. **Protein Lipidation Protocols,** edited by *Michael H. Gelb, 1999*
115. **Immunocytochemical Methods and Protocols (2nd ed.),** edited by *Lorette C. Javois, 1999*

METHODS IN MOLECULAR BIOLOGY™

Kinesin Protocols

Edited by

Isabelle Vernos

European Molecular Biology Laboratory,
Heidelberg, Germany

Humana Press  **Totowa, New Jersey**

999 Riverview Drive, Suite 208
Totowa, New Jersey 07512

This publication is printed on acid-free paper. ∞
ANSI Z39.48-1984 (American Standards Institute) Permanence of Paper for Printed Library Materials.

Cover design by Patricia F. Cleary.

Cover image provided by Dr. E. Mandelkow: X-ray structure of the motor protein kinesin from rat brain (Protein Data Bankcode 3kin). The model shows the two "heads" of the dimeric complex (top and bottom) which move along microtubules, using the energy derived from ATP hydrolysis. The heads are joined together by an α-helical coiled coil (middle). *See* www.mpasmb-hamburg.mpg.de.

For additional copies, pricing for bulk purchases, and/or information about other Humana titles, contact Humana at the above address or at any of the following numbers: Tel: 973-256-1699; Fax: 973-256-8341; E-mail: humana@humanapr.com, or visit our Website at www.humanapress.com

Printed in the United States of America. 10 9 8 7 6 5 4 3 2 1

Library of Congress Cataloging-in-Publication Data

Kinesin protocols / edited by Isabelle Vernos.
p. cm. -- (Methods in molecular biology ; v. 164)
Includes bibliographical references and index.
ISBN 0-89603-766-5 (alk. paper)
1. Kinesin--Laboratory manuals. I. Vernos, Isabelle. II. Series.

QP552.K46 K56 2000
572'.6--dc21

00-038895

Preface

By the end of the 1980s only two microtubule-dependent motors, the plus end-directed kinesin and the minus end-directed cytoplasmic dynein, had been identified. At the time, these two motors seemed almost sufficient to explain directional motility events on polar microtubule tracks in the cell. Nonetheless, shortly after, the tip of the iceberg began to emerge with the identification of proteins containing in their sequences a domain found in kinesin. This domain, called the "motor domain," conferred on these proteins the essential property of moving on microtubules, using the energy derived from ATP hydrolysis. Since then, the identification of new proteins belonging to the kinesin superfamily of microtubule-dependent motors has gone at such a pace that nowadays more than 200 entries with motor domain sequences are deposited in the database. Kinesin family members are found in all eukaryotic organisms tested. They present a wide range of domain organizations with a motor domain located at different positions in the molecule. Their motility properties are also variable in directionality, velocity, and such other characteristics as bundling activity and processivity. Finally, and most important, they participate in a multitude of cellular functions. Our understanding of many cellular events, such as mitotic spindle assembly and neuronal transport, to cite only two, has progressed substantially in the last few years thanks to the identification of these motors. Kinesin-like proteins (KLP) appear now to be involved in so many different cellular events that it is no longer a surprise to see researchers finding a KLP involved in their favorite cellular process. The general interest in this field is thus growing and many researchers are now faced with the task of identifying and/or characterizing a KLP to understand the process they are studying.

The aim of *Kinesin Protocols* is to provide a set of clear and concise protocols for the identification and characterization of members of the kinesin superfamily of microtubule-dependent motors. These protocols should prove to be especially useful for nonspecialists in the field, but others are actually up-to-date protocols based on recent findings that may turn out to be of interest for specialists as well. As in other books in the *Methods in Molecular Biology* series, a special emphasis has been put on the "Notes" section. There, the reader will find all the little tricks—gathered through experience by the authors—that make the difference between a successful and an unsuccessful experiment.

The protocols presented in *Kinesin Protocols* cover many different aspects of kinesin identification and characterization. The volume opens with a few chapters dealing with various approaches to the identification and purification of kinesins from different sources (Chaps. 1–6). These include methods to express and purify kinesins in different systems. Purified proteins or fragments are used to determine some of the properties intrinsic to members of this family. Methods presented in the following chapters are aimed at characterizing microtubule-enhanced ATPase activity (Chap. 7) and motility properties at different levels (Chaps. 8 and 9). Although most KLPs indeed have the property to move directionally on microtubules, new types of activities have recently been found for some members of the class. Several ways to test their microtubule destabilizing activity are presented in Chap. 10. Some examples of how to address functional studies are presented in the following few chapters (Chaps. 11–17). Although the function of KLPs is generally thought to be the transport of cargoes, it has become clear that they also play an important role in the organization of microtubules in three dimensions. Chapter 18 describes some very new methods to address this aspect of KLP function. Finally, two chapters present technically more demanding protocols for the study of kinesins at the structural level. One chapter describes methods that have been successful in crystallizing kinesin motor domains (Chap.19) and the other chapter presents protocols to study the structure of the kinesin–microtubule complex (Chap. 20).

Obviously, every reader will select and read first the chapter(s) of interest in *Kinesin Protocols*. Nonetheless, the content of the entire volume is recommended to everyone working in the field as a means to gain a better understanding of how best to handle kinesins experimentally. Some redundancy or overlap among chapters has proved unavoidable because certain basic experimental principles may be used for different purposes. We are confident that our book will both help the reader solve current research problems and stimulate the design of new experimental approaches adapted to the kinesin of interest in their work.

Isabelle Vernos

Contents

Contributors

Fabienne Beuron • *Imperial Cancer Research Fund, London, UK*

Haralabia Boleti • *Institut Pasteur, Unité de Biologie des Interactions Cellulaires, Paris, France*

Scott T. Brady • *Department of Cell Biology and Neuroscience, University of Texas Southwestern Medical Center, Dallas, TX*

Heather M. Brown • *Section of Molecular and Cellular Biology, University of California at Davis, Davis, CA*

Nick Carter • *Molecular Motors Group, The Marie Curie Research Institute, Surrey, UK*

Rob Cross • *Molecular Motors Group, The Marie Curie Research Institute, Surrey, UK*

Arshad Desai • *Cell Biology and Biophysics Programme, European Molecular Biology Laboratory, Heidelberg, Germany*

Sharyn A. Endow • *Department of Microbiology, Duke University Medical Center, Durham, NC*

Ernst-Ludwig Florin • *Cell Biology and Biophysics Program, European Molecular Biology Laboratory, Heidelberg, Germany*

Vladimir I. Gelfand • *Department of Cell and Structural Biology, University of Illinois at Urbana-Champaign, Urbana, IL*

Laura M. Ginkel • *Department of Physiology and Biophysics, University of Washington School of Medicine, Seattle, WA*

David D. Hackney • *Department of Biological Science, Carnegie Mellon University, Pittsburgh, PA*

Nobutaka Hirokawa • *Department of Cell Biology and Anatomy, Graduate School of Medicine, University of Tokyo, Tokyo, Japan*

Andreas Hoenger • *Structure Programme, European Molecular Biology Laboratory, Heidelberg, Germany*

J. K. Heinrich Hörber • *Cell Biology and Biophysics Program, European Molecular Biology Laboratory, Heidelberg, Germany*

Anthony A. Hyman • *Max Planck Institute for Molecular Cell Biology and Genetics, Pfotenhauerstrasse, Dresden, and European Molecular Biology Laboratory, Heidelberg, Germany*

Sylvia Jeney • *Cell Biology and Biophysics Program, European Molecular Biology Laboratory, Heidelberg, Germany*
Wei Jiang • *Department of Biological Science, Carnegie Mellon University, Pittsburgh, PA*
Eric Karsenti • *European Molecular Biology Laboratory, Heidelberg, Germany*
Janardan Kumar • *Department of Cell Biology, Duke University Medical Center, Durham, NC*
Sergei A. Kuznetsov • *Institute of Cell Biology and Biosystems Technology, Faculty of Biological Sciences, University of Rostock, Rostock, Germany*
Nathalie Le Bot • *European Molecular Biology Laboratory, Heidelberg, Germany*
Lisa C. Lindesmith • *Department of Cell Biology, Duke University Medical Center, Durham, NC*
Eckhard Mandelkow • *Max-Planck-Unit for Structural Molecular Biology, Hamburg, Germany*
Gerardo Morfini • *Department of Cell Biology and Neuroscience, University of Texas Southwestern Medical Center, Dallas, TX*
Robert L. Morris • *Department of Biology, Wheaton College, Norton, MA*
Jens Müller • *Max-Planck-Unit for Structural Molecular Biology, Hamburg, Germany*
François Nédélec • *Cell Biology and Cell Biophysics Programme, European Molecular Biology Laboratory, Heidelberg, Germany*
Erik Nielsen • *Max Planck Institute for Molecular Cell Biology and Genetics, Pfotenhauerstrasse, Dresden, and European Molecular Biology Laboratory, Heidelberg, Germany*
Yasuko Noda • *Department of Cell Biology and Anatomy, Graduate School of Medicine, University of Tokyo, Tokyo, Japan*
Niovi Santama • *Molecular Biology and Biochemistry Laboratory, University of Cyprus and Cyprus Institute of Neurology and Genetics, Nicosia, Cyprus*
Jonathan M. Scholey • *Section of Molecular and Cellular Biology, University of California at Davis, Davis, CA*
Fedor Severin • *Max Planck Institute for Molecular Cell Biology and Genetics, Pfotenhauerstrasse, Dresden, and European Molecular Biology Laboratory, Heidelberg, Germany*
David J. Sharp • *Section of Molecular and Cellular Biology, University of California at Davis, Davis, California*
Michael P. Sheetz • *Department of Cell Biology, Duke University Medical Center, Durham, NC*

MARYANNE F. STOCK • *Department of Biological Science, Carnegie Mellon University, Pittsburgh, PA*
WILLIAM SULLIVAN • *Department of Biology, University of California at Santa Cruz, Santa Cruz, CA*
THOMAS SURREY • *Cell Biology and Cell Biophysics Programme, European Molecular Biology Laboratory, Heidelberg, Germany*
GYÖRGYI SZEBENYI • *Department of Cell Biology and Neuroscience, University of Texas Southwestern Medical Center, Dallas, TX*
MANFRED THORMÄHLEN • *Max-Planck-Unit for Structural Molecular Biology, Hamburg, Germany*
MING-YING TSAI • *Department of Cell Biology and Neuroscience, University of Texas Southwestern Medical Center, Dallas, TX*
M. CAROLINA TUMA • *Department of Molecular, Cellular, and Developmental Biology, Yale University, New Haven, CT*
MING-YING TSAI • *Department of Cell Biology and Neuroscience, University of Texas Southwestern Medical Center, Dallas, TX*
ISABELLE VERNOS • *European Molecular Biology Laboratory, Heidelberg, Germany*
KIMBERLY W. WALIGORA • *Department of Microbiology, Duke University Medical Center, Durham, NC*
CLAIRE E. WALCZAK • *Medical Sciences Program, Indiana University, Bloomington, IN*
LINDA WORDEMAN • *Department of Physiology and Biophysics, University of Washington School of Medicine, Seattle, WA*
BRENT D. WRIGHT • *Section of Molecular and Cellular Biology, University of California at Davis, Davis, CA*
MARINO ZERIAL • *Max Planck Institute for Molecular Cell Biology and Genetics, Pfotenhauerstrasse, Dresden, and European Molecular Biology Laboratory, Heidelberg, Germany*

1

Purification of Kinesin from the Brain

Sergei A. Kuznetsov and Vladimir I. Gelfand

1. Introduction

The kinesin superfamily constitutes a structurally diverse group of microtubule-based motor proteins that use the energy of Mg–ATP hydrolysis to transport organelles along microtubules ***(1)***. Purification of kinesins is required for both the characterization of their motile properties and studies of their regulation.

Two approaches for kinesin isolation have been used. The first is isolation of native protein from cytosol (*see* also Chapter 9); the second is isolation of recombinant kinesin from bacteria or cultured insect cells transformed with plasmids encoding kinesin (*see* Chapters 4 and 6). As more and more genes encoding different kinesin-like proteins are cloned, recombinant proteins expressed in bacterial or baculovirus systems are becoming a main source of protein for biophysical studies aimed mainly to characterize the structure of kinesins and mechanism for transforming of the energy of ATP hydrolysis to movement along microtubules ***(2,3)***. Recombinant DNA technology also allows domain-swapping experiments that help in understanding the role of individual domains of kinesins in generation of force and direction of movement ***(1,2,4–6)*** (*see* Chapter 5). Biochemical isolation of kinesins from cells is not the method of choice if the recombinant protein can be used instead, because even conventional kinesin is not an abundant protein; isolation usually takes several days and the yield is relatively small. However, several questions cannot be addressed with recombinant proteins, which is the reason that this chapter is included in the book.

First, many kinesins are multimeric complexes, and therefore biochemical isolation is the best method for characterizing the subunit composition of native kinesins and finding nonmotor subunits ***(7)*** (*see* Chapter 17). Several studies indicated that nonmotor subunits as light chains of conventional kinesin are

From: *Methods in Molecular Biology*, Vol. 164: *Kinesin Protocols*
Edited by: I. Vernos

essential for kinesin function in vivo ***(8)*** and play an important role in the regulation of kinesin motor activity ***(9–11)***.

Biochemical isolation allows the study of interactions of motor proteins with other components that may be involved in motor binding to membranes or to other proteins ***(12)*** (*see* Chapters 12 and 13).

Another important question that can only be properly studied on a biochemically purified protein is what kind of posttranslational modifications are present in the protein. As phosphorylation is probably involved in the regulation of activity or the interaction of motor proteins with organelles ***(13,14)***, a proper protocol of protein purification is essential for mapping the sites of posttranslational modification and for the analysis of the role of these modifications in the function of the protein.

We describe here a procedure for kinesin purification from bovine brain that was originally developed in 1986 ***(15)***. Using the kinesin preparation isolated by this method, we were able to characterize kinesin ATPase activity and determined its quaternary structure ***(16,17)***. Several investigators (i.e., **refs. *17*** and ***18***) have successfully used modifications of this method, which has been adapted for the commercial production of conventional kinesin by Cytoskeleton (Denver, CO).

Because our method of kinesin isolation is based on its association with microtubules polymerized from purified tubulin, one can use this protocol not only for kinesin isolation but also for the purification of microtubules and tubulin from bovine brain.

2. Materials

1. Bovine brains (five to six brains, 2.0 kg) are obtained as fresh as possible and chilled on ice.
2. Buffer A: working buffer for kinesin isolation (10 L): 50 m*M* imidazole/HCl (pH 6.7–6.8), 0.5 m*M* $MgCl_2$, 0.1 m*M* EDTA, 1 m*M* 2-mercaptoethanol. It is important for 2-mercaptoethanol to be added in all buffers just before use.
3. Buffer A (pH 7.2): for brain extraction during kinesin isolation (3–4 L).
4. Buffer A/150: buffer A with 0.15 *M* KCl (5–7 L).
5. Buffer A/500: buffer A with 500 m*M* KCl (1–2 L).
6. Buffer B: working buffer for microtubule isolation (1 L): 50 m*M* imidazole/HCl (pH 6.7–6.8), 0.5 m*M* $MgCl_2$, 50 m*M* KCl, 1 m*M* EGTA, 0.1 m*M* EDTA, 1 m*M* 2-mercaptoethanol.
7. Buffer B (pH 7.2): for brain extraction during microtubule isolation (0.5 L).
8. Buffer B with 12 *M* glycerol for microtubule polymerization (0.5 L).
9. 100 m*M* phenylmethylsulfonyl fluoride (PMSF) in dimethylsulfoxide (DMSO).
10. 100 m*M* ATP (pH 6.7) in distilled water.
11. 100 m*M* inorganic tripolyphosphate (PPP_i) (cat. no. T-5633, Sigma) in buffer B.
12. 5 m*M* Taxol in DMSO.

13. DEAE–cellulose (DE-52, Whatman) and phosphocellulose (P-11, Whatman) precycled according to the procedure of manufacturer and equilibrated with buffer A (*see* **Note 1**).
14. Sephacryl S-300 (Pharmacia) packed in a 2.6 × 90-cm column.

3. Method

An original method of kinesin purification ***(19)*** as well as several other modifications ***(20)*** call for incubation of the crude extract with Taxol-stabilized microtubules in the presence of AMP–PNP, which yields preparations with low ATPase activity ***(19,20)***. Therefore, we use preliminary column chromatography steps for partial purification of kinesin, and only after these steps do we perform an affinity pelleting of microtubule-bound kinesin in the presence of PPP_i. This approach helps to remove contaminating proteases that could degrade kinesin before incubating it with microtubules at room temperature.

The isolation of kinesin takes 3 d and is carried out at 4°C unless otherwise stated.

3.1. First Day

1. Preparation of bovine brain extract for kinesin isolation. Brain tissue is cleaned of blood clots and meninges and homogenized in 250-g batches in 250 mL buffer A (pH 7.2) for 1–2 min in a blender (*see* **Note 1**). The homogenate is centrifuged at 17,700*g* for 30 min (10,000 rpm, JA-10 rotor, Beckman) and PMSF is added from a freshly prepared stock to a final concentration of 1 m*M*. After this step, all the buffers for kinesin isolation are supplemented with 0.1 m*M* PMSF (*see* **Note 2**). The supernatant (1.5 L, 20–30 mg/mL of protein concentration) is centrifuged again at 30,000*g* for 60 min (14,000 rpm, JA-14 rotor, Beckman).
2. Batch DEAE–cellulose chromatography of bovine extract. The brain extract is mixed with 800 mL settled DEAE–cellulose and the mixture gently stirred for 1 h. The suspension is filtered through a 2-L Büchner funnel with glass filter (pore size G1–G2) and the resin is washed with 3 L of buffer A while on the filter. The proteins are eluted with 2–3 L of buffer A/150 while DEAE–cellulose is on the filter. For elution, 8–10 250-mL portions of buffer A/150 are passed through the DEAE–cellulose filter cake and each 250-mL fraction is collected separately. Fractions with a protein concentration of more than 1 mg/mL are pooled and used for further purification.
3. Batch phosphocellulose chromatography. The eluate (2–3 L) is mixed with 150–200 mL of settled phosphocellulose. The mixture is stirred for 1 h, filtered through a 0.5-L Büchner funnel with a glass filter, and washed with 1 L of buffer A/150. The resin is suspended in buffer A/150 and packed into a chromatography column (5 cm in diameter). The proteins (including kinesin) are eluted overnight with 0.5 L of buffer A/500. Then, 25-mL fractions are collected.
4. Microtubule preparation from brain extract. Microtubules from bovine brain for the affinity step of kinesin purification are prepared on the same day. Three hun-

dred grams of bovine brain are homogenized in 300 mL buffer B (pH 7.2) for 1–2 min in a blender (*see* **Note 1**). The homogenate is centrifuged at 20,000*g* for 30 min (10,000 rpm, JA-10 rotor, Beckman). ATP is added to the supernatant to a final concentration 0.1 m*M* and the extract is centrifuged again at 150,000*g* for 30 min (35,000 rpm, Type 35 rotor, Beckman). Buffer B with 12 *M* glycerol is added to a final concentration of 4 *M* glycerol. Microtubule polymerization in the extract with 4 *M* glycerol is induced by incubation for 1 h at 37°C. Microtubules are pelleted by centrifugation at 150,000*g* for 60 min (35,000 rpm, Type 35 rotor, Beckman). Pellets are resuspended in 50 mL buffer B containing 4 *M* glycerol and the microtubules are stored overnight at 4°C.

3.2. Second Day

1. The peak protein fractions from phosphocellulose column are pooled (about 150 mL with a protein concentration of 1.0–1.2 mg/mL) and dialyzed against 2 L of buffer A. After 1.5–2 h of dialysis, when the KCl concentration in dialysate has reached 100–150 m*M* (*see* **Note 3**), proteins are applied to a 20-mL column of DEAE–cellulose equilibrated with buffer A/150. The flowthrough fraction is dialyzed against 2 L of buffer A with 1 m*M* EGTA for 1.5–2.0 h until the KCl concentration in the dialysate is less than 50 m*M*. Following dialysis, the solution is clarified by centrifugation at 100,000*g* for 30 min (30,000 rpm, Type 35 rotor, Beckman) and used for affinity purification on microtubules.
2. Purification of tubulin from microtubule proteins and polymerization of purified tubulin. Microtubules resuspended in buffer B with 4 *M* glycerol are pelleted by centrifugation at 150,000*g* for 40 min (40,000 rpm, Type 40 rotor, Beckman) at 20°C. Microtubule pellets are resuspended in 25–30 mL of cold buffer B and depolymerized on ice for 20 min. Aggregates are removed by centrifugation at 100,000*g* for 30 min in the cold (30,000 rpm, Type 40 rotor, Beckman) and the microtubule protein solution (20–25 mL with protein concentration about 10 mg/mL) is applied to a 50-mL phosphocellulose column equilibrated with buffer B (*see* **Note 1**). The flowthrough fractions containing pure tubulin are collected (*see* **Note 4**). Purified tubulin (40–50 mL, protein concentration about 5 mg/mL) is polymerized by the addition of Taxol to a final concentration of 20 μ*M* and incubation for 30 min at 37°C (*see* **Note 5**).
3. Cosedimentation of kinesin with microtubules. For affinity purification, 150 mL of the kinesin-enriched fraction from **step 1** (**Fig. 1D**) is mixed with 50 mL of the microtubule preparation and the mixture is supplemented with 2.5 m*M* PPP_i. After 20 min incubation at room temperature, 40–50 mL of the kinesin–microtubule mixture is loaded onto a 20-mL layer of 4 *M* glycerol in buffer B containing 5 μ*M* Taxol and 2.5 m*M* PPP_i in 70-mL tubes and pelleted at 150,000*g* for 1 h at 20°C (35,000 rpm, Type 35 rotor, Beckman).
4. Kinesin elution from microtubules and gel filtration. The pellets containing microtubules with bound kinesin (**Fig. 1E**) are extracted with 10–12 mL of 5 m*M* ATP in buffer A/150 and 20 μ*M* Taxol. Dissociated proteins are separated from microtubules by centrifugation at 150,000*g* for 20 min (40,000 rpm, Type 40

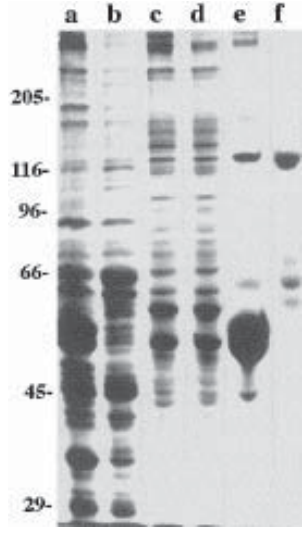

Fig. 1. Electrophoretic analysis of brain kinesin purification. Lanes: a, crude brain supernatant; b, DEAE–cellulose eluate; c, phosphocellulose eluate; d, second DEAE-cellulose eluate; e, microtubules with bound kinesin; f, purified kinesin after concentration on DEAE–cellulose.

rotor, Beckman) and further purified by gel-filtration chromatography. ATP-eluted kinesin is applied to a Sephacryl S-300 column and eluted with buffer A without PMSF (*see* **Note 6**). The column is run overnight at 25 mL/h and 6-mL fractions are collected.

3.3. Third Day

1. Kinesin concentration on a DEAE–cellulose column. The fractions are analyzed by SDS-PAGE and the kinesin containing fractions are pooled and concentrated on a 2 mL column of DEAE–cellulose eluted with buffer A/150 (*see* **Note 7**). A typical kinesin yield is 0.5–1 mg from 1 kg of bovine brain. The purity of kinesin is 90–95% (**Fig. 1F**).

4. Notes

1. Because the correct pH is very important for ion-exchange chromatography, it is critical to check that DEAE–cellulose and phosphocellulose columns are properly equilibrated and that the pH of the buffer entering and eluting from the column are identical.
2. The pH of the extract after brain homogenization should be 6.7–6.8. If necessary, it can be adjusted with dilute HCl or KOH.

3. For estimation of the KCl concentration during dialysis, measure the conductivity of the solution. Use 1:100 dilutions of buffer A with 50 and 150 m*M* KCl as a standard.
4. Phosphocellulose is a very strong cation-exchange resin and is sufficient to separate tubulin and microtubule-associated proteins. However, for a successful separation, do not use an elution rate of more than one column volume in 45 min.
5. Normally, tubulin polymerization requires GTP. However, the addition of GTP or ATP prevents kinesin binding to microtubules. Therefore, it is recommended to use a high tubulin concentration (more than 3 mg/mL) and induce tubulin polymerization by Taxol.
6. A better fractionation of small volumes of kinesin by gel filtration could be performed with fast protein liquid chromatography (FPLC) on Superose 12 (Pharmacia).
7. More concentrated kinesin can be obtain by FPLC using MonoQ HR 5/5 column (Pharmacia). In this case, elution should be performed with 300 m*M* KCl in buffer A.

Acknowledgments

Work in the lab of S. A. K. has been supported by the grant from International Human Frontier Science Program (RG-512/95M); work in the lab of V. I. G. has been supported by the grants from the National Science Foundation (MCB 9513388) and National Institutes of Health (GM-52111).

References

1. Vale, R. D. and Fletterick, R. J. (1997) The design plan of kinesin motors. *Annu. Rev. Cell Dev. Biol.* **13**, 745–777.
2. Cross, R. A. (1997) Molecular motors: the natural economy of kinesin. *Curr. Biol.* **7**, R631–R633.
3. Romberg, L., Pierce, D. W., and Vale, R. D. (1998) Role of the kinesin neck region in processive microtubule-based motility. *J. Cell Biol*. **14**, 1407–1416.
4. Henningsen, U. and Schliwa, M. (1997) Reversal in the direction of movement of a molecular motor. *Nature* **389,** 93–96.
5. Endow, S. A. and Waligora, K. W. (1998) Determinants of kinesin motor polarity. *Science* **281**, 1200–1202.
6. Sablin, E. P., Case, R. B., Dai, S. C., Hart, C. L., Ruby, A., Vale, R. D., and Fletterick, R. J. (1998) Direction determination in the minus-end-directed kinesin motor ncd. *Nature* **395**, 813–816.
7. Scholey, J. M. (1996) Kinesin-II, a membrane traffic motor in axons, axonemes, and spindles. *J. Cell Biol*. **133**, 1–4.
8. Gindhart, J. G. Jr., Desai, C. J., Beushausen, S., Zinn, K., and Goldstein, L. S. (1998) Kinesin light chains are essential for axonal transport in Drosophila. *J. Cell Biol.* **141**, 443–454.
9. Thaler, C. D. and Haimo, L. T. (1996) Microtubules and microtubule motors: mechanisms of regulation. *Int. Rev. Cytol*. **164**, 269–327.

10. Hackney, D. D., Levitt, J. D., and Wagner, D. D. (1991) Characterisation of alpha 2 beta 2 and alpha 2 forms of kinesin. *Biochem. Biophys. Res. Commun*. **174**, 810–805.
11. Verhey, K. J., Lizotte, D. L., Abramson, T., Barenboim, L., Schnapp, B. J., and Rapoport, T. A. (1998) Light chain-dependent regulation of Kinesin's interaction with microtubules. *J. Cell Biol*. **143**, 1053–1066.
12. Holleran, E. A., Karki, S., and Holzbaur, E. L. (1998) The role of the dynactin complex in intracellular motility. *Int. Rev. Cytol*.**18**, 69–109.
13. Blangy, A., Lane, H. A., d'Herin, P., Harper, M., Kress, M., and Nigg, E. A. (1995) Phosphorylation by p34cdc2 regulates spindle association of human Eg5, a kinesin-related motor essential for bipolar spindle formation in vivo. *Cell* **83**, 1159–1169.
14. Page, B. D., Satterwhite, L. L., Rose, M. D., and Snyder, M. (1994) Localization of the Kar3 kinesin heavy chain-related protein requires the Cik1 interacting protein. *J. Cell Biol.* **124**, 507–519
15. Kuznetsov, S. A. and Gelfand, V. I. (1986) Bovine brain kinesin is a microtubule-activated ATPase. *Proc. Natl. Acad. Sci. USA* **83**, 8530–8534.
16. Kuznetsov, S. A., Vaisberg, E. A., Shanina, N. A., Magretova, N. N., Chernyak, V. Y., and Gelfand, V. I. (1988) The quaternary structure of bovine brain kinesin. EMBO J. **7**, 353–356.
17. Hackney, D. D. (1988) Kinesin ATPase: rate-limiting ADP release. *Proc. Natl. Acad. Sci. USA* **85**, 6314–6318.
18. Hackney, D. D. (1991) Isolation of kinesin using initial batch ion exchange. *Methods Enzymol.* **196**, 175–181.
19. Vale, R. D., Reese, T. S., and Sheetz, M. P. (1985) Identification of a novel force-generating protein, kinesin, involved in microtubule-based motility. *Cell* **42**, 39–50.
20. McIntosh, J. R. and Porter, M. E. (1989) Enzymes for microtubule-dependent motility. *J. Biol. Chem*. **264**, 6001–6004.

2

RT-PCR for the Identification of Developmentally Regulated Novel Members of the Kinesin-like Superfamily

Niovi Santama

1. Introduction

The kinesin-like motor protein superfamily comprises to date about 100 members present in essentially all the major eukaryotic phyla (reviewed in **ref.** ***1***), including over 30 in the mouse alone ***(2)***. The common feature of the kinesin-like proteins is a highly conserved 350-amino-acid "motor domain" (30–40% sequence identity across species) that includes even more highly conserved ATP- and microtubule-binding sites ***(3)***.

It is exactly the presence of the conserved motor domain and motor-domain "signature" sequences that has facilitated enormously the cloning and identification of further novel kinesin-like proteins both by conventional homology screening of cDNA libraries and by the application of reverse transcription–polymerase chain reaction (RT-PCR) methodology. In the later, oligonucleotide probes complementary to consensus motor motifs are used to coamplify motor-domain sequences from multiple kinesin-like proteins. Subsequent characterization of the product mixture can reveal the existence of novel motor cDNAs in a cell type, tissue, or organ of choice of a given organism (examples included in **refs.** ***4–7***, among others).

The RT-PCR strategy detailed in this chapter describes successive steps of RNA isolation and cDNA production, use of cDNA in PCR using degenerate oligonucleotide primers to coamplify kinesin-like motor sequences, and a method for fast and easy subcloning of the mixed PCR product. Protocols (and an experimental example) for the selection of developmentally regulated kinesin-like proteins from mouse hippocampus are also included. The source of RNA extraction and cDNA preparation in our experiments was mouse hip-

From: *Methods in Molecular Biology*, Vol. 164: *Kinesin Protocols*
Edited by: I. Vernos

pocampal cells in a primary culture, a well characterized system in which mostly synchronized embryonic neurons develop in vitro through distinct stages of differentiation ***(8)***. Nevertheless, the methods described are readily applicable and adaptable to any other material (i.e., cell lines, tissues, or organs from any organism of interest).

It must be highlighted that once the subcloning of PCR products is achieved in this or similar protocols, the question that needs to be addressed and resolved will determine subsequent strategy. There are two approaches:

1. If the aim is to identify as many new members of the kinesin-like superfamily as possible, then this can be achieved by extensive sequencing of different selected clones. These clones, which are partial because they only contain the motor domain, can then be used to fish out full-length cDNAs either by screening appropriate cDNA libraries or by 5' and 3' rapid amplification of cDNA ends (RACE).
2. Alternatively, or in addition, it may be desirable to identify from the pool of clones those subject to developmental or cell-specific regulation. The relevant protocol offered in this chapter is one approach devised to explore this question. In this case, pools of kinesin-like cDNAs must be prepared independently from the two developmental stages or cell types that are to be compared. One pool will be subcloned and the second pool can be labeled and used as a mixed probe to screen by Southern blotting the series of clones of the first and vice versa. This is a first-step approach which is more reliable for revealing qualitative differences, but even quantitative differences can be detected if results are interpreted carefully. As such, it must always be complemented and confirmed by alternative methods of investigation such as comparative PCR of the two sources of RNA using cDNA-specific primers ***(9)*** or *in situ* hybridization ***(10)***.

2. Materials

2.1. Design and Preparation of Degenerate Primers

1. Custom-made, degenerate, synthetic oligonucleotides (usually 20–25 nucleotides), cleaved from the solid matrix, deprotected, and dialysed against distilled water (*see* **Note 1**).
2. Sephadex G25 (Amersham Pharmacia Biotech) prespun and packed in 1-mL disposable sterile plugged syringes.
3. TEN buffer: 10 m*M* Tris-HCl (pH 8.0), 1 m*M* EDTA (pH 8.0), 100 m*M* NaCl.

2.2. RT-PCR

2.2.1. Poly-A$^+$ RNA Isolation and Construction of cDNA

To avoid the action of RNases, double-distilled sterile DEPC-treated water (treated with diethyl pyrocarbonate at 1:1000 dilution and autoclaved), sterile plasticware and glassware baked at 150°C overnight should be used for the

preparation of all solutions. All handling is carried out with gloves. Specific RNase inhibitors should be included as indicated in the protocol.

1. QuickPrep micro mRNA purification kit (Amersham Pharmacia Biotech, Sweden) for the direct isolation of poly-A^+ RNA from hippocampal cells in vitro. The kit includes the following:
   a. Oligo(dT)–cellulose at 25 mg/mL in storage buffer.
   b. Extraction buffer (guanidium thiocyanate/N-lauroyl sarcosine).
   c. High-salt buffer: 10 m*M* Tris-HCl (pH 7.5), 1 m*M* EDTA, 0.5 *M* NaCl.
   d. Low-salt buffer: 10 m*M* Tris-HCl (pH 7.5), 1 m*M* EDTA, 0.1 *M* NaCl.
   e. Elution buffer: 10 m*M* Tris-HCl (pH 7.5), 1 m*M* EDTA.
   f. Microspin columns.
2. Advantage RT-for-PCR kit (Clontech Laboratories, Inc. Palo Alto, CA) for the reverse transcription of poly-A^+ RNA to cDNA. The kit contains the following:
   a. MMLV reverse transcriptase at 200 U/µL, oligo.
   b. $(dT)_{18}$ primer at 20 µ*M*.
   c. 5X conc. reaction buffer: 250 m*M* Tris-HCl (pH 8.3), 375 m*M* KCl, 15 m*M* $MgCl_2$.
   d. dNTP mix at 10 m*M* for each deoxynucleotide.
   e. RNase inhibitor at 40 U/µL.

2.2.2. PCR

1. Expand Long Template PCR polymerase mix (Boehringer LaRoche, Germany).
2. 10X conc. polymerase buffer: 500 m*M* Tris-HCl (pH 9.2), 160 m*M* $(NH_4)_2SO_4$, 22.5 m*M* $MgCl_2$ (supplied with the polymerase by the manufacturer).
3. Custom-made oligonucleotide primers (as in **Subheading 2.**1) each to be used at a final concentration of 20 pmole per reaction.
4. dNTP mix at 10 m*M* for each deoxynucleotide (Amersham Pharmacia Biotech).
5. cDNA template, prepared as in **Subheading 3.2.1**.
6. Thin-walled micro PCR tubes (0.2 mL) (Perkin-Elmer GmbH, Germany).

2.3. T/A Cloning of PCR Products

1. T/A cloning kit (InVitrogen, The Netherlands), containing:
   a. Linearized T/A cloning vector pCR2.1.
   b. T4 DNA ligase (4 Weiss U/µL).
   c. 10X conc. ligation buffer: 60 m*M* Tris-HCl (pH 7.5), 60 m*M* $MgCl_2$, 50 m*M* NaCl, 1 mg/mL bovine serum albumin (BSA), 70 m*M* β-mercaptoethanol, 1 m*M* ATP, 20 m*M* dithiothreitol, 10 m*M* spermidine.
   d. Ready-to-use 50-µL aliquots of strain TOP10F' competent *Escherichia coli* bacteria for transformation.
2. SOC medium: 2% tryptone, 0.5% yeast extract, 10 m*M* NaCl, 2.4 m*M* KCl, 10 m*M* $MgCl_2$, 10 m*M* $MgSO_4$, 20 m*M* glucose.
3. LB-agar plates containing 50 µg/mL ampicillin, 100 µ*M* iso-propyl-thio-galactopyranoside (IPTG), 40 µg/mL X-gal.

2.4. Labeling of Mixed Probe and Southern Hybridization

1. Expand DNA polymerase, 10X conc. reaction buffer and oligo primers as in **Subheading 2.2.2**.
2. dNTP mix containing 10 m*M* of dATP, dGTP, dTTP, 5 m*M* dCTP and additionally 2 μCi (or 0.3 pmol) of α-^{32}P CTP (specific activity 3000Ci/mmole).
3. "Gene Screen" hybridization transfer membrane (NEN Research Products, Du Pont).
4. 10X conc. SSC: 1.5 *M* sodium chloride, 150 m*M* sodium citrate (pH 7.0).
5. 1 *M* Na_2HPO_4 buffer (pH 7.2) ("sodium phosphate buffer").
6. Church buffer: 0.5 *M* sodium phosphate buffer, 7% sodium dodecyl sulfate (SDS), 1 m*M* EDTA.

3. Methods

3.1. Design and Preparation of Degenerate Primers

1. Prior to probe labeling, purify the crude oligonucleotide by applying it, in a total volume of 100 μL, to the top of a prespun and packed Sephadex G25 1-mL column that has been washed several times with sterile TEN buffer. Hold the spun column in a small Falcon tube containing a decapped Eppendorf tube at the bottom and centrifuge at 1600*g* for 3 min (*see* **Note 2**).
2. Collect the effluent, containing the oligonucleotide probe, in the decapped tube and then transfer to a fresh tube. Determine the concentration spectrophotometrically at 260 nm (*see* **Note 3**).
3. Make working dilutions of each oligo at 20 pmol/μL in water and store at –20°C.

3.2. RT-PCR

3.2.1. Poly-A$^+$ RNA Isolation and Construction of cDNA

1. To prepare poly-A$^+$ RNA, scrape up to 10^7 cells with a rubber policeman in 0.4 mL extraction buffer, vortex well, add 0.8 mL elution buffer, and mix again by vortexing (*see* **Note 4**).
2. After centrifuging at 10,000*g* for 1 min, place this cleared homogenate on top of the pellet of 1 mL of oligo(dT)–cellulose.
3. Mix gently, incubate slurry for 3 min on a rocking table and then centrifuge at 10,000*g* for 10 s.
4. Remove supernatant by aspiration, resuspend resin in 1 mL of high-salt buffer, centrifuge as in **step 3**, and repeat this wash for a total of five times.
5. Wash twice using low-salt buffer.
6. Resuspend the resin in 0.3 mL of low-salt buffer, transfer to a MicroSpin column, centrifuge at 10,000*g* for 5 s, and wash column three more times with 0.5 mL low-salt buffer.
7. Place column in a clean sterile tube and elute poly-A$^+$ RNA with 0.2 mL of elution buffer, prewarmed at 65°C. This fraction will contain about 80–90% of the recoverable mRNA and a second elution step with a further 0.2 mL of warm elution buffer is optional.

8. Determine the concentration of RNA in the final eluate spectrophotometrically (*see* **Note 5**) and, if necessary, precipitate to concentrate solution (*see* **Note 6**).
9. To prepare the first strand of cDNA using the stock solutions of **Subheading 2.2.1.**, place 10 ng of purified poly-A^+ RNA into a sterile 0.5-µL Eppendorf tube and make up to 12.5 µL with sterile DEPC-treated water. Perform this and all subsequent steps on ice unless otherwise specified.
10. Add 1 µL of the oligo$(dT)_{18}$ primer, heat the mix at 70°C for 2 min and quench rapidly on ice.
11. Add in order 4 µL of 5X conc. reaction buffer, 1 µL dNTPs, 0.5 µL RNase inhibitor; mix well and incubate for 42°C for 1 h (*see* **Note 7**).
12. To stop cDNA synthesis and destroy any DNase activity, heat at 94°C for 5 min and then dilute to a final volume of 100 µL with DEPC-treated water. Aliquot cDNA in convenient volumes (20 µL) and store at –80°C, avoiding repeated freezing and thawing. For a typical 50-µL PCR reaction, it is recommended to use 5–10 µL of this cDNA.

3.2.2. PCR

1. The recommended amplification protocol is as follows (*see* **Note 8**):
   a. Denaturation at 94°C for 2 min.
   b. 33 cycles of denaturation at 94°C for 10 s/annealing at 50°C for 30 s/amplification at 68°C for 1 min.
   c. Final amplification at 68°C for 5 min.
   d. Cooling at 4°C until sample retrieval.
2. For each PCR reaction, prepare on ice two separate master mixes and combine them just prior to inserting the tubes in the PCR thermocycler (*see* **Note 7**).

   Mix 1 contains the following added in order from the stocks solutions (**Subheading 2.2.2.**): sterile distilled H_2O up to 25 µL, 2.5 µL of dNTP mix, 1 µL of each of the appropriate pair of primers, 5–10 µL of template cDNA (prepared as described in **Subheading 3.2.1.**).

   Mix 2 contains: sterile distilled H_2O up to 25 µL, 5 µL of 10X conc. buffer, and 0.75 µL Expand polymerase enzyme mix.

   Combine mixes 1 and 2, mix and place tube in PCR thermocycler already set to 94°C (hot start) and commence program. No mineral oil overlay is necessary if the thermocycler model allows use of a heated lid.
3. Check 5–10 µL of each reaction by 1% agarose gel electrophoresis and maintain reaction tubes on ice for <24 h if subcloning of PCR products by T/A cloning will follow (*see* **Note 9**). A characteriztic example of the amplification results using this protocol is shown in **Fig. 1A**.

3.3. T/A Cloning of PCR Products

1. From each PCR, set up a ligation reaction by mixing in order sterile distilled water to 10 µL, 50–150 ng of the PCR product (*see* **Note 10**), 1 µL of 10X conc. ligation buffer, 50 ng of the pCR2.1 vector, and 1 µL T4 DNA ligase.

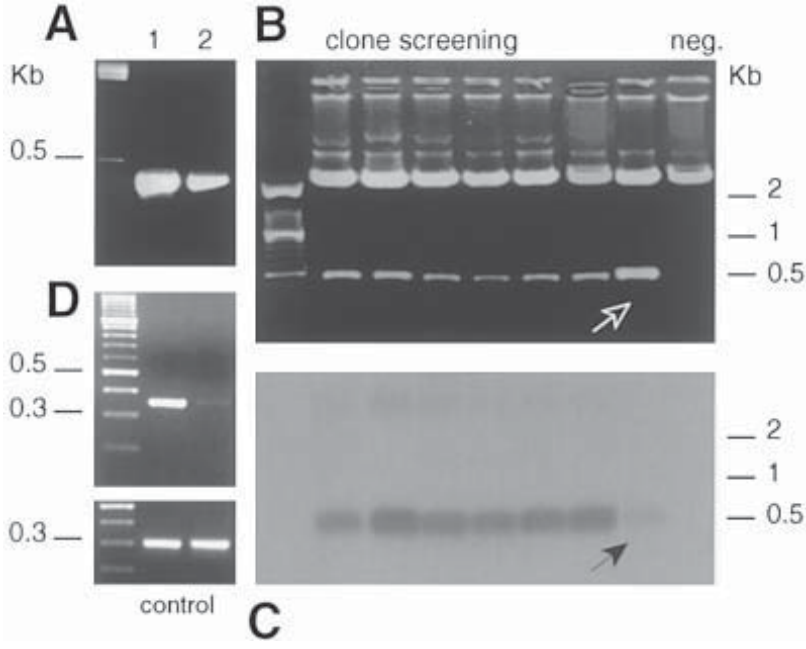

Fig. 1. An example of identification of a novel kinesin-like protein in mouse hippocampus by the concerted methodology described in this chapter. **(A)** RT-PCR using the degenerate primers described in **Note 1** and cDNA derived from stage 3 (immature; lane 1) or stage 5 (mature) hippocampal cultures (lane 2) as a template. The mixed PCR products of each stage were subcloned in vector pCR2.1. **(B)** Agarose gel showing a collection of some of the stage 3-bearing, *Eco*RI-digested plasmids which were subjected to Southern blotting using labeled, stage 5, mixed PCR product as a probe. **(C)** Corresponding autoradiograph of gel in B. The clone indicated by the arrow (M8.7) is shown to hybridize less strongly, suggesting that it is a rarer transcript in stage 5, relative to the other clones shown on this gel. This clone was then sequenced. **(D)** Confirmation of the result of C by RT-PCR, using specific primers for the unique amplification of the M8.7 clone and, as template, stage 3 (lane 1) or stage 5 cDNA (lane 2). This showed that, indeed, M8.7 cDNA is drastically downregulated during the later stages of neuronal differentiation, confirming the result in C. Bottom panel shows equivalent reactions, amplifying mouse GAPDH, carried out in parallel with the same amounts of cDNA as test reactions and used as internal standards. Sequencing of the partial clone M8.7 had revealed a novel kinesin-like protein, a full-length sequence of which would shortly appear as KIFC1 ***(11)***.

2. Incubate the ligation reaction at 14°C, preferably overnight (or at least for 6 h) and proceed immediately to bacterial transformation or store reaction at –20°C.
3. For each bacterial transformation thaw one 50-µL vial of frozen competent cells (supplied by the T/A kit manufacturer), add 2 µL of 0.5 *M* β-mercaptoethanol and 2 µL of the ligation mix, and keep on ice for 30 min.

4. Heat shock bacteria for 30 s at 42°C, place on ice for 2 min, add 250 µL of SOC medium to each tube, and incubate at 37°C with rotary shaking for 1 h.
5. Spread 50 µL and 200 µL from each transformation vial on separate LB-agar plates containing 50 µg/mL ampicillin, 100 µ*M* IPTG, and 40 µg/mL X-gal and incubate at 37°C for 18 h or more for blue/white selection (*see* **Note 11**).
6. Select white colonies, each expected to be recombinants containing an insert from the PCR product, mix and grow them in small-scale, overnight liquid LB cultures (*see* **Note 12**). Clones can be analyzed for insert size with small-scale plasmid preps and subsequent *Eco*RI restriction digests as *Eco*RI sites flank the insertion site in the pCR2.1 vector (**Fig. 1B**). Sequencing for the identification of inserts at this stage can be carried out using M13 forward and reverse primers whose sequences also flank the insertion site in the vector (*see* **Note 13**).

3.4. Labeling of Mixed Probe and Southern Hybridization

1. To use the mixed PCR product of one developmental stage (in our hands, "stage 3" of mouse primary hippocampal cultures) as a probe for Southern blotting, a collection of plasmids containing products of another developmental stage ("stage 5"), label it with α-^{32}P CTP by a further PCR. Repeat the PCR reaction under exactly the same conditions as in **Subheading 3.2.2.**, but this time using 10–50 ng of the mixed PCR product obtained previously (**Subheading 3.2.2.**) as a template and the "spiked" dNTP mix containing α-^{32}P CTP (described in **Subheading 2.4.**). The labeled mixed product, separated from unincorporated nucleotides by ethanol precipitation, is resuspend in 20 µL TE and kept at –20°C to be used the same day. One microliter of the probe is measured by β-scintillation counting to check incorporation.
2. Run the collection of *Eco*RI-digested pCR2.1 plasmids, containing inserts that are derived from the PCR product mix (**Subheading 3.2.2.**), on a 0.8% agarose gel.
3. Denature gel with 0.5 *M* NaOH/1.5 *M* NaCl for 30 min and neutralize with 1 *M* Tris-HCl (pH 7.4), and 1.5 *M* NaCl.
4. Blot DNA onto a sheet of GeneScreen, presoaked in 10X conc. SSC, by capillary transfer overnight.
5. Remove GeneScreen membrane, float it on 50 m*M* sodium phosphate buffer for 20 min, bake it in a –80°C vacuum oven for 1 h and crosslink with ultraviolet (254 nm) at 0.15 J/cm^2 for 30 s.
6. Prehybridize blot with Church's buffer at 65°C for 1 h, denature probe at 94°C for 5 min and immediately dilute it to 1–2 × 10^6 cpm/mL in Church buffer for hybridization.
7. Hybridize blot with the mixed probe at 65°C overnight.
8. Wash blot with 40 m*M* sodium phosphate/1% SDS twice for 5 min at 55°C, four times for 15 min at 65°C, dry, and expose to X-ray film for 2–6 h or overnight, as required.
9. The autoradiograph will identify clones that do not hybridize to the labeled mixed probe and are likely candidates of stage-specific motor proteins (*see* **Note 14**; for

an example, *see* **Fig. 1B**,**C**). Clones can be sequenced (*see* **Subheading 3.3.**) and the partial sequences obtained (corresponding to the motor domain) can be used for pulling out full-length clones by cDNA library screening or by 5' and 3' RACE.

4. Notes

1. The aim of the RT-PCR is to amplify many known and, more interestingly, unknown members of the kinesin-like gene family and, therefore, one has to design a degenerate (mixed) oligonucleotide that incorporates sufficient sequence variation that would be complementary to as many cDNAs as possible. Primers can be designed by including base redundancies representative of all known peptide sequences, but to avoid unnecessary redundancy likely to increase the amplification of nonspecific sequences, it is very useful to carry out nucleotide multiple sequence alignments of all known kinesin-like cDNAs from the given organism and take codon usage bias into account. Some useful empirical rules for the design are the following:
   - As much as it is possible, try to avoid amino acids with six codon choices and instead select those that are specified by one or two codons.
   - At positions where there is a choice of more than two bases (three- or four-fold ambiguity), inosine (I) is recommended. Inosine can form equal-strength stable pairs with all four bases.
   - Inosine can also be used in the third position of synonymous codons.
   - The three bases at the 3' end of the primer must be perfectly matched with the target sequence (choose a single codon amino acid for the 3' end) and should not include inosine.
   - Perfect matching at the 5' is not critical and extra sequences (i.e. restriction sites) can be added if desirable.

   For the amplification of kinesin-like cDNAs from the mouse, the following primers were designed to consensus amino acid sequences that are located within the conserved motor domain. A 5' *Cla*I site was added in the upstream primer.

   upstream primer: GGATCGA TTT GC**I** TA**C/T** GG**A/G** CA**A/G** ACN GG (for amino acid sequence *FAYGQT*).

   downstream primer: CG TTC **A/T G/C**A **C/G/T**CC **T/A**GC **N**AG **G/A**TC (for amino acid sequence *DLAGSE*).
2. An alternative, simple butanol extraction of oligonucleotides can be used instead of purification with Sephadex G25. In this case, dissolve the crude oligonucleotide in 1 mL distilled water and extract two or three successive times with 400 µL of 1-butanol. Discard the upper (organic) phase after each extraction; after the last extraction, centrifuge for 3 min at 15,000*g* and rinse pellet in 70% ethanol before redissolving in TE buffer (10 m*M* Tris-HCl [pH 7.4], 1 m*M* EDTA [pH 8.0]).
3. For the determination of the oligonucleotide concentration, mix 1–5 µL of the oligonucleotide solution with 500 µL of water in a quartz cuvet and measure the absorbance at 260 nm, using water as a blank sample. To calculate the concentration, first calculate the average molarity of the oligo in millimolar (m*M*) given by

the ratio OD_{260}/E_0. E_0 is the millimolar extinction coefficient, determined as the sum of the contribution of the known extinction coefficient of each base in the oligo (i.e., T = 8.8, C = 7.3, G = 11.7, and A = 15.4 mL/μmol). The concentration of the oligo in nanograms per microliter is determined by multiplying the calculated average molarity by 330 (the average molecular mass of a nucleotide) and by the number of nucleotides present in the sequence. (For example, for the 18-mer oligo TCGACCTGGATCCAAGGA, the E_0 = [3 × 8.8]+[5 × 7.3]+[5 × 11.7]+[5 × 15.4] = 198.4. If the measured OD_{260} is 10.65, then $OD260/E_0 = 0.054$ m*M* and the oligo concentration is 0.054 × 330 × 18 = 320.8 ng/μL).

4. The maximum capacity of the Amersham Pharmacia micro mRNA purification kit is 10^7 cells or 100 mg of tissue per run. In our experience with hippocampal primary cultures, the starting material was typically 2×10^6 cells. When working with primary cells, extracted aliquots can be pooled or extraction buffer can be transferred from dish to dish until the desired amount of cells are harvested, up to the maximum column capacity. If cell lines or tissue is used and more material is available, the macro version of this kit can alternatively be used for larger-scale mRNA purification.
5. A good approximation for determining the concentration of mRNA is given by the formula [RNA] = $A_{260} \times 40$ μg/mL. The minimum measured absorbance that is reliable to be accurate is 0.05, equivalent to 2 μg/mL. The use of good quality, undegraded and pure RNA is critical for the production of representative cDNA. RNA should have an A_{260}/A_{280} ratio of >1.7 and its integrity can be evaluated on a denaturing formaldehyde/agarose gel ***(12)***.
6. To concentrate RNA solutions, precipitate RNA with the addition of 1/40 vol of 10 mg/mL glycogen and 1/10 vol of 2.5 *M* potassium acetate (pH 5.0). Add 2.5 vol of 95% chilled ethanol and keep at –20°C for at least 30 min. Collect the precipitated RNA by centrifugation at 13,000*g* at 4°C for 5 min. Resuspend in DEPC-treated water and store at –80°C.
7. Both for cDNA generation and PCR (**Subheading 3.2.2.**) it is advisable to prepare appropriate reagent "master mixes," especially if a large number of samples are being handled. The appropriate volume is then transferred from the master mix to each tube. This minimizes pipetting errors of small volumes, reduces sample-to-sample variation, and speeds up the procedure. Always prepare a slightly larger volume of master mix to ensure that there will be enough solution, even for the last tube!
8. The importance of selecting the appropriate hybridization temperature in the PCR protocol, especially when using degenerate primers, cannot be overstressed. A balance has to be struck between avoiding too permissive conditions that will increase nonspecific amplification of unrelated sequences and using too stringent temperatures that will decrease yield or fail to amplify simultaneously the whole range of desired, related sequences. The hybridization temperature can be calculated with the following rule of thumb: T_H = [(2 × No. of AT pairs)+(4 × No. of GC pairs)°C-(2–5°C)]. If inosine is present multiply the number of pairs by 2. The value of T_H should be in the range of 50–65°C for probes of 20–25 nucle-

otides in length. Where degeneracy occurs, take into account the lowest-T_H value for setting the hybridization temperature in the PCR protocol.

9. The principle of T/A cloning is based on the fact that most thermostable polymerases (but not those that exhibit 3' to 5' exonuclease activity like *Vent* and *Pfu*, which should not be used in this method) add single deoxyadenosines (A) to the 3' ends of PCR products. The linearized pCR2.1 vector supplied in the kit possesses 3' deoxythymidine (T) overhangs and this makes it possible for PCR products to ligate directly with the vector. It is critical to protect the integrity of cohesive ends in both the PCR product and vector for efficient ligation; thus, it is recommended to use fresh (less than 24 h old) products, which should be kept on ice and *not* frozen, and to avoid freeze–thaw cycles for linearized vector aliquots (use whole vector aliquot and do not refreeze or refreeze not more than twice).
10. For setting up the ligation reaction, the recommended vector:insert ratio is 1:1, but you may try ratios up to 1:3, provided you do not use more than 2–3 µL of the PCR sample as its salts may inhibit T4 DNA ligase. In my experience, the best results are obtained with the use of 0.5–1 µL of a typical PCR sample in which the product is estimated to be at least 50 ng/µL on an agarose gel.
11. The manufacturers of the T/A kit advise that about 5% of white colonies will not be recombinants but will be false positives resulting from either frame shifts of the *lacZ* gene or blunt-end self-ligation of the vector caused by degradation of 3'T overhangs. Often this percentage is higher and an advisable step is to always set up a routine control ligation reaction in which the addition of PCR product is omitted. By counting the number of white clones as a percentage of the total number of clones, this "background" can be evaluated, and if it is higher than 30–35%, it may be better to repeat the experiment with a new batch of vector.
12. The number of clones necessary to analyze depends on the complexity of the original PCR product, the ligation efficiency of your experiment (not all white clones will turn out to be recombinants; *see* **Note 11**), and the aim of the experiment. If the aim is to identify as many new motor cDNAs as possible or to compare the expression pattern between two developmental stages or different tissues, then one should aim to analyze about 100 clones. Start with the analysis of a batch of 20–25 clones to get an idea about ligation efficiency and insert variability and then continue with the analysis of further clones, accordingly.
13. Vector sequence and manuals can be viewed and downloaded from the Invitrogen Web Resource at http://www.invitrogen.com.
14. The principle of this protocol is to compare the expression of the set of kinesin-like motor proteins expressed in two distinct developmental (differentiation) stages or cell types, aiming to identify those that are uniquely expressed in each stage or that are subject to downregulation. Technically, this is detectable by the lack of hybridization of specific stage-specific clones to the mixed probe derived from the other stage being compared (this experiment can be conducted in both combinations [i.e., screening clones of one stage using the other stage cDNA pool as mixed probe and vice versa]). Those nonhybridizing clones will be good candidates for stage-specific expression (*see* example in **Fig. 1B**,**C**). Furthermore,

this technique can also reveal clones that are developmentally downregulated resulting in weak hybridization, although such results must be interpreted with more caution because they may be artifacts resulting from inadequate probe labeling or they may simply reflect the relative abundance of a specific cDNA in the mixed pool of cDNAs used as a probe. For these reasons, the results must always be confirmed be alternative methods such as RT-PCR of the two sources of RNA that are being compared, using primers specific for the candidate clones (*see* example in **Fig. 1D**) or *in situ* hybridization.

Acknowledgments

I am indebted to Dr. Carlos G. Dotti at the European Molecular Biology Laboratory, in whose lab I conducted this work, for his continuous support, hospitality, and encouragement, to Dr. Michael Way also at the EMBL for constructive discussions and advice, and to Bianca Hellias for her expert maintenance of neuronal cultures. This work was supported by a Human Capital and Mobility Fellowship from the European Union and by a short-term Fellowship from FEBS.

References

1. Moore, J. D. and Endow, S. A. (1996) Kinesin proteins: a phylum of motors for microtubule-based motility. *BioEssays* **18**, 207–219.
2. Hirokawa, N. (1998) Kinesin and dynein superfamily proteins and the mechanism of organelle transport. *Science* **279**, 519–526.
3. Vale, R. D. (1991) Motor proteins, in *Guidebook to the Cytoskeletal and Motor Proteins* (Kreis, T. and Vale, R., eds.), Oxford University Press, Oxford, pp. 175–183.
4. Stewart, R. J., Pesavento, P. A., Woerpel, D. N., and Goldstein. L. S. (1991) Identification and partial characterization of six members of the kinesin superfamily in *Drosophila*. *Proc. Natl. Acad. Sci. USA* **88**, 8470–8474.
5. Aizawa, H., Sekine, Y., Takemura, R., Zhang, Z., Nangaku, M., and Hirokawa, N. (1992) Kinesin family in murine central nervous system. *J. Cell Biol.* **119**, 1287–1296.
6. Vernos I., Heasman J., and Wylie, C. (1993) Multiple kinesin-like transcripts in *Xenopus* oocytes. *Dev. Biol.* **157**: 232–239.
7. Nakagawa, T., Tanaka, Y., Matsuoka, E., Kondo, S., Okada, Y., Noda, Y., et al. (1997) Identification and classification of 16 new kinesin superfamily (KIF) proteins in mouse genome. *Proc. Natl. Acad. Sci. USA* **94**, 9654–9659.
8. Dotti, C. G., Sullivan, C. A. and Banker, G. A. (1988) The establishment of polarity by hippocampal neurons in culture. *J. Neurosci.* **8**, 1454–1468.
9. Santama, N., Krijne-Locker, J., Griffiths, G., Noda, Y., Hirokawa, N. and Dotti C. G. (1998) KIF2β, a new kinesin superfamily protein, is associated with lysosomes and may be implicated in their centrifugal translocation. *EMBO J.* **17**, 5855–5867.
10. Santama, N. (1997) *In situ* hybridisation for the detection of neuropeptide transmitters, in *Methods in Molecular Biology*, vol. 72: *Neurotransmitter and Neuroreceptor Methods* (Rayne, R. C., ed.), Humana Press, Totowa, NJ, pp. 159–170.

11. Saito, N., Okada, Y., Noda, Y., Kinoshita, Y., Kondo, S., and Hirokawa, N. (1997) KIFC2 is a novel neuron-specific C-terminal type kinesin superfamily motor for dendritic transport of multivesicular body-like organelles. *Neuron* **18**, 425–438.
12. Sambrook, J., Fritsch, E. F., and Maniatis, T. (1989) *Molecular Cloning. A Laboratory Manual.* Cold Spring Harbor Laboratory, Cold Spring Harbor, NY.

3

Expression Cloning with Pan Kinesin Antibodies

Laura M. Ginkel and Linda Wordeman

1. Introduction

Kinesin and kinesin-related proteins comprise a family of molecular motors that utilize the chemical energy provided by the hydrolysis of ATP to perform force-generating movements along filamentous microtubules. Members of this family of microtubule motors are vital for numerous cellular activities, such as organelle transport and chromosome segregation. Kinesin-related proteins are not only linked by function, but each family member shares a similar "motor-domain" region responsible for converting the chemical energy of ATP into mechanical force (reviewed in **refs.** ***1*** and ***2***). Within this specialized motor region, there exist short, conserved sequences that are not only present in kinesin-related motors but also found in other ATP-hydrolyzing molecular motors (myosins and dyneins) and GTP-hydrolyzing G proteins (reviewed in **ref.** ***3***). In this chapter, we will describe our use of pan-specific, kinesin peptide antibodies generated against two of these short, conserved sequences for the expression cloning of members of the kinesin-related protein family. We will briefly discuss the production of the pan-specific, kinesin peptide antisera and the four conserved regions within the motor domain of the kinesin protein family previously selected for the generation of these antibodies. In more detail, we will describe the method by which our laboratory has used these pan-specific antibodies to identify and clone kinesin-related proteins.

1.1. What are Pan-Specific, Peptide Antibodies?

Peptide antibodies are generated from a short peptide sequence that corresponds to a sequence fragment of a desired protein. In comparison to the production of either polyclonal or monoclonal antisera, peptide antibodies are both relatively simple and often less time-consuming to prepare. These antibodies

From: *Methods in Molecular Biology*, Vol. 164: *Kinesin Protocols*
Edited by: I. Vernos

have proven to be very successful tools for various immunological and biochemical techniques, such as immunofluorescence, immunoblotting, and the isolation of native proteins and protein complexes by affinity purification ***(4–7)***. Pan-specific, peptide antibodies are generated against synthetic peptides corresponding to an amino acid sequence conserved among a protein family ***(8)***. We have used pan-specific, peptide antibodies made against conserved regions within the kinesin motor domain to identify new kinesin family members ***(9)*** and to determine which kinesin-related proteins are present during skeletal muscle differentiation.

1.2. Production of Pan Kinesin Peptide Antibodies

There are four regions within the motor domain of kinesin-related proteins that are highly conserved within the kinesin family (**Fig. 1**, regions I–IV). The crystal structures of the motor domains of both kinesin heavy chain (KHC) and the kinesin-related protein, ncd, have shown that three of the conserved regions are in close proximity to the nucleotide binding region, and the fourth is a putative microtubule-binding site ***(10, 11)*** (*See* Chapter 19 for crystallization methods). Interestingly, these four regions appear to be conserved motifs that are also present in the myosin and dynein motor families, as well as the signal transduction family of G proteins. The protein members of each of these families, including kinesins, bind nucleotide and undergo a conformational switch with the hydrolysis of that nucleotide. This suggests a possible, common familiar ancestry between these proteins and the employment of comparable force-generating mechanisms (reviewed in **ref. *3***).

The four highly conserved regions of the motor domain of kinesin family proteins were previously selected to generate pan-specific peptide antibodies ***(12)***. Four short, synthetic peptides were generated based on conserved amino acid residues from the comparison of five kinesin-related proteins: *Drosophila* kinesin ***(13)***, KAR3 ***(14)***, BimC ***(15)***, ncd ***(16, 17)***, and cut7 ***(18)***. The complete sequences synthesized were GYNVTIFAYGQTG (region I), NEHSSRSHS (region II), LNLVDLAGSE (region III), and HIPYRESKLT (region IV). An extremely detailed description of the protocol followed to produce these antibodies is described in **ref. *5***. Briefly, each peptide was coupled to keyhole limpet hemocyanin (KHL) to help ensure a strong immune response and injected into two rabbits for the generation of crude, polyclonal antisera. The crude antisera was then affinity purified against the antigen (the synthetic peptide) on a peptide resin column. Two of the four synthetic peptides yielded successful pan kinesin antibodies, LNLVDLAGSE (the "LAGSE" antisera) and HIPYRESKLT (the "HIPYR" antisera). These antisera crossreacted with the peptide antigen and, at a concentration of 10 µg/mL, recognized a single band of purified squid KHC on immunoblots. The GYNVTIFAYGQTG

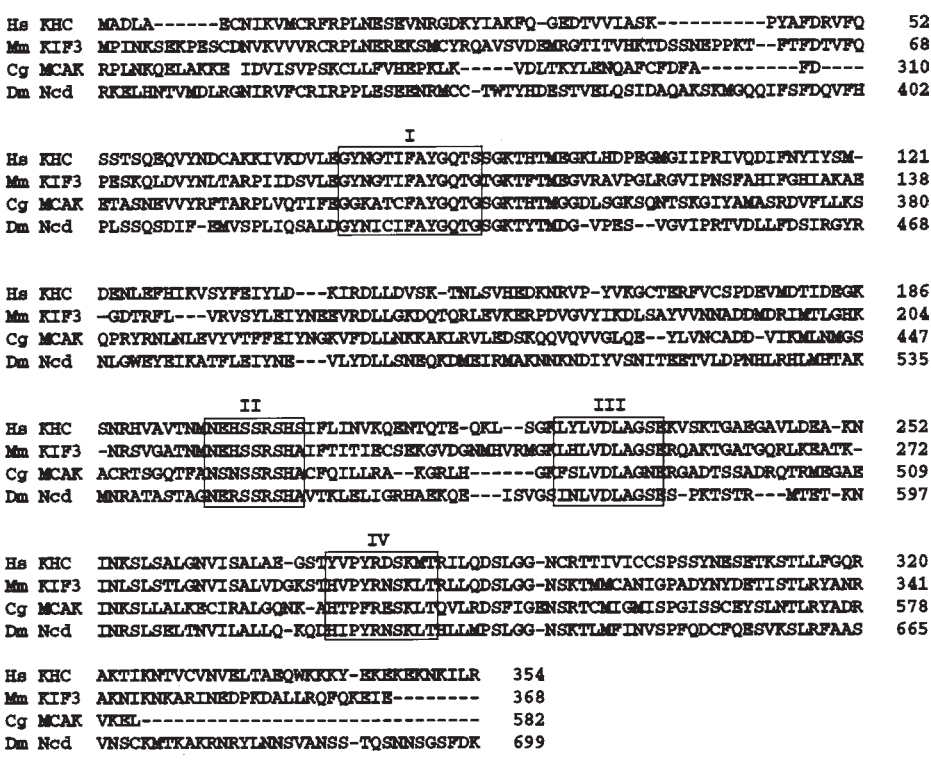

Fig. 1. Comparison of amino acid sequences of the motor domains from four kinesin-related proteins: human KHC, mouse KIF3A, hamster MCAK, *Drosophila* ncd. The boxed regions (I–IV) are the four conserved sequence fragments within the kinesin motor family. These regions were previously selected for the production of pan-specific, kinesin peptide antibodies. (From **ref.** ***12***.)

("FAYGQT") peptide did not generate a strong immune response ***(12)***. The NEHSSRSHS ("SSRSH") peptide produced a good immune response in only one of the two rabbits. This antisera crossreacted well with the peptide antigen, but barely recognized KHC over background.

Because the method for production and purification of these peptide antibodies is already easily available, we would instead like to focus on the process of selecting the amino acid sequences used in synthesizing the peptides for these antibodies. This a useful exercise because, although regions I–IV are the most obvious sections of the motor domain to select for the production of pan-specific antibodies, there are alternative regions that may be considered as possible candidates for the generation of different pan kinesin antibodies. In Field et al. ***(5)***, a review of the 40 peptide antibodies produced in that laboratory gave

a 43% success rate for those made from internally located peptide sequences. This is important to remember because any region chosen from the kinesin motor domain will also be an internal sequence. Field et al. ***(5)*** also found that the net charge of the peptide was an important parameter in predicting success. Those peptides that were strongly basic, with a net charge of +3 to +5, were most successful. Either weakly acidic or basic peptides were slightly less so, and those peptides with a net charge of zero most often failed. Furthermore, it is also useful to determine the antigenicity of the region of the protein selected for peptide antibodies. The more antigenic (less hydrophobic) segments of the protein generally yield a stronger immune response and are more likely to correspond to surface residues that will be accessible to the antibody.

Two pan-specific, kinesin antibodies that proved to be successful, LAGSE and HIPYR, are both in hydrophilic regions of the motor domain. The LAGSE and HIPYR peptides have net charges of –2.1 and +1.1, respectfully, at pH 7.0. The LAGSE region (**Fig. 1**, region III) of the kinesin motor domain is part of the nucleotide binding segment of the protein. It is contained within a loop covering the rear of the nucleotide cleft. Clustered among this same section of the three-dimensional (3D) motor-domain structure is the SSRSH region (region II) of the protein. This region is in a very similar position to a nearly identical sequence in myosin that is implicated in transmitting conformational changes from the nucleotide pocket. The crystal structure of KHC and ncd suggested that the microtubule-binding site was located within two loops of the motor domain (L8 and L12), one of them (L12) containing the HIPYR region ***(10, 11)***. It was subsequently confirmed by alanine-scanning mutagenesis that the center of microtubule binding, indeed, resides in L12. This region also corresponds to the major actin-binding domain in myosin ***(19)***. The two conserved regions of the motor domain that yielded successful synthetic peptides for antibody production are clearly more peripherally located within the motor domain structure.

The two pan-specific, kinesin antibodies that were not successful, FAYGQT and SSRSH, are both in hydrophobic regions of the motor domain. The FAYGQT and SSRSH peptides have net charges of –0.1 and +0.4, respectfully. The failure of these peptides to produce either an adequate or consistent immune response may be the result of their lack of antigenicity and having a net charge close to zero. Both of these regions (**Fig. 1**, regions I and II) are positioned within the nucleotide-binding environment. Interestingly, as stated earlier, both the SSRSH and LAGSE regions of the motor domain are clustered in the back of the nucleotide-binding pocket. The lack of antigenicity of the SSRSH peptide suggests that, in comparison to the LAGSE region, the SSRSH segment of the nucleotide pocket is more embedded within the structure. The FAYGQT region is within the classic P-loop of the protein. It cradles the α- and β-phosphates of the bound nucleotide and is, therefore, more internally

located within the nucleotide-binding region ***(10, 11)***. This peptide was also difficult to handle because of its poor solubility in water.

The pan-specific, peptide antibodies that were previously produced were designed to recognize any member of the kinesin motor family. At that time, the family of kinesin-related proteins was still fairly small. The kinesin family has grown such that it is now separated into three major classes dictated by the position of the motor domain: NH_2-terminal motor domain (N type), COOH-terminal motor domain (C type), or middle motor domain (M type). In **Fig. 1**, both KHC and KIF3 are examples of N type motors. MCAK is a M type motor, and ncd is a C-type motor. Each class of kinesin-related motors continues to expand, occupying divergent roles within the cell ***(1, 2)***. A possible strategy for generating pan-kinesin peptide antisera different from those already produced is to narrow the search for new kinesins that fall within a certain class (N, C, or M type). Careful sequence alignments of such kinesin-related proteins may reveal some interesting, yet subtle, regions of similarity that could be selected for peptide synthesis and antibody production ***(20)***.

2. Materials

2.1. Are Kinesin-Related Proteins Present in Your System?

2.1.1. Testing HIPYR and LAGSE Antibodies on Immunoblots

1. Gradient sodium dodecyl sulfate-polyacrylamide gel electrophoresis (SDS-PAGE) gels 4–12% (Novex, San Diego, CA).
2. HIPYR and LAGSE antisera are currently commercially available (Berkeley Antibody Company, Berkeley, CA). Dilute antisera in Tris-buffered saline (TBS), pH 8.0.
3. Enzyme-conjugated secondary antibody (Jackson ImmunoResearch, West Grove, PA) (*see* **Note 1**):
   a. Alkaline phosphatase (AP)-conjugated secondary antibody proceeded by 5-Bromo-4-chloro-3-indolyl phosphate/nitro blue (BCIP/NBT) colorimetric reaction ***(21)***.
   b. Horseradish peroxidase (HRP)-conjugated secondary antibody proceeded by a photochemical reaction (ECL kit, Amersham, UK).

2.1.2. Using HIPYR and LAGSE for Immunofluorescence

1. 12-mm glass coverslips (Carolina Biological Supply, Burlington, NC).
2. 16% paraformaldehyde stock (Ted Pella, Redding, CA). Dilute to and use at 4% in 1× phosphate-buffered saline (PBS), pH 7.5. Parafilm the opened stock and keep refrigerated; this is stable for at least 1 mo.
3. Ceramic cover-slip holder (made by Coors, available through Thomas Scientific, Swedesboro, NJ).
4. To prepare a humidified, antibody incubation chamber, cover the bottom of a 15-cm plastic Petri dish with parafilm. Place two, wet, rolled-up Kimwipes along

opposite, inside edges of the dish. After coverslips are placed inside the chamber, remember to replace the chamber's lid.
5. Usually, the choice of blocking solution depends on the animal source of the secondary antibody. For example, if secondary antibodies are produced in a donkey, use 20% donkey serum diluted in PBS to block.
6. HIPYR and LAGSE antisera are currently commercially available (Berkeley Antibody Company, Berkeley, CA).
7. Fluorophore conjugated, anti-rabbit secondary antibody (Jackson Immuno–Reseach, West Grove, PA) (*see* **Note 1**).
8. AbDIL (antibody diluent): TBS (pH 8.0), 1.0% bovine serum albumin (BSA), 0.1% Triton X-100, 0.02% NaN_3.
9. Antifade mounting media (VectorLabs, Burlingame, CA). Clear nail polish (Wet 'n Wild, Sigma, St. Louis, MO).

2.2. Screening an Expression Library with Pan Kinesin Antibodies

2.2.1. Library Plating and Double, IPTG–Nitrocellulose Filter Lifts

1. Protocol is described for λZAP libraries (Stratagene, La Jolla, CA). Host bacteria: XLI-blue, tetracycline resistance.
2. LB- or NZY-agar plates (15-cm Petri dishes). NZY-top agarose: NZY media, 10 m*M* $MgSO_4$, 0.2% (w/v) maltose, 0.7% agarose.
3. SM buffer: 100 m*M* NaCl, 50 m*M* Tris-HCl (pH 7.5), 10 m*M* $MgSO_4$, 0.01% gelatin. Sterilize by autoclaving.
4. Nitrocellulose circles, 132 mm in diameter.
5. IPTG (Isopropyl β-D-thiogalactopyranoside), 10–20 m*M* in sterile water.
6. Whatman 3MM paper; plastic wrap; pencil or permanent waterproof marker; parafilm.

2.2.2. Antibody Screening Filters with Pan Kinesin Antibodies

1. TBS (Tris-buffered saline), pH 8.0.
2. Blocking solution: 5.0% dried milk in TBS (pH 8.0).
4. HIPYR and LAGSE antisera are currently commercially available from Berkeley Antibody Company (Berkeley, CA).
5. AP-conjugated anti-rabbit secondary antibody (Jackson ImmunoReseach, West Grove, PA).

2.2.3. Purification of Positive Plaques

1. Plastic transfer pipets.
2. 1.7-mL microfuge tubes.
3. Chloroform.
4. SM buffer (**Subheading 2.2.1.**).
5. 10-cm LB- or NZY-agar Petri dishes.
6. NZY-top agarose.
7. 82-mm nitrocelluose filters.

3. Methods

In this section, we will describe how to utilize the pan kinesin antisera generated by Sawin et al. ***(12)***, LAGSE and HIPYR, to identify kinesin-related proteins by screening an expression library. This procedure can be used for expression cloning with any two pan-specific antisera. To further illustrate our techniques, we will parallel our discussion with data from our laboratory.

3.1. Are Kinesin-Related Proteins Present in Your System?

Before beginning an often lengthy expression screen in search for kinesin-related proteins, it is wise to first assess the possible expression, if any, of these proteins in your system. The expression of kinesin-related proteins in your system can be determined by immunoblots and/or immunofluorescence.

3.1.1. Testing HIPYR and LAGSE Antibodies on Immunoblots

Because a library screen is essentially a Western blot, it is useful to test the specificity and behavior of the chosen antibodies on immunoblots.

1. Prepare crude cell lysates of the cell line or tissue from which the cDNA expression library chosen for the screen is made (*see* **Note 2**).
2. Separate proteins by SDS-PAGE as per standard methods ***(22)***. Gradient SDS–polyacrylamide gels (4–12%) can be very useful for this procedure because they give a wider effective range of protein separation.
3. Transfer the proteins onto nitrocellulose and process using standard Western blot techniques ***(21)***. If labeling blots with the HIPYR or LAGSE antisera, incubate for 2 h at 5 µg/mL at room temperature (*see* **Note 3**). Incubate with an enzyme-conjugated secondary antibody for 2 h at room temperature.

Figure 2 demonstrates how HIPYR and LAGSE antibodies perform on immunoblots. One can use whole-cell lysates, purified or partially purified organelles, or specific tissues to test antibody performance. C2C12 cells can be triggered to differentiate into skeletal myofibrils upon the depletion of mitogen growth factors from the media (differentiation media). Each blot in **Fig. 2A** displays crude cell lysates of myoblasts (undifferentiated cells, lane 1) and a time-course of differentiating myofibrils (lanes 2–7), separated on a 7.5% SDS-PAGE gel and probed with the HIPYR and LAGSE antisera. Most of the identified kinesin-related proteins fall with the molecular mass range of 80–190 kDa ***(1)***. The blots in **Fig. 2A** show many proteins that fall within that range. It is important to realize that these may or may not be kinesin-related proteins. Although these antibodies are affinity purified and thus will not result in spurious cross-reactivity, some non-kinesin proteins may have epitopes that are shared with the short, conserved kinesin sequences that may cross-react with the peptide antibodies. In addition, although both the HIPYR and LAGSE anti-

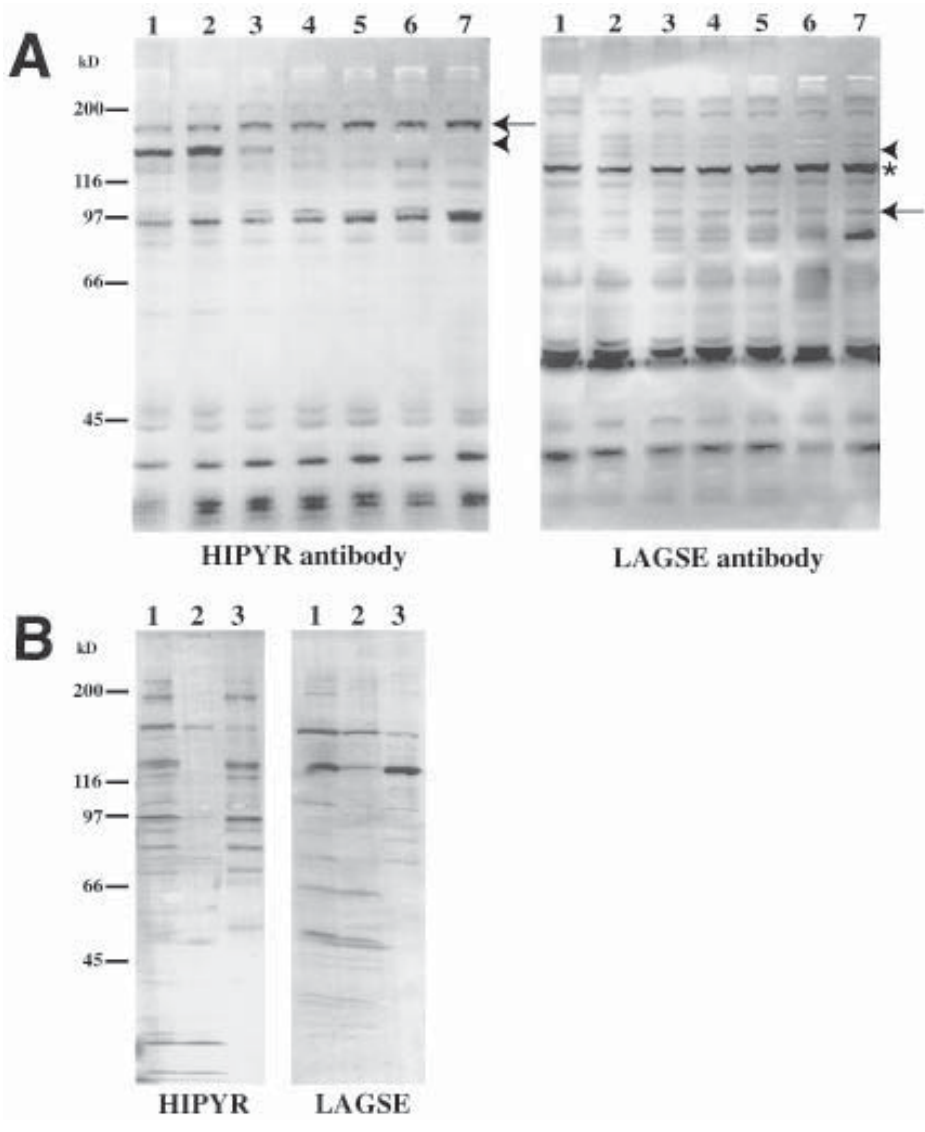

Fig. 2. Immunoblots testing the HIPYR and LAGSE antibodies on C2C12 and CHO cell lysates. Time-course of C2C12 differentiation **(A)**. Lane 1, undifferentiated C2C12 myoblasts; lanes 2–5, 1–4 d differentiation; lane 6, 1 wk differentiation; lane 7, 2 wk differentiation. Star (*) on LAGSE blot denotes an approx 120 kDa protein that may represent KHC. Arrows and arrowheads indicate increasing and decreasing expression levels of proteins, respectively. Microtubule-pelleting assay of CHO cell lysates **(B)**. Lane 1, high-speed supernatant; lane 2, microtubule-depleted supernatant; lane 3, microtubule pellet. Approximately equal amounts of protein are loaded within each lane.

sera were produced to recognize kinesin-related motor domains, they recognize different sequences/epitopes. Therefore, it should not be surprising to see different results when comparing the two blots. For example, the mouse KHC is 117 kDa. There is a strong band in the LAGSE blot of approximately that size that may be KHC (star). However, the HIPYR blot shows only a faint band in that region. If, indeed, that band is KHC, for one reason or another, the LAGSE antisera crossreacts stronger with that protein than HIPYR. Finally, if you are studying a developmental process, such as skeletal muscle differentiation, it can be useful to assess the potential kinesin-related protein expression over a developmental time-course. In **Fig. 2A**, there appears to be both increases (arrows) and decreases (arrowheads) of putative kinesin family proteins. This information can be useful in helping to narrow the search for these proteins within a particular stage of development.

Alternatively, the kinesin expression in your system can be determined by a microtubule-pelleting assay. Polymerized microtubules can be added to an ATP-depleted, high-speed supernatant of a crude cell lysate ***(23)***. Microtubules are pelleted through a glycerol cushion and resuspended. **Figure 2B** shows two immunoblots of a microtubule pelleting assay from CHO cells. The high-speed supernatant (lane 1), microtubule-depleted supernatant (lane 2), and microtubule pellet (lane 3) have been probed with HIPYR and LAGSE antisera. A microtubule-pelleting assay can be performed either with ATP-depleted material or by using the nonhydrolyzable ATP analog AMP–PNP to promote the rigor binding of kinesins to microtubules. Enrichment of HIPYR and LAGSE crossreacting bands in the microtubule pellet, especially those that can be extracted with ATP (not shown), can serve as further confirmation that a band on the blot represents a kinesin-related protein.

3.1.2. Using HIPYR and LAGSE Antibodies for Immunofluorescence

The HIPYR and LAGSE antibodies can also be used for immunofluorescence to determine if there may be kinesin-related proteins in your system. We will describe our basic method of performing immunofluorescence with the pan kinesin antibodies on tissue culture cells.

1. Plate cells onto a 12-mm round, glass coverslip (*see* **Note 4**) placed in a 24-multiwell plastic dish with 1 mL of media. Incubate cells as normal.
2. When ready to fix the cells, remove the coverslip with forceps and transfer to the fixation solution. At first, it is wise to use the standard fixative for your cells. With the C2C12 cells, the HIPYR and LAGSE antibodies are most visible with a 4% paraformaldehyde fixation, 20 min, at room temperature.
3. After fixation, transfer the coverslip into a ceramic cover-slip holder immersed in 100 mL of PBS to wash for at least 5 min. All wash steps are performed in this manner.

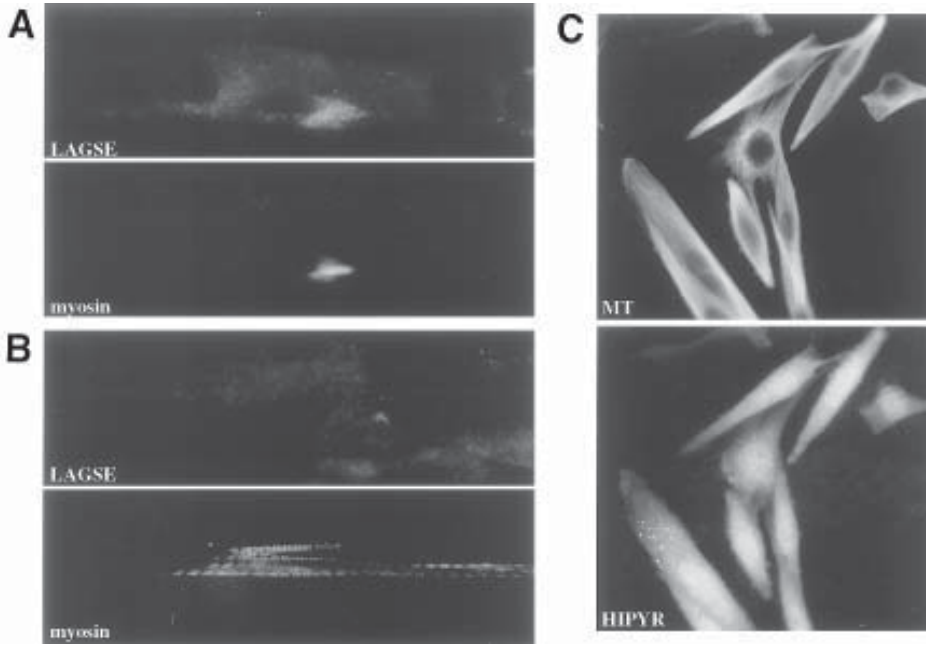

Fig. 3. Immunofluorescence of LAGSE and HIPYR antibodies in C2C12 cells and myofibrils. **(A**,**B)** Cells are double labeled with LAGSE antisera and an antibody to skeletal muscle myosin and examined by immunofluorescence microscopy. In **(A)**, an accumulation of putative kinesin-related proteins colocalizes with a mass of skeletal muscle myosin. In a more mature myofibril **(B)**, where myosin striations are visible, the colocalization is abolished. **(C)** Cells are double labeled with HIPYR antisera and an antibody to tubulin.

4. Transfer the washed coverslip to a humidified, antibody chamber (cell side up!). Add 20 µL of blocking solution to the cells to decrease nonspecific crossreactivity. Incubate for at least 30 min.
5. Wash the coverslip for 5 min and return to humidified chamber for primary antibody incubation. For the HIPYR and LAGSE antisera, we incubate cells with 15 µL of 5–10 µg/mL antibody diluted in AbDIL. Incubation time can vary from 30 min to 2 h at room temperature; overnight incubations should be done at 4°C.
6. Wash the coverslip for 5 min, and return to humidified chamber. Incubate cells with 15 µL of secondary antibody for 30 min to 2 h.
7. Wash the coverslip for at least 10 min and mount onto a microscope slide (cell side down!) with antifade mounting media. Affix the coverslip to the microscope slide with clear nail polish.

Figure 3 shows staining of C2C12 myoblasts and myofibrils with both the HIPYR and LAGSE antibodies. When labeling cells with antisera that has not been affinity purified, it is important to perform peptide block control experiments to insure that the labeling is specific. As the HIPYR and LAGSE antibodies are affinity purified, we only performed secondary antibody control experiments (data not shown) to carefully titrate the concentration of secondary antibody and reduce any nonspecific crossreactivity. As might be expected from a family of proteins that consist of many vesicle motors, the pan kinesin antisera labels in a fairly punctate-like manner in the cell. **Figure 3A**,**B** shows cells that are double, immunofluorescently labeled with the LAGSE antisera and an antibody to skeletal muscle myosin. In **Fig. 3A**, the cell has been incubated in differentiation media for 1–2 d and has just started to express and accumulate skeletal muscle myosin. It is an immature myofibril, as no myosin striations, indicative of assembled sarcomeres, are present. Interestingly, there is a similar accumulation of putative kinesin-related proteins in the same region. When looking at a more mature myofibril containing myosin striations (**Fig. 3B**), the colocalization of putative kinesin-related proteins and myosin is gone. We are searching for kinesin-related proteins that may participate in the assembly of the developing skeletal muscle myofibril. These immunofluorescence studies proved useful because it helped to narrow our search for kinesin proteins to very early stages of myofibril formation. At that point of differentiation (1–4 d of C2C12 cell differentiation), it appears as though putative kinesin proteins are both still prominent and located in an intriguing region in the cell. Likewise, we made a cDNA expression library from C2C12 cells that had been differentiating for 2–3 d to be screened with the pan kinesin antibodies. Figure 3C shows a field of C2C12 cells that are double labeled with the HIPYR antisera and an antibody against tubulin. Putative kinesin-related protein labeling is seen throughout the cell (*see* **Note 5**).

3.2. Screening an Expression Library with Pan Kinesin Antibodies

Pan kinesin antibodies can be used to obtain a cDNA clone of kinesin family members by screening a λ-phage cDNA expression library. These libraries can be either purchased or made. When a cDNA expression library is produced, the information encoded within the mRNA of a particular cell line, tissue, or organism is converted into the more stable, double-stranded DNA. The cloned, DNA fragments are then inserted into a self-replicating λ vector so that, when introduced into bacteria, the DNA insert is transcribed from a promoter that is functional in *Escherichia coli*. The resulting recombinant proteins can be identified and isolated by a screen of that library with a primary antibody (in this case, the

pan kinesin antisera). The success of an expression screen greatly depends on the quality of the cDNA library. The averge size of the DNA inserts is an important factor when choosing a library to screen. To increase the chances of isolating a full-length clone of the protein of choice, expression libraries with longer-sized inserts are definitely favorable. Our laboratory has successfully used the HIPYR and LAGSE antisera to clone kinesin family proteins from both a library that was purchased (Chinese Hamster Ovary λZAP library, Stratagene, La Jolla, CA) and an oligo(dT)-primed library that was created in the lab.

The following protocol is specific for screening λZAP (Stratagene, La Jolla, CA) expression libraries with two different pan kinesin peptide antisera. By using two pan-specific antisera and isolating those plaques that are positive with both, this helps ensure the isolation of true kinesin-related proteins and minimizes cloning of proteins from nonspecific crossreactivity of one of the antibodies. Before beginning the screen, it is important to determine the phage titer of the library. This permits the plating of the correct number of plaque forming units (PFUs) per Petri dish. This is done by plating serial dilutions of the library to be screened and counting the resulting plaques to determine the PFUs per milliliter.

3.2.1. Library Plating and Double, IPTG-Nitrocellulose Filter Lifts

1. Grow a 3-mL fresh culture of host bacteria overnight. Dilute the culture 1:100 in 25 mL LB (plus antibiotic) supplemented with 10 m*M* $MgSO_4$ and 0.2% (w/v) maltose. Continue to grow for a couple of hours (do not surpass an OD_{600} of 1.0). Pellet the bacteria gently at 5000*g* for 10 min and resuspend in half the original volume with sterile 10 m*M* $MgSO_4$ (*see* **Note 6**). When ready to plate, dilute the cells to OD_{600} = 0.5 with sterile 10 m*M* $MgSO_4$. Use the bacteria immediately after diluting.
2. Preincubate agar plates at 42°C for 1 h before plating. For screening a mammalian library, plate a total of 10^6 PFUs with approx 50,000 PFUs per 15-cm Petri dish (20 dishes). For each dish to be plated, combine freshly diluted bacteria and 5×10^4 PFUs of library (diluted in SM buffer) in a Falcon 2059 (*see* **Note 7**). Refrigerate the bacteria and phage for 10 min (*see* **Note 8**), then incubate for 15 min in a 37°C water bath. Add 7–10 mL of NZY-top agarose, warmed to 52°C, and gently mix (by vortexing, or pipetting up and down). Pour onto prewarmed agar plates, quickly distribute evenly across the agar surface (avoid air bubbles), and allow to solidify at room temperature (approx 10 min).
3. Incubate the plates, upside down, at 42°C until small plaques are just visible on a bacterial lawn (3–6 h). Check often while waiting for plaques to appear.
4. While waiting for plaques to appear, soak nitrocellulose filters (one for each dish) in 10–20 m*M* IPTG. A total of 40 IPTG filters are needed for 20 dishes. Label each filter specifying number and antibody (s*ee* **Note 9**).

5. As soon as plaques are visible, overlay dry IPTG filters upon the forming plaques (one per dish) (*see* **Note 10**). Mark the orientation of the IPTG filter so that once the filter is removed, positive plaques can be traced back to the correct position on the agar plate. Also, label the plate with the same number as on the filter. These are the first set of filters for the screen.
6. Place the plates back into the incubator, but lower the temperature to 37°C. Incubate at 37°C for 4 h.
7. Carefully remove the IPTG filters from the agar plate and place on Whatman 3MM paper to dry. When lifting the filter from the plate, be careful not to disturb the bacterial lawn. Place the second set of IPTG filters on the plates. Match the number of the plate with the filter number and, again, mark the orientation of the filter upon the agar.
8. Incubate the plates (with the second set of IPTG filters) at 37°C for 4 h (*see* **Note 11**).
9. Again, carefully remove the second set of IPTG filters and dry on Whatman 3MM paper. Parafilm the lid of the agar dish to the base and store at 4°C until ready to select out positive plaques.

3.2.2. Antibody Screening Filters with Pan Kinesin Antibodies

1. Let IPTG filters that have been incubated with the phage dry for at least 30 min before processing for kinesin-positive plaques. Wash filters in TBS (pH 8.0) with gentle shaking. Because there are two sets of filters (one for each antisera), wash the sets in separate containers in which they will remain for the course of the antibody processing. The wash solution will turn yellow as bacteria are being cleaned from the filters. Continue to change the wash solution until it no longer changes color.
2. Remove the wash solution and incubate filters for 1 h with blocking solution with agitation. After the block, thoroughly wash the filters again with TBS to remove any residual blocking solution.
3. Incubate the filters with the pan kinesin antisera diluted in TBS (pH 8.0) with agitation. To help reduce crossreactivity with negative plaques, incubate at a low concentration of antibody (*see* **Note 12**) for a long period of time (approx 6–8 h at room temperature). Use at least 5 mL per 132-mm filter. After primary antibody incubation, collect the antibody solution and filter through a 0.22-µm filter to be used again (*see* **Note 3**).
4. Wash filters with TBS (pH 8.0). Because there may be 20 filters that are being processed in one container, it is important to wash extensively with TBS so that any residual primary antibody is removed. We wash for a total of 1 h, changing the TBS solution four times.
5. Incubate filters with alkaline phosphatase-conjugated anti-rabbit secondary, 1:2000 in TBS (pH 8.0). Because a low concentration of primary antibody was used, incubate in secondary antibody for a long time (approx 4 h at room temperature).

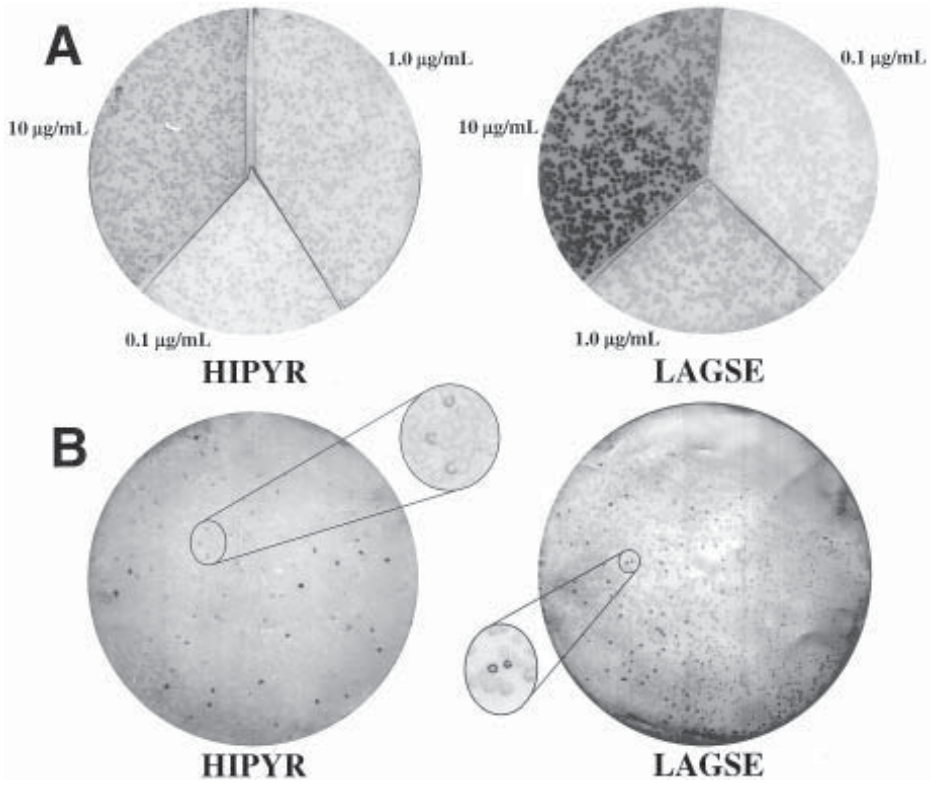

Fig. 4. Examples of HIPYR and LAGSE antibody labeling in a C2C12 λZAP expression library. **(A)** Three concentrations of each antisera, 0.1, 1.0, and 10 µg/mL, were tested to determine at what concentration to use the antibodies for the screen. The LAGSE antisera crossreacts with a bacterial protein(s) as seen by the dark labeling at 10 µg/mL. **(B)** Examples of HIPYR (1.0 µg/mL) and LAGSE (0.1 µg/mL) positive plaques. Positive plaques are darker in comparison to the neighboring, nonpositive plaques.

6. Wash filters with TBS for 1 h, changing solution four times. Develop filters by BCIP/NBT ***(21)*** until background plaques are visible. Dry filters on Whatman 3MM paper. While drying, circle the positive plaques and make special note of those plaques that are positive with both antisera (*see* **Note 13** and **Fig. 4B**).

3.2.3. Purification of Positive Plaques

1. Each positive plaque needs to be purified away from the neighboring, nonpositive plaques. This is done by excising the small bit of agar that surrounds and includes the positive plaque (*see* **Note 14**). Place the agar plug into a microfuge tube containing 1 mL of SM buffer plus 40 µL chloroform. Do this separately for each positive plaque.

2. Rotate the microfuge tube containing the agar plug overnight at 4°C so that the phage is leached from the agar.
3. Replate the phage from each microfuge tube (protocol same as in **Subheading 3.2.1.**) on 10 cm agar plates with 3–5 mL of top agarose. Remember that each tube will have to be re-titrated. Use 82-mm nitrocellulose filters. Process filters as in **Subheading 3.2.2**.
4. Repeat this process until a pure, positive plaque is isolated.

Our lab has used this protocol to clone kinesin-related proteins from two λZAP libraries. One of the libraries was made from the mouse myoblast cell line, C2C12. In order to focus our search for kinesin-related proteins that may be participating in the assembly of the developing myofibril, the C2C12 library was made from cells that had just begun to differentiate and assemble sarcomeres. From the C2C12 screen, 18 double-positive clones were purified. The DNA was extracted and excised, and the 3' and 5' ends of the clone were sequenced. Eleven of the clones matched the sequence for conventional KHC. Five of the clones were the kinesin-related protein KIF3A, and one of the clones was the kinesin-related protein KIF3B. Finally, there was one novel clone that was purified. DNA sequence fragments from both ends of the clone matched no known sequence in the databases. The size of the insert was determined by restriction digests and was shown to be unusually long. To determine if this was indeed a novel kinesin, the clone was sequenced using degenerate primers to both the FAYGQT and LAGSE regions (regions I and III, **Fig. 1**). No sequence was generated from these attempts, indicating that hybridization of the primers to the DNA did not occur. After sequencing further into the clone and not finding any matches to kinesin-related proteins, it was assumed that this clone was not a protein of that family. Finally, it is important to point out that along with the 18 double-positive clones, there were approximately another 60 clones that crossreacted with only one of the pan kinesin antisera. These clones have not been sequenced, but some could represent members of the kinesin family that are divergent in one of the conserved regions used to produce the pan-specific antibodies.

Figure 5 summarizes the results of a screen of 600,000 plaques of a λ Uni-Zap CHO-K1 library (Stratagene). The library was screened with anti-LAGSE because that antisera exhibited crossreactivty with kinetochores in mitotic CHO cells ***(12)***. Seventeen positive clones were isolated and plaque purified as described earlier. The excised plasmids were digested with a combination of restriction enzymes that would cut out the cloned fragment and cut at least once within the cloned fragment but would not cut the pBluescript II vector. The DNA digests were run on a 0.8% DNA gel and blotted onto nitrocellulose by capillary action. The blot was probed as described in Sambrook et al. ***(22)*** with a T4 kinase, ^{32}P-labeled 100,000-fold degenerate LVDLAGSE primer at

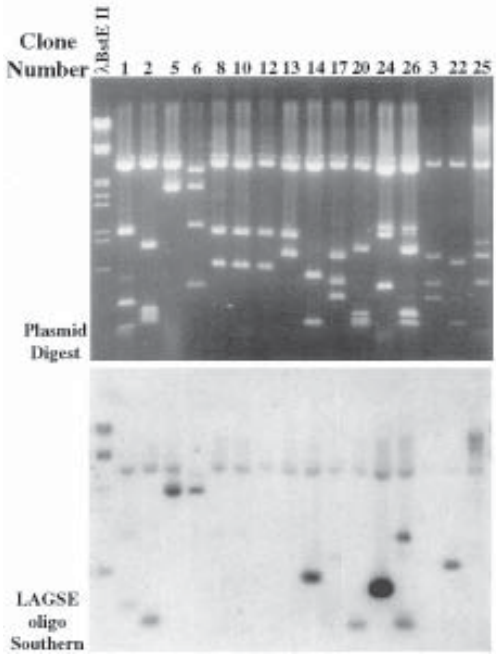

Final Sequencing Data	Peptide-sera Crossreactivity HYPIR	LAGSE
1-PI transfer protein (PI)	-	+++
2-Kinesin-related (22)	+++	++
5-Kinesin-related	++	++
6-Kinesin-related	++	++
8-PI	-	+++
10-PI	-	+++
12-PI	-	+++
13-Not kinesin-related	-	+
14-Kinesin-related	++	++
17-DNA binding protein B	-	+
20-Kinesin-related (26)	+++	++
24-Kinesin heavy chain	++	+
26-Kinesin-related (20)	+++	++
3-DNA binding protein B	-	+
22-Kinesin-related (2)	+++	++
25-DNA binding protein A	-	+

Fig. 5. Analysis of positive clones isolated from an anti-LAGSE screen of a CHO cDNA library. **Top left:** *Eco*R1/*Xho*1/*Sty*1 triple digest of positive excised plasmids. **Bottom left:** A Southern blot of the same DNA gel probed with a ^{32}P-labeled degenerate LAGSE oligo. The ultimate identity of the clones is verified by DNA sequencing and the crossreactivity of the purified plaques with both anti-HYPIR and anti-LAGSE antibodies. Only kinesin-related proteins showed some degree of crossreactivity with both antisera and also hybridized to the degenerate LAGSE oligo.

very low stringency. Certain clones exhibited a tendency to hybridize to the oligo. Subsequent sequence data revealed that the clones that hybridized to the degenerate oligo were almost exclusively kinesin-related proteins. Furthermore, the extent of crossreactivity of the purified plaques identified in the anti-LASGE screen was tested with both anti-HIPYR and anti-LAGSE antibodies. Those plaques that did not crossreact with anti-HIPYR, even if they exhibited extremely strong anti-LAGSE crossreactivity, were not kinesin-related proteins. Hence, kinesin-related proteins exhibited some degree of crossreactivity with both anti-HIPYR and anti-LAGSE and reflected homology with DNA sequences derived from conserved regions of the kinesin motor domain.

In conclusion, a careful screen of a unidirectional cDNA CHO-K1 expression library with anti-LAGSE antibodies resulted in a number of clones in which approx 50% of the clones were kinesin-related proteins. There are sev-

eral methods one can use to partially characterize the clones prior to DNA sequencing, not the least of which is confirming crossreactivity with both antikinesin peptide antibodies. However, the increasing ease of automated DNA sequencing combined with the ever-growing number of DNA sequences in the databases makes it feasible to classify newly isolated positive clones with only one DNA sequencing run. Expression cloning with pan-kinesin antibodies is a reasonable alternative to PCR-based mass cloning efforts. This technique has the advantage that if the quality of the library is high, long clones can be obtained. The disadvantage is that expression screening is more labor intensive than PCR screens, and for this reason, it is generally not practical to attempt this more than once.

4. Notes

1. Most of our secondary antibodies are purchased from Jackson ImmunoResearch Labs (West Grove, PA). When receiving the antibody, the protein is reconstituted as directed in the packing material. Unwanted debris is removed with centrifugation at 10,000*g* for 10 min. Aliquots of the secondary antibody are stored in 50% glycerol at –20°C. Enzyme-conjugated secondary antibodies for immunoblotting are used at 1:2000 in TBS (pH 8.0). Fluorophore-conjugated secondary antibodies for immunofluorescence are used at 1:25 to 1:100 in AbDIL (*see* **Subheading 2.1.2.**, **step 6**).
2. Preparation of crude lysates from tissue culture cells: For each time-point, remove cultured cells from a 10-cm tissue culture dish with 1 mL PBS + 5 m*M* ETDA. We find that two to three dishes of the mouse myoblast cell line, C2C12, yield a manageable cell pellet. Pellet cells by centrifugation at 1000 rpm for 5 min, wash one time with PBS, and repellet. Resuspend the pelleted cells in 25–50 µL of 2% SDS, depending on the pellet size. Incubate the resuspended cells in boiling water for 10 min, and cool on ice. Lysates can be passed through a 20-gage, and then 26-gage, needle to help sheer the DNA. Spin the lysate at 10,000*g* for 10 min at 4°C to remove unwanted debris and determine a crude protein concentration of the lysate with an A280 reading (OD 1 = approx 1 mg/mL protein). Dilute lysates 1:1 with final sample buffer minus the usual SDS (100 m*M* DTT, 60 m*M* Tris-HCl [pH 6.8], 0.01% bromophenol blue). The samples are now ready to load on the gel. When trying to assess the presence of kinesin-related proteins in your system, it is important to remember that detection is limited by the level of protein expression. It is useful to test the crude cell lysate over a range of protein concentrations when first starting this process. We found that 0.1 mg of the cell lysate gave a strong signal in our cells.
3. Primary antibodies are often fairly precious. After using the primary antibody (in our case, anti-HIPYR and anti-LAGSE) for Western blot analysis, the antibody-containing solution is sterilized through a 0.22-µm syringe filter and stored at 4°C. The solution can then be reused a number of times, filtering after each use. Often, mild crossreactivity of an antibody is progressively reduced with this pro-

cedure; however, if it seems as though the detectability is decreasing after multiple uses, discard that solution, and redilute more primary antibody.

4. Use of the small, 12-mm glass coverslips helps to conserve antibody. Many times, tissue culture cells (especially from primary cultures) behave differently on glass surfaces in comparison to tissue culture plastic. To avoid this, it may be necessary to first coat glass coverslips with pure extracellular matrix proteins (e.g., collagen, laminin) that may simulate the in vivo matrix environment. Alternatively, the coverslips may be coated with a cell and tissue adhesive material. We have used and had success with Cell-Tak (Collaborative Biomedicals/Becton Dickinson Labware), Matrigel (Becton Dickinson Labware), and ProNectin F recombinant attachment factor (Stratagene).
5. In **Fig. 3**, it appears as though the HIPYR antibody staining is more prominent than that of the LAGSE antibody. This is more a result of the imaging of these cells than actual levels of protein expression. In **Fig. 3A**, the camera's light detector was positioned on the accumulation of the putative kinesin proteins. Because this region was obviously brighter than the rest of the cell, the exposure time was shorter than that used when imaging the HIPYR antibody. This prevents overexposure of the film and allows proper imaging of the region that was selected (the putative kinesin accumulation).
6. After resuspending the pelleted bacteria in one-half the volume with sterile 10 m*M* $MgSO_4$, the cells can be stored at 4°C for up to 48 h. After that time, the cells should be discarded.
7. Do not exceed 300 µL of diluted phage in SM buffer per 600 µL of bacteria.
8. Refrigerating the bacteria and phage for 10 min before warming to 37°C helps to give the phage some extra time to attach to the host bacteria for a more efficient infection.
9. Slowly submerge the nitrocellulose filters into the IPTG solution, starting with one edge. After the filter is properly wet, remove with forceps, and touch the edge to some plastic wrap to help shake off excess liquid. Place wet filters on clean Whatman 3MM paper to dry. Mark the filters by numbering with a pencil or permanent waterproof marker. Because, in the end, there will be two IPTG filters for each plate, it is important to label each filter with a number and antibody. For example, if there are 20 plates, and both the LAGSE and HIPYR antisera will be used, label the filters L1–L20 and H1–H20. If there are excess IPTG filters, they can be stored at –20°C. Store filters between sheets of plastic wrap and enclose within foil. When using stored filters, bring to room temperature before placing on agar. Be aware that these filters are slightly harder to manipulate.
10. To properly place the IPTG filters upon the agar plates, hold opposite edges of the filter with gloved hands (or forceps) and bend in the middle. Place the bent region of the filter upon the agar (in the middle of the plate) and slowly lay down the sides. As the filter makes contact with the agar, allow it to become wet. Avoid air bubbles.
11. It is already a long day before the incubation with the second set of IPTG filters can begin. Therefore, instead of placing these plates in the 37°C incubator for an additional 4 h, they can be left on the benchtop overnight. Incubating the plates at

room temperature does not seem to inhibit protein expression. Alternatively, if the plates are kept at 37°C overnight, the plaques will become too large. Ideally, after the second incubation, the plaques should not be touching each other (just barely touching is acceptable). If this occurs, the phage have been plated too densely, often making it more difficult to recognize and isolate positive plaques. When the plaques first appear, assess how closely they are spaced, and vary the incubation times accordingly; however, do not incubate the IPTG filters at 37°C for less than 2 h.

12. Before beginning the primary antibody incubation, it is very important to first determine at what concentration the antibodies will be used. An antibody screen of a expression library is essentially a Western blot. The phage-incubated IPTG filters are first incubated with a primary antibody followed by incubation with an enzyme-conjugated secondary antibody. Those plaques (proteins) that crossreact with the primary antibody are then visualized. It is important that a colorimetric detection system (e.g., alkaline phosphatase) rather than a photochemical system (e.g., ECL, Amersham, UK) is used to visualize the positive plaques. When trying to determine if a plaque is truly positive, the color of the plaque will be judged in comparison to background staining of neighboring plaques. It is much easier to make this judgement with a colorimetric detection system. The concentration of the primary antibody should be picked by determining what concentration of antibody gives a low, yet visible background staining on nonpositive plaques. This step can be tricky because occasionally an antibody can crossreact with bacterial proteins also contained within the plaques. In those cases, the antibody concentration needs to be titrated so that positive plaques are visible over bacterial protein crossreactivity. **Figure 4A** demonstrates how the LAGSE and HIPYR antisera were tested for three different concentrations on phage-incubated, IPTG filters. Each antisera was tested at 0.1, 1.0, and 10 µg/mL diluted in AbDIL. The LAGSE antisera does crossreact with a bacterial protein(s), as visible by the dark staining at 10 µg/mL. From this concentration test, we decided to use the HIPYR antisera at 1.0 µg/mL and the LAGSE antibody at 0.1 µg/mL.
13. **Figure 4B** demonstrates how positive plaques appear. Sometimes, it is useful to look at a possible, positive plaque under high magnification (with a dissection scope) to help determine its authenticity.
14. An easy method of excising positive plaques is by using a plastic, transfer pipet (no need to be sterile) that has had the tip removed with a razor, making the hole slightly larger. The hole should be large enough to accurately include the positive plaque when excising the agar, yet still small so to minimize carrying over too many nonpositive plaques. Place the developed filter circle on a light box and carefully arrange the agar plate from which the paper was lifted upon it so that both are in the same orientation. Locate the positive plaques on the agar dish and press the end of the transfer pipet into the agar until it touches the bottom of the Petri dish. Carefully remove the pipet so that the agar plug remains inside its end, and squirt the plug into a 1.7-mL microfuge tube. Be sure to use a different transfer pipet for each positive plaque.

Acknowledgments

This work was supported by an American Heart Association Grant-in-Aid (9650028N) and a Shannon Award (AR44346A) from the National Institutes of Health to L. W., and PHS-NRSA T32GM07270 to L.M.G.

References

1. Moore, J. D. and Endow, S. A. (1996) Kinesin proteins: a phylum of motors for microtubule-based motility. *Bioessays* **18**, 207–219.
2. Hirokawa, N. (1998) Kinesin and dynein superfamily proteins and the mechanism of organelle transport. *Science* **279**, 519–526.
3. Vale, R. D. (1996) Switches, latches, and amplifiers: common themes of G proteins and molecular motors. *J. Cell Biol.* **135**, 291–302.
4. Brown, C. D., Barnes, K., and Turner, A. J. (1998) Anti-peptide antibodies specific to rat endothelin-converting enzyme-1 isoforms reveal isoform localisation and expression. *FEBS Lett.* **424**, 183–187.
5. Field, C. M., Oegema, K., Zheng, Y., Mitchison, T. J., and Walczak, C. E. (1998) Purification of cytoskeletal proteins using peptide antibodies. *Methods Enzymol.* **298**, 525–541.
6. Blotnick, E., Miller, C., Groschel-Stewart, U., and Muhlrad, A. (1995) Immunochemical probing of the functional role of the 238–246 and 567–574 sequences of myosin heavy chain. *Eur. J. Biochem.* **232**, 235–240.
7. Monaghan, P., Clarke, C., Perusinghe, N. P., Moss, D. W., Chen, X. Y., and Evans, W. H. (1996) Gap junction distribution and connexin expression in human breast. *Exp. Cell. Res.* **223**, 29–38.
8. Cole, D. G., Cande, W. Z., Baskin, R. J., Skoufias, D. A., Hogan, C. J., and Scholey, J. M. (1992) Isolation of a sea urchin egg kinesin-related protein using peptide antibodies. *J. Cell Sci.* **101**, 291–301.
9. Wordeman, L. and Mitchison, T. J. (1995) Identification and partial characterization of mitotic centromere-associated kinesin, a kinesin-related protein that associates with centromeres during mitosis [see comments]. *J. Cell Biol.* **128**, 95–104.
10. Sablin, E. P., Kull, F. J., Cooke, R., Vale, R. D., and Fletterick, R. J. (1996) Crystal structure of the motor domain of the kinesin-related motor ncd [see comments]. *Nature* **380**, 555–559.
11. Kull, F. J., Sablin, E. P., Lau, R., Fletterick, R. J., and Vale, R. D. (1996) Crystal structure of the kinesin motor domain reveals a structural similarity to myosin [see comments]. *Nature* **380**, 550–555.
12. Sawin, K. E., Mitchison, T. J., and Wordeman, L. G. (1992) Evidence for kinesin-related proteins in the mitotic apparatus using peptide antibodies. *J. Cell Sci.* **101**, 303–313.
13. Yang, J. T., Saxton, W. M., and Goldstein, L. S. (1988) Isolation and characterization of the gene encoding the heavy chain of Drosophila kinesin. *Proc. Natl. Acad. Sci. USA* **85**, 1864–1868.
14. Meluh, P. B. and Rose, M. D. (1990) KAR3, a kinesin-related gene required for yeast nuclear fusion. *Cell* **60**, 1029–1041; erratum: *Cell* **61(3),** 548.

15. Enos, A. P. and Morris, N. R. (1990) Mutation of a gene that encodes a kinesin-like protein blocks nuclear division in A. nidulans. *Cell* **60**, 1019–1027.
16. McDonald, H. B. and Goldstein, L. S. (1990) Identification and characterization of a gene encoding a kinesin-like protein in Drosophila. *Cell* **61**, 991–1000.
17. Endow, S. A., Henikoff, S., and Soler-Niedziela, L. (1990) Mediation of meiotic and early mitotic chromosome segregation in Drosophila by a protein related to kinesin [see comments]. *Nature* **345**, 81–83.
18. Hagan, I. and Yanagida, M. (1990) Novel potential mitotic motor protein encoded by the fission yeast cut7+ gene. *Nature* **347**, 563–566.
19. Woehlke, G., Ruby, A. K., Hart, C. L., Ly, B., Hom-Booher, N., and Vale, R. D. (1997) Microtubule interaction site of the kinesin motor. *Cell* **90**, 207–216.
20. Vale, R. D. and Fletterick, R. J. (1997) The design plan of kinesin motors. *Annu. Rev. Cell Dev. Biol.* **13**, 745–77.
21. Lane, D. and Harlow, E. (1988) *Antibodies: A Laboratory Manual*. Cold Spring Harbor Laboratory, Cold Spring Harbor, NY.
22. Sambrook, J., Maniatis, T., and Fritsch, E. F. (1989) *Molecular Cloning: A Laboratory Manual*. Cold Spring Harbor Laboratory, Cold Spring Harbor, NY.
23. Vallee, R. B. and Collins, C. A. (1986) Purification of microtubules and microtubule-associated proteins from sea urchin eggs and cultured mammalian cells using Taxol, and use of exogenous Taxol-stabilized brain microtubules for purifying microtubule-associated proteins. *Methods Enzymol.* **134**, 116–127.

4

Expression of Kinesin in *Escherichia coli*

Maryanne F. Stock and David D. Hackney

1. Introduction

Kinesin can generally be expressed to high levels in *Escherichia coli* and this provides an excellent means for obtaining significant amounts of purified constructs. For detailed work, it is essential to have a native construct uncompromised by extraneous tags, and this can readily be obtained. *See* **refs. *1–3*** for examples of vector construction using the T7 RNA polymerase system.

Kinesin head domains bind tightly to phosphocellulose even though they do not have a large net positive charge at neutral pH (predicted pI for *Drosophila* kinesin DKH340 and DKH346 are 7.4 and 6.3). This may represent a nonspecific analogy to the interaction of the head domains with the extensive negative surface charge on the outside surface of the microtuble (MT). This tight affinity for phosphocellulose makes chromatography on phosphocellulose a useful initial step that recovers kinesin in high yield and purification from crude extracts. Kinesin heads also bind to positively charged surfaces and the combination of chromatography on phosphocellulose and DEAE resins provides sufficient purification for most purposes. The protocol presented here is derived from the original purification of kinesin from bovine brain by Kuznetsov and Gelfand ***(4)*** (*see* Chapter 1), except that the phosphocellulose step is done first. Because of the tight binding of kinesin to phosphocellulose, quantitative adsorption is more easily obtained from lysis buffers of high ionic strength with phosphocellulose than with DEAE resins.

Constructs that include all or most of the stalk and tail domains are more difficult to purify. The total level of expression is low and essentially all of what is expressed aggregates into insoluble inclusion bodies when expressed at 37°C. Even though total expression is lower, net yields of soluble protein can

From: *Methods in Molecular Biology*, Vol. 164: *Kinesin Protocols*
Edited by: I. Vernos

be increased by expression at <25°C. Because of the low ratio of soluble kinesin to contaminating *E. coli* proteins, purification of long kinesins is considerably more demanding than for isolated head domains. Constructs containing the C-terminal half of the stalk precipitate from the solution at low concentrations of ammonium sulfate and this provides considerable purification in a simple step. The highly asymmetric shape of the extended coiled-coil of long constructs makes gel filtration particularly attractive as they migrate ahead of the majority of *E. coli* proteins.

2. Materials

1. LB media: 10 g tryptone, 5 g yeast extract, and 5 g NaCl per liter. Autoclave to sterilize.
2. Lysis buffer: 50 m*M* Bicine/NaOH (pH 8.1), 4 m*M* $MgCl_2$, 0.4 m*M* EDTA, and 5 m*M* mercaptoethanol.
3. MgM buffer: 20 m*M* 3-(N-Morpholine) propanesulforic acid (Mops)/NaOH (pH 7.0), 2 m*M* $MgCl_2$, 0.1 m*M* EDTA, and 0.01% (v/v) m*M* mercaptoethanol.
4. 50MgM: MgM buffer supplemented with 50 m*M* NaCl.
5. MgKA buffer: 50 m*M* imidazole/HCl (pH 6.7), 2 m*M* $MgCl_2$, 0.05 m*M* EDTA, and 0.01% (v/v) m*M* mercaptoethanol.
6. A25 buffer: 25 m*M* N-(2-acetamide)-2-aminoethanesulfonic acid (ACES)/KOH (pH 6.9); 2 m*M* magnesium acetate, 2 m*M* EGTA, 0.1 m*M* EDTA, and 0.01% (v/v) m*M* mercaptoethanol.
7. Phenylmethylsulfonyl fluoride (PMSF), saturated solution in 95% ethanol (*see* **Note 1**).
8. Pepstatin: 1 mg/mL in methanol.
9. Leupeptin: 2.5 mg/mL in A25 buffer with extra NaOH to approx pH 7.5.
11. ATP: disodium salt.
12. Isopropyl β-D-thiogalactopyranoside (IPTG): 0.5 *M* in water and sterilized by filtration.
13. Lysozyme.
14. Phosphocellulose: P11 (Whatman) (*see* **Note 2**).
15. DEAE resin: DEAE BioGel (Bio-Rad).
16. Sonifier: Branson model 450 with wide tip.

3. Methods

Except as indicated, all operations are performed at 0–4°C and all solutions are supplemented with ATP to ≥ 0.1 m*M* (*see* **Note 3**).

3.1. Expression of Constructs

1. A 200-mL culture is grown overnight at 37°C in LB media with vigorous shaking and used to inoculate 1.8 L of fresh media in a 4-L flask. The diluted cells are then grown for an additional 1.5 h at 37°C.

2. IPTG is added to 0.05 m*M* to induce expression of the recombinant protein and the cells are shaken for an additional 4–6 h at 37°C.
3. The cells are chilled on ice and collected by centrifugation for 6 min at 6000*g* (6000 rpm in Sorvall GS3 rotor) (*see* **Note 4**).
4. The pelleted cells are stored frozen in the centrifuge bottles (*see* **Note 5**).

3.2. Alternate Expression for Proteins with Limited Solubility

Most long kinesin constructs, as well as many constructs of other proteins, are largely insoluble when expressed at 37°C. Methods to evaluate solubility are given below. If this is a problem, then the yield of soluble protein can usually be increased by induction at a lower temperature.

1. Perform growth of cells as in **Subheading 3.1.**, **step 1.**
2. Chill the cells briefly in wet ice to lower the temperature below 20°C before the addition of IPTG.
3. Continue induction by shaking at approx 22°C.

3.3. Lysis and Initial Purification on P11

1. Frozen cells from 12 L of culture are thawed and resuspended in 400 mL of cold lysis buffer.
2. Gently stir the cells with a magnetic stirrer and add 0.15 mL leupeptin, 0.3 mL pepstatin, 0.2 mL PMSF, 0.1 g ATP, and 0.1 g lysozyme. Incubate for 10–15 min on ice (*see* **Note 1**).
3. Sonify cells to complete lysis and to fragment DNA. During the sonfication process, add an additional 0.1 g ATP and 0.2 mL PMSF (*see* **Note 6**).
4. Centrifuge (25,000*g* for 15 min) and discard pellet. Save a sample for sodium dodecyl sulfate-polyacrylamide gel electrophoresis (SDS-PAGE) before and after centrifugation to determine the extent of lysis.
5. Add 18 mL packed P11 to the supernatant and stir for 10 min. Filter on a 12.5-cm Buchner funnel with #1 filter paper. Save a sample of the filtrate for SDS-PAGE. Do not let the filter cake go dry. Rinse on the filter with 50MgM buffer (*see* **Note 7**).
6. Resuspend washed P11 in 50MgM and load onto a 2.5 × 10-cm column. Rinse the column with 50 mL of 50MgM.
7. Elute the kinesin with 450 m*M* NaCl in MgM buffer. Collect 4-mL fractions and pool the peak of the protein (*see* **Note 8**).
8. Evaluate the extent of lysis and binding to P11 by SDS-PAGE. Load samples of the crude extract, the clarified supernatant, and the P11 filtrate. If lysis is complete, the majority of the bands in the crude extract and clarified supernatant will be of the same intensity. Formation of inclusion bodies is indicated by a selective decrease in the level of the expressed protein following centrifugation. Binding of the expressed protein to P11 is indicated by its selective depletion in the filtrate compared to the clarified supernatant (*see* **Note 9**)

3.4. Further Purification of Short Constructs

1. The P11 fraction from **Subheading 3.3.**, **step 7** is dialyzed overnight versus 1 L of MgKA buffer.
2. The dialysate is diluted with an equal volume of water and clarified by centrifugation (25,000*g* for 15 min).
3. The supernatant is loaded onto a 1.5 × 27-cm column of DEAE BioGel equilibrated with MgKA buffer. The column is washed with approx 30 mL of MgKA and then eluted with a gradient of 0–125 m*M* NaCl in MgKA (100 × 100 mL with 4-mL fractions). The fractions are analyzed by SDS-PAGE to locate the peak of kinesin and evaluate the purity (*see* **Note 10**).
4. The kinesin pool is concentrated by loading on a 1 × 3-cm column of P11. Kinesin is eluted with a step to 800 m*M* NaCl in A25 buffer. Fractions of 0.5 mL are collected and the peak is pooled.

3.5. Further Purification of Long Constructs

1. Ammonium sulfate is added with stirring to the P11 fraction from **Subheading 3.3.**, **step 7** to a total of 0.23 g per gram of original solution. The precipitated protein is collected by centrifugation (25,000*g* for 15 min), the pellet is drained well and then dissolved in minimal MgM buffer with 1 *M* NaCl (≤ 1 mL).
2. The kinesin is chromatographed on a 1.5 × 45-cm column of BioGel A5 m in MgM buffer with 1 *M* NaCl and the peak fractions are pooled.
3. The kinesin can be concentrated and further purified by batch elution from a small DEAE BioGel column. The pool from gel filtration is dialyzed versus MgKA buffer, loaded onto a 1 × 3-cm DEAE column, and eluted with a step gradient to 150 m*M* NaCl. (*see* **Notes 10** and **11**).

3.6. Storage

Both long and short constructs are conveniently stored at –80°C following dialysis against A25 buffer with 50 m*M* KCl, 50% glycerol, and 2 m*M* dithiothreitol (DTT).

4. Notes

1. Phenylmethanesulonyl fluoride is highly toxic and appropriate care should be exercised. To minimize exposure of personnel and to minimize exposure of the main PMSF stock to moisture, it is convenient to aliquot approx 200 mg solid PMSF into 5-mL glass test tubes and store sealed at –20°C. Immediately before use, add 2 mL of 95% ethanol to one tube and mix to make a saturated solution. PMSF is hydrolyzed in buffers over the course of hours, or faster. Thus, diluted solutions represent a greater hazard when fresh. To hydrolyze PMSF in any unused stock solution, add an excess of KOH in methanol.
2. To prepare P11, suspend in cold 0.5 N NaOH and filter wash on filter with 0.5 *N* NaOH. Repeat wash with more NaOH, but include 0.5% (v/v) Triton X-100.

Rinse the filter cake with deionized water to remove excess NaOH and then wash twice as above by resuspension with cold 0.5 *N* HCl. Rinse the filter cake with deionized water to remove excess HCl and then resuspend in MgKA buffer and add sufficient NaOH to bring the pH to approx 7.0. Refilter and resuspend in MgKA buffer. For long-term storage, add sodium azide to 0.02% (w/v), with appropriate care for toxicity of sodium azide. Used P11 can also be recycled by this procedure.

3. Kinesin is unstable in the absence of a nucleotide ***(1)***. Even transient exposure to solutions without significant ATP or ADP can result in decreased specific activity.
4. To reduce the number of centrifuge bottles, additional culture can be repelleted in the same bottles after discarding the supernatants.
5. Cells that have never been frozen do not lyze as readily as a frozen cell. Consequently, it is recommended to subject the cells to a freeze–thaw cycle even if they will be used without storage.
6. Cell suspension should be in a glass beaker and the beaker should be in a slurry of wet ice for good heat transfer. Sonify in 30-s pulses with continuous stirring and allow ≥ 30 s between pulses for heat exchange. Generally, about 4 × 30 s at full power is sufficient to reduce the viscosity produced by the released DNA, but this will vary considerably depending on the exact power output of the sonifier.
7. Pour a 2.5 × 10-cm column of P11 in MgM buffer with 50 m*M* NaCl and then empty the contents of this column into the supernatant. After filtration, this will yield the correct amount of P11 to refill this column.
8. Although all constructs containing the head domain bind tightly to P11, different constructs elute at somewhat different salt concentrations. A 50- to 450-m*M* step will give good recovery and a level of purification that is generally sufficient when combined with the subsequent steps. Additional purification can be obtained by the use of a salt gradient or step concentrations that are optimized for a particular construct. Gradient elution will require the use of SDS-PAGE for localization of the peak of kinesin.
9. For staining with Coomassie Blue R , 10 µL of a 1/10 dilution is appropriate.
10. Used DEAE BioGel columns can be reused if carefully stripped of adsorbed proteins. The column should be extensively washed in MgKA buffer with 1 *M* NaCl and then shifted to room temperature and washed with the same buffer containing 0.1% SDS (w/v) and 0.02% sodium azide. After washing, the column is stored at 4°C in the buffer containing SDS. Under some circumstances, the SDS will precipitate in the cold. Thus, to reuse the column, return it to room temperature and wash with buffer in the absence of SDS. As a final step to totally purge SDS, pass a solution of bovine serum albumin in 1 *M* NaCl through the column before equilibration with the final buffer for chromatography.
11. Some long kinesin constructs tend to aggregate at low ionic strength. To avoid extensive precipitation, do not dialyze concentrated solutions. In some cases, it may also be necessary to have some salt in the dialysis solution.

Acknowledgments

This work was supported by grant NS28562 from the National Institutes of Health.

References

1. Huang, T.-G. and Hackney, D. D. (1994) Drosophila kinesin minimal motor domain expressed in Escherichia coli. Purification and kinetic characterization. *J. Biol. Chem*. **269**, 16,493–16,501.
2. Jiang, W., Stock, M., Li, X., and Hackney, D. D. (1997) Influence of the kinesin neck domain on dimerization and ATPase kinetics. *J. Biol. Chem*. **272**, 7626–7632.
3. Stock, M. F., Guerrero, J., Cobb, B., Eggers, C. T., Huang, T.-G., Li, X., and Hackney, D. D. (1999) Formation of the compact conformer of kinesin requires a C-terminal heavy chain domain and inhibits microtubule-stimulated ATPase activity. *J. Biol. Chem*. **274**, 14,617–14,623.
4. Kuznetsov, S. A. and Gelfand, V. I. (1986) Bovine brain kinesin is a microtubule-activated ATPase. *Proc. Natl. Acad. Sci. USA* **83**, 8530–8534.

5

Plasmids for Expression of Chimeric and Truncated Kinesin Proteins

Kimberly W. Waligora and Sharyn A. Endow

1. Introduction

The construction of mutant or chimeric proteins enables researchers to identify regions of a protein that are involved in a particular function. The technique of overlap polymerase chain reaction (PCR) ***(1)*** allows one to make a number of mutants in a timely fashion.

In the field of motor proteins (specifically kinesin ***[2]*** and ncd ***[3,4]***), a number of researchers are trying to identify the regions of the proteins that are responsible for the determination of polarity ***(5–7)***. In this chapter, we describe the techniques we use to construct various mutant or chimeric proteins. In addition, we briefly explain the protocols we use to determine optimal protein expression, preparation of motor protein lysates, and how we ultimately assay for motor polarity.

2. Materials

2.1. Plasmid Construction

1. Oligonucleotides for PCR are designed so that they either contain a unique restriction site or are adjacent to an internal site. The oligonucleotides we use are synthesized by the Duke University DNA Synthesis Facility.
2. Vent polymerase (New England Biolabs, Beverly, MA).
3. 10X ThermoPol buffer: [1X = 10 m*M* KCl, 20 m*M* Tris-HCl (pH 8.8), 10 m*M* $(NH_4)_2SO_4$, 2 m*M* $MgSO_4$, 0.1% Triton X-100], and 100 m*M* $MgSO_4$ (New England Biolabs, Beverly, MA).
4. Nucleotides: 25 m*M* dNTP mix diluted to 1.25-m*M* stock (Stratagene, La Jolla, CA).
5. Qiagen QIAEX II gel extraction kit (Santa Clarita, CA) to purify PCR fragments from agarose gel slices.
6. Transformations are done by the standard $CaCl_2$ protocol ***(8)***.

From: *Methods in Molecular Biology*, Vol. 164: *Kinesin Protocols*
Edited by: I. Vernos

7. Luria Broth (LB): 10 g bactotryptone, 5 g yeast extract, 10 g NaCl per L of H_2O is used to grow overnight cultures of wild-type and mutant clones for selection and characterization of chimeric plasmids.
8. Plasmid preps for PCR and sequencing are prepared using the Qiagen plasmid QIA prep spin and plasmid mini kits (Santa Clarita, CA), respectively.
9. Double-stranded DNA sequencing is performed manually using the Sanger method ***(9)***. Sequenase, DNA polymerase termination mixes, and ^{35}S-dATP are purchased from Amersham Pharmacia Biotech (Piscataway, NJ).

2.2. Motor Protein Expression

1. M9ZB media: for 1 L, mix 860 mL of ZB (10 g N-Z-amine A, 5 g NaCl per 860 mL), 100 mL 10X M9 salts (1 g NH_4Cl, 3 g KH_2PO_4, 6 g Na_2HPO_4 per 100 mL), 40 mL of 10% glucose, 1 mL of 1 *M* $MgSO_4$, 50 µg/mL ampicillin (stock 50 mg/mL in H_2O), and 5 µg/mL chloramphenicol (stock 25 mg/mL in ethanol).
2. PME buffer: 10 m*M* phosphate buffer (pH 7.4), 1 m*M* EGTA, 1 m*M* $MgCl_2$, is used for washing cells after harvesting.
3. Isopropyl β-D-thiogalactopyranoside (IPTG) (dioxene-free; Amersham Pharmacia Biotech, Piscataway, NJ) is prepared as a 1 *M* stock in H_2O and stored at –20°C.
4. 1X Sodium dodecyl sulfate-polyacrylamide gel electrophoresis (SDS-PAGE) sample buffer: 50 m*M* Tris-HCl (pH 6.8), 2 m*M* EDTA, 1% SDS, 8% (v/v) glycerol, 143 m*M* mercaptoethanol, and 0.01% bromophenol blue.
5. Phenylmethylsulfonyl fluoride (PMSF) is prepared as a 200-m*M* stock in ethanol and stored at –20°C.
6. Protease inhibitor cocktail (200X concentrated): 1 µg/mL leupeptin, 1 µg/mL pepstatin A, 2 µg/mL TAME (Nα-*p*-tosyl-L-arginine methyl ester), and 2 µg/mL aprotinin (all from Sigma Chemical Co., St. Louis, MO).

2.3. Motility Assays

1. PM buffer: 100 m*M* piperazine-*N*,*N'*-*bis*(2-ethanesulfonic acid) (PIPES) (pH 6.9), 2 m*M* EGTA, 1 m*M* $MgCl_2$.
2. Microtubules, PC-purified tubulin ***(10)*** and N-ethylmaleimide (NEM)-modified tubulin ***(11)*** stored at –70° C.
3. Coverslips are cleaned by sonication for 20 min in 10% (w/v) Alconox detergent (Alconox, Inc., New York, NY) in water. They are rinsed three times in water with sonication for 10 min. The cover slips are then rinsed two times with 95% ethanol with sonication and stored in 95% ethanol in an airtight container.
4. VALAP: a mixture of vaseline:lanolin:paraffin (1:1:1) is heated gently until melted, then allowed to solidify and stored covered at room temperature.

3. Methods

3.1. Plasmid Construction

Overlap PCR is the method of choice for us in that it is a fast, simple, and highly efficient way to make the mutants and chimeras we design. This par-

ticular method involves two steps: (1) the amplification of two mutant fragments and (2) the fusing of the mutant fragments to one another by amplification of the overlap fragment, ultimately leading to the mutant or chimeric construct (**Fig. 1A**).

1. The first step is to design the oligonucleotides (which are complementary to each other) so that they contain the mutation or junction we want to make (*see* **Note 1**). In the first step, two reactions are set up. Each reaction uses one flanking primer that hybridizes near one or the other end of the targeted sequence and the mutated oligonucleotide that hybridizes at the site at which the mutation or new junction is to be introduced. By setting up two separate reactions, the two fragments generate an overlap of the two mutated primers. Because of the overlap, the two fragments can be hybridized by denaturing and annealing them in a subsequent reaction.
2. In the second step, these fragments, together with the two initial flanking primers, are used to amplify the full-length sequence that now contains the mutation or new junction (**Fig. 1A**).
3. A typical PCR reaction mixture contains 0.1–100 ng of template DNA, 10 µL 10X ThermoPol buffer, 2 µL of 100 m*M* $MgSO_4$, 16 µL of 1.25 m*M* nucleotide mix, 1 µ*M* of each primer, and 1 U Vent polymerase, and is adjusted to 100 µL with sterile dH_2O. The samples are overlaid with 60 µL of mineral oil (Sigma Chemical Co., St. Louis, MO) and typically subjected to 30 cycles of denaturation (1 min, 98°C), annealing (1 min 30 s, 55°C) and extension (2 min, 72°C) using a Perkin-Elmer Cetus DNA Thermo Cycler.
4. When generating new mutants, overlap PCR is generally the ideal method. However, when we want to add or delete a base or bases near a unique restriction site, a simple one-step PCR is used. Here, only one mutant oligonucleotide is used, keeping in mind that it needs to contain an unique restriction site (**Fig. 1B**).
5. After recovery of plasmids containing the final PCR product, a quick screen is done to see if the plasmids do in fact contain the mutation. A short oligonucleotide of approx 12–15 basepairs is designed so that the last base at the 3' end is the first base of the mutation or new junction. This permits only the mutated PCR fragment to be amplified and thus is an efficient way to screen candidate clones by PCR (**Fig. 1C**) (*see* **Note 1**). The selected plasmids are then grown in 50- to 100-mL cultures of LB containing the selective antibiotic (e.g., ampicillin), at 37°C with shaking. The purified double-stranded DNA is then sequenced to verify that the mutation or junction is correct.

3.2. Motor Protein Expression

1. The mutants or chimeras are transformed into an *E. coli* T7 polymerase expression strain BL21(DE3)pLysS ***(12)*** by the $CaCl_2$ method and plated on LB agar plates containing ampicillin (for selection of the expression plasmid) and chloramphenicol (for selection of the pLysS plasmid).

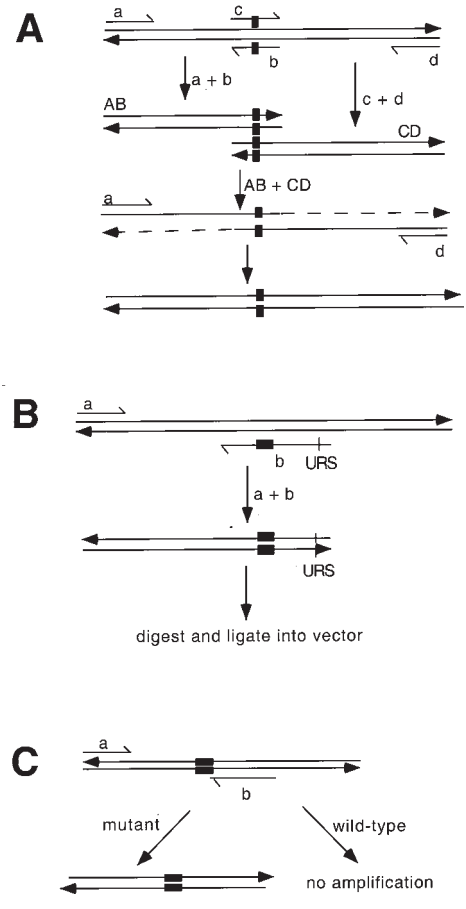

Fig. 1. Schematic illustrations of overlap PCR mutagenesis, single primer mutagenesis and screening by PCR. **(A)** Primers are indicated by lowercase letters (a, b, c, d); PCR products are indicated by uppercase letters (AB, CD); black boxes denote the mutated base. The first step of overlap PCR mutagenesis is to amplify the AB and CD products separately. The AB and CD products are denatured and allowed to anneal to one another, and then amplified by primers a and d, resulting in the final PCR product that contains the mutated base(s). **(B)** Primers are indicated by lowercase letters (a, b). The black box in primer b denotes the presence of a mutation and URS indicates an unique restriction site. After amplification, the PCR product is digested and cloned into an appropriate vector. **(C)** Primers are indicated by lowercase letters (a, b). The 3' end of Primer b ends with the first base of the mutation or new junction. The only PCR products obtained are the mutant products, amplified from colonies containing the mutation or new jucntion. These colonies can be grown in 50- to 100-mL cultures to prepare DNA for sequence analysis.

2. To determine the optimal induction time, a 25-mL culture is grown in M9ZB media overnight with shaking at 22°C. After 10–12 h, when the $OD_{550} = 0.6$, the cultures are induced at 22°C by adding IPTG to 0.4 m*M*. One-milliliter aliquots are taken at $t = 0, 1, 2, 3, 4, 6$ h. The cells are centrifuged and the pellet is resuspended in 100 µL 1X SDS-PAGE sample buffer. The samples are boiled for 2–5 min and 10 µL loaded on a 10% SDS-polyacrylamide gel ***(13)***. Separation of induced protein bands by SDS-PAGE and staining with Coomassie blue allow the determination of the molecular weight of the induced protein and the optimal induction time.
3. Once the optimal induction time n is determined, the procedure is scaled up to 500-mL cultures. One-milliliter aliquots are taken at $t = 0$ and n h and analyzed by SDS-PAGE in order to ensure that the cells are induced and also to check for protein size and presence of any degradation. Cells are harvested and washed with PME buffer + 50 m*M* NaCl + 0.5–1 m*M* PMSF. PMSF is added at this point to protect the induced protein from any protease activity. The pellets are then flash frozen in liquid N_2 and stored at –70°C (*see* **Note 2**).

3.3. Motility Assays

1. In order to assay motility, clarified lysates of the motor proteins need to be prepared. Frozen induced bacterial cell pellets are thawed on ice and resuspended in cold PME buffer + 50 m*M* NaCl containing 1:200 diluted protease inhibitor cocktail. The resuspended pellet is flash frozen in liquid N_2 and quickly thawed at 37°C. Once thawed, PMSF is added to 1 m*M* and DNase to 40 µg/mL and the cells are incubated on ice for 15–20 min. The lysate is then centrifuged at 39,000*g* (4°C) for 30 min and transferred to a Beckman TLA-100 ultracentrifuge tube and centrifuged for 30 min at 155,000*g* (2°C). The supernatent contains the expressed motor protein and is used for the motility and directionality assays.
2. Axoneme–microtubules (MT) complexes are prepared immediately before the assays is done. First, salt-extrated axonemes ***(14)*** are diluted (1:10) in PM buffer and centrifuged at 12,000 rpm for 10 min at room temperature (RT). The pellet is resuspended in 9 µL containing 1 m*M* Mg-GTP, 20 µg NEM-modified tubulin, and 20 µg PC-purified tubulin and incubated for 2 min at 37°C. The reaction is stopped by the addition of 7 µL of PM containing 40 µ*M* Taxol (prewarmed to 37°C) and transferred to room temperature. Typically, the axoneme–MT complexes are diluted 1:5 with PM buffer before performing the assays.
3. In vitro motility assays are performed with the mutant proteins to check for movement on microtubules (MTs). This is done by coating clean glass cover slips with 6–8 µL of 0.5 OD_{280} anti-glutathione *S*-transferase (GST) antibody, rinsing twice with 25 µL of PME buffer and then coating with the mutant GST-motor fusion protein one to three times (final volume 6–8 µL), and adding 1- to 1.6-µL microtubules and 0.9 µL of 50 m*M* Mg–ATP. The cover slip is sealed onto a clean glass slide with VALAP and observed using video-enhanced differential interference contrast microscopy (*see* **Note 3**). Any microtubule motility is recorded on videotape.

4. Once motility is acertained, polarity assays are done on each construct and compared to the wild type. The polarity assays are done the same way as the motility assays with the addition of axoneme–MTs instead of MTs.
5. We determine velocities by manually tracking the leading ends of MTs using a mouse controlled cursor overlaid on a video image and a tracking program designed specifically for this purpose (courtesy of N. Gliksman and T. Salmon, University of North Carolina Chapel Hill, NC).

4. Notes

1. When designing the oligonucleotides for PCR in **Subheading 2.1.**, we estimate the melting temperature (T_m) of each of them to ensure that the two oligonucleotides used in a PCR reaction have a similar T_m. The formula used to calculate the T_m of each oligonucleotide is T_m (°C) = 4(G + C) + 2(A + T) ***(1)***. This results in a better yield because each primer has the same chance to anneal to the DNA ***(1)***. In addition, we decided to use Vent polymerase over *Taq* because of its increased fidelity and yield of amplified DNA in our PCR reactions. However, when screening for our mutants using the oligonucleotide primer that primes on the mutant but not on the wild type (**Fig. 1C**), we use *Taq* polymerase (New England Biolabs, Beverly, MA) because it does not have the 3' to 5' exonuclease activity that would correct the mismatch and permit synthesis from wild-type clones.
2. A few modifications were made in order to optimize motility. First, we resuspend the induced cell pellets in 0.5–0.8 mL of buffer per gram of cells, the least amount of buffer possible, in order to get a concentrated lysate of motor proteins. Second, we add salt (50 m*M* NaCl) to the buffer to help solubilize the protein. A Western blot of the lysates can be done to determine if the expressed protein is soluble and also to ensure that no degradation of the protein has occurred.
3. We found that some of our motor lysates were not able to bind microtubules to the cover slip. To determine if the motor is not able to bind to microtubules or if the concentration of motor is not high enough, we use AMP–PNP instead of ATP in our motility assays. If the motor is able to bind microtubules, bound microtubules should be observed evenly distributed across the cover slip. It should then be possible to observe motility by increasing the concentration of motor in the lysate. If the motor is not able to bind microtubules to the cover slip, microtubules will be present in solution but not bound to the cover slip in the presence of AMP–PNP. It is then necessary to alter the motor construct or redesign the mutant in order to obtain a motor capable of binding to microtubules.

References

1. Ho, S. N., Hunt, H. D., Horton, R. M., Pullen, J. K., and Pease, L. R. (1989) Site-directed mutagenesis by overlap extension using the polymerase chain reaction. *Gene*, **77**, 51–59.
2. Bloom, G. S. and Endow, S. A. (1995) Motor proteins 1: kinesins. *Protein Profile* **2**, 1109–1111.

3. McDonald, H. B., Stewart, R. J., and Goldstein, L. B. B. (1990) The kinesin-like ncd protein of Drosophila is a minus-end directed microtubule motor. *Cell* **63**, 1159–1165.
4. Walker, R. A., Salmon, E. D., and Endow, S. A. (1990) The *Drosophila* claret segregation protein is a minus-end directed motor molecule. *Nature* **347**, 780–782.
5. Case, R. B., Pierce, D. W., Hom-Booher, N., Hart, C. L., and Vale, R. D. (1997) The directional preference of kinesin motors is specified by an element outside of the motor catalytic domain. *Cell* **90**, 959–966.
6. Endow S. A. and Waligora, K. W. (1998) Determinants of kinesin motor polarity. *Science* **281**, 1200–1202.
7. Henningsen, U. and Schilwa, M. (1997) Reversal in the direction of movement of a molecular motor. *Nature* **389**, 93–95.
8. Sambrook, J., Fritsch, E. F., and Maniatis, T. (eds.) (1989) *Molecular Cloning: A Laboratory Manual*. Cold Spring Harbor Laboratory Press, Cold Spring Harbor, NY.
9. Sanger, F., Nicklen, S., and Coulson, A. R. (1977) DNA sequencing with chain-terminating inhibitors. *Proc. Natl. Acad. Sci. USA* **74**, 5463–5467.
10. Williams, R. C., Jr., and Lee, J. C. (1982) Preparation of tubulin from brain. *Methods Enzymol.* **85**, 376–385.
11. Hyman, A., Drechsel, D., Kellogg, D., Salser, S., Sawin, K., Steffen, P., et al. (1990) Preparation of modified tubulins. *Methods Enzymol.* **196**, 303–319.
12. Studier, F. W., Rosenberg, A. H., Dunn, J. J., and Duberdorff, J. W. (1990) Use of T7 RNA polymerase to direct expression of cloned genes. *Methods Enzymol.* **185**, 60–89.
13. Laemmli, U. (1970) Cleavage of structural proteins during the assembly of the bacteriophage T4. *Nature* **227**, 680–685.
14. Allen, C. and Borisy, G. G. (1974) Structural polarity and directional growth of microtubules of *Chlamydomonas* flagella. *J. Mol. Biol*. **90**, 381–402.

6

Preparation of Recombinant Kinesin Superfamily Proteins Using the Baculovirus System

Nobutaka Hirokawa and Yasuko Noda

1. Introduction

Microtubules and associated motor proteins provide an important structural basis for intracellular motility such as organelle transports, mitosis, meiosis, and cilia and flagellar motility. Organelle transports are very important for cellular morphogenesis and activities, conveying and targeting indispensable materials to the correct destination, often at considerable velocities. In order to clarify this trafficking mechanism by motor proteins, systematical search for novel, putative members of this family have been achieved and a series of cDNA, containing consensus sequences encoding both the ATP-binding and the microtubule-binding domains of kinesin heavy chain, were cloned and characterized from murine brain libraries ***(1–3)***. They form kinesin superfamily proteins (KIFs). Now, 10 members (KIF1A, KIF1B, KIF2, KIF3A, KIF3B, KIF4, KIF5A, KIF5B, KIF5C, KIFC1, KIFC2, KIFC3) have been identified and characterized ***(4–10)***.

These new putative motors can be categorized into three types, according to the relative position of their motor domains: N-terminal-motor-domain type, such as KIF1A, KIF1B, KIF3A, KIF3B, KIF4, and KIF5; middle-motor-domain type, such as KIF2, and C-terminal-motor-domain type, such as KIFC1, KIFC2, and KIFC3. Molecular cell biological approaches have been used to characterize all these novel motor proteins, including cloning and sequencing techniques, observation of molecular structures by electron microscopy (EM), in vitro motility assays, and immunological approaches to elucidate the distribution of the molecules. These works have revealed a sophisticated network of motor proteins, with redundancy and specificity.

From: *Methods in Molecular Biology*, Vol. 164: *Kinesin Protocols*
Edited by: I. Vernos

Because it is sometimes difficult to discriminate subtle differences among these proteins that coexist in the cell, the expression of individual recombinant proteins is a helpful method to investigate the localization and function in vivo, as well as the structure and motile activity in vitro of specific proteins.

To obtain recombinant proteins, it is possible to use a prokaryote (*Escherichia coli*) (*see* Chapters 4, 5, and 15) or eukaryote (baculovirus-Sf9) expression systems. In general, the former is a quick and less expensive way to get a high yield of protein and is suitable for the projects requiring large amounts of protein, such as polyclonal antibody production. The latter is superior in increasing the possibility of proper folding and supporting posttranslational modifications and, thus, is ideal for the examination of the fine structure and function of the original protein.

In the case of studies on families of proteins that closely resemble one another, expression in the baculovirus system is inevitable to characterize particular motor protein, because their detailed examination requires native and active protein forms. In addition to the full-length product, partial fragments of the protein are sometimes needed to prepare unique antigens or to suppress the function of endogenous motor molecules. We have tried many constructs and succeeded in expressing many kinds of KIFs.

Splendid progress in molecular biology has enabled recombinant protein expression to become steadier and handier during the last several years. Nowadays, we usually express motor proteins with a tag that enables short-step, high-quality purification (KIF3B, KIF1A, KIFC2) ***(7,8,10)***. Although one-step purification is not sufficient, it dramatically decreases the contamination of endogenous motor proteins of Sf9 cells. Moreover, the high efficiency of transfection rate has saved laborious screening of baculovirus clone with the target gene.

This chapter introduces the procedures for the preparation of recombinant KIFs in the baculovirus expression system. It consists of four parts: (1) construction of vector, (2) transfection into Sf9 cells, (3) amplification and purification of the virus, and (4) expression and purification of the recombinant motor protein.

2. Materials

2.1. Construction of Vector

1. Bac-to-Bac™ baculovirus expression systems (Gibco-BRL).
   - pFastBac donor plasmid.
   - MAX efficiency DH10Bac competent cells.
2. Luria agar.
3. Bluo-gal.
4. Isopropyl β-D-thiogalactopyranoside (IPTG).
5. Kanamycin.

6. Gentamicin.
7. Tetracyclin.
8. QIAGEN Plasmid midi kit (QIAGEN Inc., Chatsworth, UK).

2.2. Transfection of Sf 9 Cells with Recombinant Bacmid DNA

1. Sf9 (*Spondoptora frugiperda*) cells (ATCC #CRL 1711).
2. Grace's cell-culture medium supplemented (TNM-FH) (Gibco, cat. no. 350-1605).
3. Heat-inactivated fetal calf serum (FCS), checked for supporting cell growth in advance.
4. Cell FECTIN reagent from Bac-to-Bac™ baculovirus expression systems (Gibco-BRL).
5. Six-well culture plate (Nunc International, cat. no. 152795).

2.3. Amplification and Purification of Virus

1. Culture flasks, 25, 80, and 175 cm^2 (correspondent to the scale of culture) (Nunc, cat. nos. 163371, 147589, and 156502).
2. A 96-well culture plate (optional for end-point dilution) (Nunc, cat. no. 167008).

2.4. Expression and Purification of Recombinant Motor Protein

1. Chelating Sepharose fast flow (Pharmacia) charged with 50 m*M* $NiSO_4$.
2. NAP5 desalting column (NAP5 Sephadex G-25, Pharmacia).
3. PHM buffer: 25 m*M* piperazine-N,N-bis[2-ethanesulfonic acid] [PIPES], 25 m*M* HEPES, 1 m*M* $MgCl_2$ (pH 7.4).
4. Elution buffer (500 m*M* imidazole [pH 7.4]).
5. Protease inhibitor cocktail, (1000X): 1 *M* phenylmethylsulfonyl fluoride [PMSF], 100 mg/mL leupeptin, 1 g/mL pepstatin A, 10 mg/mL tosylarginylmethylester in dimethylsufoxide.
6. Culture flasks, 25, 80, and 175 cm^2 (correspondent to the scale of culture) (Nunc, cat. no. 163371, 147589, and 156502).

3. Methods

3.1. Construction of the Vector

A transfer vector is constructed using the pFastBac donor plasmid ***(11)*** (Gibco-BRL Life Technologies, Gaithersburg, MD). (Formerly, we used the pBacPAK8 transfer vector system, but the transfection efficiency and expression rate has been improved in the new system.) To generate full-length recombinant N-terminal-type KIF molecules with a polyhistidine tag, we usually use the PCR method with *Taq* polymerase to introduce six histidine codons in-frame and a stop codon at the COOH terminus, in addition to the enzyme restriction sites on both ends. In the case of C-terminal-type KIFs (KIFCs), we introduce the histidine tag at the NH_2-terminus. For proper translation, the 5' noncoding region before the consensus start codon is preserved with care (ATAAATGCC).

The FastBac plasmid inserted with recombinant protein gene is transformed into MAX efficiency DH10Bac cells (Gibco-BRL) and placed on Luria agar plates containing 100 µg/mL Bluo-gal, 40 µg/mL IPTG, 50 µg/mL kanamycin, 7 µg/mL gentamicin, and 10 µg/mL tetracyclin. Serial dilutions of cells (10^{-1}–10^{-3}) enable the visualization of white colonies of recombinant Bacmid. Bacmid DNA is verified and isolated for transfection with the QIAGEN Plasmid midi kit.

3.2. Transfection of Sf 9 Cells with Recombinant Bacmid DNA

Sf9 cells are transfected with a mixture of recombinant Bacmid DNA and CellFECTIN reagent according to the protocol of Bac-to-Bac™ baculovirus expression systems.

1. The 9×10^5 Sf9 cells in log-phase growth are seeded to each 35-mm dish in a six-well plate with 2 mL of medium supplemented with FCS and incubated for 1 h.
2. Dilute 5 µL of miniprep Bacmid DNA into 100 µL of medium without FCS and mix thoroughly.
3. Dilute 6 µL of CellFECTIN reagent into 100 µL medium and mix.
4. Combine the two solutions, mix, and incubate for 15–45 min at room temperature and add 800 µL medium.
5. Wash cells gently with the medium, aspirate the medium and add the solution in **step 4**. (Do not dry up the cells.)
6. Incubate for 5 h in an incubator.
7. Remove medium and add 2 mL of medium with FCS.
8. After 48 h, check cells for the expression of recombinant protein. The supernatant is centrifuged at 500*g* for 5 min, transferred to a fresh tube, and stored at 4°C protected from light. Under these conditions, it is stable for up to 3 mo. For longer storage, freezing with liquid nitrogen and preserving at –80°C is recommended (*see* **Note 1**).

3.3. Amplification and Purification of the Virus

From the initial transfection, viral titers are estimated to be $(2–4) \times 10^7$ plaque-forming units per milliliter (PFU/mL). Infection of monolayer culture at a multiplicity of infection (MOI) of 0.1 results in an approx 100-fold amplification after 48 h incubation.

When it is planned to be use the recombinant motor protein in repeated experiments, the isolation of recombinant virus by end-point dilution is recommended. For large-scale infection, we usually use the third or fourth harvested medium after purification.

1. Plate 100 µL of 2×10^5 cells/mL Sf9 cells in log-phase growth to each well of a 96-well culture plates.
2. Dilute the virus inoculum to 2×10^5, 2×10^4, and 2×10^3 PFUs/mL. Add 100 µL of each diluted medium to 32 wells of the 96-well plate and incubate for 7 d.

3. Check each well for the presence of pathological changes such as inclusion bodies. Aspirate the medium from several wells infected with virus with a lower titer. Store the supernatant for virus stock and examine the cells for the expression of recombinant protein.

3.4. Expression and Purification of Recombinant Motor Protein

In order to obtain a fully active form of purified recombinant motor protein, our first goal is to get the protein in the soluble fraction. To optimize the infection conditions, preliminary experiments are necessary, changing the MOI from 1 to 10 and the harvesting time from 24 h to 96 h. For each condition, cells are homogenized with PHM buffer supplemented with protease inhibitors and centrifuged at 10,000*g* for 15 min, yielding supernatant and pellet fractions. Samples are electrophoresed and the presence of the recombinant band is checked after gel staining. It is also necessary to optimize buffer conditions for purification that largely depend on the molecule itself. Changes of pH sometimes drastically improve the solubility of proteins (*see* **Notes 2–4**).

When the recombinant motor protein is recovered in the soluble fraction, a one-step purification with a polyhistidine tag can be performed. Because 1 mL of resin usually binds 4–8 mg of histidine-tagged protein (it depends on the size or conformation of the protein and sometimes the yields is much lower), the volume of the column also depends on the scale of the experiment.

1. Wash an immobilized Ni^{2+} column (chelating Sepharose FF) with PHM buffer (*see* **Note 5**).
2. Resuspend infected Sf9 cells with PHM buffer supplemented with protease inhibitors, homogenize with a teflon homogenizer, and clarify by ultracentrifugation at 100,000*g* for 30 min.
3. Apply the resultant supernatant to preequilibrated column and wash the column with the buffer.
4. Elute with elution buffer and collect fractions (*see* **Note 5**).
5. Check the protein concentration of fractions and select fractions of high yield.
6. Apply these selected fractions to a desalting column and change the buffer to PHM (*see* **Note 6**).

4. Notes

1. Although progress in technology has greatly improved the transfection procedure, low efficiency of transfection can occur, which is usually caused by the following:
   a. Viability of Sf9 cells. Sf9 cells in log-phase growth with a viability over 97% should be used for transfection. Fresh stocks must be used within 3 mo. Overconfluent cultures are detrimental for cell viability. Replate the cells every 3 or 4 d. Because Sf9 cells need much oxygen, minimize the medium depth (4 mL to a 25-cm^2 flask and 12 mL to a 80-cm^2 flask) and loosen the cap maximally ***(12)***.

b. Purity of recombinant Bacmid DNA. Impurity of DNA preparation decreases the efficiency of transfection. We usually prepare recombinant DNA using the QIAGEN plasmid midi kit.
c. Uninfectivity of Sf9 cells. Infectivity to baculovirus differs among cell lines. Changing the cell line (e.g., Sf21, or High 5) sometimes improves the transfection and expression rate of proteins.

2. A low yield of expressed protein can be improved by changing the following parameters:
   a. Increasing the viability of Sf9 cells.
   b. Improving the infection conditions, which involves the time-course, MOI, and cell-density improvements.
   c. Checking the untranslated region of the vector. Changing the 5' noncoding region to the frequently used starting codon consensus in Sf9 cells sometimes improves the translation efficiency ***(13)***.
   d. Even though transfection efficiency has improved dramatically, it is not perfect. When unpurified virus inoculum is used repeatedly, the expression rate gradually decreases because of the higher productivity of untransfected virus. So, the purification of virus by end-point dilution is inevitable if large amount of high-titer stock is needed for experiments.
3. When the band of recombinant protein is not clear on SDS-PAGE gels, it is sometimes helpful to compare it with corresponding samples from Sf9 cells or Sf9 cells infected with wild-type baculovirus.
4. Overexpression of recombinant proteins sometimes causes the insolubility of protein that form inclusion bodies within the cells that can be lysed with guanidine or urea treatment, only to recover a denatured form without activity in the soluble fraction. Thus, instead of trying various conditions, the reconstruction and expression of the protein with a fusion partner save much time and effort. We experienced partial expression of KIF protein fused with thioredoxin or glutathione *S*-transferase (KIFC2) that induced proper folding and solubilized the target protein ***(8)***.
5. One-step purification can be improved by changing the buffer conditions. Some proteins remain bound to the Sepharose after washing with buffer containing 1 *M* NaCl. This step removes contamination bands drastically. The elution of proteins from the chelating Sepharose can sometines be done with lower concentrations of imidazole (below 150 m*M*), decreasing the inactivation of the protein ***(8)***. Purification protocols largely depend on each particular protein and can be optimized through various trials.
6. One-step purification with a histidine tag does not completely remove the contaminating bands derived from Sf9 cells and baculovirus. Sometimes, inactive forms of the recombinant protein may disturb the analysis of the active form. Nucleotide-dependent microtubule binding of the motor protein is sometimes a useful way to purify the active fraction.

References

1. Aizawa, H., Sekine, Y., Takemura, R., Zhang, Z., Nangaku, M., and Hirokawa, N. (1992) Kinesin family in murine central nervous system. *J. Cell Biol*. **119**, 1287–1296.
2. Hirokawa, N. (1998) Kinesin and dynein superfamily proteins and the mechanism of organelle transport. *Science* **279**, 519–26.
3. Nakagawa, T., Tanaka, Y., Matsuoka, E., Kondo, S., Okada, Y., Noda, Y., et al. (1997) Identification and classification of 16 new kinesin superfamily (KIF) proteins in mouse genome. *Proc. Natl. Acad. Sci. USA* **94**, 9654–9.
4. Kondo, S., Sato-Yoshitake, R., Noda, Y., Aizawa, H., Nakata, T., Matsuura, Y., and Hirokawa, N. (1994) KIF3A is a new microtubule-based anterograde motor in the nerve axon. *J. Cell Biol*. **125**, 1095–1107.
5. Nangaku, M., Sato-Yoshitake, R., Okada, Y., Noda, Y., Takemura, R., Yamazaki, H., and Hirokawa, N. (1994) KIF1B, a novel microtubule plus end-directed monomeric motor protein for transport of mitochondria. *Cell* **79**, 1209–1220.
6. Noda, Y., Sato-Yoshitake, R., Kondo, S., Nangaku, M., and Hirokawa, N. (1995) KIF2 is a new microtubule-based anterograde motor that transports membranous organelles distinct from those carried by kinesin heavy chain or KIF3A/B. *J. Cell Biol*. **129**, 157–167.
7. Okada, Y., Yamazaki, H., Sekine-Aizawa, Y., and Hirokawa, N. (1995) The neuron-specific kinesin superfamily protein KIF1A is a unique monomeric motor for anterograde axonal transport of synaptic vesicle precursors. *Cell* **81**, 769–780.
8. Saito, N., Okada, Y., Noda, Y., Kinoshita, Y., Kondo, S., and Hirokawa, N. (1997) KIFC2 is a novel neuron-specific C-terminal type kinesin superfamily motor for dendritic transport of multivesicular body-like organelles. *Neuron* **18**, 425–438.
9. Sekine, Y., Okada, Y., Noda, Y., Kondo, S., Aizawa, H., Takemura, R., and Hirokawa, N. (1994) A novel microtubule-based motor protein (KIF4) for organelle transports, whose expression is regulated developmentally. *J. Cell Biol*. **127**, 187–201.
10. Yamazaki, H., Nakata, T., Okada, Y., and Hirokawa, N. (1995) KIF3A/B: a heterodimeric kinesin superfamily protein that works as a microtubule plus end-directed motor for membrane organelle transport. *J. Cell Biol*. **130**, 1387–1399.
11. Luckow, V. A., Lee, S. C., Barry, G. F., and Olins, P. O. (1993) Efficient generation of infectious recombinant baculoviruses by site-specific transposon-mediated insertion of foreign genes into a baculovirus genome propagated in Escherichia coli. *J. Virol*. **67**, 4566–4579.
12. Richardson, C. D., (1995) Baculovirus expression protocols, in *Methods in Molecular Biology*, vol. 39 (Walker, J. M., ed.), Humana, Totowa, NJ, p. 418.
13. Ayres, M. D., Howard, S. C., Kuzio, J., Lopez-Ferber, M., and Possee, R. D. (1994) The complete DNA sequence of Autographa californica nuclear polyhedrosis virus. *Virology* **202**, 586–605.

7

Assays for Kinesin Microtubule-Stimulated ATPase Activity

David D. Hackney and Wei Jiang

1. Introduction

Methods for assay of ATPase rates can be classified into broad categories depending on whether an ATP-regenerating system or a continuous coupled assay is employed versus quenching at discrete times for subsequent analysis for production of Pi or ADP (or, more rarely, for the loss of ATP).

Use of an ATP-regenerating system such as pyruvate kinase and phosphoenolpyruvate (PEP) provides a useful way to maintain low concentrations of ATP. In the presence of pyruvate kinase and PEP, the ADP, which is produced by hydrolysis of ATP, is rapidly rephosphorylated back to ATP with the coupled formation of pyruvate. The free-energy change for this reaction strongly favors phospho-transfer from PEP to ADP, and significant ADP accumulation does not occur until almost all of the PEP is exhausted. An ATP-regenerating system is particularly useful when the starting ATP concentration is below the K_m value. Without a regenerating system it is difficult to obtain a true initial rate because the ATP concentration and the hydrolysis rate start decreasing immediately on initiating the reaction. With pyruvate kinase and PEP, the ATP concentration remains constant and the rate remains linear for long periods and can be more easily monitored even when [ATP] << K_m. Rapid recycling of ADP also keeps the steady-state ADP concentration very low. This is useful when the ATPase rate is desired in the absence of product inhibition by ADP, but it is a disadvantage if the K_i for ADP is desired. Pi does accumulate during the reaction, but it is a poor inhibitor of kinesin.

If lactate dehydrogenase and NADH are also present, then the reduction of pyruvate to lactate results in the coupled oxidation of NADH that can be monitored by the change in absorbance at 340 nm. This provides a convenient

From: *Methods in Molecular Biology*, Vol. 164: *Kinesin Protocols*
Edited by: I. Vernos

coupled spectrophotometric assay for the steady-state ATPase rate. The regeneration of ATP is useful even when the reaction is to be monitored by the assay of Pi, because of the extended linear phase of the reaction at low ATP concentrations. Other kinases such as creatine kinase can be used for recycling ATP, but pyruvate kinase has the advantage that it can be readily coupled to lactate dehydrogenase to produce an absorbance change and its substrate, PEP, is comparatively stable if acid is used to quench the reaction. The method in **Subheading 3.1.** uses this coupled assay system to continuously monitor the progress of the ATPase reaction by the change in absorbance at 340 nm.

If the reaction is quenched at discrete times, there are numerous methods for analysis of the products ADP and Pi, including direct colorimetric or fluorescence assays, use of ^{32}P as a label, and coupled enzymatic assays. It is also possible to follow the reaction by the accompanying proton liberation at neutral pH. Most assays for Pi have taken advantage of the unusual properties of the complex formed between molybdate and Pi under acid conditions. In the oxidized state, the phosphomolybdate complex absorbs in the near ultraviolet (UV) to give a pale yellow color, but it can be readily converted to a reduced complex with a strong blue color. This reduction forms the basis for the Sumner method with ferrous sulfate as the reductant ***(1)***. The oxidized phosphate complex has a hydrophobic surface and can be readily extracted into organic solvents, whereas ADP and ATP remain in the aqueous phase. This provides a useful means for separation of Pi from ATP and ADP (*see* **refs. *2*** and ***3***). The hydrophobic surface of the phosphomolybdate complex can also bind dye molecules. The malachite green method ***(4)*** described in **Subheading 3.3.** and **3.4.** utilizes the shift in the wavelength for the maximum absorbance of this dye upon binding to the oxidized phosphomolybdate complex.

Radiochemical methods have the advantage of high sensitivity, which allows reactions to be conducted in small volumes that conserve valuable kinesin preparations and microtubules. The ^{32}P label can be incorporated into either the α or γ positions of ATP to give labeled ADP or Pi, respectively, on hydrolysis. These can be separated from the starting ATP by thin-layer chromatography, ion-exchange chromatography, adsorption of ATP and ADP on charcoal, and extraction of Pi into organic solvents as the complex with molybdate. Use of ^{32}P has the disadvantage of the short half-life of ^{32}P and the need for special and increasingly complex regulatory requirements. In addition, commercial preparations of ^{32}P usually contain 1–2% or more of hydrolysis products and also a considerable amount (up to 35% in some cases) of ^{32}P-labeled material that cannot be hydrolyzed by kinesin to ADP and Pi (*see* **ref. *5*** for a discussion of this problem and the controls that need to be applied). The sensitivity of the malachite green assay for Pi is sufficiently high that it can replace the radiochemical methods in all but

the most demanding circumstances or when ATPase rates must be determined in the presence of high initial Pi concentrations.

2. Materials

1. 200 m*M* Mg–ATP: Dissolve 1.2 g of Na_2ATP (Sigma, Grade I) in 4 mL cold water and keep on ice; with stirring, add cold 2 N KOH to pH 7 (approx 1 mL); then add 2 mL of 1 *M* magnesium acetate. Add additional KOH if needed to keep the pH at approx 7.0. Dilute a small sample to determine the ATP concentration by A_{259} using an extinction coefficient of 15.4/m*M*/cm; add sufficient additional water to bring the final concentration to approx 200 m*M*; then determine the exact final concentration by A_{259}. Store in small aliquots at –80°C.
2. PEP: 200 m*M* potassium PEP in water. Adjust pH to 7.0 with 2 N KOH (store in small aliquots at –80°C).
3. 80PM buffer: 80 m*M* piperazine-N,N-bis(2-ethanesulfonic acid) (PIPES)/NaOH at pH 6.9, 2 m*M* EGTA, 1 m*M* $MgSO_4$, and 2 m*M* dithiothreitol (DTT).
4. A25 buffer: 25 m*M* *N*-(2-acetamido)-2-aminoethanesulfonic acid (ACES)/KOH at pH 6.9, 2 m*M* magnesium acetate, 2 m*M* potassium EGTA, 0.1 m*M* potassium EDTA, and 1 m*M* of 2-mercaptoethanol.
5. NADH: 70 m*M* in water (store in small aliquots at –80°C).
6. Pyruvate kinase: 10 mg/mL (Sigma, Type III) in A25 buffer (store at –80°C).
7. Lactate dehydrogenase: 10 mg/mL (Sigma, Type XXX-S) dialyzed versus A25 buffer (store at –80°C).
8. Taxol: 15 m*M* in dimethyl sulfoxide (DMSO) (store at –20°C).
9. Tubulin: Purified from bovine brain by two cycles of polymerization and chromatography on phosphocellulose to remove microtubule-associated proteins (MAPs) as described by Williams and Lee ***(6)*** except that the final resuspension and phosphocellulose chromatography is done in 80PM buffer containing 0.05 m*M* GTP (*see* **Note 1**) (*see also* Chapters 1 and 9).
10. Microtubules (MTs): Polymerized from MAP-free tubulin and stabilized with Taxol. Tubulin (300 mg in 55 mL 80PM) is warmed to 37°C for 2 min to initiate polymerization; Taxol is added in small aliquots with gentle stirring to 65 μ*M* (1.2 molar ratio); held at 25°C for 15 min; then centrifuge for 50 min at 235,000*g* in a Beckman Ti45 rotor at 25°C. The microtubule pellet is washed by homogenization in 70 mL of A25 buffer and recentrifuged. The washed pellet is resuspended in A25 buffer with 8 μ*M* Taxol and centrifuged 1.5 min at 13,000*g* to remove aggregated material. Store in small aliquots at –80°C after rapid freezing in liquid nitrogen. The tubulin concentration is determined by absorbance at 275 nm in 6 *M* guanidine·HCl using an extinction coefficient of 1.03 mL/mg/cm/s and a molecular mass of 110 kDa for the tubulin heterodimer (*see* **Notes 2** and **3**).
11. Perchloric acid: 0.6 N in water (store at 4°C) (*see* **Note 4**).
12. Molybdate reagent: 1% ammonium molybdate (Sigma) in 0.8 N HCl. Prepare by gradual addition of solid ammonium molybdate to cold 0.8 N HCl with vigorous stirring. (Store at 4°C for less than 1 mo; discard if a precipitate develops or if standard curve shifts.)

13. Malachite green: 0.05% (w/v) in water (store at 4°C).
14. Pi standard solution: 0.100 *M* KH_2PO_4.
15. Labware: The malachite green Pi assay is so sensitive that it is prone to a false high reading because of phosphate contamination of labware and reagents. Use only detergents that are free of phosphate for cleaning labware. Avoid using glassware, as it binds Pi. If glassware must be used, it should be given final rinses in 1 N HCl and deionized water and then air-dried. Generally, new plastic tubes and cuvets do not contain Pi, but this should be tested with each lot.

3. Methods

ATPase reactions are described here with A25 buffer, but they could be done with many other buffers. The concentration required for half-maximal stimulation by MTs increases rapidly with salt concentration and it may not be possible to approach saturation with MTs in buffers of high ionic strength. Pyruvate kinase requires potassium and reactions utilizing this enzyme cannot be performed in the absence of potassium. The activity of pyruvate kinase is largely independent of pH between 6.5 and 8.0, but decreases rapidly at a lower pH. The activity of lactate dehydrogenase is largely independent of pHs between 6.0 and 7.0, but decreases rapidly at higher pH.

3.1. Continuous Coupled Assay with Regeneration of ATP

1. Equilibrate 0.98 mL of A25 buffer containing 1 m*M* Mg–ATP, 2 m*M* PEP, 0.25 m*M* NADH, 3–10 μg/mL pyruvate kinase, approx 3 μg/mL lactate dehydrogenase, and 8 μ*M* Taxol in a semimicrocuvet at 25°C (*see* **Subheading 3.2.** for determination of the optimal level of pyruvate kinase and lactate dehydrogenase) (*see* **Notes 5–7**).
2. Add microtubules, mix, and then immediately add kinesin and mix (total volume of microtubules and kinesin at approx 20 μL) (*see* **Notes 8–10**).
3. Record the decrease in A_{340} versus time and determine the slope of the linear region following the transient for response of the coupled enzymes (*see* **Subheading 3.2.**).
4. Calculate the ATPase rate using an absorbance decrease at 340 nm of 6.22/m*M*/cm for oxidation of NADH.

3.2. Determination of Response Time of Coupled Assay

High concentrations of lactate dehydrogenase and especially pyruvate kinase inhibit the MT-stimulated ATPase of kinesin and the amounts must be carefully controlled to provide efficient recycling of ATP without producing significant inhibition of kinesin *(7)*. As the activity of pyruvate kinase is variable from batch to batch and from supplier to supplier, the controls should be rechecked for each new batch.

1. Prepare a cuvet with a 1-mL reaction mixture as in **Subheading 3.1.**, **step 1**, except omit pyruvate kinase and increase lactate dehydrogenase to 20 μg/mL to ensure that it is not limiting.

2. Add pyruvate kinase to approx 3 µg/mL.
3. Add 10 µL of 5 m*M* ADP and observe the decrease in A_{340} with time.
4. The A_{340} should decrease by 0.3 and the transient should obey first-order kinetics. Estimate the half-life of the transient. If the half-life is less than 5 s or more than 30 s, repeat the measurement at a different level of pyruvate kinase. Calculate the amount of pyruvate kinase required to give a half-life of approx 5 s and use this amount in the ATPase assay.
5. Repeat **steps 1–4** with excess pyruvate kinase and limiting lactate dehydrogenase to determine how much lactate dehydrogenase to use. Adjust the lactate dehydrogenase level in the ATPase reaction to have a half-life of around 2 s.
6. As a control on the inhibition by pyruvate kinase, determine the ATPase rate of kinesin at several high concentrations of pyruvate kinase. Perform these assays with a single concentration of MTs that produces less than half maximal activation. Extrapolate to the amount of inhibition expected at the lower pyruvate kinase level determined in **Subheading 3.2.**, **step 4**.

3.3. Assay by Rate of Production of Pi

1. Reactions are performed as for **Subheading 3.1.**, **steps 1** and **2**, but omit lactate dehydrogenase and NADH. If regeneration of ATP is not desired, also omit pyruvate kinase and PEP (*see* **Note 11**).
2. At various times remove an aliquot of the reaction for assay of Pi by the malachite green method (**Subheading 3.3.**).

3.4. Malachite Green Assay for Pi

1. At desired times, stop reaction by addition of a small aliquot (≤ 20 µL containing ≤ 10 nmol Pi) to 0.6 mL ice cold 0.8 *M* perchloric acid; incubate on ice for 1–5 min; and centrifuge 1 min at 13,000*g* at 4°C to remove precipitated protein (*see* **Note 12**).
2. Add 0.5 mL supernatant to 0.5 mL molybdate reagent in a disposable cuvet, mix, add 50 µL of malachite green stock, mix and read A_{650} after 1 min against a reagent blank (*see* **Notes 13** and **14**).
3. Determine concentration of Pi by comparison with a standard curve generated using dilutions of the standard Pi solution (1 nmol of Pi in a 1-mL final assay volume should give an A_{650} of around 0.1) (*see* **Notes 15** and **16**).

4. Notes

1. Microtubule-associated proteins (MAPs) are potent inhibitors of the MT-stimulated ATPase of kinesin and care must be taken to totally remove them.
2. GTP is an alternative substrate for kinesin. The final steps in the preparation of tubulin are performed with only 50 µ*M* GTP and the polymerized tubulin is thoroughly washed in buffer without GTP to minimize carryover of free GNP into the final MT preparation.
3. The washing and final resuspension of the MTs can be performed in other buffers to match particular applications. A25 is used here so that reactions can be con-

ducted in the absence of added salt if desired, while still allowing reactions to be done in the presence of salts added directly to the reaction mix.

4. Perchloric acid is an oxidizer and a potential explosive danger. Although dilute aqueous solutions do not pose a severe hazard, solutions should not be evaporated to dryness and local disposal regulations should be determined.
5. The reaction volume can be reduced if microcuvets are employed. It is often useful to have the contents of the cuvet stirred during the reaction using a magnetic stirrer mounted below the cuvet.
6. ATP and PEP stocks contain variable amounts of ADP and pyruvate. These contaminants will consume some of the NADH that is initially added to a reaction mix. Consequently, additional NADH may need to be added to obtain a stable A_{340} of ≥ 1 before the addition of kinesin.
7. Taxol is only slightly soluble in water. To prevent local precipitation when adding Taxol from concentrated solutions in DMSO, always mix immediately after addition and avoid adding Taxol to solutions at < 25°C.
8. A kinesin motor-domain concentration of 10–30 n*M* is optimal for short monomer and dimer constructs that have maximum rates of 40–60 s^{-1}. Care should be taken to keep the concentration of kinesin as low as possible because the concentration of MTs required for half-maximal stimulation is highly dependent on the concentration of kinesin in the assay ***(8)***. Higher concentrations are required for longer constructs if they fold into the compact conformer (the 7 S species for homodimers or the 9 S species for heterotetramers ***[9]***). These compact conformers have greatly reduced extents of stimulation by MTs ***(10)***. Higher concentrations will also be required if the basal rate in the absence of MTs is desired.
9. Kinesin motor domains bind to many surfaces. In order to obtain the low concentration of kinesin that is required in the ATPase assay, it is often not possible to dilute directly from the storage stock of kinesin, and an intermediate dilution must be made. It is necessary to redetermine the protein concentration in this intermediate stock as significant loss resulting from adsorption may occur. See **ref. *7*** for a more extensive treatment of this problem.
10. Frozen aliquots of MTs should be rapidly thawed by incubation in a water bath at 25°C. Concentrated stocks are stable for several hours at 25°C and should not be chilled.
11. When reactions need to be performed at very high MT concentrations, a large fraction of the total volume must be derived from the stock solution of MTs. In this case, the reagents in the reaction mix of **Subheading 3.1.**, **step 1** can be prepared at 5X concentration so that 80% of the final reaction volume can be contributed by the stock of MTs.
12. The assay can be made more sensitive if desired by increasing the ratio of the sample volume to that of the perchloric acid quench. For maximum sensitivity, quench 0.5 mL of reaction mix with 0.1 mL of cold 3 N perchloric acid. A significant precipitate of potassium perchlorate will develop when the reaction contains a high concentration of potassium salts. The total volume can also be reduced by using microcuvets.

13. Disposable plastic cuvets are preferable over glass or quartz cuvets, both because they are generally free of Pi and because a colored film accumulates on the walls of the cuvets after repeated use.
14. The A_{650} will increase to a plateau value in approx 30 s. Record the plateau value. Over longer times the absorbance will slowly fall, often accompanied by precipitation of the dye.
15. The reagent blank should have an A_{650} of ≤ 0.05 versus water. Higher values indicate phosphate contamination.
16. At an A_{650} of approx 1, all of the malachite green is complexed to Pi, and additional Pi does not result in a further increase in A_{650}. If a measured absorbance is > 0.9, repeat the measurement on a smaller aliquot.

Acknowledgments

This work was supported by grant NS28562 from the National Institutes of Health.

References

1. Sumner, J. B. (1944) A method for the colorimetric analysis of phosphorus. *Science* **100**, 413–414.
2. Hackney, D. D., Stempel, K. E., and Boyer, P. D. (1980) Oxygen-18 probes of enzymic reactions of phosphate compounds. *Methods Enzymol.* **64**, 60–83.
3. Hackney, D. D. and Clark, P. K. (1985) Steady state kinetics at high enzyme concentration: the myosin ATPase. *J. Biol. Chem*. **260**, 5505–5510.
4. Penney, C. L. and Bolger, G. (1978) A simple microassay for inorganic phosphate, II. *Anal. Biochem*. **89**, 297–303.
5. Jiang, W. and Hackney, D. D. (1997) Monomeric kinesin head domains hydrolyze multiple ATP molecules before release from a microtubule. *J. Biol. Chem*. **272**, 5616–5621.
6. Williams, R. C., Jr. and Lee, J. C. (1982) Preparation of tubulin from brain. *Methods Enzymol.* **85**, 376–385.
7. Huang, T.-G. and Hackney, D. D. (1994) Drosophila kinesin minimal motor domain expressed in Escherichia coli. Purification and kinetic characterization. *J. Biol. Chem*. **269**, 16,493–16,501.
8. Hackney, D. D. (1994) The rate limiting step in microtubule-stimulated ATP hydrolysis by dimeric kinesin head domains occurs while bound to the microtubule. *J. Biol. Chem*. **269**, 16,508–16,511.
9. Hackney, D. D., Levitt, J. D., and Suhan, J. (1991) Kinesin undergoes a 9 S to 6 S conformational transition. *J. Cell Biol*. **115**, 388a.
10. Stock, M. F., Guerrero, J., Cobb, B., Eggers, C. T., Huang, T-G., Li, X., and Hackney, D. D. (1999) Formation of the compact conformer of kinesin requires a C-terminal heavy chain domain and inhibits microtubule-stimulated ATPase activity. *J. Biol. Chem*. **274**, 14,617–14,623.

8

An Improved Microscope for Bead and Surface-Based Motility Assays

Nick Carter and Rob Cross

1. Introduction

We describe the construction and operation of an optimized microscope for kinesin motility assays, using either microtubules (MTs) sliding over kinesin-coated surfaces or the motility of kinesin-coated beads on immobilized single microtubules. A Zeiss Axiovert was modified by replacing the standard Zeiss condenser and mechanical stage with an improved arrangement that provides much better mechanical stability and very high resolution differential interference contrast (DIC) imaging of unstained microtubules using standard tungsten lamp illumination. The microscope can be used routinely for MT surface-sliding assays, using low-volume flow cells constructed by sandwiching together two cover slips. The design allows for the optional addition of optical trapping and high-resolution tracking hardware, for recording of single-molecule mechanical transients.

2. Materials

2.1. Microscope

2.1.1. Optical Layout

1. Standard Zeiss Axiovert 135TV.
2. ×100 N.A. 1.3 oil-immersion objective.

2.1.2. Condenser

1. Objective lens (Zeiss Fluar, ×40, N.A. = 1.3, iris).
2. Custom built condenser tube with field aperture.
3. Objective lens and DIC slider mount supplied by Technical Video.

From: *Methods in Molecular Biology*, Vol. 164: *Kinesin Protocols*
Edited by: I. Vernos

2.1.3. Stability

1. Vibration isolation workstation (Newport).
2. Custom built stage.
3. Piezoelectric stage (Physik Instrumente, P-730.20), for fine XY.
4. Micrometer drive (Physik Instrumente, M-312.00), for coarse XY.

2.1.4. Video Camera, Video Processing, and Video Recording

1. Charged coupled device (CCD) video camera (Watec WAT-501ex).
2. Hamamatsu Argus 20 video processor.
3. sVHS VCR (Panasonic A-5400).
4. Grabber card in the personal computer (PC) (DT2855, Data Translation).
5. RETRAC software. The videotape was analyzed using RETRAC, a program written specifically for filament tracking. It has two main components. One allows the user to capture frames from a live video source or VCR, and a second that allows the user to track moving objects, with simultaneous calculation of velocity and counting statistics. RETRAC is freeware and available for download from our website (http://mc11.mcri.ac.uk/motorhome.html).

2.1.5. Optical Trapping

For optical trapping, a 3-W continuous-wave (CW) Nd:YAG (Uniphase STA 1064-3E, CW) is used.

2.2. MT Gliding Assays

1. 55 × 22-mm cover slips (BDH, 406/0188/44) and 22 × 22-mm cover slips (BDH, 406/0187/33).
2. 1M K–piperazine-*N*,*N*-bis(2-ethanesulfonic acid) (PIPES). PIPES dissolves around its isoelectric point of approx pH 6.5. Take 500 mL water and add 65 g solid KOH; then, after cooling if necessary, slowly add 302 g PIPES buffer (Sigma P-6757). Once everything is dissolved, monitor the pH and roughly adjust by adding more KOH pellets as necessary. Allow the warm solution to cool and then fine-adjust the pH using 5 *M* KOH. Be careful not to overshoot, as there is no way back.
3. 100 m*M* NaGTP stock solution. Nucleoside triphosphates such as GTP and ATP undergo rapid hydrolysis at acidic pH, so efforts should be made to control the pH when dissolving and storing them. Dissolve 1 g NaGTP (Sigma G8877) in 15 mL of 10 m*M* Na–PIPES (pH 6.9), monitoring the pH. Rapidly reneutralize the pH by titrating in 5 *M* KOH. Finely adjust the pH, then make the volume up to 19.11 mL. Store frozen at –20°C in aliquots of 5–2000 µL. Do not add $MgCl_2$ to the stock solution (it precipitates).
4. 100 m*M* Mg–ATP stock solution. Dissolve 5.87 g NaATP (Sigma A7699 ATP ultra or Boehringer 519 987) in 60 mL of 10 m*M* K–PIPES (pH 6.9), continuously monitoring the pH and holding as close as possible to neutral using concentrated KOH. Once the ATP is dissolved, add 10 mL of 100 $MgCl_2$ and readjust the pH to 6.9. Adjust the volume to 100 mL and freeze in aliquots of 5–5000 µL.

5. Taxol (paclitaxel) stock solution. Wear gloves and work in the fume hood. Inject 2.93 mL anhydrous dimethyl sulfoxide (DMSO) (Aldrich 27685-5) into a 25-mg bottle of Taxol (Sigma T 7402). Dissolve by vortexing and store as 2- to 20-µL aliquots at –20°C. Taxol is stable in DMSO but unstable in water . It is insoluble in aqueous buffers above about 18 µ*M*. DMSO is explosive if it gets wet. Store small volumes at room temperature over beds of Sephadex G-50.
6. 0.2 *M* Na–EGTA. Dissolve 15.2 g EGTA (Sigma E 4378) in 190 mL water. Adjust pH to neutral by adding concentrated NaOH, then make volume to 200 mL. Store at room temperature.
7. 1 *M* MgCl2. 20.33 g $MgCl2{\cdot}6H_2O$ to 100 mL water. Sterile filter and store at room temperature.
8. BRB80 (Brinkley reassembly buffer). Most of our motility assay buffers are based on BRB80. BRB80 is 80 m*M* K–PIPES, 1 m*M* $MgCl_2$, 1 m*M* EGTA (pH 6.9). Make up as a 10X stock, store at 4°C, and dilute freshly for use.
9. Purified tubulin. Tubulin at about 1–200 µ*M* (protocol for tubulin preparation on our webpage) in BRB80 should be flash frozen in 10- to 25-µL aliquots in the presence of 30% glycerol by immersion in liquid nitrogen, and stored either at –7°C or preferably in liquid nitrogen.
10. Taxol-stabilized microtubules. Thaw an aliquot of tubulin (typically 200 µ*M*) and add stock 100 m*M* Na–GTP to 1 m*M* and $MgCl_2$ to 2 m*M*. Warm to 37°C and incubate for 20 min. Add Taxol (paclitaxel) from a 10 m*M* stock in DMSO to 20 µ*M* final. Dilute microtubules 1000-fold for use using BRB80 buffer supplemented with 20 µ*M* Taxol. Keep at room temperature, because the MTs tend to depolymerize if kept on ice.
11. Motility buffer for his-tagged motors with nickel–NTA polystyrene beads: 80 m*M* PIPES (pH 7.0), 1 m*M* $MgCl_2$, 0.1% of 2-mercaptoethanol (because lower pH, DTT, and EGTA reduce his–nickel binding).
12. Oxygen scavenging system: 3 mg/mL glucose, 100 µg/mL glucose oxidase, and 20 µg/mL catalase. The glucose oxidase and catalase are made up as a 50X stock solution in BRB80+ 50% glycerol and can be stored frozen at –20°C. The glucose solution is made separately as a 50X stock and stored frozen.

3. Methods

3.1. Microscope

3.1.1. Optical Layout

The optical arrangement, including the beam path for an infrared trapping laser, is shown in **Fig. 1**. The basic microscope is a standard Zeiss Axiovert 135TV. A 100× N.A. 1.3 oil-immersion objective gives good DIC transmission imaging under green light and good infrared transmission (in the opposite direction) for optical trapping. The Zeiss mechanical stage and condenser are replaced with a custom arrangement. For optical trapping, infrared laser light is led via a beam expanding telescope into the epifluorescence port of the microscope. A hot mirror is installed below the objective to bring the trapping light

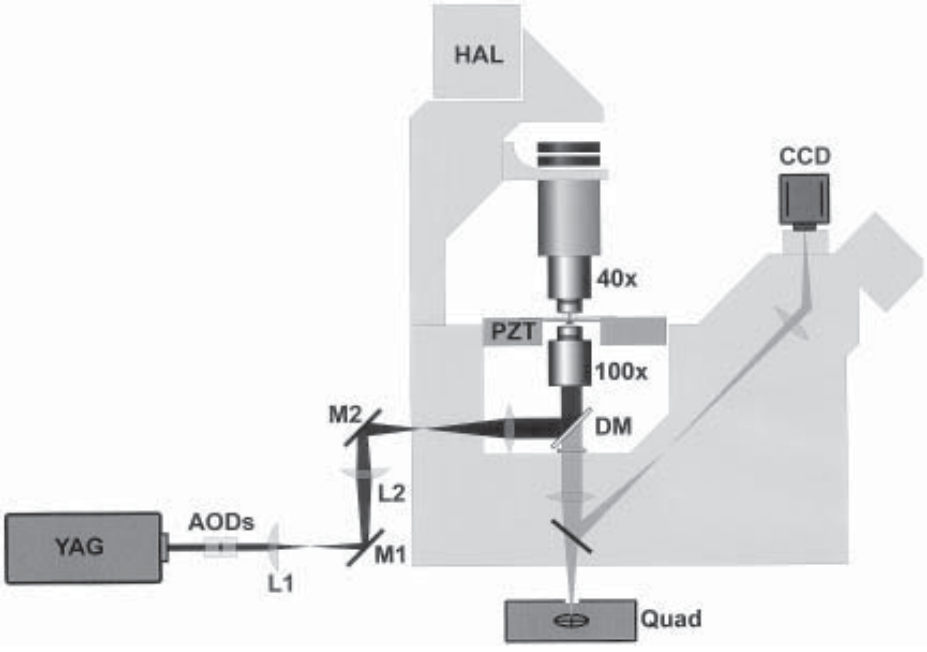

Fig. 1. Schematic showing the arrangement of the laser trap optics. The beam from a Nd:YAG laser (YAG) is steered using a pair of orthogonally mounted AODs. After steering, the beam is expanded using a combination of two external lenses (L1 and L2) and the "tube lens" in the microscope. The periscope (M1, M2) guides the trapping laser light into the microscope and provides the essential adjustment for trap alignment (by beam walking). A dichroic mirror (DM) reflects the laser light up through the objective (100x) to the specimen, but allows the shorter wavelength visible light to pass through. A second infrared blocking filter is mounted below DM. For high-resolution DIC imaging, a second objective lens is used as a condenser (40x). The trapped bead position is measured in the *X*- and *Y*-axes using a quadrant photodiode (Quad), mounted below the Keller port.

up into the specimen plane. Green light transmitted by the specimen passes through this hot mirror and is reflected into a CCD camera mounted on the trinocular. Optionally, the mirror that directs this light into the camera can be slid out, allowing the light to pass directly through the Keller port onto a position detector for bead-tracking experiments.

3.1.2. Condenser

We replaced the Zeiss condenser with an objective lens (Zeiss Fluar, ×40, N.A. = 1.3). The attachment for the objective lens and DIC slider was supplied by Technical Video (www.technicalvideo.com). This was mounted on the end

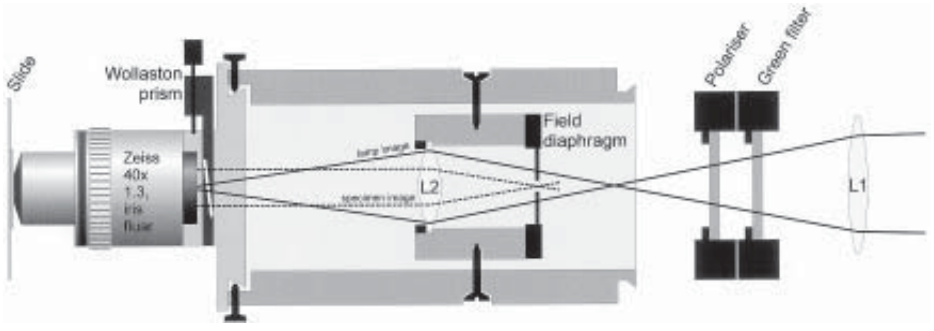

Fig. 2. The optics in the custom-made condenser. An objective lens is used as a condenser to provide the illuminating light for high-resolution DIC. The polarizer and green filter are the standard Zeiss components. Lens L2 (f = 65 mm, 40 mm in diameter) replaces that in place below the 45° mirror on the Axiovert. In combination with lens L1 (f = 30, 25 mm in diameter), a lamp filament image is produced that overfills the back aperture of the objective lens. An iris positioned a distance f (30 mm) from L1 provides the diaphragm for setting Köhler illumination.

of an aluminum tube that also contained an auxiliary lens and an iris diaphragm (**Fig. 2**). The new condenser gives better resolution and contrast than the standard model, allowing us to see microtubules by video-enhanced DIC using the standard Zeiss 100-W tungsten lamp, which is less expensive and much more stable than the brighter 100-W mercury lamp illumination usually necessary to see unstained MTs by DIC. Construction details are given in **Subheading 3.4.1.**

3.1.3. Stability

The microscope sits on a vibration isolation workstation (Newport). The Zeiss stage has been replaced with a sandwich of fixed 8-mm aluminum plates, and this assembly is bolted directly to the optical table. An XY stage with subnanometer positioning and repeatability (Physik Instrumente, P-730.20) is mounted between these plates. The specimen is clipped to a small X-Y micrometer drive (Physik Instrumente, M-312.00) which rides on the nanopositioning stage. This arrangement combines manual, coarse, mechanical X-Y positioning and fine, computer-driven, piezoelectric nanopositioning, allowing the user to scan manually over long distances and then implement nanometer-precision positioning at arbitrary locations on the specimen surface.

3.1.4. Video Camera, Video Processing, and Video Recording

We used an inexpensive CCD video camera (Watec WAT-501ex). The video signal was processed using two-frame averaging and real-time background sub-

traction using a Hamamatsu Argus 20 video processor. The Argus 20 has two video out lines, one of which was connected to an sVHS VCR (Panasonic A-5400) and the other to a grabber card in the PC (DT2855, Data Translation), allowing short video clips to be captured directly into computer memory via RETRAC software (*see* below).

3.1.5. Optical Trapping

In addition to DIC imaging of sliding MTs, the optical layout allows for trapping and tracking of kinesin-coated beads moving on immobilized MTs ***(1–3)***. **Figure 1** shows the beam path for light from the trapping laser, a 3W CW Nd:YAG (Uniphase STA 1064-3E, CW). Here, we describe the arrangement for a fixed optical trap and a movable stage, but it is possible also to steer the optical trap on the *X*- and *Y*-axes using twin acousto-optic deflectors (AODs).

3.2. MT Gliding Assay Flow Cells

For double-objective lens microscopy, specimens must be mounted in flow cells comprising two cover slips. We use a large 55 × 22-mm cover slip (BDH, 406/0188/44) and a small 22 × 22-mm cover slip (BDH, 406/0187/33).

The motility surface is on the larger cover slip. The glass surface is cleaned by immersing the cover slip in ethanol. Remove from the ethanol and quickly clean and dry the cover slip by dragging through a folded lens tissue. Rapidly removing the excess ethanol prevents the streaking that occurs if it is allowed to evaporate slowly (*see* **Note 1**). If required, a nitrocellulose coating can be applied at this stage. We apply a drop (5 µL of 1% nitrocellulose in amyl acetate) directly to the glass and wipe it across using a lens tissue so that drying occurs almost instantly.

The flow cell is made up by applying two lines of grease (Dow Corning, high- vacuum grease). It is not necessary to use spacers other than the grease itself, because it does not matter if the upper cover slip is not perfectly level. As shown in **Fig. 3**, these specimens can easily be made self-sealing by applying the grease in two curves with extra grease at the edges. The solutions can be flowed through and the small cover slip pressed down (applying pressure over the grease with a clean blunt object such as tweezers) to seal in the final solution. The sample volume can be adjusted by changing the separation of the lines of grease, we typically work with a final volume between 4 and 8 µL (*see* **Note 2**).

All solutions used in our gliding assay are based on BRB 80 (*see* **Note 3**). A typical flowthrough procedure for the gliding assay is the following:

1. Use a micropipet flow in one flow cell volume of the motor solution (usually between 0.1 and 20 µ*M*, depending on the motor density required). A surface-

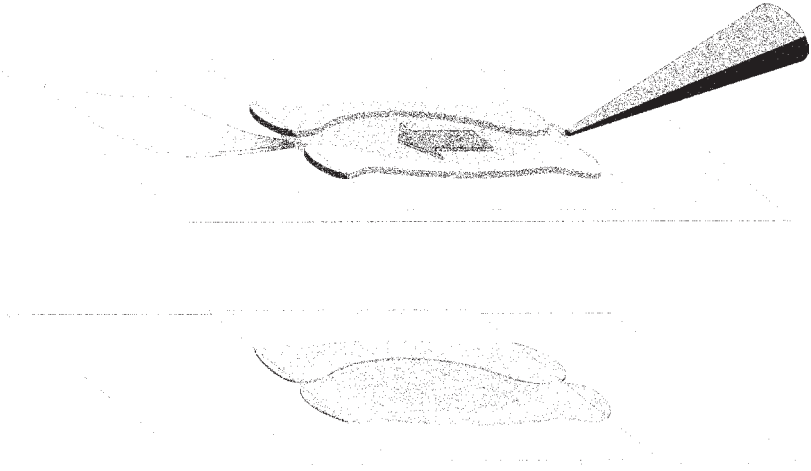

Fig. 3. Preparation of self-sealing flow cells. Dual-cover-slip flow cells can be easily sealed by applying the grease in two curves with extra grease at the ends. The upper diagram shows how assay solutions can be washed through the sample using a micropipet and some filter paper. The final volume can be sealed in the flow cell (lower) by applying pressure to the upper cover slip.

blocking protein is also recommended (we use casein at 0.1 mg/mL). Make a mental note of the approximate flow cell volume. The solution is drawn into the cell by capillarity. Allow the motor to adsorb to the surface for 2–5 min at room temperature (*see* **Note 4**).

2. Wash out nonadsorbed motor with 2 vol of assay buffer, applying the solution to one side of the chamber using a micropipet and drawing the solution gently through the cell using the capillary action of the torn edge of a strip of Whatman 3MM, placed at the exit of the chamber (**Fig. 3**) (*see* **Note 5**).
3. Flow in 2 or more volumes of MTs in motility buffer with 10–20 μ*M* Taxol and the required ATP concentration. As soon as the last volume has flowed in, seal the flow cell, apply immersion oil to both the top and bottom and mount on the microscope (*see* **Notes 5** and **6**).

3.2.1. Microscope Set Up for Video Enhanced DIC

Initial alignment for Köhler illumination is done conventionally ***(4,5)*** by focusing roughly on the specimen and then focusing and centering the condenser assembly by imaging the field diaphragm. MTs on the cover-slip surface are best found using the grease surface on the edge of the flow cells as a guide. Arrange the flow cell so that the objective lens is viewing the grease. Focus within the grease by eye. On focusing down, the grainy appearance of the grease will suddenly disappear and you have found the glass surface. On

moving the stage to view the solution the microscope should be very close to focusing on the motility glass surface (usually within 1 μm).

Now switch to the camera, adjusting fine focus to find the surface. Set the illuminating light intensity to almost saturate the camera (this is the point where signal to noise is maximal). With the contrast on the Argus set to max, MTs should be visible without background subtraction. Defocus slightly so that no surface features are visible and collect a background image (BSUB on the Argus) and begin the real-time background subtraction. MTs should now be clearly visible when the surface is focused. Image noise can be reduced by increasing frame averaging (*see* **Note 7**).

The enhanced video signal is recorded to sVHS videotape. Time-lapse recordings are made using RETRAC and the DT2855 frame grabber card. Frames are captured from the live video signal or from the recorded video.

3.2.2. Velocities from the MT Gliding Assay

For the greatest ease of manual microtubule tracking, the magnification and video system should produce images in which MTs appear to be 4–8 pixels wide. Typically the captured frame should be in the region of 30–60 μm across (assuming the captured frames are full size (e.g., 768 × 576 for CCIR, or 640 × 480 for NTSC). These frame dimensions are easily achieved on the Axiovert with a camera with a ⅓-in. CCD chip and using a ×63 or ×100 objective lens.

Despite recent advances in digital data storage, videotape remains the least expensive and most convenient way of storing real-time video. This is likely to change in the next few years, but for the moment, we use VHS videotapes.

Velocity estimation can only be as good as the digitized field size calibration. The best way to calibrate the setup is to use a graticule slide, a slide with etched lines at 1- or 10-μm intervals (available from microscope manufacturers). RETRAC, our tracking software has a function that simplifies calibration in both the *X*- and *Y*-axes separately. Independent calibrations for the *X*- and *Y*-axes is sometimes important, even if your capture card claims to have "square pixels," the other components in the system may not necessarily maintain the correct video aspect ratio. On a similar note, if you swap CCD cameras you should recalibrate, even if the manufacturers claim the same CCD chip size.

The simplest way to track is to follow the tip of a moving microtubule. For maximum accuracy the time lapse between frames should be adjusted to minimize the effects of operator error when tracking using the mouse. In practice, we try to collect 20 frames, and adjust the time lapse so that the microtubules move across the full field during this time. In comparison to actin filaments, MTs are quite rigid and follow relatively straight paths in the gliding assay (**Fig. 4A**). This makes MT velocity estimation simpler and more forgiving of changes in frame capture rate than actin.

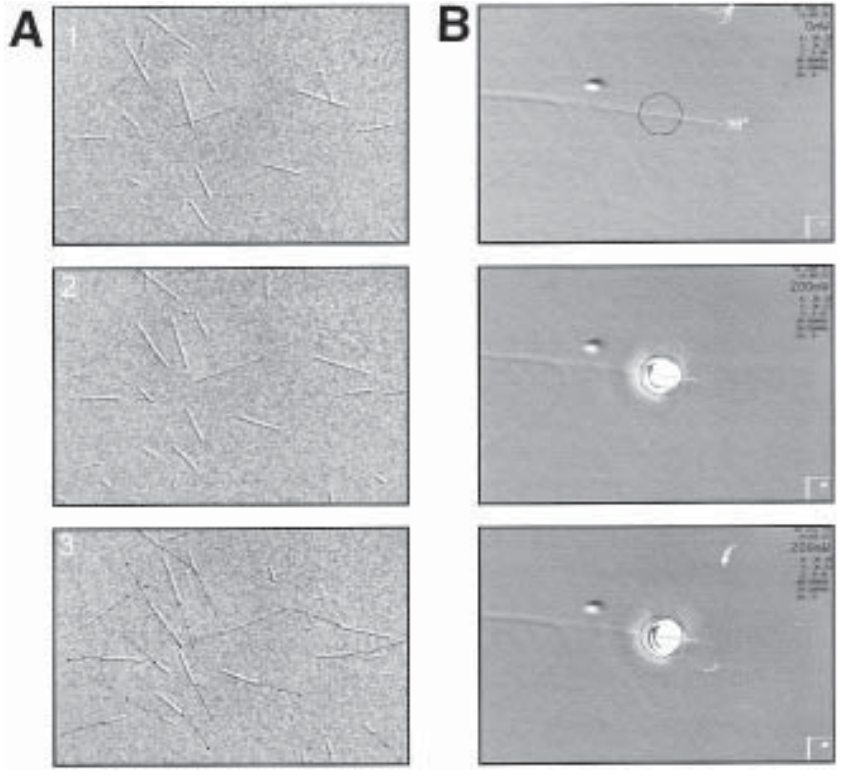

Fig. 4. DIC images showing examples of **(A)** a surface-based multimolecule, and **(B)** bead-based single-kinesin-molecule motility assays. In **(A)**, a nitrocellulose coated cover slip has been decorated with casein and the fast kinesin nkin. Three consecutive images are shown, each 1.5s apart. The field displayed is 43.4 × 28.7 μm. Single microtubules glide over the motor-coated surface. The MT tracking data for these images are overlayed on frame 3. In DIC, microtubules that are in the same plane as the Wollaston prism (here upper right to lower left) have much less contrast. In **(B1)**, a single MT adsorbed to the glass surface is marked for location (XYZ) and orientation using a video overlay. The optical trap position is shown with the central overlaid circle. A trapped polystyrene bead complete with attached kinesin molecule is positioned over the MT **(B2)**. After some seconds of diffusional rotation of the bead, the motor is able to bind to the MT and pull the bead out of the trap center until it reaches maximal force **(B3)**. Here, the bead runs approx 200 nm until it reaches stall force, a similar event to that shown by bead position data in **Fig. 5**. Typically after a few seconds at stall force, the motor detaches and the bead moves quickly back to the trap center. In **(B)** the field dimensions are 17.2 × 11.3 μm. It is an inherent property of DIC microscopy that small objects appear larger than they really are. The MTs appear to be 200–300 nm and the bead appears to be 1.5 μm in diameter; their true diameters are 25 nm and 800 nm respectively.

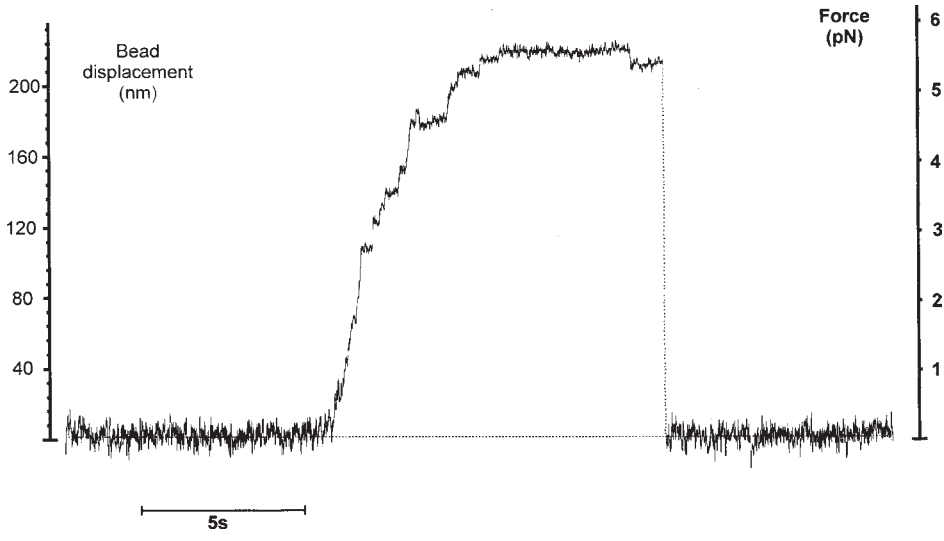

Fig. 5. An example single-kinesin-molecule optical trap recording. The record was made from a his-tagged kinesin attached to a Ni–NTA polystyrene bead (1 μm in diameter). The data show the bead position data during a single-kinesin-molecule interaction with a microtubule (off-axis bead position data not shown). As the kinesin pulls the bead out of the center of the trap, the force acting on the molecule increases (linearly) until it reaches a maximum force of just over 5 pN (trap stiffness 0.025 pN/nm). Progress at forces over 2 pN is sufficiently slow to resolve single 8-nm forward (and backward) steps of the molecule. Data were stored at 5 kHz per channel and filtered with a 101-point (20 ms) averaging filter. The concentration of ATP was 10 μ*M*.

3.3. Single Molecule Optical Trapping

It is possible to study single-molecule motility by diluting out the motor until MTs attach via single motor molecules to the surface ***(6)***. An alternative that allows loads to be applied is for microtubules to be immobilized on the glass surface; motors are then attached to silica or polystyrene beads, and the bead–motor constructs are set to move along the microtubule tracks. In the simplest arrangement, beads carrying motors are captured out of solution by driving them into a fixed optical trap, by moving the servo stage. Once the beads are captured, further manipulation of the stage is used to bring the microtubule within range of the motor. The stage is then parked and interactions of the motor with the track recorded on video tape as excursions from the trap center. The trap may also be switched off at this point, to allow the motor to make unconstrained runs. Developments of this basic arrangement add steering of the trap and bead tracking at a higher time resolution. In all cases, the same sample preparation is used.

3.3.1. Optical Trapping Flow Cell Preparation

1. The solutions used in the single-molecule samples are based on BRB80, except when using his-tagged motors with nickel–NTA polystyrene beads (*see* **Subheading 2.2.**, **item 11**). An oxygen scavenging system is used in all our trapping solutions. Solutions are supplemented with glucose and the enzymes immediately before washing into the flow cell. This is not necessary if you are not using fluorescence or a laser trap, or if trapping at low power.
2. Silica beads (0.5–1.0 µm in diameter) are decorated with purified kinesin as follows. Surfactant present in the bead stock is removed by centrifuging a couple of minutes at 1000 or 2000*g* is usually sufficient to settle silica beads on a benchtop centrifuge. The beads are resuspended in motility buffer with 50–100 µg/mL casein. It may be necessary to pass the solution through the micropipet several times to break up clumps formed because of loss of surfactant. The presence of the casein should now prevent beads from clumping together. The kinesin motor can now be added. Care should be taken to mix the beads well (vortex or micropipet) soon after the motor is added to give consistent kinesin labeling. Any unbound kinesin can be removed by a final stage of centrifugation and resuspension in the casein blocking buffer (*see* **Notes 8** and **9**).
3. Microtubules are washed into the flow cell and given 5–10 min to adsorb to the glass. There must be no casein in this first solution, as this competes with the MTs for adsorption to the glass. The MTs still in solution are washed out with two to three flow cell volumes of motility buffer with 50–200 µg/mL casein (*see* **Note 10**). This solution also blocks (casein coats) the glass surface and helps prevent the beads from sticking when they are added. After a couple of minutes of block time, the motor-labeled beads are flowed through in the motility buffer with casein and the desired concentration of ATP (*see* **Note 11**).

3.4. Hardware Considerations for Viewing Single MTs in DIC

The main changes required to make a research quality microscope capable of resolving single MTs in DIC are as follows: increase the illumination, increase the contrast in the video signal, and perform some real-time digital image enhancement.

Increasing the amount of light increases the number of bits in the digitised image that encode the shading across a MT. More light leads to less graininess in the final image; that is, it improves the signal-to-noise ratio. Remember that the crossed polarizers in the microscope remove most of the lamp light. This, together with the high magnifications involved, means that you will be unlikely to saturate your camera.

One method of providing more light is to use a mercury lamp. Technical Video provide the necessary equipment, including a light guide that provides a good uniform source for DIC illumination. Alternatively, the more stable 100-W tungsten–halogen source can be used along with an objective as a condenser (*see* **Subheading 3.4.1.**).

Because of the extremely high-contrast settings necessary to view single MTs in DIC, some method of on-line digital image processing is essential to produce reasonable images. The Hamamatsu Argus image processor provides the contrast enhancement and real-time image processing functions necessary. The frame averaging reduces image noise, but do not be tempted to set a high frame averaging. Depending on the MT velocity, high frame averaging can make the MT ends less distinct and so make tracking more difficult. Software in development (freeware, *see* our website) will allow you to capture full-motion grayscale video with real-time background subtraction on a Windows PC, performing some of the Argus functions. Note that if recording to videotape with this software, the VGA card must have a video-out option.

Unless your building has particularly dynamic flooring, expensive vibration isolation optical tables should not be necessary for the gliding assay. Most minor vibration problems can be resolved by sitting the microscope on a metal plate that is cushioned with foam or bubble-pack.

3.4.1. Constructing a Condenser for High-Resolution DIC

Of all the microscope modifications described here, this is the "simplest" to reproduce and provides a great improvement in the quality of DIC images over the Zeiss equipment. However, it should be noted that some engineering and careful adjustment of optical components is required.

Technical Video (www.technicalvideo.com) can provide an objective/condenser mount for a Zeiss Axiovert microscope that gives some improvement in DIC resolution. This kit makes it possible to see (just) single undecorated MTs in tungsten-illuminated DIC. However, there are two main drawbacks with this system: first, most of the illuminating light is lost because of considerable overfill of the back aperture, and second, a Köhler illumination position cannot be attained because of the lack of an iris. This kit does provide an objective lens and Wollaston mount that will pay for itself in saved engineering time. You will have to produce your own condenser tube (113 mm long, 65 mm outside diameter) with a lens and iris mount. Make sure you can adjust the center position of the lens. Paint the inside with a matte black. The lens L1, iris, and the objective lens can be centered with the aid of the Bertrand lens on the Axiovert optovar.

The choice of objective lens used for your condenser is an important one. There are several points to consider. First, an iris is very useful; this becomes the condenser aperture diaphragm, allowing you to find the optimal balance of contrast and resolution in your image. Compared to the imaging objective lens, the condenser objective should have an equivalent or preferably higher N.A. to provide the maximum resolving power. Choose a lower magnification than the imaging objective lens. Make sure the working distance is enough for your application, remembering that you will probably be viewing the lower cover

slip of the cover-slip sandwich. We chose to use the Zeiss Fluar ×40, 1.3 N.A., with an iris. This is the least expensive high-magnification, high-N.A. lens with an iris and a usable working distance for our samples.

The combination of the two lenses puts more light down through the objective. The upper lens L2 (focal length f = 65 mm) replaces the standard Zeiss lens and screws into the tilting condenser carrier just below the 45° mirror. The lamp filament image at the back of the objective overfills the back aperture. For accurate Köhler illumination, the field diaphragm must be 30 mm (L2 focal length) from L2. The field diaphragm will then be in focus and centered when the objective/condenser is in its best (Köhler) illuminating position.

There are some disadvantages to the dual cover slip/dual objective style of microscopy. The cover-slip sandwich must be thin (less than 100 µm in our case), which rules out some samples, although is quite acceptable for most in vitro motility assays. Both cover slips need immersion oil, and this soon becomes second nature. Note that most standard Zeiss slide mounts are unsuitable for the dual-cover-slip samples.

3.4.2. Modifications for Optical Trapping

A profound understanding of optics is not essential to convert a standard microscope for optical trapping. More essential is a healthy fear of invisible but blindingly bright radiation. The complexity of the task really depends on the type of recordings you are planning to make. At its simplest, a trap can be used as a micromanipulator to place motor-coated beads onto MTs to follow their movement using video. Such a trapping microscope does not require the mechanical stability, electronics, or software development required to record single-molecule steps.

Several high-quality reports have described the general principles for design and calibration of optical trapping apparatus ***(2,7)***. This section will cover some aspects of improving microscope stability to the nanometer level.

3.4.2.1. Laser Stability

Before buying a laser for making single-molecule recordings, ask the manufacturer for information on beam-pointing stability. Better still, measure the beam-pointing stability. With the short beam path in our apparatus (**Fig. 1**), a tiny 1 µrad change in beam direction at the laser corresponds to approx 8 nm of trap displacement in the specimen plane. Thus, in order to resolve the kinesin steps of 8 nm (or smaller?), the laser-pointing stability should be better than 1 µrad.

Laser drift is usually related to heating in the laser head, so a good thermal contact between the laser and the optical table can help. Lasers that have a cooling fan incorporated may have better temperature stability but vibrate too much for single-molecule recordings.

3.4.2.2. Beam Pathway Stability

For the same reasons, it is a good idea to keep the laser beam path as short as is practical; this reduces the "optical leverage" and thus reduces the influence of beam pointing on the trap position. Similarly, keep the optics close to the table using small rigid mounts.

To measure the stepwise progress of single kinesin molecules, vibration isolation is an absolute necessity. We use a table from Newport, which in combination with the high mechanical stability of the described microscope, provides sufficient isolation that we can walk around on the wooden floor of the room during measurements.

Carefully ducting the beam path is not only important for laser safety. Small air currents can have a surprisingly large influence on beam pointing. Also, keeping the beam path draftproof, as well as lightproof, keeps dust off the sensitive optical components in the light pathway.

3.4.2.3. Beam Steering

The AODs are located in the beam pathway in a position where beam steering produces a rotation of the expanded beam at the back aperture of the objective and, hence, a translation of the trap position. This also ensures that there is minimum light loss (i.e., minimum change in trap geometry and stiffness) when the trap is moved far from the central position ***(8)***.

3.4.2.4. Stage Stability

When not steering the laser, a trapped bead is locked relative to the position of the objective lens, whereas the target microtubule is locked to the stage. Any unwanted movement of the objective lens relative to the stage will translate directly to undesirable drift of the motor across or away from the microtubule. This movement can be both vibrational or slower drift of the stage and can be surprisingly large in amplitude.

Slow stage drift is almost always thermal in origin. A slow increase in room temperature during the day can cause unacceptable drift of the sample over the objective. Temperature-controlled environments can be made/bought for microscope stages or whole microscopes, but unless they are very well insulated, they still introduce thermal gradients that lead to drift. Controlling the room temperature with air conditioning gives the most stable environment. Direct the air-conditioning output away from the microscope to reduce the effects of thermal gradients and the temperature cycling. Keep sunlight and any apparatus that run hot away from the microscope stage.

As a general rule, try to overengineer everything on the microscope stage that is not mounted on the piezoelectric stage. First, thicker plates react more slowly to changes in room temperature, even the slow 1°C or 2°C of thermal

cycling from the air conditioning will be significant when measuring nanometers. Second, the increase in mass of the microscope stage will tend to reduce the influence of extraneous vibrations, whether picked up mechanically through the table or air-borne (acoustic).

The objective lens is gripped by polytetrafluoroethylene (PTFE) on the lower aluminum plate. This allows normal focusing but considerably reduces XY drift.

Using a bead position detector, it is quite simple to measure stage stability. Prepare a slide with beads fixed on the surface. Simply drying a bead solution onto the cover-slip surface can often be sufficient. Use a final flowthrough (sealed as in **Fig. 3**) to wash out any beads that are not stuck down. A solitary surface bead can now be used with the bead position detector to measure any stage drift. Take care because some beads that appear solidly attached to the surface may have residual Brownian that will only show up on the position detector. Vibrations and resonance of the microscope can also be studied by applying Fourier methods to this bead position data.

4. Notes

1. Methods other than fluorescence for imaging single MTs include dark field ***(9)*** and phase as well as DIC microscopy ***(5)***. All these methods are sensitive to irregularities and contamination of the cover-slip surface. This should be considered an advantage rather than an inconvenience when compared to fluorescence microscopy, because by showing uneven, badly coated, or dirty cover-slip surfaces, quality control is introduced. The experimenter is forced to deal with problems (such as dirty glass or particles in assay solutions) that would be invisible using fluorescence microscopy. Generally, the surface of cover slip benefits from ethanol washing, although you should expect some variability, even between cover slips from the same box.
2. Any evaporation from the edges of the flow cell during slide preparation can be avoided by covering it with a moisture chamber (just an inverted Petri dish with moistened tissue stuck to the inside). The sealed flow cells are useful in the gliding assay as well as in the single-molecule experiments. Removing the evaporation problem ensures that the solution ionic strength remains unchanged. Particularly where very low motor densities are used, there will be little change in ATP concentration and sealed slides will show the same gliding velocity for 1 h or more (although an ATP-regenerating system may be necessary when working at low ATP concentrations).
3. Motor activity can also be sensitive to thiol oxidation, so you may find that including 5 m*M* DTT in the motility buffer improves motility.
4. Some motor proteins bind better to the glass surface than others. Erratic motility may be the result of the protein denaturing on the glass, or binding in such a way that its force-generating conformational change is inhibited. Areas of uncoated glass can also bind microtubules and inhibit sliding. Increase motor concentration if possible or try infusing the motor twice over and/or reducing or eliminat-

ing the wash step prior to infusing microtubules. Including casein at 50–200 μg/mL in the assay buffer efficiently protein-coats the glass. Such a coating can, in some cases, increase the sliding velocity observed ***(9)***. For some motors, a hydrophobic surface such as nitrocellulose allows more motor to bind. There are several ways to apply a thin coating of nitrocellulose to the glass surface. We find that those methods that rely on slow evaporation of solvent do not produce a "clean" surface (meaning appears clear in DIC). The nitrocellulose is dissolved in amyl acetate, take care because this is a highly flammable mixture.

5. A single flow cell volume does not replace the previous contents of the flow cell. Try flowing through a dye and you will see that there is by no means a clean replacement of the flow cell contents. Particularly at the edges near the grease there is much slower flow. Take care to wash through several flow cell volumes, particularly where concentrations are important (e.g., if you want to be confident in your final ATP concentration).
6. When working at low concentrations of ATP, it may be necessary to use an ATP-regenerating system. There are no rules here because if you are working at very low motor densities, there will be a relative "ocean" of ATP available, even at low concentrations. This is complicated by the fact that it is hard to know just how much motor bound to the surface and how much was washed out when the flow cell was prepared. The best indication is that if you see the sliding velocity gradually falling with time, this suggests that ATP concentration is falling.
7. For ease of tracking, it is important to consider the number and length of MTs in the assay. Overcrowding the surface can make tracking trickier than it need be. Similarly, if MTs are very long, the number of trackable MT ends is too low. The stock of MTs can be shortened by breaking them up by shearing. This can be done by micropipetting the MT solution with the pipet tip pushed to the end of the Eppendorf tube and forcing the solution through the small gap (two or three times should be enough; try to avoid bubbles).
8. Silica or polystyrene? Because of higher density, silica beads sink faster than polystyrene beads. For samples on an inverted microscope, this is an advantage. If, for example, you are planning to do a bead-based motility assay without laser trap assistance, then for convenience silica beads should be used. The slow rate at which silica beads will diffuse into MTs on the lower glass surface will still be several orders of magnitude higher than that for polystyrene because most polystyrene beads will remain up in solution much of the time. One of the disadvantages of silica is that it has a lower refractive index than polystyrene. For this reason, silica beads produce a smaller signal on the bead position detector and also require more laser power to produce a given trap stiffness. The high sink rate for silica can mean that bead stock must be remixed for every flow cell, particularly when carefully trying to control the final bead density. A final note about beads is not to believe the bead size standard deviations claimed by manufacturers. Care should be taken when making recordings that the trapped bead is not much larger/smaller than the others. The trap calibrations that require a radius will give inaccurate stiffness estimations.

9. When making single-kinesin-molecule recordings it is important to repeat the bead preparation, reducing the amount of motor added until motor loading is very low. We continue reducing motor until approximately half of the beads neither run in the presence of ATP nor bind to MTs in zero ATP conditions (rigor).
10. Immobilizing microtubules — surface cleaning and treatment. With our method of cover-slip cleaning with ethanol, sufficient MTs attach firmly to the glass surface to make single-molecule recordings. Other reports show that coating the glass with 4-aminobutyl-dimethyl-methoxysilane provides extremely well-attached MTs. We are currently working on this method of silanation and so cannot provide a protocol. MTs that can be seen to be poorly attached to the surface (where some Brownian motion is visible) do not provide a good substrate for making recordings. They introduce a compliance that makes the resolution of single steps difficult. As can be seen from the trace in **Fig. 5**, attachment of the motor to the MT stiffens the system substantially. This can be seen by comparing the amplitude of the Brownian movement of the bead at the start and end of the trace (no attachment) to that in the plateau at maximum force. In records such as this, the stiffness of the bead–cover slip link (i.e., bead–motor–MT–glass) can be typically 10 times that of the trap stiffness.
11. Sealed samples are essential when making single-molecule recordings. The evaporation from the edges of nonsealed samples causes a slow flow of solution passed the trapped bead. This flow can cause free beads to drift by; these beads can interfere with the bead detector signal making recordings useless, or beads can drift into the trap.

References

1. Block, S. M., Goldstein, L. S., and Schnapp, B. J. (1990) Bead movement by single kinesin molecules studied with optical tweezers [see comments]. *Nature* **348**, 348–352.
2. Svoboda, K. and Block, S. M. (1994) Force and velocity measured for single kinesin molecules. *Cell* **77**, 773–784.
3. Svoboda, K. and Block, S. M. (1994) Biological applications of optical forces. *Annu. Rev. Biophys. Biomol. Struct.* **23**, 247–285.
4. Inoue, S. and Spring, K. R. (1997) *Video Microscopy: The Fundamentals*. Plenum, New York and London.
5. Salmon, E. D. and Tran, P. (1998) High-resolution video-enhanced differential interference contrast (VE-DIC) light microscopy. *Methods Cell. Biol*. **56**, 153–184.
6. Howard, J., Hudspeth, A. J., and Vale, R. D. (1989) Movement of microtubules by single kinesin molecules. *Nature* **342**, 154–158.
7. Simmons, R. M., Finer, J. T., Chu, S., and Spudich, J. A. (1996) Quantitative measurements of force and displacement using an optical trap. *Biophys. J*. **70**, 1813–1822.
8. Molloy, J. E. (1998) Optical chopsticks: digital synthesis of multiple optical traps. *Methods Cell. Biol*. **55**, 205–216.
9. Howard, J., Hunt, A. J., and Baek, S. (1993) Assay of microtubule movement driven by single kinesin molecules. *Methods Cell Biol*. **39**, 137–147.

9

Use of Photonic Force Microscopy to Study Single-Motor-Molecule Mechanics

Sylvia Jeney, Ernst-Ludwig Florin, and J. K. Heinrich Hörber

1. Introduction

With the intensive study of functional properties of motor proteins at the single-molecule level, many new insights were gained on the correlation between the kinesin structure and its function. Recent work on kinesins has demonstrated that the neck and the first hinge region of the motor play an important role in kinesin directionality, velocity, and ATPase activity ***(1–4)***. The investigation of the three-dimensional (3D) mechanical properties in this context can provide the information to understand how structural changes stipulate the molecular function. A 3D view is essential, as mechanical properties can be anisotropic and motor molecules, in general, move in space to fulfill their function.

One approach to this problem is the application of photonic force microscopy (PFM). It relies on a combination of optical tweezers and a 3D position detector ***(5,6)***, which is used in conjunction with a thermal position fluctuation analysis method based on Boltzmann statistics ***(7)***. This technique provides access to 3D energy landscapes with a resolution of one-tenth the thermal energy ***(8)***. The spatial and temporal resolutions are in the nanometer and microsecond regions, respectively.

A common scheme in optical tweezers experiments is the use of small latex or glass beads coated with the biomolecules of interest. These functionalized beads are manipulated with the optical tweezers and their interactions probed. In this chapter, we detail the methods for mechanical investigation with particular reference to kinesin. Despite this focus, the technology described here is of general purpose and has a widespread applicability (e.g., on questions related to cellular transport phenomena).

From: *Methods in Molecular Biology*, Vol. 164: *Kinesin Protocols*
Edited by: I. Vernos

In the following, we first describe the biochemical isolation of kinesins from cells, which can be performed where no recombinant proteins are available (*see* Chapters 1, 4 and 6 for other purification methods). This is a straightforward 1-d, high-yield procedure for kinesin purification from chicken brain developed by Hanry Yu (personal communication). We present the protocols for the preparations of protein-coated beads and an adequate sample chamber. A brief introduction to instrument design (described in detail elsewhere, e.g., **refs. *9*** and ***10***) is provided along with the experimental setup and data analysis. Finally, we outline how to extract information about the molecular mechanics from the recorded 3D energy landscapes.

2. Materials

2.1. Kinesin

1. Approximately 25 fertilized chicken eggs after 12–13 d incubation at 37°C (*see* **Note 1**).
2. PMEE' (working buffer for kinesin isolation): 35 m*M* piperazine-*N*,*N*-*bis* (2-ethanesulfonic acid) (PIPES) (pH 7.2), 5 m*M* $MgCl_2$, 1 m*M* EGTA, 1 m*M* EDTA; stored at –20°C.
3. PMEE' + 25% sucrose; PMEE' + 20% sucrose; PMEE' + 5% sucrose; all stored at –20°C.
4. Protease inhibitor 1: 0.2 mg/mL Pepstatin A, 2.0 mg/mL N^{α}-*p*-tosyl-L-arginine methyl ester (TAME), 2.0 mg/mL *N*-tosyl-L-phenylalanine chloromethyl ketone (TPCK), stored 200X at –20°C in 50% EtOH/H_2O.
5. Protease inhibitor 2: 0.2 mg/mL leupeptin, 2.0 mg/mL soybean trypsin inhibitor (SBTI), stored 200X at –20°C in H_2O.
6. Phenylmethylsulfonyl fluoride (PMSF) stored at –20°C in 2-propanol (*see* **Note 2**).
7. 1 *M* dithiothreitol (DTT) in PMEE', 200 m*M* GTP in distilled H_2O (pH 6.7), 10 m*M* Taxol in water-free dimethylsulfoxide (DMSO; *see* **Note 3**), D-glucose in powder, 5'-Adenylylimidodiphosphate (AMP-PNP) in powder, hexokinase, 100 m*M* ATP in distilled H_2O (pH 6.7), all stored at –20°C.
8. Releasing buffer: PMEE', 1X protease inhibitor 1, 1X protease inhibitor 2, 1 m*M* DTT, 0.5 m*M* GTP, 20 µ*M* Taxol, 10 m*M* ATP, 20 m*M* $MgCl_2$.

2.2. Microtubules

1. A reliable source of tubulin should be accessible. Several protocols on how to purify and cycle tubulin from bovine brain are available in the literature ***(11)*** (*see also* Chapter 1). High-quality tubulin can also be purchased (e.g., Cytoskeleton, Denver CO). To produce a tubulin preparation suitable for in vitro assays, the purified tubulin should be cycled to select for active subunits and remove free nucleotides (*see* Chapter 10). Store tubulin at –80°C or in liquid nitrogen (N_2liq).
2. Polymerization buffer (BRB80+GTP): 80 m*M* PIPES (pH 6.8), 2 m*M* $MgCl_2$, 1 m*M* EGTA (*see* **Note 4**), 1 m*M* GTP.
3. Stabilization buffer: BRB80, 15 µ*M* Taxol (*see* **Note 4**).

2.3. Bead Coating

The beads commonly used for optical trapping in biology are made of latex or silica and have sizes ranging from 0.2 to 1 μm in diameter.

Assay buffer: 80 m*M* PIPES (pH 6.9), 4 m*M* $MgCl_2$, 1 m*M* EGTA, 1 mg/mL casein, 50 m*M* KCl, 1 m*M* DTT, 20 μ*M* Taxol.

2.4. Flow Cell

Flow cells are constructed as described in **ref. *12*** but double-stick tape (Tesa, Germany) can also be used instead of grease to stick the cover slips together. The cover slips are cleaned with 2% Hellmanex in H_2O (Hellma, Germany) or saturated KOH in ethanol and modified with (3-Trimethoxysilylpropyl)-diethylenetriamine (DETA) (Huls, Germany) in 1 m*M* acetic acid.

2.5. Instrument

A detailed description of the theoretical background of optical trapping and trap construction can be found in the literature (in particular, **refs. *9*, *10*,** and ***13***). Provided here is a description of our experimental apparatus, which is restricted to the components necessary for PFM.

The optical arrangement is described in **Fig. 1** by following the light path. The optical tweezers are implemented around a conventional inverted light microscope with standard DIC equipment (Axiovert 35, Zeiss, Germany). The complete setup is built on a vibration isolated optical table (Newport, Germany).

To resolve the movement of the bead coated with the biomolecules, it is required that the bead position in the trap can be determined with high spatial and temporal resolution. **Figure 2** shows the arrangement of the position detection in more detail. The motion of the bead, trapped close behind the geometric focus, is detected by measuring changes in intensity with the quadrant photodiode (QPD). These intensity changes are the result of the alteration in the interference pattern caused by the movement of the bead. The object's position detection can be explained by a far-field interference effect between the illuminating light and the light scattered by the trapped particle ***(6,14)***. The lateral and axial movement of the trapped object can be measured simultaneously with nanometer resolution and a maximum bandwidth of several megahertz, which is limited practically to 100 kHz by the data acquisition rate of the PC. Both differential signals from the QPD serve as the lateral position signal; the total laser intensity signal corresponds to the axial position signal. All three signals are digitized (one dimension per channel) by a transputer data acquisition board featuring two A/D converters with 16 MB memory on board and a digital signal processor (DSP) programmable in ADWinBasic (AD-Win 5F, Jäger Elektronik, Germany).

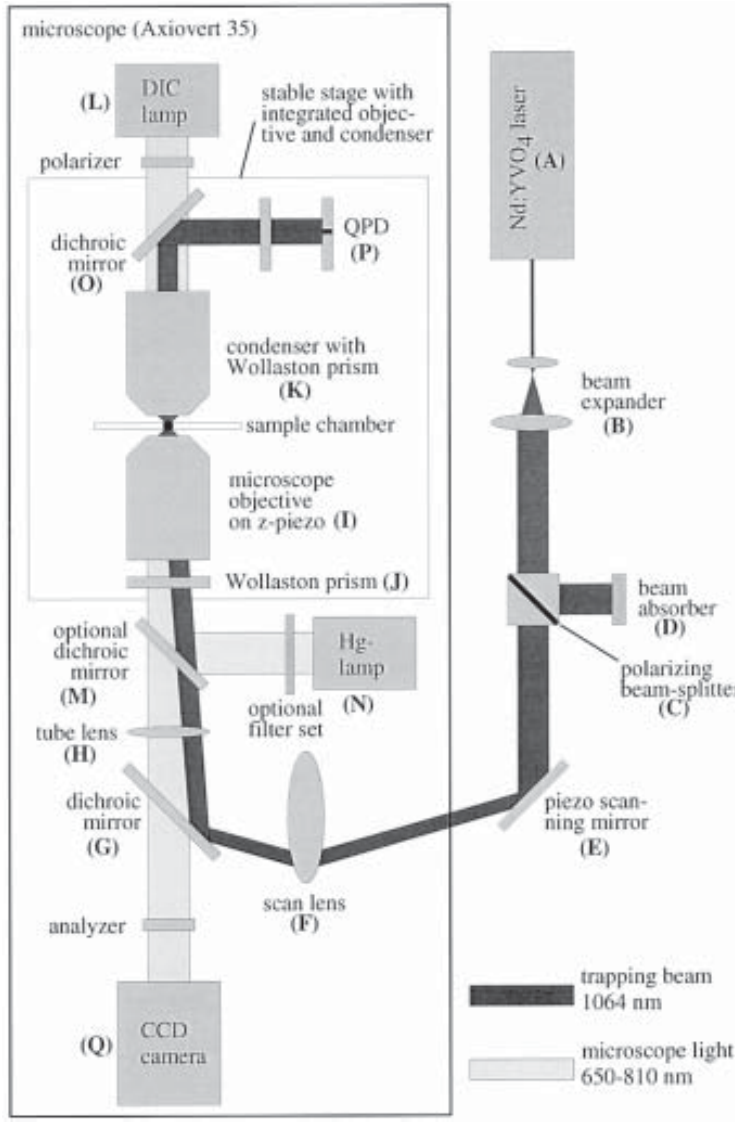

Fig. 1. Scheme of the PFM. The trapping beam is emitted by a diode-pumped Nd:YVO_4 laser (A) in the near infrared (wavelength: 1064 nm, T20-B10–106Q, Spectra Physics, Germany) with a maximum power of 3 W in continuous-wave mode. To achieve a high-intensity gradient necessary for a good trapping efficiency, the back aperture of the focusing device is overilluminated with the laser light by about 1.5 times. This is accomplished by adapting the effective diameter of the laser beam with a beam expander (B). For stability purposes, the laser is run at high power and the laser intensity in the focus is regulated afterward by a polarizing beam splitter (C). A beam

Because the commercially available microscope sample stages do not provide the necessary mechanical stability for measurements on single molecules, a more rigid stage was custom built. This new sample stage guarantees a high stability with respect to drift and mechanical vibrations. The lateral displacement of the sample chamber is performed by a scan stage with capacitive position sensors and a digital feedback (NPS3220, NPS-XY-100A, Queensgate, UK). The sample holder is screwed onto the scan stage and can be moved 100 μm in *x* and *y* with a precision of less than 1 nm.

The microscope images are recorded by a capacitive coupled device (CCD) camera supplemented with a camera controller (C5405-01 and C2400, Hamamatsu, Japan) and stored on an S-VHS video film. In order to visualize microtubules (MTs) the image signal can be amplified and the background subtracted by a real-time image processor (Argus 20, Hamamatsu, Japan).

2.6. Data Analysis

There are several commercially available software packages for data acquisition such as Lab View (National Instruments) or Visual Basic (Microsoft). For data analysis, we use IgorPro (Wavemetrics). The 3D reconstruction of

---

absorber (D) is placed next to it to collect the discarded light. The beam is then deflected onto a scanning mirror (E), which is glued on a piezo that can be tilted around both axis (PSH2zNV, power supply: ENV 400/1, Piezosysteme Jena, Germany). The scanning mirror together with the scan lens (F) allows a lateral translation of the laser focus in the object plane of maximum 3.9 μm in *x* and *y*. Inside the microscope, the beam is directed by a dichroic mirror (G) through the tube lens (H) onto the high-numerical-aperture (N.A.) oil-immersion objective (I) (Neofluar 100x, N.A. = 1.3, Zeiss), which focuses the laser beam in the object of the microscope, generating a diffraction limited spot in the sample chamber. The objective is mounted on a piezoelectric actuator (I) (PI-foc, P721.00, Physik Instrumente, Germany), permitting the shifting of the laser focus along the optical axis over a range of 100 μm. The PI-foc and the scanning arrangement move the laser focus in three dimensions and, therefore, serve as a 3D manipulator for the trapped object. The standard DIC equipment features a Wollaston prism (J) placed under the objective and a second one in the condenser (K). The DIC illumination (L) used here is restricted to a wavelength of about 700 nm. Optionally, a dichroic mirror (M) and a Hg lamp (N) can be placed together with a filter set (BP-546 nm for excitation, LP-590 nm for emission) into the light path in order to use fluorescence microscopy. For this purpose, the MT and the bead have to be labeled with a fluorophore like Rhodamine. The laser light scattered by a trapped particle is collected by the condenser lens (K) and projected by a second dichroic mirror (O) onto the quadrant photodiode (P) (S5981, Hamamatsu, Japan). Both dichroic mirrors (DELTA Lys. and Optic, Denmark) reflect the laser light and transmit the light for DIC illumination, which is guided onto a CCD camera (Q) (Hamamatsu, Japan).

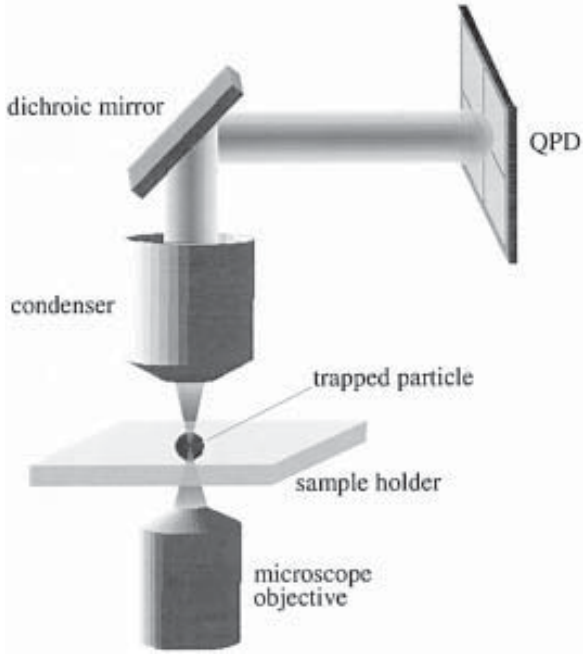

Fig. 2. Arrangement of the forward scattered light position detection by a quadrant photodiode (for details, *see* text). The QPD is placed in the back focal plane of the condenser and fixed magnetically on an iron plate in order to enable the lateral manual adjustment of the detector relative to the projected beam.

position histograms and energy landscapes are represented with AVS (Advanced Visual Systems Inc.).

3. Methods

3.1. Kinesin Purification

1. Pop off the eggs, cut the embryo's heads, extract the brain, and put it in PMEE' on ice.
2. Wash the brains twice in PMEE' by spinning it at 1000*g* for 3 min at 4°C.
3. You obtain approx 4–5 g of brain, freeze the quantity you do not need (*see* **Note 5**) in N_2liq and keep at –80°C.
4. Homogenize by adding 1 mL of homogenization buffer (PMEE', 1X protease inhibitor 1, 1X protease inhibitor 2, 1 m*M* DTT, 1 m*M* PMSF) per gram of brain. Homogenize 10 times, wait 5 min, and repeat 10 times (*see* **Note 6**).
5. Organelles and membranes are washed away from the homogenate by centrifugation (first at 20,201*g*, 4°C, in a Sorvall superspeed centrifuge, SS34 rotor for 15 min and then at 215,577*g*, 4°C, in a Beckman ultracentrifuge, SW60 rotor for 20 min).

7. The supernatant now contains cytoskeletal and associated proteins. By adding 1 m*M* GTP and 200 µ*M* Taxol, the supernatant is incubated for 15 min at 37°C to promote endogenous microtubule (MT) polymerization.
8. 2 m*M* AMP–PNP and 1 *M* D-glucose is added to the viscous MT solution to induce a rigor-state binding of the motors to MT. Add separately 2 U/mL hexokinase, mix the MT solution gently, and put it at 37°C for 15 min.
9. The MT–motor complexes are then isolated from the residual proteins through a 500-µL PMEE'/25% sucrose cushion containing 20 µ*M* Taxol (at 121,262*g*, 25°C, for 15 min, in a Beckman ultracentrifuge with SW60 rotor).
10. The MTs are in the pellet, which is resuspended in 600 µL PMEE' supplemented with 1X protease inhibitor 1, 1X protease inhibitor 2, 1 m*M* DTT, 0.5 m*M* GTP, and 20 µ*M* Taxol. To wash away the sucrose, the MTs are centrifuged for 10 min at 25°C, 214,200*g* (Beckmann ultracentrifuge, TLS 55 rotor).
11. Resuspend the MTs in 400 µL releasing buffer to release the motors without destroying the polymers.
12. After a 15-min incubation at room temperature, the MTs are centrifuged (at 214,200*g*, 25°C, in a TLS55 rotor for 15 min).
13. The supernatant (= ATP release) with the motor proteins is loaded onto a 5–20%-sucrose density gradient (*see* **Note 7**) to separate the kinesin molecules from other motor proteins in a high-speed centrifuge (at 250,100*g*, 4°C, in a SW60 rotor for 4 h).
14. Finally 400 µL fractions are collected successively and analyzed by gel electrophoresis (8%, sodium dodecyl sulfate-polyacrylamide gel electrophoresis [SDS-PAGE]) to identify the fraction containing kinesin.

The proteins gained by this method have very good activity and stick well to silica beads. They can be stored for several months in N_2liq or at –80°C. After each new isolation the enzymatic activity of the molecules should be checked routinely in a MT gliding assay (for this method, consult the other chapters of this volume).

3.2. Taxol Stabilized Microtubules

Cycled tubulin (about 10 mg/mL) is centrifuged (in a TLA100 rotor at 213,483*g* for 10 min at 4°C) to remove any aggregated tubulin. MTs are polymerized from this tubulin in polymerization buffer at 37°C for 40 min and fixed with stabilization buffer. Their concentration is adjusted in stabilization buffer to give a loose coating of the cover slip.

3.3. Bead Coating

The coating of beads with motor molecules is achieved by following a standard protocol ***(16)***.

1. The microbeads are washed by centrifugation three times in distilled water (H_2Odist) (*see* **Note 8**).

2. In the experiments described here, only the binding between one kinesin molecule and a MT is of interest. Therefore the beads are preincubated at twice their final concentration in assay buffer with 2 m*M* AMP–PNP or without any nucleotides (*see* **Note 9**) for 5 min at 4°C.
3. Kinesin is diluted to twice the final concentration in assay buffer.
4. Afterward, the bead solution is added very quickly (within a few seconds) to an equal volume of kinesin solution. The kinesin is allowed to adsorb onto the beads for 1 h at 4°C on a rotating wheel.

This is a reliable coating method for kinesin proteins isolated from brain cells or for recombinant proteins as long as the tail of the kinesin heavy chain is present in the purified molecule (*see* **Note 10**).

The challenge in bead functionalization is to attach to one microbead a controlled number of kinesin molecules in the correct orientation, leaving the motor domain free for an eventual interaction with a MT (*see* **Notes 10** and **11**). There are several ways to control that only a single kinesin interacts with a MT at a time:

1. To facilitate a binding ratio of one kinesin to one bead, a solution at a molar kinesin-to-bead ratio of 1:1 mixed rapidly (within a few seconds) should be prepared. We use our beads at a final concentration of 0.20–0.05 pM, depending on the bead size and the sample chamber geometry. It is an appropriate concentration range for laser trapping, because a too high bead concentration can lead to the trapping of more than one bead, disturbing the measurements. The exact value has to be adjusted to experimental conditions.
2. The number of kinesin molecules on a bead that interact with a MT can also be estimated by a statistical method ***(16,17)***. A kinesin-coated bead directed with the tweezers upon a MT moves along it, in the presence of 2 m*M* ATP (*see* **Note 9**), with a probability $P(n)$ or fails to bind with a probability $1\text{-}P(n)$, where n is the number ratio of kinesins to beads at mixing. $P(n)$ should be measured at different ratios and plotted. If a single kinesin molecule moves the bead, then $P(n) = 1 - \exp(-n/\rho)$ and corresponds to the Poisson probability that a bead carries one or more motors ***(18)***.
3. Another way to test for the number of motors interacting with a MT is to measure the maximum force the molecule is able to exert upon the laser trap while moving along the MT (*see* **Note 9**). The force measured in the MT direction should not exceed 5–6 pN, which is the maximal force for one molecule, as reported previously ***(15)***.
4. The success of bead coating is crucial for motility experiments done in the presence of ATP. When too little kinesin is bound to the spheres, leaving a too high concentration of active kinesin in the assay solution, the long kinesin constructs adhere to the chamber surface and transport the MT away like in a gliding assay (*see* Chapter 8). This happens with full-length proteins when the active kinesin-to-bead ratio is higher than 100. It seems that the previous coating of the bead

with casein does not allow many kinesins to attach. A simultaneous interaction of two molecules with the same MT can therefore also be excluded by geometrical considerations.

3.4. Sample Chamber

An important aspect for the sample preparation is the immobilization of MT on the glass surface of the sample chamber. Weakly attached MT would disturb the experiment. Our sample chamber is a conventional microscope perfusion chamber with a volume of about 30 µL constructed with two strips of double-sided tape sticking a microscope glass slide to a 22-mm cover slip. Fluids perfuse into the chamber by capillary forces and are exchanged by pipetting at one end of the chamber and sucking at the other end with filter paper ***(13)***.

To guarantee a tight binding of the MT to the cover-slip surface, the lower cover slip, which will be reached by the laser trap, is silanized according to the following protocol (*see* **Note 12**):

1. The cover slips are first washed by boiling them for 15 min in a saturated KOH-ethanol solution (*see* **Note 13**) and rinsed several times in ethanol absolute or distilled water. Additionally, the cover slips can also be left overnight in a 2% Hellmanex in H_2Odist. solution and rinsed in H_2Odist. Each rinsing should be done in a sonication bath for several minutes.
2. Prepare and let 1 m*M* acetic acid with 1% DETA solution hydrolyze for 5 min.
3. Incubate the clean cover slips for 2 min in the DETA solution.
4. Rinse and sonicate in H_2Odist.
5. Dry the cover slips at 150°C for 15 min.

3.5. Bead Assay and Data Recording

A MT solution is perfused into the microscope chamber at high flow rates, which ensures that they bind with their long axis parallel to the flow field (*see* **Note 14**). The MT are allowed to adhere to the pretreated lower glass slide for 10 min. The chamber is then washed with assay buffer to remove unadhered MT. Furthermore, this wash coats the cover slip with casein, which minimizes unspecific adhesions between the kinesin-coated beads and the chamber surface. After 5 min, the motor-coated beads are added. Either a single bead is captured from solution with the trap and approached to a MT or a bead already attached to a MT is trapped. The MT orientation is controlled by DIC microscopy. Once all the solutions needed for the experiments are introduced, the flow conduit of the chamber is sealed with silicon grease to avoid evaporation.

The 3D-position fluctuations of the trapped bead are measured using an optimal sampling rate of the acquisition card in order to acquire enough points for reasonable counting statistics, which requires a minimum of 10,000 points.

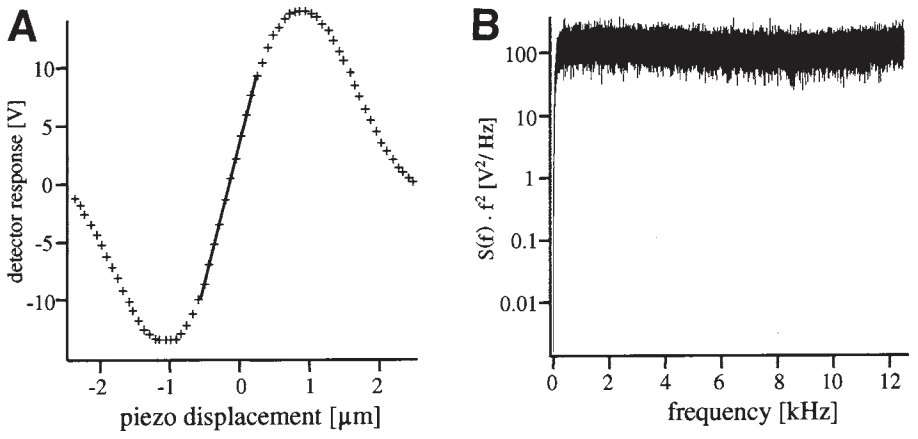

Fig. 3. **(A)** Detector response curve (+++) to the scanning of a fixed 0.9-µm glass bead by the laser focus. The amplitude of the motion of the piezo-scanner was 4 µm and the frequency was 3.3 Hz. The continuous line represents a linear fit of the detector signal. **(B)** Power spectral density $S(f)$ of the position fluctuation of a trapped 0.9-µm silica glass bead at about 5 µm above the cover-slip surface, multiplied with the square of the frequency (f^2). The height of the plateau used for the calibration can be easily determined from the graph.

They are then amplified with low-noise preamplifiers and displayed on a digital oscilloscope.

3.6. Position Signal Calibration

The calibration of the detector should be done during the actual experiment with the same bead sizes and sample chamber. Two reliable methods for a calibration in all three dimensions can be applied:

1. The first consists of fixing a microsphere on the lower cover glass of the microscope chamber and positioning it in the laser focus (*see* **Note 15**). The laser focus is then moved periodically over the sphere either laterally with the scanning mirror, to calibrate the *x*- or *y*-signal, or along its optical axis with the PI-foc (*see* **Fig. 1**), to calibrate the *z*-signal. The detector signal is then plotted vs the driving voltage (**Fig. 3A**). The inherent hysteresis of the piezoelectric actuators can be corrected as described previously ***(5)***. Depending on the bead size, the calibration curves have a linear region and the slope corresponds to the detector sensitivity in units of volts per meter. The detector response is linear in the range of about 0.7 µm laterally and 1.2 µm axially for a glass bead diameter of 0.9 µm (*see* **Fig. 4A**).
2. The detector sensitivity depends on the light intensity, on the bead size, and decreases with the distance of the focus from the cover-slip surface because of

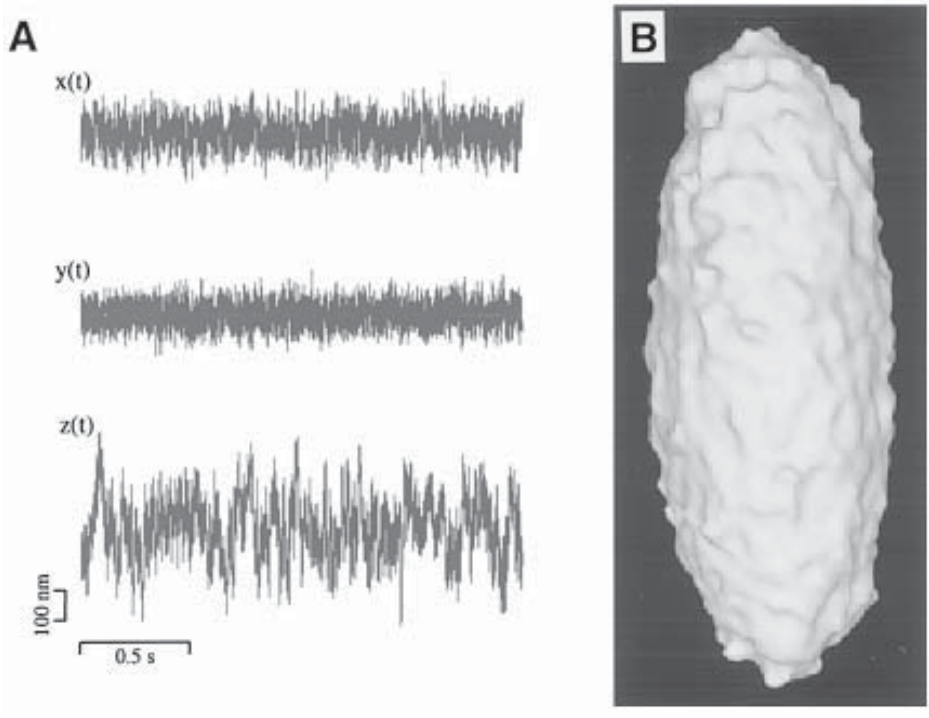

Fig. 4. Three-dimensional position fluctuation analysis applying Boltzmann statistics. **(A)** Typical 3D position fluctuation recordings of an optically trapped bead (430 nm in diameter) at low laser power in aqueous solution at 2 μm from the cover-slip surface. The sampling rate was 25 kHz. The peak-to-peak fluctuations have a maximum of 200 nm in the lateral directions (x and y) and 500 nm along the optical axis (z). **(B)** 3D energy isosurface (approx 5 k_BT above the global minimum) of the trapping potential calculated from 3D position histograms with 500,000 position vectors using the data shown in **(A)**.

spherical aberrations. Therefore, the calibration becomes more accurate when it is done with the identical sphere used in the experiment as well as at constant temperature. A convenient, straightforward method to do this has been proposed by Allersma et al. ***(5)*** using the power spectrum of the displacement fluctuations of an optically trapped bead in solution measured in three dimensions. The power spectral density (in units of m^2/Hz) resembles a Lorentz curve as long as the detector response is linear ***(18)***. The detector sensitivity β for a bead of radius r in a medium of viscosity γ can be estimated without knowing the trap stiffness from an uncalibrated voltage power spectrum $S_V(f) = \beta^2 S(f)$ (in units of V^2/Hz). Multiplication of $S_V(f)$ with the square of the frequency (f^2) results in a function reaching a plateau for frequencies above the corner frequency f_c of the spectrum. As

shown in **Fig. 3B**, the plateau value P can be measured and used to calculate the detector sensitivity β in volts per meter:

$$P = \beta^2 S_0 f_0^2 = \beta^2 \, k_B T / 6\pi^3 \eta r \;\Rightarrow\; \beta = \sqrt{6\pi^3 \eta r P / k_B T}$$

3.7. Laser Trap Calibration: Potential Profiling

Once the 3D time series of the thermal position fluctuations of the bead in the laser trap are measured and quantified (an example is shown in **Fig. 4A**), the trapping potential can be calibrated. The method presented here characterizes the 3D potential of the laser focus acting on the trapped particle by analyzing its 3D position fluctuations. The trap stiffness is calculated from the curvature of the potential profile for each dimension.

During the observation time, the particle moves, driven by thermal energy inside a volume defined by the optical arrangement of the trap. In thermal equilibrium, the probability $P(\mathbf{q})d\mathbf{q}$ of finding a small particle in a given potential $V(\mathbf{q})$ inside a given volume $d\mathbf{q}$ follows the Boltzmann distribution:

$$P(\mathbf{q})d\mathbf{q} = C^{-1} \exp(-V(\mathbf{q})/k_B T) \, d\mathbf{q} \tag{1}$$

where $\mathbf{q} = (x,y,z)$ is the position vector of the particle and C obeys the normalization condition $\int P(\mathbf{q})d\mathbf{q} = 1$. **Equation 1** states that the probability density distribution to find the bead at a certain position is directly correlated to the potential. Therefore, the analysis of the position fluctuations can be used to calculate directly the 3D potential by the relation:

$$V(\mathbf{q}) = -k_B T \ln P(\mathbf{q}) + k_B T \ln C \tag{2}$$

The last term defines a constant energy offset and can be neglected.

All the measured position vectors $\mathbf{q}$ of the bead are used to calculate a 3D position histogram, representing the probability density $P(\mathbf{q})$ to find the particle at position $\mathbf{q}$. A 3D probability density distribution $P(\mathbf{q})$ can be then transformed into a 3D energy landscape using **Eq. 2**. **Figure 4B** displays a typical 3D isopotential surface of a sphere in the laser trap at approx $5k_BT$, calculated using the 3D position fluctuation histograms gained from the recordings in **Fig. 4A** and equation ***(2)***. More than 90% of all positions are within the volume enclosed by this isosurface. The volume has an ellipsoidal shape elongated along the optical axis (z-axis), as expected from the intensity distribution in the focal spot of a high numerical aperture (N.A. = 1.3) objective lens. The elongation is due to a weaker force constant along the z-axis, allowing larger bead fluctuations compared to the lateral directions. The asymmetric axis ratio depends also on parameters such as the bead diameter. In the lateral plane (x- and y-axis), the 3D profile has ideally rotational symmetry.

The 3D information can now be used to analyze the trapping potential along defined axes. In the case of the bead trapped in the potential of laser tweezers,

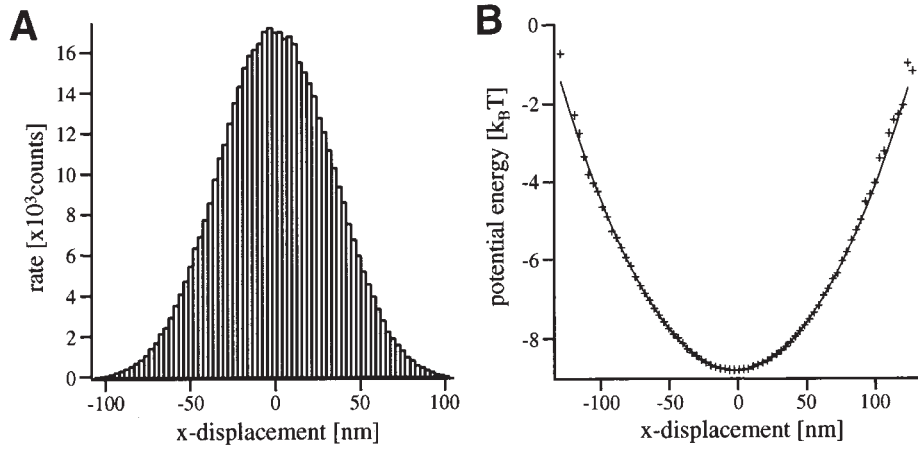

Fig. 5. **(A)** The measured 1D probability distribution of the lateral positions x(t) of a 430-nm trapped glass sphere at about 2 µm above the cover-slip surface. The Gaussian distributed histogram was plotted from the original dataset shown in **Fig. 4A**. **(B)** The lateral potential energy is given in units of k_BT and the 0-position is chosen arbitrarily at the potential minimum. A parabolic curve (continuous line) fits very well to the data indicating the harmonicity of the potential.

these axes are chosen along and perpendicular to the optical beam axis. From the calibrated time series in each dimension x, y, or z (**Fig. 4A**), the one-dimensional (1D) probability distribution of the particle's position is determined and plotted in **Fig. 5A** (shown only for $x[t]$). From this, a potential profile can be derived by **Eq. 2** (**Fig. 5B**). The one-dimensional position histogram shows a Gaussian distribution. The corresponding potential obtained is harmonic and confirms that for small displacements, optical tweezers can be considered as acting like a linear spring on the particle with a direction-dependent spring constant k_i ($i = x$, y, or z):

$$V(x, y, z) = \tfrac{1}{2}k_x x^2 + \tfrac{1}{2}\, k_y y2 + \tfrac{1}{2}k_z z^2$$

The energy profile has the highest precision around its minimum, since the energy minimum is at the same time the most probable bead position and the most populated region in the histogram (**Fig. 5A**). The spring constant k_i is given by the curvature (second derivative) of $V(\mathbf{q})$, which can be fitted by a parabolic function.

Because no assumption about the shape of the potential has been made, the method applies also to anharmonic potentials. It can be used for force measure-

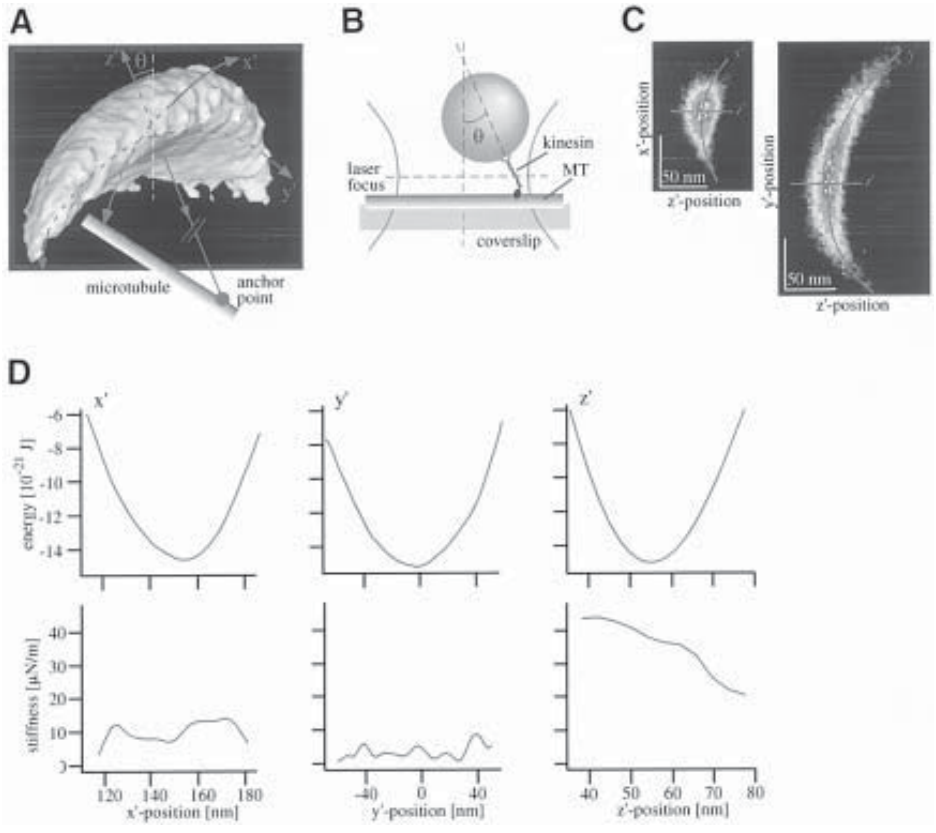

Fig. 6. Kinesin mechanics. **(A)** 3D energy isosurface experienced by a trapped bead tethered to a MT via a single kinesin molecule. The *z*' line pointing toward the kinesin's anchor and on the MT indicates the orientation of the linker axis through the global potential minimum. θ represents the axial tilt angle of the energy landscape of a bound bead relative to the one of an unbound bead. The three lines *x*', *y*', and *z*' indicate the directions relative to the molecular axes used for slicing. **(B)** In the special case of the experiment presented here as an example, the bead was pulled about 140 nm out of the trap center in the *x* direction and pushed approx 50 nm away from the glass surface by the binding of the kinesin molecule. **(C)** Slices of the 3D energy landscape shown in **(A)** cut according to the planes *x*'*z*' and *y*'*z*' with respect to the MT and tether axis. The lines named *x*', *y*', and *z*' show the directions along which a one-dimensional potential profile is extracted. **(D)** Calculated potential and stiffness versus extension profiles along each direction given by the lines *x*', *y*', and *z*'.

ments in three dimensions and, in addition, it provides access to 3D energy profiles, regardless of their shape, with a resolution of one-tenth of the thermal energy and subnanometer spatial resolution.

3.8. Molecular Mechanics

In order to study molecular mechanics, we analyze the position fluctuation of a bead tethered by the molecule of interest in its natural environment. By following the procedure described earlier for the determination of the trapping potential, we can characterize the potential acting on the bead when tethered by a single kinesin molecule to a MT fixed on the cover slip.

The energy isosurface depicted in **Fig. 6A** is the 3D energy landscape experienced by a trapped bead tethered to a MT via a single kinesin. The profile also shows which positions the bead can reach above the MT under these conditions. Comparing this potential profile to the one of the bead only in the laser focus (**Figs. 4B** and **6A**, both landscapes are drawn at the same scale), one can see that the additional tethering of the bead to a MT by the motor molecule strongly restricts the movement of the bead. Furthermore, the energy landscape of the tethered bead is tilted by an angle θ with respect to the optical axis in the *xz*-plane of the laser potential. This tilt is the result of the relative position of the focus to the anchoring point of the kinesin molecule on the MT. **Figure 6B** indicates schematically that during this experiment, the laser beam axis and the long axis of the molecule were not parallel.

With the presented tools, we can investigate the mechanical properties of kinesin according to relevant axes (*x*', *y*', and *z*' in **Fig. 6A**) of the molecular structure by extracting 1D energy profiles from the 3D profile, as explained earlier. One axis, referred to as the *z*'-axis, is parallel to the kinesin stalk, which is, in most cases, tilted relative to the optical axis. The origin of the kinesin stalk vector corresponds to the point of highest probability for the bead center position, actually the minimum of the potential. At this point, the curvature of the energy landscape is calculated and its normal determines the direction of the kinesin stalk vector. The anchor point, the tether axis and the center of the bead are then aligned on a common axis, as shown in **Fig. 6B**. Another interesting direction, called the *x*'-axis, along which a characteriztic stiffness of kinesin is observed, lays in a plane defined by the MT and the stalk axis in such a way that the stalk axis is perpendicular to it. The corresponding third direction (*y*'-axis) is placed perpendicular to the MT and the stalk axes. The new planes spanned by the defined lines are referred to as the *x*'*z*'- and *y*'*z*'-planes and are used to cut the 3D energy landscape into 2D energy profiles (referred to as "slices") (*see* **Fig. 6C**).

From the 1D energy profiles, force and stiffness versus extension profiles can be calculated in three dimensions by differentiation, along a path defined by the MT and tether orientations (**Fig. 6D**). Interesting parameters in the 1D profiles are, for example, the potential width giving a lower estimate for the molecular length or its shape, indicating here the anharmonic and anisotropic

nature of molecular hinges. We discovered, for example, that the kinesin molecule is able to withstand forces against compression along the stalk and that it generates a restoring force against bending. A significant rotational stiffness of the kinesin molecule and a maximum stiffness of 200 μN/m along its stalk were measured. Because the 3D stiffness was found to vary with mutations of the motor domain and was strongly correlated to the nucleotide-binding state of the motor, the stiffness could be mainly attributed to the neck region next to the motor domain ***(19)***.

The precision of the energy profiles is determined by the number of statistically independent points in each bin of the 3D histogram. To ensure that the mechanical properties of kinesin dominate the energy landscape, the trap stiffness for all measurements should be at least one order of magnitude smaller than the average kinesin stiffness. This guarantees only a small contribution of the laser stiffness to the measured resulting stiffness.

4. Notes

1. The skull of the embryo at 13 d is already very hard, this complicates the extraction of the brain. The brain should be prepared fresh, as a kinesin preparation from frozen brain contains less active motors.
2. Prewarm PMSF to dilute crystals.
3. Taxol in DMSO can only be frozen once, for aliquoting precool the Eppendorf tubes on ice; the solution readily freezes on ice.
4. BRB80 can be stored at 5X for several months at 4°C; the 200 m*M* GTP stock solution is stored at –20°C; the polymerization buffer is prepared fresh on ice. The stabilization buffer is prepared and used fresh at room temperature.
5. We usually use 4 g of brains, which yields to a quantity of kinesin sufficient for several months of experiments. Therefore, the indicated buffer quantities are optimized for 4 g of brains. Kinesin purification from frozen brains produces proteins with lower activity.
6. During homogenization, only the cellular membrane should break; the nuclear membrane should be preserved, avoiding the contamination of the cytosol with DNA.
7. The gradient should be prepared very carefully, because this is, according to our experience, the most delicate step of this protocol.
8. The maximum time and speed for centrifugation depend on the bead size and should be provided by the manufacturer. Bead aggregates can be resolved by sonication.
9. When used for kinesin motility experiments, the assay buffer is supplemented with a varying amount of ATP and the ATP-regeneration system (1 μg/mL creatine kinase and 2 m*M* creatine phosphate) ***(15)***.
10. Our experience has shown that the noncoiled-coil tail present in most full-length motor constructs is essential for the correct and direct attachment of kinesin to a glass or latex substrate. This phenomenon is also observed for constructs of other

proteins. For example, the conditions for attachment of one spectrin molecule to a SiN_4–AFM cantilever is more favorable when the protein includes a tail a few amino acids long (Lenne, P. F., personal communication).

11. It is assumed that the casein molecules present in the assay buffer at saturating concentrations favor the erection of the kinesin molecule and orient its heads away from the bead surface, leaving the motor domain free for an eventual interaction with a MT. This could explain why motor activity and affinity to MT is increased by the presence of casein.
12. A silanized cover slip should not be kept more than 2 d. A good control of the successful attachment of the MT to the glass is to add a solution of kinesin and ATP to the sample chamber after MT coating. If the attachment is too weak, the MT should release from the surface because of the presence of kinesin between the glass surface and the MT.
13. The KOH–ethanol solution should be saturated but the KOH should still dilute well.
14. For a good binding of the MTs with their long axis parallel to the flow field, the flow chamber should have a maximum thickness of 100 μm. In thicker chambers, vortices can arise in the flow and perturb the MT arrangement.
15. During scanning, the laser focus should be placed slightly below the sample, approaching the bead closer to its trapping position ***(6)***. This corresponds better to the situation of the actual experiment.

Acknowledgments

We would like to thank Hanry Yu for providing us with the kinesin protocol and Rolf Eckert and Alan Hamill for reading the manuscript.

References

1. Henningsen, U. and Schliwa, M. (1997) Reversal in the direction of movement of a molecular motor. *Nature* **389,** 93–95.
2. Case, R. B., Pierce, D. W., Hom-Booher, N., Hart, C. L., and Vale, R. D. (1997) The directional preference of kinesin motors is specified by an element outside of the motor catalytic domain. *Cell* **90,** 959–966.
3. Endow, S. A. and Waligora, K. W. (1998) Determinants of kinesin motor polarity. *Science* **281,** 1200–1202.
4. Grummt, M., Woehlke, G., Henningsen, U., Fuchs, S., Schleicher, M., and Schliwa, M. (1998) Importance of a flexible hinge near the motor domain in kinesin-driven motility. *EMBO J.* **17,** 5536–5542.
5. Allersma, M. W., Gittes, F., deCastro, M. J., Stewart, R. J., and Schmidt, C. F. (1998) Two-dimensional tracking of ncd motility by back focal plane interferometry. *Biophys. J.* **74,** 1074–1085.
6. Pralle, A., Prummer, M., Florin, E.-L., Stelzer, E. H. K., and Hörber, J. K. H. (1999) Three-dimensional position tracking for optical tweezers by forward scattered light. *Microsc. Res. Tech.* **44,** 378–386.

7. Florin, E.-L., Pralle, A., Stelzer, E. H. K., and Hörber, J. K. H. (1998) Photonic force microscope calibration by thermal noise analysis. *Appl. Phys. A* **66,** S75-S78.
8. Florin, E.-L., Jeney, S., Stelzer, E. H., and Hörber, J. K. H. (2000). Three-dimensional position fluctuation analysis reveals a new view on single molecule mechanics. *Proc. Natl. Acad. Sci. USA*, submitted.
9. Svoboda, K. and Block, S. M. (1994) Biological applications of optical forces. *Annu. Rev. Biophys. Biomol. Struct.* **23,** 247–285.
10. Sheetz, M. P. (ed.) (1998) Laser Tweezers in Cell Biology, *Methods Cell Biology Services* 55. Academic Press.
11. Hyman, A., Drechsel, D., Kelogg, D., Salser, S., Sawin, K., Steffen, P., et al. (1991) Preparation of modified tubulins. *Methods Enzymol.* **196**, 478–485.
12. Howard, J., Hunt, A. J., and Baek, S. (1993) Assay of microtubule movement driven by single kinesin molecules. *Methods Cell Biol.* **39**, 137–147.
13. Block, S. M. (1990) Optical tweezers: a new tool for biophysics. *Noninvas. Tech. Cell Biol. (Mod. Rev. Cell Biol.)* **15**, 375–402.
14. Gittes, F. and Schmidt, C. F. (1998) Interference model for back focal plane displacement detection in optical tweezers. *Opt. Lett* **23** , 7–9.
15. Svoboda, K. and Block, S.-M. (1994) Force and velocity measured for single kinesin molecules. *Cell* **77**, 773–784.
16. Block, S. M., Goldstein, L. S., and Schnapp, B. J. (1990) Bead movement by single kinesin molecules studied with optical tweezers. *Nature* **348,** 348–352.
17. Kojima, H., Muto, E., Higuchi, H., and Yanagida, T. (1997) Mechanics of single kinesin molecules measured by optical trapping nanometry. *Biophys. J.* **73,** 2012–2022.
18. Gittes, F. and Schmidt, C. F. (1998) Signals and noise in micromechanical measurements. *Methods Cell Biol.* **55,** 129–156.
19. Jeney, S., Florin, E.-L., Hancock, W., Howard, J. and Hörber, J. K. H. (2000) Mechanical anisotropy of kinesin molecules revealed by thermal fluctuation analysis. In preparation.

10

Assays for Microtubule-Destabilizing Kinesins

Arshad Desai and Claire E. Walczak

1. Introduction

The kinesin superfamily is a large family of microtubule (MT)-stimulated ATPases that couple the energy of ATP hydrolysis to force production (reviewed in **refs.** ***1*** and ***2***). Conventional kinesin was identified as a motor protein that could translocate along MT polymers. Since the molecular cloning of kinesin ***(3)***, well over 100 additional proteins have been identified that share high sequence homology with the catalytic domain of kinesin. Many of these kinesin-related proteins (KRPs) have also been shown to be MT-based motor proteins using in vitro motility assays (reviewed in **ref.** ***2,*** *see also* Chapters 5, 8, and 12).

Although kinesin and many KRPs share high-sequence homology in their catalytic domain, recent evidence suggests that some kinesin superfamily members may not act as conventional motor proteins but may be microtubule-destabilizing enzymes ***(4–6)***. The first hints at this function came from studies on the yeast Kar3 protein. Analysis of the in vitro motility of a bacterially expressed fragment of Kar3p revealed that it slowly depolymerizes MTs from the minus ends as it translocates along MTs toward the minus end ***(5)***. The most striking example of the ability of some KRPs to destabilize MTs came from studies of the *Kin*I KRPs XKCM1 and XKIF2 ***(4)***. Both XKCM1 and XKIF2 were shown to directly destabilize MTs in an ATP-dependent manner. Their ability to destabilize MTs does not involve classical motor activity. Furthermore, this MT-destabilization activity can be distinguished mechanistically from that of conventional kinesin and other kinesin family motors.

Here, we describe the biochemical assays used to analyze the effect of MT-destabilizing kinesins on various MT substrates. We first describe how to prepare dynamic and stabilized MTs and the fixed time-point and real-time assays

From: *Methods in Molecular Biology*, Vol. 164: *Kinesin Protocols*
Edited by: I. Vernos

that can be done using MT substrates. We also describe immunofluorescence assays to analyze the localization of kinesins on MTs. Finally, we describe a tubulin dimer binding assay that can be used to test the mechanism of action of the destabilizing KRP. These assays will be useful to discern the mechanism of other KRPs that have been proposed to act as MT-destabilizing enzymes based on genetic studies ***(6–9)***. In addition, these assays will be useful to analyze the mechanism of other MT dynamics regulators.

2. Materials

1. Pure enzyme preparation: We use recombinant XKCM1 or XKIF2 purified from insect Sf–9 cells using conventional chromatographic techniques ***(4)***. The final preparation was eluted from a MonoS cation-exchange column in BRB80, 1 m*M* dithiothreitol (DTT), 10 µ*M* Mg–ATP, 300 m*M* KCl, and 1 µg/mL each of leupeptin, pepstatin A, and chymostatin. Fractions were supplemented with 10% sucrose (w/v), aliquoted, frozen in liquid nitrogen, and stored at –80°C (*see* **Note 1**).
2. Recycled tubulin: We use phosphocellulose-purified bovine brain tubulin that has been cycled at least one additional time after purification using standard procedures (http://skye.med.harvard.edu/newprotocols/toc.html). All tubulin is stored in aliquots at –80°C in IB (50 m*M* K–glutamate, 0.5 m*M* $MgCl_2$). Tubulin concentration is determined using $\varepsilon_{\text{tubulin,280 nm}} = 115{,}000/M \cdot \text{cm}$.
3. Fluorescent tubulin: Tubulin polymer is labeled with fluorescent dyes using standard procedures ***(10)*** (http://skye.med.harvard.edu/newprotocols/toc.html).
4. BRB80 buffer: 80 m*M* piperazine-*N*,*N*-*bis*[2-ethanesulfonic acid] (PIPES), 1 m*M* $MgCl_2$, 1 m*M* EGTA (pH 6.8) with KOH. This buffer is also made as a 5X stock for many of the experiments. Sterile filter and store at 4°C (*see* **Note 2**).
5. Mg–ATP (Sigma A-2383). The disodium salt of ATP is made up as a 0.5 *M* stock in water to which an equimolar amount of $MgCl_2$ is added so the final concentration of the solution is 0.5 *M* $MgCl_2$ and 0.5 *M* ATP. Solution is sterile filtered and stored in aliquots at –20°C.
6. Mg–5'-Adenylylimido-diphosphate (AMP–PNP) (Sigma A-2647). The dilithium salt of AMP–PNP is made up as a 0.1 *M* stock in water to which an equimolar amount of $MgCl_2$ is added so the final concentration of the solution is 0.1 *M* $MgCl_2$ and 0.1 *M* AMP–PNP. Solution is sterile filtered and stored in aliquots at –20°C.
7. Mg–GTP (Sigma G-8877). The disodium salt of GTP is made up as a 0.1 *M* stock in water**.** Solution is sterile filtered and stored in aliquots at –20°C.
8. Mg–GDP (Sigma G-7127). The disodium salt of GDP is made up as a 0.1 *M* stock in water. Solution is sterile filtered and stored in aliquots at –20°C.
9. GMP–CPP: Unfortunately, there is no commercial source of guanylyl-(α-B)-methylene-diphosphate (GMP–CPP) and it must be synthesized in-house ***(11)***. All stocks are at 0.1 *M* GMP–CPP in water. They are stored in aliquots at –20°C.
10. Axonemes: Axonemes are prepared according to standard procedures as described previously ***(12)***. They are stored at –20°C in 50% v/v glycerol, 5 m*M* PIPES, 0.5 m*M* EDTA, 1 m*M* of 2-mercaptoethanol (pH 7.0) with KOH.

11. BRB80/1% glutaraldehyde: This is 1X BRB80 containing 1% final concentration of glutaraldehyde. Make fresh before use.
12. BRB80/30% glycerol: Make by adding glycerol to 1X BRB80 buffer. This solution can be stored at 4°C.
13. Spin-down tubes: These are 15-mL Corex tubes that have been modified to hold a cover slip at the bottom of the tube so that samples can be readily centrifuged onto cover slips. They have been described previously (***13,*** *see also* Chapter 15).
14. Flow chambers: These are microscope slides that have been modified to create a flow cell and are used routinely in studies of microtubule dynamics and motility assays. They have been described previously (***14,*** *see also* Chapters 8, 9, and 12).
15. Oxygen scavenging mix (OSM): 200 µg/mL glucose oxidase, 35 µg/mL catalase, 4.5 mg/mL glucose, 0.5% of 2-mercaptoethanol. This is made fresh daily from concentrated stocks of each of the components.
16. Taxol: Paclitaxel (Sigma T7402). Taxol is made as a 10 m*M* stock in dimethyl sulfoxide (DMSO) and stored in aliquots at –20°C.
17. TBS-Tx: 20 m*M* Tris-HCl (pH 7.4), 150 m*M* NaCl, 0.1% Triton X-100. Store at room temperature.

3. Methods

3.1. Preparation of Microtubule Substrates

The effects of kinesins on MT dynamics can be assayed by using three types of MT substrates. The first type of substrate is a dynamic MT. For this experiment, we use MTs that have been polymerized off axoneme seeds in the presence of GTP. These samples can be analyzed by either fixed-time-point assays (**Subheading 3.2.1.**) or in real-time (**Subheading 3.2.2.**). The other two types of substrates are MTs stabilized with the nonhydrolyzable GTP analog GMP-CPP or with the MT-stabilizing drug Taxol (**Subheading 3.3.**).

3.1.1. Preparation of Dynamic MTs Nucleated from Axonemes

1. Make 225 µL of 20 µ*M* tubulin mix on ice such that at 15 µ*M*, the BRB80 concentration is 1× and the GTP concentration is 0.5 m*M*. For a recycled tubulin stock of 150 µ*M* concentration, the reaction mix would be as follows: 60 µL of 5X BRB80; 30 µL of 150 µ*M* recycled tubulin; 1.5 µL of 100 m*M* GTP; water to 225 µL.
2. Incubate tubulin mix at 0°C for 5 min, spin at 350, 000*g* for 5 min at 2°C (90,000 rpm in a TLA100 rotor). Transfer supernatant to a cold tube on ice.

3.1.2. Preparation of GMPCPP MTs

GMP–CPP is the best current GTP analog for tubulin polymerization. GMP–CPP is a potent nucleator of microtubules. Therefore, at tubulin concentrations of 1 mg/mL or higher, very numerous and short microtubules are formed in the presence of GMP–CPP. If longer GMP–CPP microtubules are desired, nucleation can be limited by diluting the tubulin to 2–3 µ*M* (0.2–0.3 mg/mL). We

generally make a 1- to 3-mg/mL CPP tubulin mix and store it at –80°C in small aliquots. Directly polymerizing this mix results in short GMP–CPP seeds. Diluting the mix while thawing it results in the formation of longer GMP–CPP microtubules.

1. On ice, mix unlabeled tubulin and labeled tubulin (1–3 mg/mL final) at an appropriate ratio in 1X BRB80 with 1 m*M* DTT and 0.5–1 m*M* GMP–CPP. Incubate at 0°C for 5–10 min.
2. Clarify mix in TLA100 rotor at 90 K (350,000*g*) for 5 min at 2°C.
3. For the visual assay (**Subheading 3.3.1.**), freeze supernatant in 5- to 10-µL aliquots in liquid nitrogen and store at –80°C.
4. To form long GMP–CPP microtubules, thaw a CPP mix tube by adding in enough warm BRB80 with 1 m*M* DTT such that the final tubulin concentration is 2–3 µ*M* (pipet in 37°C BRB80 with 1 m*M* DTT, mix by gently pipetting up and down until the frozen seed mix pellet is thawed, then place in a 37°C water bath). Incubate at 37°C for 30 min or longer. Free GMP–CPP can be removed as described in **Subheading 3.1.3.** or the CPP microtubules can be used directly for assays.
5. For the sedimentation assay (**Subheading 3.3.2.**), polymerize the supernatant at 37°C for 30 min. Pellet the polymerized MTs in a TLA100 rotor at 350,000*g* (90K 5 min at 25–30°C), discard the supernatant, and resuspend the pellet in 0.8X–1X the starting volume of BRB80 with 1 m*M* DTT.
6. Microtubule concentration (i.e., the concentration of tubulin dimer in MT polymer) in the resuspended pellet is determined from the A_{280} of an aliquot of the sedimented and resuspended MTs diluted in BRB80 with 5 m*M* $CaCl_2$ and incubated at 0°C for 10 min to induce depolymerization (using $\varepsilon_{\text{tubulin,280 nm}} = 115{,}000/M \cdot \text{cm}$). The appropriate resuspension buffer diluted in parallel is used as a blank (*see* **Note 3**).

3.1.3. Preparation of Taxol-Stabilized MTs

1. On ice, mix unlabeled tubulin and labeled tubulin (visual assay, **Subheading 3.3.1.**) or unlabeled tubulin alone (sedimentation assay, **Subheading 3.3.2.**) at an appropriate ratio in 1X BRB80 with 1 m*M* DTT and 1 m*M* GTP. Incubate at 0°C for 5 min.
2. Clarify mix in TLA100 rotor at 350,000*g* (90K) for 5 min at 2°C. Incubate supernatant at 37°C for 1–2 min.
3. Add Taxol stepwise to equimolar as follows (for 1 mg/mL tubulin) (*see* **Note 4**).
4. Pipet in the Taxol and immediately flick the tube to mix it in.
5. Add 1/100 vol 10 µ*M* Taxol; incubate at 37°C for 5–10 min.
6. Add 1/100 vol 100 µ*M* Taxol; incubate at 37°C for 5–10 min.
7. Add 1/100 vol 1000 µ*M* Taxol; incubate at 37°C for 15 min.
8. Pellet microtubules over a warm 40% glycerol in a BRB80 cushion. Spin at 75K for 15 min (300,000*g*) in a TLA100.3 rotor, aspirate, and wash the sample–cushion interface, and rinse the pellet and resuspend in warm BRB80, 1 m*M* DTT, and 10–20 µ*M* Taxol (Taxol should be at least equimolar and preferably in excess to the tubulin).

3.2. Assays on Dynamic MTs

The effects of kinesins on MT dynamics are first assessed on dynamic MTs nucleated off *Tetrahymena* axonemes ***(12)***. *Tetrahymena* axonemes are ciliary fragments that serve as nuclei for MT polymerization. The effect of kinesins on MTs polymerized off axonemes can be assessed using both fixed (**Subheading 3.2.1.**) and real-time (**Subheading 3.2.2.**) assays as described in the following.

3.2.1. Fixed-Time-Point Assay

The effect of a purified kinesin or partially pure fraction on MT assembly is assayed on 15 µ*M* tubulin polymerized off *Tetrahymena* axonemes at 37°C in the presence of ATP. In addition to the concentration of the kinesins tested, the time of incubation, the adenine nucleotide, the final salt concentration, as well as the tubulin concentration can be varied. The kinesin can also be added after allowing MT assembly for some duration although we prefer to do this experiment live using video-enhanced differential interference contrast (VE-DIC) (**Subheading 3.2.2.**). Note that tubulin requires GTP for polymerization and GTP can be used as a substrate by some kinesins ***(15)*** so that any interpretation of nonhydrolyzable adenine nucleotide analogs added into the reaction must take into account this possibility.

The following protocol is for six reactions (a convenient number to pellet in one HB-6 rotor):

1. Prepare assay mixes on ice:
   a. 30 µL tubulin mix (**Subheading 3.1.1.**).
   b. 2 µL of 30 m*M* MgATP.
   c. Purified kinesin or fraction and KCl such that the final volume is 40 µL and the final concentration of KCl is 50–75 m*M* (all reactions to be compared must have similar KCl concentration, i.e., +/– 5 m*M*).
2. Mix and add axonemes (<1 µL for typical axoneme preparations), mix again, and transfer 10 µL to a new tube on ice (*see* **Note 5**).
3. Transfer the 10-µL reactions to 37°C. Stagger tubes by 30 s.
4. After 7 min at 37°C, add 100 µL BRB80/1% glutaraldehyde (at room temperature), mix gently with a cut-off P200 tip, and incubate at room temperature for 3 min. Dilute with 900 µL BRB80 (equilibrated at room temperature), mix by gentle inversion, and load 100 µL onto a 5 mL BRB80/30% glycerol cushion in a spin-down tube.
5. Sediment at 16°C for 20 min at 10,000 rpm (15,000*g*) in an HB-6 rotor.
6. Aspirate partially, rinse sample–cushion interface two times with BRB80, aspirate completely, and postfix in –20°C methanol for 5 min.
7. Rehydrate two times with TBS-Tx and perform antitubulin immunofluorescence as described in **ref. *12***. An example of typical results is shown in **Fig. 1A**.

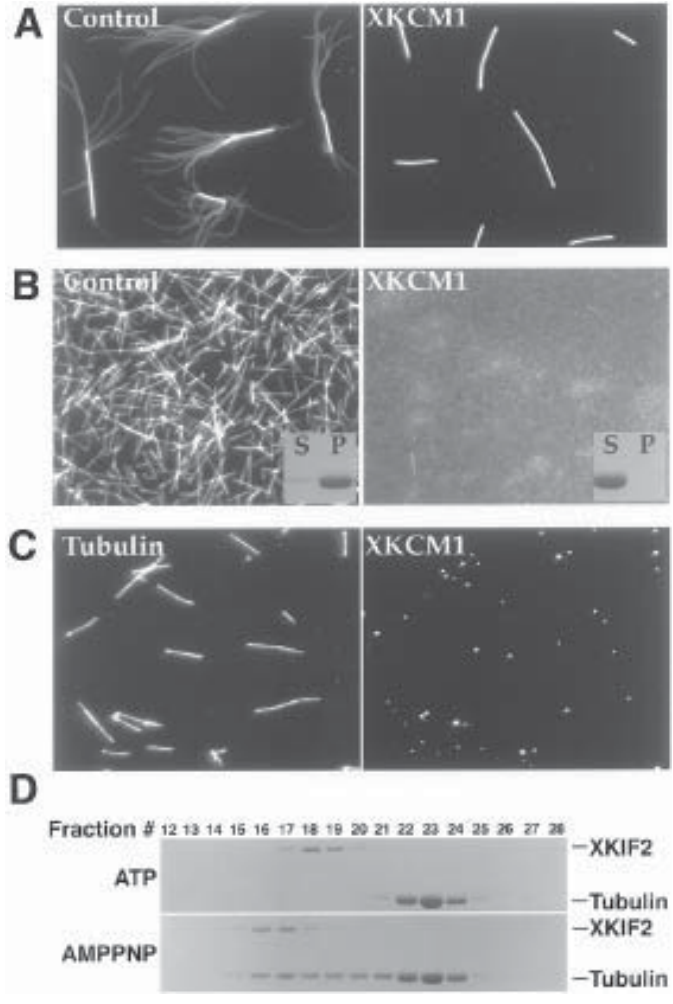

Fig. 1. Examples of results from various assays used to detect microtubule destabilization activity. **(A)** Results from fixed-time-point assay on dynamic microtubules showing microtubules incubated with a control buffer (left-hand panel) or XKCM1 (right-hand panel). **(B)** Results from a qualitative visual fluorescence assay on stabilized microtubule substrates showing GMP–CPP microtubules incubated with a control buffer (left-hand panel) or XKCM1 (right-hand panel). The inset shows the results of the same samples run on a sedimentation analysis. **(C)** Results from the immunofluorescence analysis showing the localization of tubulin (left-hand panel) and XKCM1 (right-hand panel) during microtubule depolymerization. **(D)** Results from the tubulin dimer binding assays showing the nucleotide dependency of XKIF2 binding to tubulin as analyzed by gel-filtration chromatography. Reproduced from Desai, et al. (1999) *Cell* **96,** 69–78; ©Cell Press, Cambridge, MA.

3.2.2 Real-Time Assay

To assess the effect of a kinesin on prepolymerized MTs we utilize flow cells and real-time VE-DIC analysis. Briefly, we use double stick-tape flow cells made from clean cover slips (http://skye.med.harvard.edu/newprotocols/toc.html) and axonemes as nucleating structures for MTs.

1. Axonemes are adsorbed to flow cell surfaces for 3 min, the surface blocked with 5 mg/mL bovine serum albumin (BSA) for 5 min, after which the chamber is rinsed with 3–4 chamber volumes of BRB80.
2. Two to three chamber volumes of tubulin mix (**Subheading 3.1.1.**) is introduced (the mix is prepared in BRB80 buffer containing GTP and ATP).
3. After approx 10 min, when significant MT assembly is evident from both ends of axonemes, we flow in a mix of the kinesin diluted into the initial tubulin mix and record the effect on the prepolymerized MTs. Storage buffer diluted similarly is used as a control (*see* **Note 6**)

3.3. Assays on Stabilized MT Substrates

To characterize how a kinesin destabilizes MTs, we analyze its effect on MTs stabilized by the drug Taxol or by polymerization with GMP–CPP, a GTP analog that is essentially nonhydrolyzable by tubulin over the time-course of most experiments. Because Taxol and GMP–CPP eliminate the intrinsic GTP hydrolysis-driven destabilization mechanism of tubulin, depolymerization of stabilized MTs requires input of free energy and multiple rounds of action. Thus, these substrates are very useful to analyze if the action of a destabilizer is catalytic and, if so, to analyze the details of the reaction mechanism. In this section, we describe a quick qualitative visual assay to test if a kinesin depolymerizes such MTs (**Subheading 3.3.1.**) as well as a more rigorous sedimentation assay (**Subheading 3.3.2.**). In addition we describe a microscopy assay to look at the depolymerization reaction in real time (**Subheading 3.3.3.**).

3.3.1. Qualitative Visual Fluorescence Assay

Fluorescent-stabilized MTs are polymerized from a mixture of unlabeled and labeled tubulin (generally with tetramethylrhodamine) as described in **Subheading 3.1.2.** or **Subheading 3.1.3.** depending on whether they are stabilized with GMP–CPP or Taxol. We generally use a ratio of 1 part labeled tubulin to 7 parts unlabeled tubulin.

In this assay, the adenine nucleotide, the type and amount of kinesin as well as the final salt concentration can be varied. To rigorously assess the effects of these manipulations, the sedimentation assay described in **Subheading 3.3.2.** should be performed on the variations (*see* **Note 7**).

1. At room temperature, mix the following:
   a. 1 µL of 15 m*M* Mg–ATP or 50 m*M* Mg–AMP–PNP.
   b. 1 µL 5X BRB80.
   c. 1–3 µL purified kinesin or fraction to be tested; for a new protein the final KCl concentration should be varied between 0 and 100 m*M*.
2. Add 5 µL of 2–3 µ*M* GMP–CPP MTs or 2 µ*M* Taxol-stabilized MTs (in BRB80 containing 10–20 µ*M* Taxol; the final Taxol concentration should be two to three times the final tubulin concentration).
3. After 5 min, 10 min, and so forth, at room temperature, squash 1.5 µL under an 18 × 18-mm cover slip and view by epifluorescence microscopy. A typical example is shown in **Fig. 1B**.

3.3.2. Sedimentation Assay

Taxol and GMP–CPP MTs are polymerized from unlabeled tubulin as described in **Subheadings 3.1.2.** and **3.1.3.** Polymerized MTs are sedimented and resuspended to around 10–15 µ*M* in BRB80 with 1 m*M* DTT (for GMP–CPP MTs) and BRB80, 20 µ*M* Taxol, and 1 m*M* DTT (for Taxol-stabilized MTs). The stabilized MT stock concentrations are then adjusted to two times the final desired MT concentration using the appropriate resuspension buffer (*see* **Note 8**).

1. For a 100-µL reaction, prepare a 50-µL mix at room temperature comprised of 1X BRB80, 1 m*M* DTT, Mg–ATP (2–4 m*M*) or Mg–AMP–PNP (10 m*M*), the kinesin to be tested, and KCl such that the final KCl concentration in 100 µL will be 50–75 m*M*. To this mix, add 50 µL of 4 µ*M* stabilized MTs (final 2 µ*M* tubulin in MT polymer). Incubate at room temperature for 15–30 min.
2. Sediment 80 µL in a TLA100 rotor at 90,000 rpm (350,000*g*) for 5 min at 23°C. The residual 20 µL can be frozen in liquid nitrogen and used to estimate total recovery if desired.
3. Remove supernatant as thoroughly as possible and save; resuspend pellet in 80 µL BRB80, 5 m*M* $CaCl_2$, and the same KCl concentration as for the reaction, and incubate on ice for 10 min.
4. Analyze 20–25 µL of the supernatant and the resuspended pellet on a 10% sodium dodecyl sulfate-polyacrylamide gel electrophoresis (SDS-PAGE) gel followed by Coomassie staining. The amount of tubulin in the supernatant and pellet can be quantified by densitometry of a scanned Coomassie-stained gel. In addition, Western blotting of approx 5 µL supernatant and the pellet can be used to assess the kinesin used in the assay fractionates.

3.3.3. Real-Time Assay

We used real-time analysis of XKCM1-induced depolymerizing GMP–CPP MTs to show that the depolymerization action of this kinesin acted on ends and not via a severing mechanism and also to determine the polarity of action — an important criterion to distinguish between motility-based targeting to ends and

direct targeting to ends. The assay we used allowed us to film depolymerization of GMP–CPP MTs and then unambiguously assign polarity to the substrate MTs.

1. Coat double-stick-tape flow cell surfaces with the MT glue for 3 min (*see* **Note 9**).
2. Block the flow cell surfaces with 5 mg/mL BSA in BRB80. This preparation binds MTs to the cover-slip surface without significantly releasing, moving, or depolymerizing them in the presence of ATP in the time-scale of this assay.
3. Introduce segmented GMP–CPP MTs into the flow cell for 2 min — adjust the time and concentration of the segmented MTs to result in a "good" density on the surface (*see* **Note 10**).
4. Rinse extensively with BRB80, 1 m*M* DTT, 1.5 m*M* Mg–ATP, and 1X OSM.
5. Introduce the kinesin to be tested into the flow cell. In our case, 20 n*M* XKCM1, preincubated for 10 min on ice with a 30-fold molar excess of either anti-XKCM1 antibody or an irrelevant rabbit IgG adjusted to BRB80, 1 m*M* DTT, 1.5 m*M* Mg–ATP, 1 mg/mL BSA, and 1X OSM.
6. Monitor the reaction using timelapse fluorescence microscopy with a 60×, 1.4 N.A. Nikon objective and a video/cooled CCD camera. We routinely collect one image every 10–20 s, with each exposure being 0.5–1 s.
7. After 10–15 min, introduce approx 200 n*M* K560 into the flow cell and record the motility of the observed MTs to retroactively and unambiguously assign their polarity.

3.4. Immunofluorescence Assay

To determine if the kinesin of interest targeted specifically to the ends of the microtubules or if it bound all along the walls of the microtubules, it is necessary to carry out immunofluorescence analysis of the kinesin localization during the depolymerization reaction. For immunofluorescence analysis of kinesins on GMP–CPP MTs, it is necessary to have a glutaraldehyde-resistant primary antibody to the kinesin. We have had good success obtaining glutaraldehyde-resistant antibodies by pretreating antigens prior to injection with glutaraldehyde.

1. Mix 50 n*M* XKCM1 with 1–2 µ*M* GMP–CPP MTs in 1.5 m*M* Mg–ATP or 5 m*M* Mg–AMP–PNP in BRB80, and 1 m*M* DTT.
2. After 3 min (ATP) or 15 min (AMP–PNP) at room temperature, fix 3 µL with 30 µL of BRB80/1% glutaraldehyde equilibrated at room temperature and incubate at room temperature for 3 min.
3. Dilute with 800 µL of BRB80 equilibrated at room temperature and sediment 50 µL onto a cover slip (gently mix by inversion just before withdrawing the 50 µL).
4. For the sedimentation, put 5 mL BRB80 in a spindown tube and underlay (using a cut-off 1-mL pipet tip) with 2 mL of BRB80, and 10% glycerol. Pipet the 50 µL fixed diluted reaction on top of the BRB80 and sediment 1–1.5 h at 12–13K

(25,000*g*) in a HB-6 rotor at 20°C. If the MTs are too dense or too sparse, adjust the amount sedimented in subsequent experiments.

5. After sedimentation, postfix in –20°C methanol for 5 min, rehydrate, and process for indirect immunofluorescence using glutaraldehyde-resistant anti-XKCM1 and anti-tubulin antibodies. The results of such an experiment performed with XKCM1 in the presence of 5 m*M* Mg–AMP–PNP is shown in **Fig. 1C** (*see* **Note 11**).

3.5. Tubulin Dimer Binding Assays

In our analysis of *Kin*I kinesins, we found that ATP hydrolysis is not required for MT end targeting or for induction of a conformational change at the MT end. Therefore, we hypothesized that it is used to recycle XKCM1/XKIF2 by dissociating them from tubulin dimer. With dynamic MT substrates, disruption of the end structure would presumably induce a catastrophe, releasing a small number of XKCM1/XKIF2-tubulin dimer complexes and a much larger number of free-tubulin dimers as the unstable GDP–tubulin core of the MT depolymerizes. The XKCM1/XKIF2-tubulin dimer complex would need to dissociate to allow the XKCM1/XKIF2 to act again at a new MT end. This hypothesis predicts that an XKCM1/XKIF2-tubulin dimer complex should persist in the presence of AMP–PNP but not ATP. To test this, we developed a gel filtration chromatography assay to analyze the interaction of *Kin*I kinesins versus K560 with tubulin dimer in the presence of ATP or AMP–PNP. The assay is designed for small-scale analysis using a Pharmacia SMART system, thus requiring only small amounts of protein and nucleotide analogs (*see* **Note 12**).

1. The SMART system should be set at 20°C. Prepare ATP column buffer or AMP–PNP column buffer consisting of 1X BRB80, 75 m*M* KCl, 200 µ*M* Mg–ATP or 200 µ*M* Mg–AMP–PNP, 20 µ*M* GDP, and 1 m*M* DTT.
2. Make 80 mL buffer without nucleotides or DTT, degas, then add nucleotides plus DTT and wash one pump into the buffer. To do this, pour 40 mL buffer into a 50-mL conical flask, transfer the pump frit to the buffer (use a plastic transfer pipet to suck off water adhered to the sides of the frit), and while the pump is washing, pour in the other 40 mL of buffer. With some practice, one can use approx 60 mL for three runs needed per experimental condition. **Note:** The buffer volumes described are for 10-mL pumps; some systems are equipped with 20-mL pumps which will require twice the buffer volume. The buffer volume is minimized primarily because of the expense of AMP-PNP.
3. Rinse system and 20-µL loop well with the column buffer. Install the Superose 6 column and equilibrate at 20 µL/min for 2 h followed by 40 µL/min for 1 h (20 column volumes).
4. Mix either 10 µ*M* tubulin, 2 µ*M* kinesin to be tested, or 10 µ*M* tubulin alone, or 2 µ*M* kinesin alone in a buffer of the following final composition: BRB80, 75 m*M* KCl, 1 m*M* DTT, 50 µ*M* GDP, 3 m*M* Mg–ATP/3 m*M* Mg–AMP–PNP. Mix

all buffer and nucleotide components before adding the proteins. Incubate at room temperature for 15 min, then spin filter using a 0.45-µm Ultrafree MC filter at 7000 rpm (4,000*g*) in an Eppendorf microfuge for 2 min at room temperature. Fractionate the filtrate on the Superose 6 at 40 µL/min, collecting 50-µL fractions. The total program is 2.9 mL after the start of injection; collect fractions between 0.5 and 2.2 mL after the start of injection.

5. Add 17 µL of 4X sample buffer to each 50-µL fraction and analyze 30–35 µL on a 10% SDS-PAGE gel, followed by Coomassie-staining. An example of a typical run is shown in **Fig. 1D**.

4. Notes

1. It is important to measure the salt concentration of the eluted fractions from each of the different preparations and to make up a control buffer that corresponds exactly to this buffer composition for all of the assays described.
2. When working with microtubules, especially with microtubules stabilized with GMP–CPP, it is essential to make all buffers as potassium salts. It has been shown that the combination of glycerol and sodium ions can induce hydrolysis of GMP–CPP and, thus, decrease the stability of these microtubule preparations ***(17)***.
3. GMP–CPP MTs are cold-labile so they should not be stored on ice.
4. If Taxol is added all at once, it will cause tubulin precipitation! If polymerizing 2 mg/mL tubulin, use 2 µ*M*, 20 µ*M*, and 200 µ*M* steps.
5. The axoneme concentration must be optimized for each prep such that 1 µL of the reaction (the volume pelleted onto the cover slip) results in a "good" density when viewed using a 60× objective. "Good" density is when the axonemes are not too sparse but are also not so dense as to prevent easy photography and length measurements of the nucleated MTs.
6. A major problem with the analysis of kinesins using such an assay is the tendency of the kinesins to adsorb to flow cell surfaces and, as a consequence, to rigor bind MTs to surfaces as well as to remove the kinesin from solution. This problem disallows use of such an assay to quantitatively assess the effects of kinesins on the individual parameters of microtubule dynamics. Nevertheless, this assay was extremely important in our analysis because it provided direct evidence that XKCM1 is a catastrophe-inducing kinesin.
7. Using this type of quick assay, we can detect depolymerization activity in lysates of insect cells infected by baculoviruses coding for *Kin*I kinesins but not control virus-infected cells. In addition, we can monitor depolymerization activity during purification.
8. In our assays the final concentration of MTs used was low (2 µ*M*) because the released end product from the depolymerization induced by *Kin*I kinesins is competent to repolymerize. To minimize complications in interpretation arising from potential repolymerization, we performed the analysis at low MT concentrations. Analysis of varying MT concentration could possibly be performed using nocodazole to trap released tubulin dimer and prevent repolymerization. How-

ever, potential interference from nocodazole at MT ends might complicate interpretation of such an analysis.

9. MT glue is a preparation used to coat a flow cell such that it will bind MTs but not release, move, or depolymerize them in the presence of ATP. We used a very dilute SP-Sepharose fraction from a insect cell lysate expressing low levels of XKIF2 that satisfied these three criteria. Alternatives include *N*-ethylmalemide (NEM)-treated *Xenopus* extract or a mutant kinesin although different adherence methods may significantly affect the observed rates of depolymerization.
10. Segmented GMP–CPP MTs that have dimly labeled plus and minus end segments polymerized off brightly labeled GMP–CPP MT seeds were prepared by diluting bright GMP–CPP seeds (1:2 rhodamine labeled:unlabeled tubulin) into 1.5 µ*M* dim GMP–CPP tubulin mix (1:11 rhodamine labeled:unlabeled tubulin) and incubating at 37°C for 1–2 h. All GMP–CPP mixes contained 500 µ*M* GMP–CPP
11. In addition to this method, morphological analysis of GMP–CPP MTs incubated with XKCM1 can also be performed using negative-stain electron microscopy. In this case reaction mixes are pipetted onto a glow-discharged carbon and formvar-coated copper grid, negative-stained using uranyl acetate and viewed in an electron microscope (*see* **ref. *4*** for further details).
12. For each two-protein (i.e., *Kin*I kinesin-tubulin or K560-tubulin) combination there are three runs in ATP column buffer and three runs in AMP–PNP column buffer (each protein alone plus the two-protein mixture). The reaction mixes should be prepared from frozen stocks, incubated and immediately injected onto the column after filtration. After the three runs in one nucleotide state are done, equilibrate the column in the other nucleotide state as described in **Subheading 3.5.**, **step 2**, and then do the other three reactions.

Acknowledgments

C. E. W. was supported by the USAMRMC Breast Cancer Research Program and the National Institute of Health and A. D. by a Howard Hughes Medical Institute predoctoral fellowship. The authors wish to thank Tim Mitchison in whose lab these assays were initially developed.

References

1. Hirokawa, N., Noda, Y., and Okada, Y. (1998) Kinesin and dynein superfamily proteins in organelle transport and cell division. *Curr. Opin. Cell Biol.* **10,** 60–73.
2. Vale, R. D. and Fletterick, R. J. (1997) The design plan of kinesin motors. *Annu. Rev. Cell Dev. Biol.* **13,** 745–777.
3. Yang, J. T., Laymon, R. A., and Goldstein, L. S. B. (1989) A three-domain structure of kinesin heavy chain revealed by DNA sequence and microtubule binding analyses. *Cell* **56,** 879–889.
4. Desai, A., Verma, S., Mitchison, T. J., and Walczak, G. E. (1999) Kin I kinesins are microtubule-destahilizing enzymes. *Cell* **96,** 69–78.

5. Endow, S. A., Kang, S. J., Satterwhite, L. L., Rose, M. D., Skeen, V. P., and Salmon, E. D. (1994) Yeast Kar3 is a minus-end microtubule motor protein that destabilizes microtuhules preferentially at the minus ends. *EMBO J.* **13,** 2708–2713.
6. Saunders, W., Hornack, D., Lengyel, V., and Deng, C. (1997) The *Saccharomyces cerevisiae* kinesin-related motor Kar3p acts at preanaphase spindle poles to limit the number and length of cytoplasmic microtubules. *J. Cell Biol.* **137,** 417–431.
7. Cottingham, F. R. and Hoyt, M. A. (1997) Mitotic spindle positioning in Saccharomyces cerevisiae is accomplished by antagonistically acting microtubule motor proteins. *J. Cell Biol.* **138,** 1041–1053.
8. DeZwaan, T. M., Ellingson, E., Pellman, D., and Roof, D. M. (1997) Kinesin-related KIP3 of Saccharomyces cerevisiae is required for a distinct step in nuclear migration. *J. Cell Biol.* **138,** 1023–1040.
9. Huyett, A., Kahana, J., Silver, P., Zeng, X., and Saunders, W. S. (1998) The Kar3p and Kip2p motors function antagonistically at the spindle poles to influence cytoplasmic microtubule numbers. *J. Cell Sci.* **111,** 295–301.
10. Hyman, A., Drechsel, D., Kellogg, D., Salser, S., Sawin, K., Steffen, P., et al. (1991) Preparation of modified tubulins. *Methods Enzymol.* **196,** 478–485.
11. Hyman, A. A., Salser, S., Drechsel, D. N., Unwin, N., and Mitchison, T. J. (1992) Role of GTP hydrolysis in microtubule dynamics: information from a slowly hydrolyzable analogue, GMPCPP. *Mol. Biol. Cell* **3,** 1155–1167.
12. Mitchison, T. J. and Kirschner, M. W. (1984) Dynamic instability of microtubule growth. *Nature* **312,** 237–242.
13. Evans, L., Mitchison, T., and Kirschner, M. (1985) Influence of the centrosome on the structure of nucleated microtubules. *J. Cell Biol.* **100,** 1185–1191.
14. Vale, R. D. (1991) Severing of stable microtubules by a mitotically activated protein in *Xenopus* egg extracts. *Cell* **64,** 827–839.
15. Shimizu, T., Toyoshima, Y. Y., and Vale, R. D. (1993) Use of ATP analogs in motor assays, in *Motility Assays for Motor Proeins* (Scholey, J. M., ed.), Academic San Diego, CA, pp. 167–176.
16. Caplow, M., Ruhlen, R. L., and Shanks, J. (1994) The free energy for hydrolysis of a microtubule-bound nucleotide triphosphate is near zero: all of the free energy for hydrolysis is stored in the microtubule lattice. *J. Cell Biol.* **127,** 779–788.
17. Caplow, M. and Shanks, J. (1996) Evidence that a single monolayer tubulin-GTP cap is both necessary and sufficeint to stabilize microtubules. *Mol. Biol. Cell* **7,** 663–675.
18. McNally, F. J. and Vale, R. D. (1993) Identification of katanin, an ATPase that severs and disassembles stable microtubules. *Cell* **75,** 419–429.
19. Hartman, J. J., Mahr, J., McNally, K., Okawa, K., Shimizu, T., Vale, RD., and McNally, F. (1998) Katanin, a microtubule-severing protein, is a novel AAA ATPase that targets to the centrosome using a WD4O-containing subunit. *Cell* **93,** 277–287.

11

Green Fluorescent Protein as a Tag for Molecular Motor Proteins

Sharyn A. Endow

1. Introduction

Following the discovery that the green fluorescent protein (GFP) fluoresces when expressed in foreign organisms ***(1)*** and that it can serve as a reporter in living cells when fused to another protein ***(2)***, GFP has come into wide use. GFP offers advantages over other reporters in that it fluoresces in live cells and its fluorescence does not require the addition of any substrates, cofactors, or accessory proteins. This means that GFP-tagged proteins can be used to follow the dynamics of specific proteins in living cells, making it feasible to carry out experiments that previously were either difficult or not possible to perform. GFP fusion proteins can also be targeted for expression in given cellular compartments and it is possible to ensure that all of the protein is labeled by transferring the gene fusion into a null mutant, representing a great increase in efficiency compared to previous methods of fluorescent labeling of proteins. Moreover, GFP fluorescence is long-lasting, and its sensitivity to pH and temperature has enabled workers to use GFP fusion proteins to measure pH in specific cellular compartments ***(3)*** and to follow protein localization in temperature-shift experiments ***(4)***.

For the molecular motor proteins, GFP has been used to study the localization of specific motors in the cell ***(5,6)*** and the dynamics of processes in which they are involved (e.g., spindle assembly ***[7,5,8–10]*** and pigment granule dispersion/aggregation ***[11]***), and to label motors for single-motor in vitro motility assays ***(12,13)***. Nonetheless, the use of GFP to study molecular motor proteins has not yet been fully exploited. The ability to visualize GFP-tagged motors in live cells should allow workers to investigate the regulation and motility of the motors in vivo, as well as use the fluorescence properties of GFP to study motor

From: *Methods in Molecular Biology*, Vol. 164: *Kinesin Protocols*
Edited by: I. Vernos

biophysics and structure–function in vitro. The first structure–function study of a molecular motor protein using GFP to detect movement of a motor region has recently been reported for myosin ***(14)*** and is discussed in **Subheading 2.3.**

2. Properties of GFP

2.1. GFP Fluorescence

The fluorescence excitation and emission properties of GFP are similar but not identical to those of fluorescein isothiocyanate (FITC). This means that it is possible to use filter sets designed for FITC to excite GFP and collect its fluorescence, although neither the FITC excitation nor emission filters are optimized for GFP. Several workers have designed custom GFP filter sets ***(15)***, which are now available commercially. However, the recovery of mutant GFPs that fluoresce much more brightly than wild-type GFP ***(16–18)*** has greatly reduced the need to use custom GFP filter sets. The use of the brighter fluorescing GFPs is especially advantageous for laser-scanning confocal microscopy because it is usually not possible to optimize the laser for GFP excitation. Perhaps the most widely used of the brighter GFPs are S65T GFP ***(16)*** and enhanced green fluorescent protein (EGFP) ***(17)***, which is available commercially. These GFPs can be excited using a Hg or Xe lamp and standard FITC filter sets in a fluorescence microscope or the 488-nm line of a Kr–Ar laser for confocal microscopy, and the fluorescence can be collected using the emission filter in the FITC set. Several of the mutant GFPs are shifted in emission wavelength, giving them a different color fluorescence (*see* **ref. *15*** for a table of these GFPs). These different color GFPs are useful for double-label imaging ***(19)***, as well as other applications.

2.2. Photobleaching of GFP

One of the remarkable uses of GFP has been its application in fluorescence recovery after photobleaching (FRAP) experiments to study protein dynamics and transport in living cells ***(20–22)***. These groundbreaking experiments have resulted in conceptual advances that could lead to an understanding of fundamental aspects of cell function. The experiments are performed by using intense laser irradiation to photobleach a GFP fusion protein in a defined region of the cell and then monitoring the fluorescence recovery of the region, which is brought about by diffusion or transport of the GFP fusion protein back into the region (**Fig. 1A**). Both the kinetics of recovery and the cellular structures that are labeled prior to photobleaching and during recovery can provide information about the cellular process under study.

Although photobleaching recovery techniques were developed prior to the use of GFP ***(23,24)***, previous studies were limited to membranes because meth-

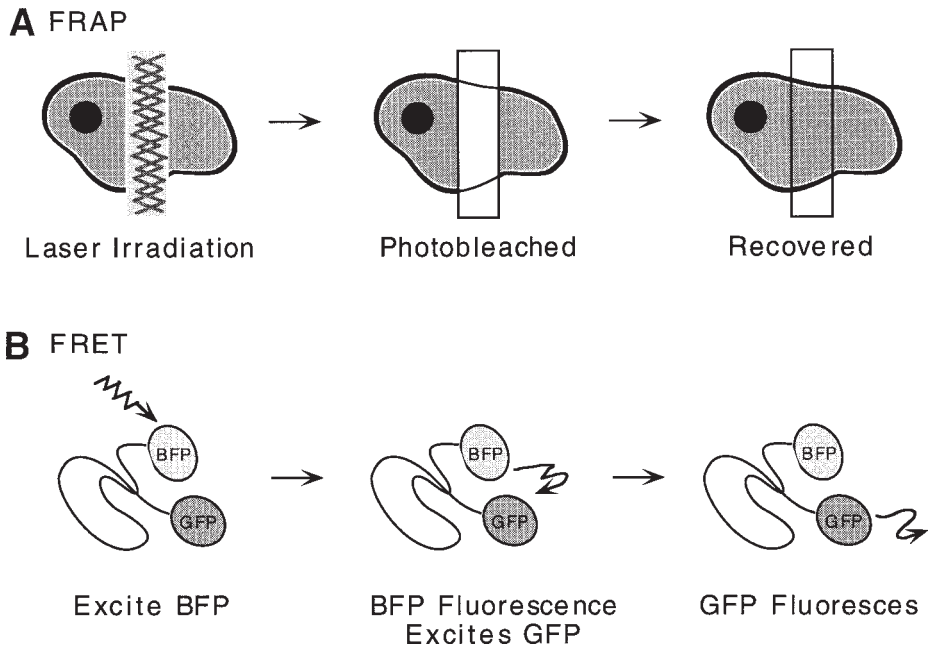

Fig. 1. FRAP and FRET with GFP. **(A)** FRAP is performed by irradiating a GFP fusion protein in a cell to photobleach the GFP, then monitoring the fluorescence recovery of the photobleached region. Both the kinetics of recovery and the GFP labeled structures prior to photobleaching and during fluorescence recovery can provide information about the cellular process under study. **(B)** FRET is performed by fusing to a given protein (or to different proteins) two fluorescence molecules that are excited by light of different wavelengths and emit different color fluorescence. The fluorescent molecules are chosen so that the fluorescence of one can excite the other. The two molecules in the example shown are GFP and BFP. The experiment is performed by the investigator exciting BFP, the BFP fluorescence then excites the GFP, and the GFP fluorescence is monitored by the investigator. Any movement of the protein regions to which BFP or GFP are attached will increase or decrease the fluorescence intensity. This permits the BFP and GFP to serve as reporters for the movement.

ods for fluorescent labeling could not accurately target specific internal cellular structures. The ability to express GFP fusion proteins that label specific subcellular structures has opened new possibilities for the use of photobleaching recovery experiments, and some of these should be directly applicable to the study of molecular motor proteins in the cell. Although photobleaching methods have not yet been used to study molecular motors, these methods represent a powerful means for obtaining information about motor function in vivo that cannot easily be obtained in other ways.

Photobleaching experiments require the use of a mutant GFP that does not show photoactivation, a process which results in brighter fluorescence with increased excitation by 395- or 490-nm light ***(1,25)***. Photoactivation does not occur in several of the GFP mutants that have been described, including S65T GFP ***(16)***, and one of these mutants should be used for photobleaching experiments rather than wild-type GFP.

2.3. Fluorescence Energy Transfer Using GFP

Green fluorescent protein can also be used in fluorescence resonance energy transfer (FRET) experiments to detect movement of one region of a protein relative to another or interactions of a given protein with a second protein. Fluorescence energy transfer requires the use of two fluorescent molecules attached to the protein or proteins under study that are excited by different wavelengths of light and emit different wavelengths of fluorescence, such that the fluorescence emitted by one excites the other (**Fig. 1B**). During an experiment, one fluorescent molecule is excited by the investigator who then measures the fluorescence from the second molecule. The intensity of fluorescence depends on the proximity of the second fluorescent molecule to the first, which can change during the course of the experiment if movement occurs in the protein regions to which the fluorescent molecules are attached or if interactions between the two fluorescently labeled proteins change. Changes in the emitted fluorescence intensity can be readily detected and recorded using sensitive detectors.

Fluorescence energy transfer has recently been used to demonstrate that the coiled-coil rod of myosin recoils like a lever arm during ATP hydrolysis ***(14)***. This was done by fusing GFP and BFP (blue fluorescent protein, a mutant of GFP) to either end of the myosin S1 motor domain and expressing the fusion protein. The GFP and BFP were in close proximity to one another in the fusion protein, making it possible for the workers to excite BFP, whose fluorescence, in turn, excited GFP, and to monitor the GFP fluorescence (**Fig. 1B**). The BFP fluorescence is transient, rather than long-lasting like GFP fluorescence, making BFP an excellent fluorescence donor for exciting GFP in these experiments. Changes in fluorescence intensity were measured with different added nucleotides (ATP, ADP) and the time-course of changes in fluorescence intensity was followed after adding ATP, permitting the workers not only to detect the movement between the GFP and BFP but also to determine the step in ATP hydrolysis at which the movement takes place. The results of these experiments provide direct evidence for the "swinging lever arm" hypothesis of myosin function ***(26)*** and represent major progress in understanding how myosin works.

It should also be possible to perform similar experiments with other molecular motors to detect motor movements or conformational changes during nucleotide hydrolysis. However, the large size of GFP (27 kDa) compared to the

motor domain of the kinesin proteins (approx 40 kDa) make these experiments less favorable for the kinesin motors than for myosin with its much larger S1 head (approx 95 kDa). Fluorescence energy transfer is a highly sensitive way to detect motor structural changes or movements in vitro and has the added advantage of permitting these movements to be correlated with steps in the ATP hydrolysis cycle; thus, the coupling between nucleotide hydrolysis and the motor movements can be ascertained. Fluorescence energy transfer is also potentially capable of detecting motor activity in live cells, as well as interactions of motors with other proteins in vivo. These applications of GFP to the study of molecular motors have not yet been reported, but GFP and its variants would be ideal energy donors and acceptors for these experiments because they fluoresce readily in living cells and can be targeted to specific cellular regions.

3. Plasmid Construction and Transformation

In constructing plasmids to express *gfp* gene fusions, an appropriate GFP should be selected first. Selection of a GFP for use depends on the intended experiments; for example, S65T GFP or EGFP can be used for photobleaching experiments, but wild-type GFP should not be used in these experiments because its fluorescence initially increases or photoactivates with increased excitation light, rather than immediately photobleaching. S65T GFP and EGFP also fluoresce more brightly than wild-type GFP and are therefore more favorable for protein localization. BFP is useful as a fluorescence donor in energy transfer experiments, but it is not generally useful in localization experiments because its fluorescence is transient, rather than long-lasting like many of the other GFPs. For dual imaging, mutant GFPs with different excitation and emission wavelengths can be used to label two different proteins with different colors of fluorescence ***(19)***.

For expression in plants and humans, *gfps* with altered codon usage have been made to optimize expression in *Arabidopsis* ***(27)*** and human cells ***(28,29)***. A humanized GFP has also been found to fluoresce more brightly than wild-type GFP when expressed in plants ***(30)***, probably because of the similarity in codon usage between humans and higher plants ***(31)***. Expression of GFP in *Arabidopsis* and several other higher plants has been complicated by the presence of a cryptic splice site in the wild-type *gfp* gene ***(27)***, which has been removed in the *Arabidopsis*-optimized *gfp*.

After selecting a GFP for use, any of the usual protein expression vectors can be used for plasmid construction. These have been reviewed in detail elsewhere ***(15)***. Usual methods can be used to construct gene fusions, including introduction of a common restriction enzyme site between the genes by polymerase chain reaction (PCR), and overlap extension PCR ***(32)*** (*see* Chapter 5 for more detailed methods on constructing gene fusions). Most GFP fusion

proteins that have been reported to date contain the GFP fused to the N- or C-terminus of the target protein, although some cases of successful internal insertions of GFP into another protein are known (*see* **ref. *15*** for examples). Standard methods are used to transform *gfp* gene fusion plasmids into organisms or cells to obtain transient or stable transformants.

4. Imaging GFP

Green fluorescent protein fluorescence can be detected and recorded using any of the standard methods of detecting fluorescence. These include conventional fluorescence microscopy, microscopy with a cooled charged coupled device (CCD)-camera, and laser-scanning confocal microscopy. Initial detection of GFP can usually be performed using FITC filter sets, although some variants of GFP require special filter sets for excitation and/or fluorescence detection, and some require a special laser when used in confocal microscopy. A table of the filter sets that are recommended for use with several commonly used wild-type and mutant GFPs in various applications can be found in **ref. *15***. The new fluorescence stereomicroscopes are potentially useful for screening mutants of *Caenorhaebditis elegans*, *Drosophila*, and plants for GFP fluorescence in specific cells or tissues, as well as detecting and visualizing GFP fluorescence in whole organisms, cultured cells, and tissue slices. The new Leica MZ FLIII fluorescence stereomicroscope has a unique design that results in especially bright GFP fluorescence.

4.1. Fixed Specimens

Green fluorescent protein fluorescence is labile to many of the fixatives commonly used to preserve specimens, resulting in the destruction of fluorescence in the fixed cells. Some workers have reported the preservation of GFP fluorescence after fixation with formaldehyde ***(2,33,34)***, methanol ***(35)***, or glutaraldehyde ***(35)***, but variable results have been obtained with different GFP fusion proteins in the same or different organisms. The problems with destruction of GFP fluorescence in fixed specimens can be circumvented by using an antibody to GFP to detect the GFP fusion protein instead of attempting to preserve the GFP fluorescence in the specimen. Several GFP antibodies are now available commercially and make it possible to fix cells expressing a GFP fusion protein using standard methods, then to detect the GFP fusion protein by staining the fixed cells with the GFP antibody, giving a bright signal.

4.2. Live Imaging

The most important advantage to the use of GFP is that GFP-tagged proteins can be visualized in live cells with minimal perturbation to the cell. Preparation of specimens for live imaging is simply to mount them in a nonfluorescent

medium and take care to prevent anoxia (lack of oxygen) during the imaging. Mounting of specimens can be accomplished in many cases by replacing culture medium with a simple salt solution that lacks fluorescent compounds (flavins, aromatic amino acids, serum), immobilizing in agar, or mounting under oil prior to imaging. For live motile organisms such as *C. elegans* or *Drosophila*, anesthesia is required to immobilize the organism, although these organisms can also be immobilized for short periods of time by placing them on ice for a few minutes prior to imaging.

Anoxia can be prevented for specimens mounted under oil during long periods of time-lapse imaging by mounting the specimens on oxygen-permeable membranes in custom holders ***(36)*** rather than on glass slides, or by omitting a cover slip and using an inverted microscope.

Detailed protocols for time-lapse imaging of GFP-tagged proteins in live yeast, *Dictyostelium*, *Drosophila*, and mammalian cells using a cooled CCD camera or confocal microscopy have recently been collected and published elsewhere ***(15,37)***. Some of these methods were specifically developed to image a molecular motor fused to GFP in a particular organism using a cooled CCD camera or laser-scanning confocal microscopy. These and other protocols in the collections are directly applicable to time-lapse imaging of GFP fusions to any given molecular motor protein, although methods for specimen preparation vary with each organism.

Acknowledgments

The work in my laboratory is supported by a grant from the NIH. I thank A. J. Kim for drawing **Fig. 1**.

References

1. Chalfie, M., Tu, Y., Euskirchen, G., Ward, W. W., and Prasher, D. C. (1994) Green fluorescent protein as a marker for gene expression. *Science* **263**, 802–805.
2. Wang, S. and Hazelrigg, T. (1994) Implications for *bcd* mRNA localization from spatial distribution of *exu* protein in *Drosophila* oogenesis. *Nature* **369**, 400–403.
3. Llopis, J., McCaffery, J. M., Miyawaki, A., Farquhar, M. G., and Tsien, R. Y. (1998) Measurement of cytosolic, mitochondrial, and Golgi pH in single living cells with green fluorescent proteins. *Proc. Natl. Acad. Sci. USA* **95**, 6803–6808.
4. Lim, C. R., Kimata, Y., Nomaguchi, K., and Kohno, K. (1995) Thermosensitivity of green fluorescent protein fluorescence utilized to reveal novel nuclear-like compartments in a mutant nucleoporin NSP1. *J. Biochem.* **118**, 13–17.
5. Endow, S. A. and Komma, D. J. (1996) Centrosome and spindle function of the *Drosophila* Ncd microtubule motor visualized in live embryos using Ncd–GFP fusion proteins. *J. Cell Sci*.**109**, 2429–2442.
6. Moores, S. L., Sabry, J. H., and Spudich, J. A. (1996) Myosin dynamics in live *Dictyostelium* cells. *Proc. Natl. Acad. Sci. USA* **93**, 443–446.

7. Yeh, E., Skibbens, R. V., Cheng, J. W., Salmon, E. D., and Bloom, K. (1995) Spindle dynamics and cell cycle regulation of dynein in the budding yeast, *Saccharomyces cerevisiae*. *J. Cell Biol*. **130**, 687–700.
8. Endow, S. A. and Komma, D. J. (1997) Spindle dynamics during meiosis in *Drosophila* oocytes. *J. Cell Biol.* **137**, 1321–1336.
9. Huyett, A., Kahana, J., Silver, P., Zeng, X., and Saunders, W. S. (1998) The Kar3p and Kip2p motors function antagonistically at the spindle poles to influence cytoplasmic microtubule numbers. *J. Cell Sci.* **111**, 295–301.
10. Endow, S. A. and Komma, D. J. (1998) Assembly and dynamics of an anastral:astral spindle: the meiosis II spindle of *Drosophila* oocytes. *J. Cell Sci*. **111**, 2487–2495.
11. Tuma, M. C., Zill, A., Le Bot, N., Vernos, I., and Gelfand, V. (1998) Heterotrimeric kinesin II is the microtubule motor protein responsible for pigment dispersion in Xenopus melanophores. *J. Cell Biol*. **143**, 1547–1558.
12. Pierce, D. W., Hom-Booher, N., and Vale, R. D. (1997) Imaging individual green fluorescent proteins. *Nature* **388**, 338.
13. Romberg, L., Pierce, D. W., and Vale, R. D. (1998) Role of the kinesin neck region in processive microtubule-based motility. *J. Cell Biol*. **140**, 1407–1416.
14. Suzuki, Y., Yasunaga, T., Ohkura, R., Wakabayashi, T., and Sutoh, K. (1998) Swing of the lever arm of a myosin motor at the isomerization and phosphate-release steps. *Nature* **396**, 380–383.
15. Endow, S. A. and Piston, D. W. (1998) Methods and protocols, in *Green Fluorescent Proteins: Properties, Applications and Protocols* (Chalfie, M. and Kain, S., eds.) Wiley-Liss, New York, pp. 271–369.
16. Heim, R., Cubitt, A. B., and Tsien, R. Y. (1995) Improved green fluorescence. *Nature* **373**, 663–664.
17. Cormack, B. P., Valdivia, R. H., and Falkow, S. (1996) FACS-optimized mutants of the green fluorescent protein (GFP). *Gene* **173**, 33–38.
18. Heim, R. and Tsien, R. Y. (1996) Engineering green fluorescent protein for improved brightness, longer wavelengths and fluorescence resonance energy transfer. *Curr. Biol*. **6**, 178–182.
19. Ellenberg, J., Lippincott-Schwartz, J., and Presley, J. F. (1998) Two-color green fluorescent protein time-lapse imaging. *Biotechniques* **25**, 838–846.
20. Cole, N. B., Smith, C. L., Sciaky, N., Terasaki, M., Edidin, M., and Lippincott-Schwartz, J. (1996) Diffusional mobility of Golgi proteins in membranes of living cells. *Science* **273**, 797–801.
21. Ellenberg, J., Siggia, E. D., Moreira, J. E., Smith, C. L., Presley, J. F., Worman, H., J. and Lippincott-Schwartz, J. (1997) Nuclear membrane dynamics and reassembly in living cells: targeting of an inner nuclear membrane protein in interphase and mitosis. *J. Cell Biol*. **138**, 1193–1206.
22. Hirschberg, K., Miller, C. M., Ellenberg, J., Presley, J. F., Siggia, E. D., Phair, R. D. and Lippincott-Schwartz, J. (1998) Kinetic analysis of secretory protein traffic and characterization of golgi to plasma membrane transport intermediates in living cells. *J. Cell Biol*. **143**, 1485–1503.

23. Edidin, M. (1992) Patches, post and fences: proteins and plasma membrane domains. *Trends Cell Biol.* **2**, 376–380.
24. Edidin, M. (1994) Fluorescence photobleaching and recovery, FPR, in the analysis of membrane structure and dynamics, in *Mobility and Proximity in Biological Membranes* (Damjanovich, S., Edidin, N., Szollosi, J., and Tron, L.), CRC, Boca Raton, FL, pp. 109–135.
25. Olson, K. R., McIntosh, J. R., and Olmstead, J. B. (1995) Analysis of MAP 4 function in living cells using green fluorescent protein (GFP) chimeras. *J. Cell Biol.* **130**, 639–650.
26. Holmes, K. C. (1997) The swinging lever-arm hypothesis of muscle contraction. *Curr. Biol.* **7**, 112–118.
27. Haseloff, J. and Siemering, K. R. (1998) The uses of green fluorescent protein in plants, *in Green Fluorescent Proteins: Properties, Applications and Protocols* (Chalfie, M. and Kain, S., eds.) Wiley-Liss, New York, pp. pp. 191–220.
28. Haas, J., Park, E.-C., and Seed, B. (1996) Codon usage limitation in the expression of HIV-1 envelope glycoprotein. *Curr. Biol.* **6**, 315–324.
29. Zolotukhin, S., Potter, M., Hauswirth, W. W., Guy, J., and Muzyczka, N. (1996) A humanized green fluorescent protein cDNA adapted for high-level expression in mammalian cells. *J. Virol.* **70**, 4646–4654.
30. Chiu, W.-L., Niwa, Y., Zeng, W., Hirano, T., Kobayashi, H., and Sheen, J. (1996) Engineered GFP as a vital reporter in plants. *Curr. Biol.* **6**, 325–330.
31. Wada, K., Wada, Y., Doi, H., Ishibashi, F., Gojobori, T., and Ikemura, T. (1991) Codon usage tabulated from the GenBank genetic sequence data. *Nucleic Acids Res.* **19**, 1981–1986.
32. Ho, S. N., Hunt, H. D., Horton, R. M., Pullen, J. K., and Pease, L. R. (1989) Site-directed mutagenesis by overlap extension using the polymerase chain reaction. *Gene* **77**, 51–59.
33. Kerrebrock, A. W., Moore, D. P., Wu, J. S., and Orr-Weaver, T. L. (1995) Mei-S332, a Drosophila protein required for sister-chromatid cohesion, can localize to meiotic centromere regions. *Cell* **83**, 247–256.
34. Marshall, L. G., Jeng, R. L., Mulholland, J., and Stearns, T. (1996) Analysis of Tub4p, a yeast γ-tubulin-like protein: implications for microtubule-organizing center function. *J. Cell Biol.* **134**, 443–454.
35. Nabeshima, K., Kurooka, H., Takeuchi, M., Kinoshita, K., Nakaseko, Y., and Yanagida, M. (1995) $p93^{dis1}$, which is required for sister chromatid separation, is a novel microtubule and spindle pole body-associating protein phosphorylated at the Cdc2 target sites. *Genes Dev.* **9**, 1572–1585.
36. Davis, I., Girdham, C. H., and O'Farrell, P. H. (1995) A nuclear GFP that marks nuclei in living *Drosophila* embryos; maternal supply overcomes a delay in the appearance of zygotic fluorescence. *Dev. Biol.* **170**, 726–729.
37. Sullivan, K. F. and Kay, S. A. (eds.) (1999) *Methods in Cell Biology*, vol. 58: *Green Fluorescent Proteins*. Academic, New York.

12

In Vitro Reconstitution of Endosome Motility Along Microtubules

Erik Nielsen, Fedor Severin, Anthony A. Hyman, and Marino Zerial

1. Introduction

In higher eukaryotic cells, the secretory and endocytic membrane systems are comprised of a series of biochemically and morphologically distinct compartments. Dynamic associations with cytoskeletal networks have been shown to mediate both membrane transport between these compartments as well as maintenance of their characteriztic spatial distributions within the cell. More specifically, in endocytosis, association with microtubules and the action of microtubule-associated motor proteins are necessary for the proper positioning of late endosomes, lysosomes, and the pericentriolar recycling compartment ***(1–3)***. In addition, efficient transport of cargo between early and late endosomes, and transcytosis in polarized epithelial cells, also depend on microtubule-associated motors ***(4,5)***.

In order to study the molecular mechanisms responsible for regulating the interactions between endocytic organelles and microtubules, we, along with others ***(6)***, have developed assays to measure endosome motility on and association with microtubules in vitro. In this chapter, we will outline how we reconstitute and measure movement of endocytic organelles specifically labeled with fluorescent markers along fluorescently labeled microtubules in vitro, and we discuss some of the advantages and pitfalls of these techniques.

Generation of the components necessary to perform an assay to measure motility of organelles along microtubules in vitro can essentially be split into two parts. The first is the generation of cytosolic and organelle fractions. Although the exact protocols necessary for the generation of these fractions may vary, buffers and pH requirements for the maintenance of important biological functions, such as motor activities, in these fractions can serve as useful

From: *Methods in Molecular Biology*, Vol. 164: *Kinesin Protocols*
Edited by: I. Vernos

guides when developing motility assays with novel components. As we are interested in endosome motility along microtubules we will describe the methods we use to isolate this membrane fraction. The second is the generation of microtubules and assay chambers used in reconstituting in vitro organelle motility. These protocols should be widely applicable for visualization of movements on microtubules regardless of what membranes or molecules the investigator wishes to study. We have therefore organized the chapter into two discrete sections. The first describes the isolation of cytosol and fluorescently labeled early endosomes, and the second describes construction of the reaction chamber and synthesis of fluorescently labeled microtubules.

1.1. Preparation of HeLa Cytosol and Endosomal Membranes

1.1.1. Growth and Harvest of Cells

We use HeLa tissue culture cells that have been adapted for growth in suspension culture (s-HeLa) as the source of cytosol and early endosome fractions for our motility assays. The primary benefit of growing cells in suspension culture is the increase in cell density, which allows large numbers of cells to be grown in manageable quantities of growth medium. In addition, as the cells do not have to be released from the substrate, cell isolation is much easier. These protocols were adapted from earlier ones *(7)*, with the primary differences being slight alteration of salt concentrations of the isolation buffer and inclusion of ATP during isolation of cytosol. We generally grow 2–4 L of cells at a time ($[2–4] \times 10^9$ cells) for isolation of cytosol or endosome membranes, from which we obtain enough material for several months of in vitro motility experiments.

1.1.2. Internalization of Fluorescently Labeled Markers

Pioneering assays in which vesicle motility was reconstituted on microtubules relied on light microscopy to visualize vesicle movements *(8,9)*. Although these experiments elegantly demonstrated that membrane-bounded organelles did indeed move along microtubules and set the standard for further experimentation, they suffered from the fact that few enriched membrane fractions are completely pure. As a result, clear association of motility events with specific membrane-bounded compartments was difficult to confirm. We have attempted to overcome this complication by marking specific endocytic compartments using fluorescently labeled substrates, such as rhodamine-labeled transferrin, which can simply be included in the cell medium and are efficiently internalized by the cell. Because the rates of internalization and kinetics of association of substrate molecules have been extensively characterized for the endocytic pathway *(10)*, we have been able to utilize this technique to specifically label different compartments in the endocytic pathway. We have prima-

rily used rhodamine-labeled transferrin to label early endosomes; however, fluorescent conjugates of late endosomal and lysosomal markers, such as epithelial growth factor, and low-density lipoprotein are commercially available and these compartments theoretically could also be easily labeled using similar methods. Earlier studies used internalized latex beads that fluoresce faintly in order to visualize phagocytic compartments ***(6)***. Finally, we have also had some success using fusion proteins between small GTPases of the Rab family and green fluorescent protein to fluorescently label endocytic compartments (B. Sönnichsen, unpublished results).

1.2. The Motility Assay

1.2.1. Preparation of the Microscope Chamber

We observe motility utilizing an easy to make microscope perfusion chamber consisting of microscope slides and glass cover slips sealed on two sides with grease containing glass spacer beads ***(11)***. We generally use between 5 and 10-µL chamber volumes. Leaving two sides of the chamber open allows for easy addition and exchange of reaction buffers. Exchange of solution can be performed by wicking up the solution from one side of the chamber with a torn piece of Whatman filter paper while simultaneously adding new buffer to the opposite side with a pipetman.

1.2.2. Synthesis of Fluorescently Labeled Microtubules

We synthesize microtubules in one of two ways depending on whether we wish to analyze the extent of motility of an organelle fraction or the direction(s) in which organelles travel along microtubules. If we want to quantify the extent of motility that an organelle fraction exhibits, it is important that, first, the number of motility events that can be observed per experiment and, second, the reproducibility of this number from one experiment to the next are optimized. In both of these cases, an evenly distributed and relatively dense carpet of microtubules upon which the organelles move is required. Obtaining this is most easily done with Taxol-stabilized microtubules polymerized in vitro from purified tubulin. If, however, we want to determine the directionality of this movement, having a source of microtubules with easily identified plus and minus ends is most important. In this case, we nucleate microtubule asters on purified centrosomes stuck to the surface of the microscope chamber. In either case, to visualize microtubules by fluorescence microscopy we utilize fluorescently conjugated tubulin and polymerize microtubules using purified components. Protocols describing the purification of tubulin ***(12)*** (*see also* Chapter 1), its subsequent modification with fluorescent molecules ***(13)***, and purification of centrosomes ***(14)*** have been described in detail elsewhere and, therefore, will

not be described here. In vitro synthesis of fluorescently labeled microtubules is performed essentially as described ***(15)***.

1.2.3. Reconstituting Early Endosome Motility on Microtubules

Photobleaching is a major problem encountered during the extended illumination of fluorescently labeled microtubules and organelles that occurs while recording motility events. In order to minimize photobleaching, we utilize both a shuttered light source in combination with a sensitive video camera, and an oxygen scavenging system originally used for observation of actin filaments ***(16)*** and subsequently modified for use in microtubule-based motility assays ***(6)***. This antifade buffer consists of a mixture with catalase, glucose with glucose oxidase, β-mercaptoethanol, and hemoglobin.

1.2.4. Videomicroscopes and Data Acquisition

A variety of different light microscopes and video cameras can be used to view fluorescently labeled specimens. In essence, all one needs is a microscope with epifluorescent illumination and appropriate filters. We have used Zeiss Axioskop and Axiovert microscopes fitted with 100X/1.40 plan-Apochromat lenses. In order to reduce the amount of photobleaching during time-lapse imaging, we use a computer-controlled shutter with illumination by a 100-W mercury arc lamp attenuated with heat-reflection and heat-absorbance filters. At present, several commercial software packages are available that allow for computer control of attached video cameras. We use a relatively simple system consisting of a COHU 4910 series video camera with on-chip integration controlled by the NIH-Image software package. This camera and software combination is relatively inexpensive, yet sufficient for most imaging requirements. For more detailed information, we refer the reader to the NIH Image website, http://rsb.info.nih.gov/nih-image/Default.html.

2. Materials

2.1. Preparation of HeLa Cytosol And Endosomal Membranes

2.1.1. Growth and Harvest of Cells

1. s-HeLa cells.
2. s-MEM containing L-glutamine, nonessential amino acids (Biochrom KG, Berlin. cat. no. K-0293), fetal calf serum (5%), penicillin (10 IU/mL), and streptomycin (10 µg/mL) (store at 4°C).
3. Trypsin–EDTA (Sigma Chemical Co., cat. no. T-3924; store at 4°C).
4. Phosphate-buffered saline (PBS) buffer.

2.1.2. Internalization of Fluorescently-Labeled Transferrin

1. CO_2-independent modified Eagle's media (MEM) plus 0.2% bovine serum albumin (BSA) (store at 4°C).

2. Transferrin from human serum, conjugated to tetramethylrhodamine or fluorescein (Molecular Probes Inc., cat. nos. T-2872, and T-2871).
3. SIM buffer: 250 m*M* sucrose, 3 m*M* imidazole, 1 m*M* $MgCl_2$ (pH 7.4) (store at 4°C).

2.1.3. Preparation of Cytosol

1. KEHM buffer: 110 m*M* KCl, 50 m*M* HEPES–KOH (pH 7.4), 2 m*M* $MgCl_2$, 2 m*M* Mg–ATP (make fresh).
2. 1000× CLAAP in dimethyl sulfoxide (DMSO): chymostatin (6 mg/mL), leupeptin (0.5 mg/mL), antipain (10 mg/mL), aprotinin (0.7 mg/mL), pepstatin A (100 mg/mL) (store at –20°C).
3. 1000× p-amidinophenyl-methanesofonyl fluoride; (APMSF) (10 mg/mL) in DMSO (store at –20°C).

2.1.4. Cell Cracking

Ball-bearing Cell Homogenizer 8.020-mm size with 8.002-mm ball bearing (EMBL Workshop, Heidelberg, Germany).

2.1.5. Purifying Endosome Membranes

1. 62% (v/v) sucrose solution: 80.49 g sucrose, 3 m*M* imidazole in 100 mL H_2O (make the night before).
2. 35% (v/v) sucrose solution: 40.3 g sucrose, 3 m*M* imidazole in 100 mL H_2O (make the night before).
3. 25% (v/v) sucrose solution: 27.59 g sucrose, 3 m*M* imidazole in 100 mL H_2O (make the night before).

2.2. The Motility Assay

2.2.1. Preparation of the Microscope Chamber

1. Microscope slides (76 mm × 26 mm × 0.8/1.0 mm thick; Select Micro Slides, washed; Chance Propper Ltd.,Warley, UK, cat. no. KTH 360).
2. Glass cover slips (18 mm × 18 mm, No.1; Clay Adams, Gold Seal, Reorder No. 3305).
3. Grease with glass bead spacers: Apiezon M (Carl Roth GmbH+Co D7500 Karlsruhe 21, Art. 1683). Glass beads (200–300 µm, acid washed; Sigma Chemical Co., cat. no. G-1227).

2.2.2. Synthesis of Fluorescently Labeled Microtubules

1. Purified, cycled, unlabeled tubulin (20 mg/mL; store at –80°C).
2. Purified, cycled, fluorescently labeled tubulin (20 mg/mL; store at –80°C).
3. Purified centrosomes (store at –80°C).
4. 10 m*M* GMP–CPP (store at –20°C).
5. 0.1 *M* GTP (store at –20°C).

6. 10 m*M* taxol in DMSO (store at –20°C).
7. BRB80 buffer: 80 m*M* K–piperazine-*N*,*N*-*bis*[2-ethanesulfonic acid] (PIPES) (pH 6.8), 2 m*M* $MgCl_2$, 1 m*M* EGTA (store at room temperature).
8. G-buffer: 1 m*M* GTP in BRB80 (make fresh).

2.2.3. Reconstituting Early Endosome Motility on Microtubules

1. Antifade buffer: 10 µ*M* taxol (from 10 m*M* stock; store at –20°C), 10 m*M* glucose (from 1 *M* stock; store at 4°C), 4 m*M* $MgCl_2$, 50 µg/mL glucose oxidase (from 10 mg/mL stock; store at –20°C), 50 µg/mL catalase (from 10 mg/mL stock; store at –20°C), 0.1% of 2-mercaptoethanol (store at –20°C), into 1 mL BRB80, sit at 37°C for 1–2 min prior to use (make fresh).
2. Bovine hemoglobin (30 mg/mL; make fresh).

3. Methods

3.1. Preparation of HeLa Cytosol and Endosomal Membranes

3.1.1. Growth and Harvest of Cells

1. Grow four confluent medium-sized flasks (175 cm^2) of s-HeLa in s-MEM.
2. To release the s-HeLa cells from the flask, incubate with trypsin–EDTA at 37°C until the majority has been released into the medium. Add just enough volume to cover the surface of the flask. Then, add these cells to 400 mL of s-MEM media in a 1 L spinner flask. Place this flask on a stirrer at 37°C for 24 h.
3. The next day, transfer these spinning cells into a 3 L spinner flask containing 2 L of fresh s-MEM media.
4. Grow the cells on a stirrer at 37°C until cells reach a density of 0.8–1.2 × 10^6 cells/mL. This should take 4 d. If the cells are too dense they will not internalize, so dilute them and grow into log phase again.
5. Collect the cells by sedimentation in a Sorvall GS-3 rotor at 4500*g* for 10 min at room temperature.
6. Gently resuspend the cell pellet in PBS, swirling the flask by hand until the pellet is in solution. It is okay if there are still large chunks of aggregated cells, as long as the pellet has released from the flask.
7. Spin again in a Sorvall GS-3 rotor at 4500*g* for 10 min at room temperature.
8. Again, gently resuspend the cell pellet in 50 mL of PBS, transfer this slurry to a 50-mL Falcon tube and spin in a Sorvall tabletop centrifuge at 3000*g* for 10 min at room temperature. If preparing endosome membranes, continue with internalization protocol. If preparing cytosol, proceed directly to **Subheading 3.1.3.**

3.1.2. Internalization of Fluorescently-Labeled Transferrin

1. Transfer the cell pellet to 10–15 mL prewarmed CO_2-independent MEM plus 0.2%BSA containing 30 µg/mL transferrin conjugated to rhodamine or fluorescein-isothiocyanate (FITC).
2. Incubate the cells in a 37°C water bath for 10 min and then dilute the cells to 50 mL with ice-cold SIM buffer.

3. Spin down the cells at 4°C in a refrigerated tabletop centrifuge at 3000*g* for 10 min.
4. Wash the cells with ice-cold SIM buffer and resediment cells in tabletop centrifuge at 4°C twice more.
5. Resuspend the final cell pellet in 2 cell volumes of ice-cold SIM buffer containing freshly added 1× CLAAP, 1× APMSF, and 1 m*M* dithiothreitol (DTT). Proceed to **Subheading 3.1.4.**

3.1.3. Preparation of Cytosol

Resuspend cells in 0.7 vol of ice-cold KEHM buffer to which 1× CLAAP, 1× APMSF, and 1 m*M* DTT have recently been added. Proceed to **Subheading 3.1.4.**

3.1.4. Cell Cracking

1. Assemble the cell cracker (made at EMBL) using ball-bearing size 8.002 and two 5- or 10-mL syringes, depending on the cell volume. Precool the cracker on ice, or in a cold room.
2. Passage the cells through the cell cracker six or seven times, applying quick, short bursts of pressure to the syringe plungers while frequently alternating the direction of flow through the cell cracker (*see* **Note 1**).
3. Check under a phase-contrast microscope to assess the degree of cell breakage. To do this, simply unscrew one of the syringes from the cell cracker and remove a few microliters of sample with a pipetman (*see* **Note 2**).
4. Continue with cell breakage until the majority of cells are broken. Typically, we can observe up to 90% breakage after 10–13 passages. However, more or less passages will be required depending on the strength of the researcher.
5. If endosome membranes are to be isolated, proceed to **Subheading 3.1.5.** If cytosol is to be prepared, spin the cell homogenate in a Beckmann TLA100.4 rotor at 278,000*g* for 30 min at 4°C. Remove the supernatant, saving an aliquot for protein concentration determination, and snap-freeze the rest in liquid nitrogen. Aliquots of snap-frozen cytosol should be stored at –80°C.

3.1.5. Purifying Endosome Membranes

1. Transfer the cell homogenate from **step 4** of **Subheading 3.1.**4 to a 15- or 50-mL Falcon tube and sediment nuclei and unbroken cells in a Sorvall tabletop centrifuge at 4000*g* for 20 min at 4°C.
2. Collect the postnuclear supernatant (PNS) (*see* **Note 3**).
3. Using a refractometer, adjust the sucrose concentration of the PNS fraction to 40.6% (v/v) with an ice-cold 62% (v/v) sucrose stock solution. Begin the adjustment by adding 600 µL of 62% sucrose per 500 µL PNS.
4. Split the density-adjusted PNS obtained from 2.4 L of spinner culture into six SW40 tubes using a syringe to apply equal amounts to the bottom of each tube. Carefully overlay these fractions with 4 mL of ice-cold 35% (v/v) sucrose solu-

tion, followed by 4 mL of ice-cold 25% (v/v) sucrose solution. Balance the tubes by adding to or removing from the 25% sucrose layer.
5. Spin these tubes in a SW40 rotor at 220,000*g* for 6 h at 4°C and collect the early endosome band at the 25–35% sucrose interface (*see* **Note 4**).
6. Aliquot the early endosomes in 200-µL fractions, saving a portion for protein concentration determination, and snap-freeze the rest in liquid nitrogen.

3.2. The Motility Assay

3.2.1. Preparation of the Microscope Chamber

1. Warm approx 20 g Apiezon M grease on a heating plate until the viscosity is low enough that the grease is easy to stir. Add 2 g of 200- to 300-µm glass beads and stir until they are well mixed. Pour the mixture of grease and beads into a syringe tipped with blunted 18-gage needle. Push in the plunger and remove the majority of trapped bubbles. Let the grease cool to room temperature. This grease dispenser can be stored at room temperature and will last for several months worth of experiments.
2. Extrude two lines of grease onto a glass cover slip about 1.5 cm apart and place a cover slip on top. Gently tap the cover slip with a pipet tip to generate an even seal with the grease lines (*see* **Note 5**).
3. At this point, 5 µL of previously synthesized microtubules (*see* **Subheading 3.2.2.1.**) can be added to the perfusion chamber. Alternatively, 5 µL purified centrosomes can be added for the nucleation of microtubule asters (*see* **Subheading 3.2.2.2.**). Gently tap the cover slip down with a pipet tip to reduce the chamber volume until the 5-µL reaction fills the entire chamber.
4. If prepolymerized microtubules are being used, let the chamber sit at room temperature for 5 min to allow nonspecific sticking of the microtubules to the glass surfaces of the chamber, then proceed to **Subheading 3.2.3.** If microtubule asters are being nucleated, proceed to **Subheading 3.2.2.**2.

3.2.2. Synthesis of Fluorescently Labeled Microtubules

3.2.2.1. Synthesis of Polarity-Marked Microtubules In Vitro

1. To synthesize brightly labeled microtubule seeds, dilute 1 µL of freshly thawed, fluorescently labeled tubulin (20 mg/mL) into 5 µL BRB80 and add 0.5 µL of 10 m*M* GMP–CPP (*see* **Note 6**). Incubate this mix for 10–20 min in 37°C water bath.
2. Meanwhile, add 10 µL freshly thawed 0.1 *M* GTP into 1 mL of BRB80, producing 1 mL G-Buffer. Take 30 µL of G-Buffer and mix with 10 µL freshly thawed, cycled tubulin (20 mg/mL) and 1 mL freshly thawed, fluorescently labeled tubulin. Add this mixture to the brightly labeled microtubule seeds and incubate at 37°C for an additional 20–40 min.
3. While the microtubules are polymerizing, dilute 1 µL of 10 m*M* taxol dissolved in DMSO into 1 mL BRB80. Vortex this solution well to ensure proper suspension of the taxol (*see* **Note 7**). Prewarm a Beckmann airfuge rotor to room temperature (*see* **Note 8**).

4. Remove the polymerized microtubules from the 37°C water bath and dilute into 200 µL of BRB80 +10 µ*M* taxol solution. If polymerization was successful, one should observe a marked viscosity of the microtubule-containing solution. Transfer the diluted microtubules to an airfuge tube, make a balance tube, and sediment the microtubules at 30 psi for 5 min at room temperature.
5. Aspirate the supernatant and gently resuspend the pellet in 50 µL of BRB80 + 10 µ*M* taxol. These microtubules are now stable for up to 1 wk at room temperature. To minimize photobleaching, wrap the storage tube with aluminum foil.

3.2.2.2. In Situ Nucleation of Microtubule Asters on Purified Centrosomes

1. Perfuse 5 µL of purified centrosomes diluted to preferred concentration in BRB80 into a microscope chamber (described below). Incubate the chamber in an inverted position for 1–2 min to allow centrosomes to stick to the glass cover slip.
2. Mix 1 µL of fluorescently labeled, cycled tubulin (20 mg/mL) with 10 µL of unlabeled cycled tubulin (20 mg/mL) and dilute into 50 µL of G-Buffer. Perfuse 5 µL of this mixture into the microscope chamber using a ripped piece of Whatman filter paper; wick out the preexisting chamber fluid on the opposite side.
3. Incubate the chamber in a humid box at 37°C for 20 min to polymerize the microtubules.
4. Perfuse the chamber with 10 µL of BRB80 + 10 µ*M* taxol to remove unpolymerized tubulin and stabilize the microtubules. The microscope chamber can now be stored at room temperature for several hours.

3.2.3. Reconstituting Early Endosome Motility on Microtubules

1. Prepare fresh antifade buffer, hemoglobin, and BRB80 + 10 m*M* taxol solutions.
2. Mix 4 µL antifade buffer, 1 µL hemoglobin (30 mg/mL), 2 µL HeLa cytosol (10–15 mg/mL), and 3 µL of fluorescently labeled early endosomes (5–7 mg/mL), and perfuse all 10 µL into a microscope chamber preloaded with microtubules or microtubule asters.
3. Place a drop of immersion oil on the glass cover slip and visualize fluorescent endosomes and microtubules with appropriate immunofluorescence filters on a time-lapse video microscope. Examples of endosome motility on in vitro synthesized microtubules or microtubule asters are shown in **Figs. 1** and **2**, respectively.

4. Notes

1. Avoid the inclusion of bubbles in the syringes, as they can lead to a vapor lock of the cell cracker. Also, as high pressures are generated within the cell cracker apparatus during this procedure, it is important to wear protective goggles or glasses to prevent injury if a syringe breaks.
2. It is good to save a small aliquot of unbroken cells to compare against those processed in the cracker. Intact cells can be distinguished from broken cells by presence of cytosol around a highly refringent nucleus. Alternatively, a drop of

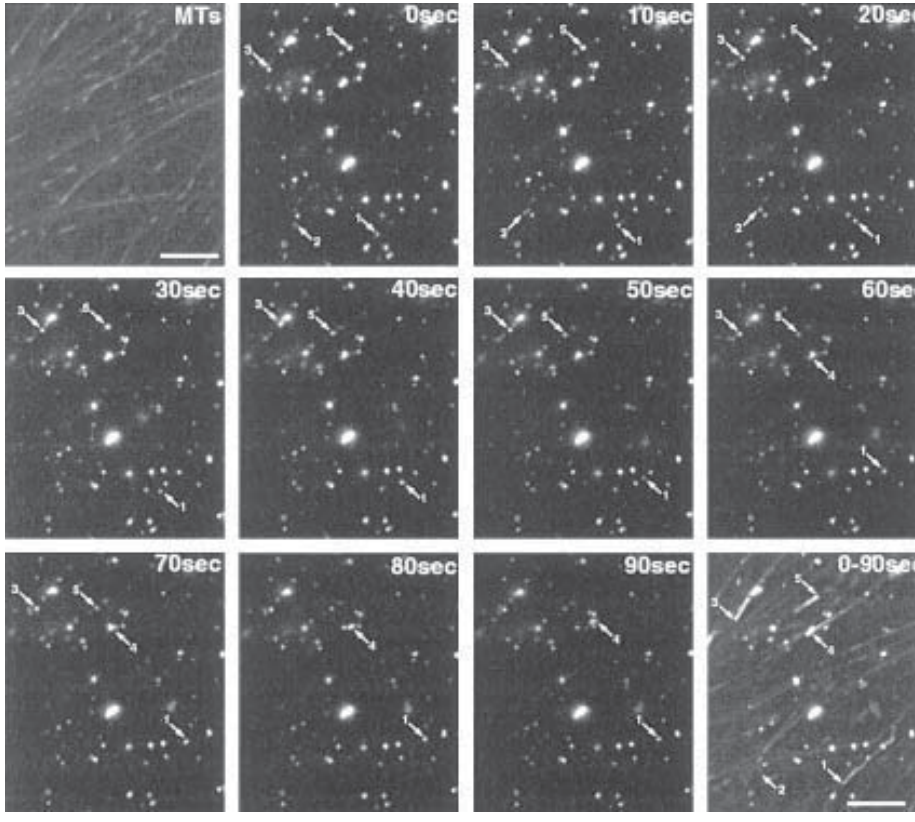

Fig. 1. Fluorescently labeled endosomes moving along in vitro synthesized microtubules. Oregon-green labeled microtubules (MTs) were adsorbed to a glass cover slip. Images of rhodamine–transferrin-labeled endosomes are shown at 10-s intervals. Moving endosomes are indicated by numbered arrows. In the final panel, a merged stack of consecutive images of fluorescently labeled endosomes (2-s intervals) is superimposed on an image of the microtubules. When represented in this manner, moving endosomes produce a series of closely spaced dots that line up with fluorescent microtubules. Scale bar: 5 μm.

1% trypan blue solution dissolved in water can be applied to the cells. Nuclei from broken cells will stain blue, whereas those of unbroken cells remain clear.

3. If it is difficult to distinguish between the supernatant and the pellet fractions, hold the tube up to a light source to help observe this interface.
4. To more easily see the endosomal membranes, place the tubes in a rack in front of a piece of black paper. We typically use a straight metal tube connected to tubing threaded through a peristaltic pump to collect the interface fractions.

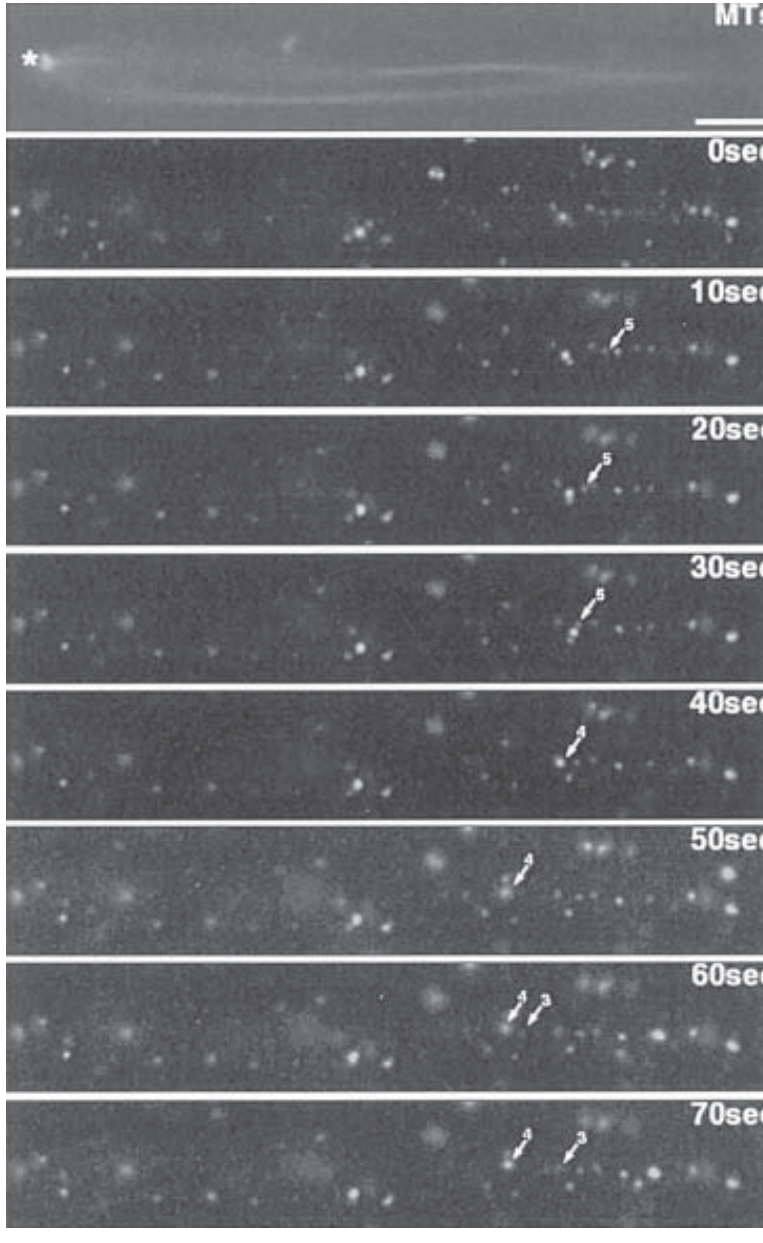

Fig. 2. Fluorescently labeled endosomes moving along microtubule asters toward both plus and minus ends. Oregon-green labeled microtubule asters (MTs) were nucleated on centrosomes (asterisk) adsorbed to a glass cover slip. Images of rhodamine–transferrin-labeled endosomes are shown at 10-s intervals. Moving endosomes are indicated by numbered arrows. *(continued)*

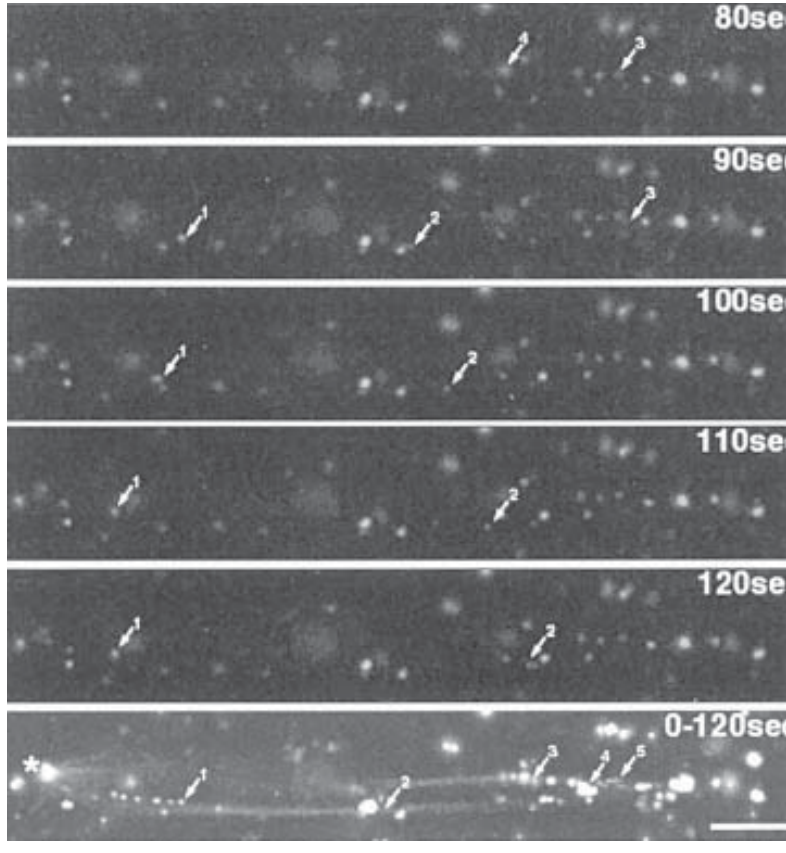

Fig. 2. *(continued)* In the final panel, a merged stack of consecutive images of fluorescently labeled endosomes (2-s intervals) is superimposed on an image of the microtubule aster. Scale bar: 5 μm.

5. When applying the grease, it is better to apply too much than too little as the chamber can be tapped down to create the proper reaction volume. The flow of buffer through the chamber and, by extension, the extent of washing in any given area of the chamber will be affected by its cross-sectional area; therefore, it pays to make the chambers as similar to one another as possible. To accurately lay the two lines of grease at set distances apart, we have found it useful to generate the chamber on a piece of graph paper using the underlying grid to apply the grease lines 1.5 cm apart.
6. GMP–CPP is unfortunately not available commercially and must be synthesized ***(17)***. Alternatively, short microtubule seeds can be synthesized in the presence of glycerol ***(15)***.

7. Taxol does not remain active through several freeze–thaw cycles; therefore, we store at the 10 m*M* taxol stock solution in 1-µL aliquots at –20°C. Additionally, as at cold temperatures, taxol precipitates out of aqueous solutions, always store at these tubes at room temperature.
8. Alternatively, microtubules can be sedimented by spinning at 100,000g in a Beckmann TLA 100 rotor for 5 min at 37°C.

Acknowledgments

The authors would like to thank Birte Sonnichsen for comments on the manuscript, and members of the Hyman and Zerial labs for helpful discussions and advice. E. N. and F. S. are supported by EMBO Long-term, and Max Planck Fellowships, respectively. This work was supported by the Max Planck Gesellschaft grants from the Human Frontier Science Program (RG-432/96), EU TMR (ERB-CT96-0020), and Biomed (BMH4-97-2410) (M. Z.).

References

1. Matteoni, R. and Kreis, T. E. (1987) Translocation and clustering of endosomes and lysosomes depends on microtubules. *J. Cell Biol.* **105**, 1253–1265.
2. Gruenberg, J., Griffiths, G., and Howell, K. E. (1989) Characterization of the early endosome and putative endocytic carrier vesicles *in vivo* and with an assay of vesicle fusion *in vitro*. *J. Cell Biol.* **108**, 1301–1316.
3. McGraw, T. E., Dunn, K. W., and Maxfield, F. R. (1993) Isolation of a temperature-sensitive variant Chinese hamster ovary cell line with a morphologically altered endocytic recycling compartment. *J. Cell Physiol.* **155**, 579–594.
4. Aniento, F., Emans, N., Griffiths, G., and Gruenberg, J. (1993) Cytoplasmic dynein-dependent vesicular transport from early to late endosomes. *J. Cell Biol.* **123**, 1373–1387.
5. Bomsel, M., Parton, R., Kuznetsov, S. A., Schroer, T., and Gruenberg, J. (1990) Microtubule- and motor-dependent fusion *in vitro* between apical and basolateral endocytic vesicles from MDCK cells. *Cell* **62**, 719–731.
6. Blocker, A., Griffiths, G., Olivo, J. C., Hyman, A. A., and Severin, F. F. (1997) Molecular requirements for bi-directional movement of phagosomes along microtubules. *J. Cell Biol.* **137**, 113–129.
7. Gorvel, J.-P., Chavrier, P., Zerial, M., and Gruenberg, J. (1991) Rab5 controls early endosome fusion *in vitro*. *Cell* **64**, 915–925.
8. Allen, R. D., Metuzals, J., Tasaki, I., Brady, S. T., and Gilbert, S. P. (1982) Fast axonal transport in squid giant axon. *Science* **218**, 1127–1129.
9. Brady, S. T., Lasek, R. J., and Allen, R. D. (1982) Fast axonal transport in extruded axoplasm from squid giant axon. *Science* **218**, 1129–1131.
10. Mellman, I. (1996) Endocytosis and molecular sorting. *Annu. Rev. Cell Dev. Biol.* **12**, 575–625.
11. Allan, V. J. (1993) Assay of membrane motility in interphase and metaphase Xenopus extracts. *Methods Cell Biol.* **39**, 203–226.

12. Mitchison, T. and Kirschner, M. (1984) Microtubule assembly nucleated by isolated centrosomes. *Nature* **312**, 232–237.
13. Hyman, A. A. (1991) Preparation of marked microtubules for the assay of the polarity of microtubule-based motors by fluorescence. *J. Cell Sci.* **14 (suppl.)**, 125–127.
14. Bornens, M. and Moudjou, M. (1999) Studying the composition and function of centrosomes in vertebrates. *Methods Cell Biol.* **61**, 13–34.
15. Howard, J. and Hyman, A. A. (1993) Preparation of marked microtubules for the assay of the polarity of microtubule-based motors by fluorescence microscopy. *Methods Cell Biol.* **39**, 105–113.
16. Kishino, A. and Yanagida, T. (1988) Force measurements by micromanipulation of a single actin filament by glass needles. *Nature* **334**, 74–76.
17. Hyman, A. A., Salser, S., Drechsel, D. N., Unwin, N., and Mitchison, T. J. (1992) Role of GTP hydrolysis in microtubule dynamics: information from a slowly hydrolyzable analogue, GMPCPP. *Mol. Biol. Cell.* **3**, 1155–1167.

13

Approaches to Study Interactions Between Kinesin Motors and Membranes

Gerardo Morfini, Ming-Ying Tsai, Györgyi Szebenyi, and Scott T. Brady

1. Introduction

Determining the subcellular location of molecular motors is an essential step in understanding their function and regulation. Although much attention has been focused on the ability of kinesin-like motors to bind reversibly to microtubules, the interaction of this family with cargo has not been extensively studied. Thus, the interactions of kinesin with membrane-bound organelles (MBOs) remains poorly understood, although kinesins are widely thought to serve as motors for movement of MBOs (*see also* Chapter 12). Methods presented in this chapter were developed to study the regulation of the membrane association of kinesins.

Immunofluorescence, nerve ligation, and pulse label axonal transport studies suggest that conventional kinesin is bound to MBOs ***(1–3)***. In standard subcellular fractionation studies, however, the majority of kinesin is recovered in soluble cell fractions ***(4)***. A possible explanation for this discrepancy between biochemical and whole-cell approaches may be that the regulation and proper compartmentalization of activities that control kinesin association with membranes in intact cells becomes disrupted during tissue homogenization. As a result, during biochemical fractionation, kinesin may become accessible to improperly regulated/localized activities that artifactually increase the amount of kinesin in the soluble fraction. Although this is useful for the purification of motor proteins, the release of kinesin from normal cargoes hampers the study of cellular functions for kinesin. By carefully controlling extraction conditions and modulating enzymatic activities that can affect protein–protein interactions during cell fractionation, the release of MBOs from kinesin can be mini-

From: *Methods in Molecular Biology*, Vol. 164: *Kinesin Protocols*
Edited by: I. Vernos

mized. These same principles may provide guidelines for characterizing the interaction of other kinesin family members with their cargoes.

In this chapter, we present both biochemical assays and live-cell detergent-extraction protocols designed to preserve or to perturb experimentally the normal membrane association of motor proteins. These methods can be modified to identify effectors that regulate the release of kinesin and kinesin-related proteins from membranes. During standard biochemical fractionation, selected effectors can be added to the homogenization buffer to determine if they influence the partitioning of kinesin motors between soluble and membrane fractions (**Subheading 3.1.1.**). After this initial screen, in a vesicle binding/releasing assay, the effects of specific enzymes can be studied (**Subheading 3.1.2.**). Finally, in whole-cell assays, candidate regulators can be tested for their effects on kinesin–membrane interactions (**Subheading 3.2.**).

There are advantages and disadvantages of both biochemical and whole-cell approaches. Advantages of the biochemical methods are that a wide range of conditions can be evaluated in a single experiment and the results are quantifiable by immunoblotting. An inherent disadvantage, however, is that normal cell structure is lost and the composition of subcellular fractions is heterogeneous and often poorly defined. In contrast, detergent extraction of whole cells, followed by immunocytochemistry for kinesins and organelle markers, allows for observing changes in the subcellular location of kinesin following various treatments, but absolute quantitation of these effects is difficult.

In summary, the methods described here serve to provide guidelines, in addition to practical details, for assessing the subcellular distribution of kinesins and for studying the regulation of association between motor proteins and membrane-bound organelles.

2. Materials

2.1. Equipment

For the biochemical studies, an ultracentrifuge with rotors suitable for submilliliter volumes, electrophoresis equipment, and protein transfer apparatus are needed. For quantitation of Western blots, it is necessary to have access to a phosphoimager system or other devices for quantitation of specific bands in electrophoresis and immunoblots. For whole-cell detergent-extraction assays, a standard tissue culture facility is required and a slide warmer is recommended to keep cells at 34–37°C during detergent extraction. Results of the whole-cell approach are analyzed on a microscope equipped for fluorescent microscopy, preferably one with a digital image acquisition system.

2.2. Reagents

All reagents are from Sigma, except when noted. Water is ultrapure reagent grade (Millipore Milli-Q filtered or equivalent; dH_2O).

2.2.1. Biochemical Assays

1. Homogenization buffer (HB): 0.32 *M* sucrose, 10 m*M* HEPES (pH 7.4), prepared on the week of the experiment from concentrated stocks and stored at 4°C.
2. Sucrose cushion: 600 m*M* sucrose in 10 m*M* HEPES (pH 7.4).
3. Effector stocks: *N*-ethyl maleimide (NEM) containing solutions should be diluted from an 0.4 *M* stock in ethanol, all prepared on the day of the experiment. None of the NEM-containing solutions, including the stock, should be stored for more than 3 h.
4. Protein concentration is determined by Coomassie Plus Protein Assay Reagent (Pierce, Rockford, IL).
5. All electrophoresis reagents are analytical grade. Immunoblotting techniques are performed following standard protocols, except when noted otherwise.

2.2.2. Whole-Cell Detergent Extraction

2.2.2.1. Stock Solutions

Avoid multiple cycles of thawing and freezing for all reagents.

1. 2× PHEM buffer: 120 m*M* piperazine-*N*,*N*-*bis*[2-ethanesulfonic acid] (PIPES), 50 m*M* HEPES, 20 m*M* EGTA, 2 m*M* $MgCl_2$ (pH 7.4) with KOH (*see* **Note 1**). The solution may be prepared, filtered and stored at 4°C for up to 1 mo.
2. GTP stocks: A 0.1 *M* solution is prepared in dH_2O, and small aliquots (200 µL) are stored at –80°C.
3. Taxol: A 10 m*M* stock solution is prepared in dimethyl sulfoxide (DMSO), and small aliquots are stored at –20°C.
4. Poly-L(D)-lysine: A solution of 0.5–1.0 mg/mL is prepared in dH_2O, sterilized by passing through a 0.22-µm filter, and individual aliquots are stored at –20°C.
5. Detergent stocks: Solutions are prepared as 10% w/v, no more than a few hours prior to starting the experiment. Longer-term storage of diluted solutions can lead to the formation of peroxide radicals.
6. Fixative stock: 2% paraformaldehyde (Fisher) in 1× PHEM buffer (pH 7.4). To prepare 100 mL, warm 40 mL of dH_2O to 65°C, then add 2 g of paraformaldehyde while stirring. The temperature should not exceed 65°C, because formic acid can form at higher temperatures. Add a few drops of 10 N NaOH to allow the paraformaldehyde to dissolve. When the solution clears, add 50 mL of 2× PHEM buffer, and when cooled to 37°C, adjust the pH to 7.4. Finally, bring the volume to 100 mL with dH_2O and pass through Whatman #3 filter paper. Store individual aliquots at –20°C for up to a month.
7. 5X sample buffer: 0.35 *M* Tris-HCl (pH 6.8), 10% w/v sodium dodecyl sulfate (SDS) (Pierce, Sequanal grade), 36% glycerol, 5% β-mercaptoethanol, 0.01% bromophenol blue.

2.2.2.2. Working Solutions

Working solutions are all prepared the day of the experiment and are warmed to 37°C before use.

1. 1× PHEM buffer is prepared by diluting 2× PHEM buffer stock with dH_2O.
2. Extraction buffer: Immediately before the experiment, 1× PHEM buffer is supplemented with 1 m*M* GTP, 10 µ*M* taxol, protease inhibitors (20 m*M* 4-[2-aminoethyl]benzenesulfonyl fluoride [AEBSF], 200 mg/mL aprotinin, 100 m*M* pepstatin, 1 m*M* leupeptin or a cocktail of mammalian protease inhibitors diluted 1:1000X [Sigma, cat. no. P-8340 or equivalent]), and the appropriate concentration of detergent.
3. Fixative: Thaw a stock aliquot and add glutaraldehyde (electron microscopy [EM] grade) to final concentration of 0.01% (*see* **Note 2**).

3. Methods

3.1. Biochemical Approaches to Study the Regulation of Interactions Between Motor Proteins and Membranes

Methods presented in this section can be used to test the effects of changes in the composition of the homogenization buffer (HB) on partitioning of kinesin motors between membrane and soluble fractions. Initially, a broad range of effectors may be considered including sulfhydryl-reactive reagents (NEM), divalent cation chelators (EDTA and EGTA), pyrophosphate, nucleotides (ADP, ATP, GTP), or nonhydrolyzable nucleotide analogs (AMP–PNP, ATP-γS) (*see* **Note 3**). Once insight into the sensitivity to effectors or regulation of motor protein association with membranes has been obtained, then more specific reagents, such as inhibitors and activators of specific enzymes or purified proteins, can be tested.

3.1.1. Biochemical Fractionation

1. Adult Sprague–Dawley rats are anesthetized and sacrificed by decapitation. Alternatively, fresh tissues from other animals or liquid-nitrogen flash-frozen tissues, can be used (*see* **Note 4**).
2. The brain is removed from the skull and slowly homogenized with 10 strokes in a Dounce glass homogenizer with the B pestle followed by 10 more strokes with the A pestle in 10 mL of ice-cold HB, with or without effectors. Because an adult rat brain increases the final volume by approx 1.6 mL, it is important to consider the expected final volume of the homogenate when calculating the concentration of the effector to be added.
3. The homogenate is first centrifuged at $11{,}000g_{max}$ for 8 min at 4°C to pellet debris, nuclei, and mitochondria (P1).
4. The supernatant (S1) is carefully removed without disturbing the first loose pellet. If necessary, this first centrifugation can be repeated.

5. S1 is further centrifuged for 1 h at 200,000g_{max} at 4°C to generate a high-speed pellet.
6. After recovering the high-speed supernatant (containing solubilized cytosolic proteins), the high-speed pellet (containing membrane proteins) are resuspended by mild sonication with a probe in 1.5 mL of HB. Avoid heating the sample while sonicating.
7. After measuring protein concentrations in both soluble and membrane fractions, the amount of total protein in each fraction is calculated.
8. An equal amount (approx 50 µg) of protein from each fraction is separated by sodium dodecyl sulfate-polyacrylamide gel electrophoresis (SDS-PAGE) and transferred to a membrane (*see* **Note 5**).
9. To quantitate results, blots are incubated with primary antibodies and probed with ^{125}I-protein A. Relative amounts of motor protein in soluble and membrane fractions are measured using a Molecular Dynamics PhosphorImager system. Typically, overnight exposures of screens are sufficient to detect a signal. Finally, the percentage of the motor protein in soluble and membrane fractions is calculated for each experimental condition. Alternatively, following immunodetection, chemiluminescent assays can be performed as recommended by the manufacturers. However, chemiluminescence methods are quite difficult to quantitate accurately and this method is best used for qualitative analysis. Regardless, the distribution for defined marker proteins other than the motor should be evaluated to confirm that membrane and soluble proteins were separated during fractionation. We check routinely for the distribution of integral membrane proteins (e.g., synaptophysin in neuronal tissue) and soluble markers (e.g., hsc70).

After this first screening, further information can be gained about the membrane pool in which motor protein levels are altered by a given effector. More homogeneous organelle fractions can be obtained by differentially fractionating the first supernatant (S1, as above) as three independent membrane pellets, V0, V1, and V2, and a final soluble fraction (S4) (**Fig. 1**). V0 is obtained by centrifuging S1 at 40,000g_{max} for 40 min; V1 is obtained by centrifuging S2 at 100,000g_{max} for 1 h; V2 is obtained by centrifuging S3 at 200,000g_{max} for 2 h. All centrifugations are run at 4°C. Each of these fractions has a distinct protein profile. Using this fractionation scheme, we were able to determine that the effects of EDTA and NEM on kinesin association with different membrane fractions were clearly distinct (Morfini, Tsai and Brady, unpublished observations).

3.1.2. Vesicle Binding/Releasing Assay

This assay was designed to test in a single experiment the effects of several candidate regulators on motor protein interactions with several membrane fractions. For this assay, either a specific membrane fraction (V0, V1, or V2, as in **Fig. 1**) or a standard microsomal fraction can be used. Microsomal vesicles are purified as follows:

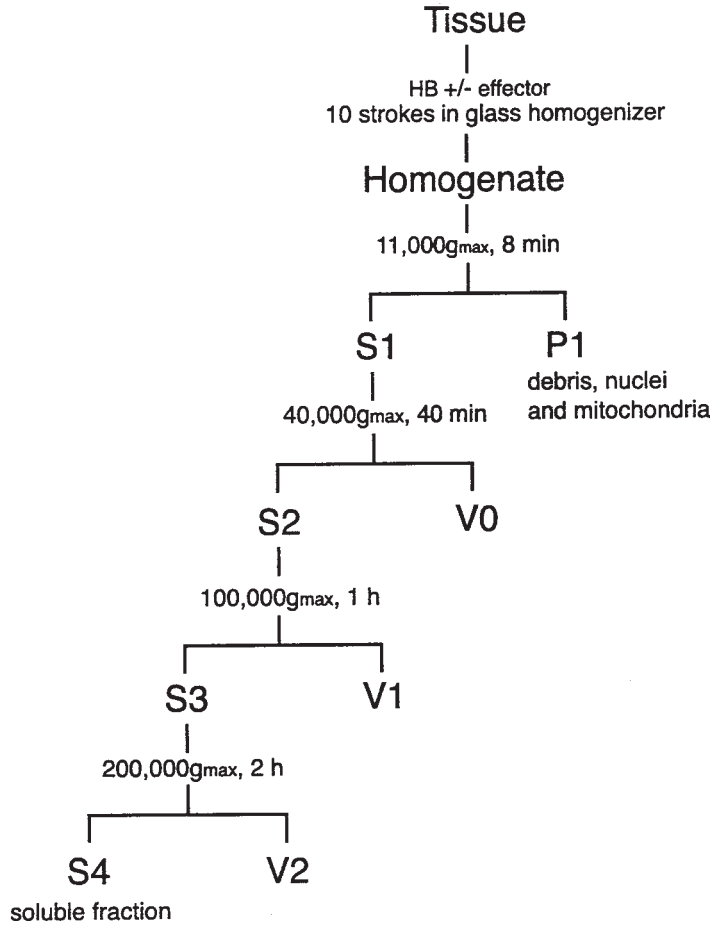

Fig. 1. Flow chart of a typical tissue fractionation by differential centrifugation. V0, V1 and V2 are membrane fractions, each enriched for distinct markers; S4 is the final soluble fraction, enriched in solubilized, cytosolic proteins.

1. Homogenize tissue in 5 vol of cold HB (w/v) as described above.
2. The homogenate is centrifuged for 15 min at 39,800g_{max} to yield a pellet and a supernatant.
3. The supernatant is further centrifuged for 40 min at 120,000g_{max}.
4. The resulting supernatant is carefully layered onto 600 m*M* sucrose in 10 m*M* HEPES (pH 7.4) and centrifuged for 2 h at 260,000g_{max}.
5. The resulting microsome pellet is carefully resuspended in HB (*see* **Note 6**).
6. Total protein concentration of resuspended microsomal vesicles is adjusted to 1 mg/mL.

7. One hundred-microliter aliquots are incubated with different effectors at 37°C (*see* **Note 7**). A time-course for the action of each effector should be established. Controls should include buffer blanks, cofactors, nucleotides, and so forth. When available, it is best to test specific inhibitors and activators of a given effector.
8. After incubation is complete, samples are layered over 600 m*M* sucrose in 10 m*M* HEPES (pH 7.4), and centrifuged at 260,000g_{max} for 20 min at 4°C.
9. The supernatants are transferred to new tubes and the pellets resuspended in a volume that equals the volume of the supernatant.
10. Pellets are resuspended in 1% SDS in 10 m*M* HEPES (pH 7.4) by vigorous shaking of tubes with an orbital shaker at room temperature for 3 h to overnight.
11. Gel loading sample buffer is added from a 5X stock to give samples in 1× sample buffer. Equal volumes of each fraction are separated by SDS-PAGE and probed for the presence of the proteins of interest by quantitative immunoblotting.

Using this vesicle assay, we showed that the chaperone hsc70 induced the release of kinesin from membranes in a nucleotide-dependent manner ***(5)***.

3.2. Whole-Cell Detergent Extraction to Study the Distribution of Kinesin Motors

A variety of cell lines and primary cultures can be used, including neuronal and nonneuronal cell types. The choice of cells depends on a number of practical and theoretical considerations. Some cell lines, such as COS-1, CHO, and mouse kidney BHK21, can be transfected relatively easily and subclones expressing various exogenous recombinant proteins are available or can be generated. These cells, however, spread poorly in tissue culture, compared to mouse NIH or Swiss 3T3 fibroblasts. Alternatively, cell lines may be selected because they exhibit well-characterized behavioral and biochemical responses to a given factor. For example, PC12 cells extend neuritelike processes in response to NGF or FGF-2 through activation of well-studied pathways. When studying motors involved in directional transport in neurons, primary cultures of hippocampal neurons are a prime model system ***(6)***. In addition, the species specificity of available antibodies can be a strong determinant of cell choice.

3.2.1. Cell Culture and Preparation

Prior to an experiment, cell lines are maintained on their preferred substrate in their optimal medium. We grow them in 5% calf serum or in serum-free medium with low concentrations of mitogens to limit division. Detergent extraction and immunocytochemistry are most conveniently performed on cells grown in four- or eight-well chamber slides (Becton Dickinson), but they can also be done on cover slips. Cells are plated on chamber slides 48 h prior to the extraction. To improve cell attachment, we coat culture slides for 1 h with 0.5 mg/mL poly-L(D)-lysine. Slides are then rinsed three times with sterile water

Table 1
Kinesin is Retained in Detergent-Extracted Cells at Concentrations that Remove Soluble Proteins

Detergent, concentration in% w/v	GFP retained in cells	Kinesin (H2) retained in cells
Extraction buffer, no detergent	+++++	+++++
Triton X-100, 0.01%	++++	++++
Triton X-100, 0.05%	++	++++
Triton X-100, 0.1%	+	+++
Triton X-100, 0.5%	+	+++
Triton X-100, 1%	+	++
Digitonin, 0.015%	++	++++
Digitonin, 0.03%	+	++++
Saponin, 0.02%	++	++++
Saponin, 0.1%	+	++++
Saponin, 0.2%	+	++++

Note: Cells were extracted for 4 min with detergents at concentrations indicated in the table. Following fixation and immunostaining for kinesin and tubulin, relative intensities of GFP fluorescence and H2 immunoreactivity were scored on a scale of + to +++++. A single plus in the GFP column refers to residual nuclear GFP. Only cells with well-preserved cytoskeleton were included.

and briefly dried in the hood. We usually prepare dishes on the day of an experiment, but dry, coated dishes can be stored at 4°C for at least 1 wk. Cells are plated at densities of approx 2500–5000 cells/cm^2 in the medium of choice. When deciding on cell-plating densities and medium supplements, the desired number of cells at the time of an experiment should be considered. A final density corresponding to approx 60% of confluency, with some spaces between cells, is optimal. Well-attached cells in the interphase withstand detergent extraction better than rounded, dividing cells.

3.2.2. Detergent Extraction of Live Cells

An understanding of the properties of detergents and use of appropriate controls are critical for obtaining meaningful information from these assays. We recommend that several detergents at various concentrations be tried on a preparation of choice, as the degree of permeabilization with different detergents, and even the same detergent at different concentrations, can vary greatly ***(7,8)*** (*see* **Note 8**).

1. Immediately before detergent treatment, cells are removed from the incubator and placed on a 34–37°C slide warmer.
2. Cells are carefully rinsed twice with 37°C 1× PHEM to remove serum and debris. The rinse is aspirated off with a 200-µL yellow pipet tip connected to a low-

pressure vacuum trap. The tip should be directed to an edge of the chamber to avoid cell detachment and/or damage.

3. Cells are immediately extracted by adding warm detergent-containing extraction buffer (0.5–1 mL) for 2–10 min. Unextracted controls, incubated in extraction buffer without detergents, should be included in each experiment. This control provides a baseline for comparing the effects of detergents on extraction of the protein of interest (*see* **Note 9**) and cell morphology. Because extraction time is critical and cells should never be allowed to dry during the entire procedure, it is recommended that two people perform the experiment.

To evaluate the subcellular distribution of a given motor protein with membranes, extraction profiles for motor proteins are compared to those of known soluble and membrane-bound proteins. The extraction of motor proteins and selected markers can be visualized simultaneously in the same cells by double immunostaining. In addition, the distribution of motor proteins in different membrane pools can be determined using organelle markers. We found that BHK21 cells stably transfected with a vector for constitutive expression of green fluorescent protein (GFP) was a particularly convenient marker for assessing the behavior of a soluble protein.

Using this approach, we established patterns of release for GFP and kinesin from BHK21 and 3T3 cells following treatment for 2–20 min with a wide range of concentration of Triton X-100, saponin, digitonin, and 3-([3-cholamidopropyl]dimethylammonio)-1-propane-sulfonate (CHAPS) (**Table 1**, **Figs. 2** and **3**). Our results confirm previous in vivo results showing that the majority of kinesin is associated with membrane-bound organelles in intact cells ***(11,12)***.

3.2.3. Evaluation of Candidate Effectors for Regulating the Association Between Kinesin Motors and Membranes in Permeabilized Cells

Cells are grown and extracted as described in **Subheading 3.2.2.**, except that putative effectors of motor proteins are included in the extraction buffer. The rationale for these experiments is that it is possible to allow passive diffusion of reagents into cells with a permeabilized plasma membrane ***(9)***. In some cases, a brief incubation in extraction buffer without effector can be advantageous; this pre-extraction step helps to remove soluble proteins that could interfere with the assay and thus may increase the efficacy of effectors. However, pre-extraction could also remove essential cofactors or accessory proteins. All considered, the investigator should determine empirically the usefulness of this step. We usually pre-extract cells for 1 min in extraction buffer. Then, the buffer is changed to an effector-containing extraction buffer and cells are incubated for an additional 4 min.

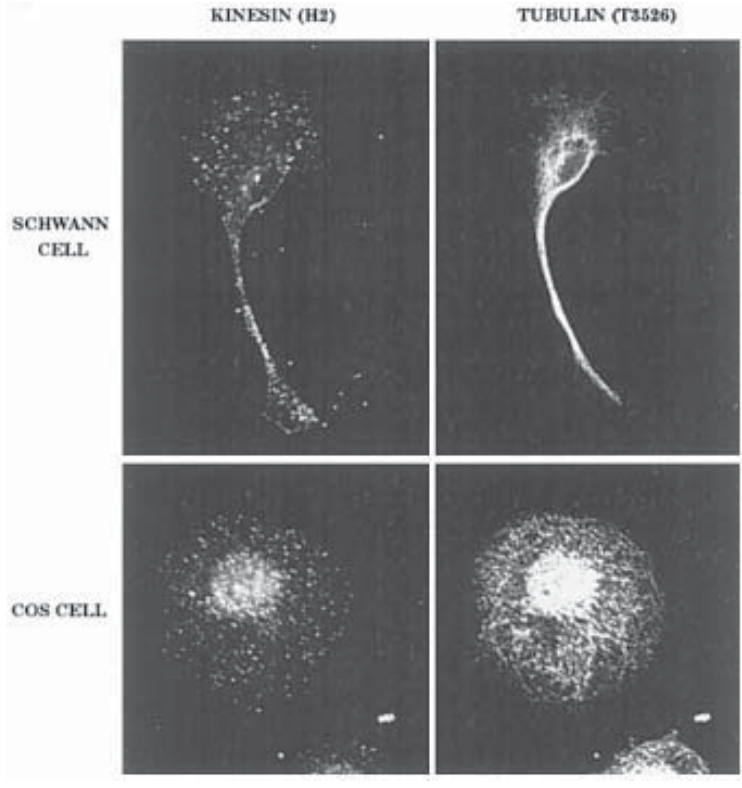

Fig. 2. Images showing punctate kinesin-staining patttern (left column) and filamentous tubulin distribution (right column) in a Schwann cell (top row) and a COS cell (bottom row). Cells were extracted for 5 min with 0.2% saponin prior to fixation. Images were acquired by laser confocal microscopy through a ×100 (N.A. 1.4) lens for the Schwann cell and a ×63 (N.A. 1.4) for the COS cell.

When the chaperone hsc70 was tested in this assay, a reduction in the number of kinesin immunoreactive vesicle-like structures was observed. Thus, results obtained from this assay were consistent with and complemented biochemical studies showing that hsc70 releases conventional kinesin from membranes ***(5)***.

3.2.4. Immunocytochemical Detection of Kinesin Motors

1. At the end of the extraction step, cells are incubated in fixative (**Subheading 2.2.2.**) for 10 min at 37°C.
2. After fixation, cells are rinsed three times in PBS and either processed immediately for immunocytochemistry or stored at 4°C in PBS for up to 1 wk.

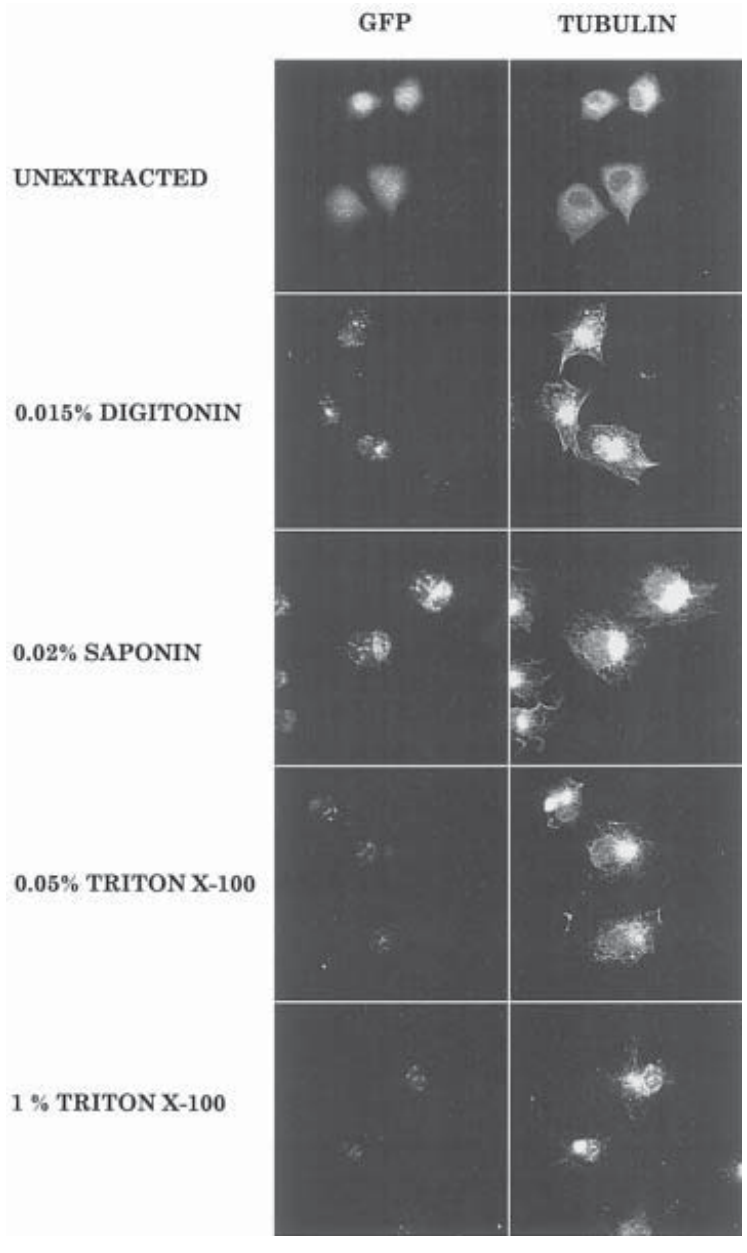

Fig. 3. Images showing the GFP and tubulin distribution before and after extraction with detergents in BHK21 cells stably transfected with a GFP vector. In unextracted cells, GFP permeated the entire cell, including the nucleus. In contrast, in extracted cells, GFP is restricted to the nucleus and a small perinuclear region. Microtubules become more obvious as soluble tubulin is extracted.

3. Prior to staining, cells are further extracted in 0.2–0.6% Triton X-100/PBS for 10–20 min. This step can reduce background resulting from nonspecific binding of extracted proteins to the coated slide.
4. Nonspecific antibody binding is blocked by incubation in blocking solution (2.5% gelatin, 2.5% BSA, and 0.01% sodium azide in PBS readjusted to pH 7.4) for 1 h.
5. Primary antibodies are diluted in blocking solution and incubated at 4°C for approx 16 h. We use the following primary antibodies: rabbit antitubulin polyclonal antibody (Sigma T-3626) at 1:200; H2 and 63–90 antikinesin mouse monoclonal antibodies ***(2,12)*** at 5–20 µg/mL.
6. Cells are washed three times in PBS, then incubated with secondary antibodies, diluted in blocking solution, for 45 min at room temperature. We used the following secondary antibodies: goat anti-rabbit IgG–Texas Red (Molecular Probes) at a dilution of 1:500; goat–anti-mouse–Oregon Green 488 at a dilution of 1:500 (Molecular Probes).
7. After incubation with antibodies, cells are washed three times in PBS.
8. After additional washes in 50 m*M* Tris-HCl (pH 8.0), slides are incubated with a nuclear marker (Molecular Probes).
9. Slides are cover-slipped with ProLong antifade (Molecular Probes) or Gel/Mount (Biomedia, Foster City, CA) (*see* **Note 10**).

3.2.5. Imaging Techniques

To get the most information out of immunocytochemistry, good quality imaging is required. We use a Zeiss Axiovert microscope, also suitable for live-cell imaging. High-numerical-aperture objectives with N.A. 1.3–1.4 (Zeiss 40× (NA 1.3) or 63× (NA 1.4) or 100× (NA 1.4) are recommended for visualizing vesicular and filamentous proteins (*see* **Figs. 2** and **3**). In some cases, laser scanning confocal microscopy can determine the positions of antigens within cells more precisely. Imaging with a cooled CCD camera, however, allows detection of lower-level signals and, with proper controls, can be semiquantitative. Confocal microscopy can be difficult to quantitate because of drift in the photomultiplier detectors. Quantitative analysis of results requires an imaging software package, such as Openlab (Improvision) or Metamoph (Universal Imaging). In addition, some imaging software packages now include deconvolution programs that improve image quality by removing background resulting from haze artifacts from light scattering, achieving much the same effect as confocal microscopy. For presentation, images were prepared using Adobe Photoshop. Although the contrast of presentation images may be enhanced using Photoshop, all images shown in the same panel should be altered simultaneously using the same algorithm to avoid distortions of the scientific information. Moreover, merging of multicolor images to show colocalization should not be done using Photoshop because different wavelengths of light have slight differences in focal point. This operation is best done using the imaging software.

4. Notes

1. For optimal preservation of the cytoskeleton during biochemical fractionation, many investigators use buffers at pH 6.9. In particular, kinesin is sensitive to pH and will begin to lose activity at pH less than pH 6.5–6.8. To ensure maximal enzymatic activities during whole-cell extraction, however, we prefer to keep the pH of all solutions at 7.4. We did not notice a change in the integrity of the cytoskeleton, in the presence of taxol, between pH 6.9 and 7.4, as assessed by immunocytochemistry.
2. The choice of fixative is critical to get an intense, reliable signal from a fixed specimen. We found that a combination of 2% paraformaldehyde and 0.01% glutaraldehyde is optimal for preserving both the cytoskeleton and GFP fluorescence. Higher concentrations of glutaraldehyde result in increased levels of autofluorescence, loss of fluorescence from GFP, and loss of antigenicity for many epitopes. Alcohol fixation does not preserve cytoskeletal structures as effectively as the formaldehyde and glutaraldehyde mixture. Investigators should determine the optimal composition and concentration of fixative for their particular epitope and antibody. We recommend testing the effect of fixative concentrations on antigen preservation by immunoblotting. Nitrocellulose membrane strips containing the protein of interest are fixed for 10 min with the fixative, washed extensively with PBS, and then immunoreactivity of the protein is evaluated by standard methods.
3. Preferentially, effectors with known mechanisms of action should be chosen. For example, we initially focused on a sulfhydryl-reactive reagent NEM and the divalent cation chelator EDTA. NEM covalently modifies free sulfhydryls on a wide variety of proteins and has been used to establish functional significance for specific sulfhydryl groups. A range of effector concentrations should be tested, given that there may be differential sensitivities among the various components. For example, several distinct NEM-sensitive factors (NSF) acting at different stages of the intracellular transport pathway were identified based on their differential sensitivities to NEM ***(10)***.
4. We fractionated both fresh and frozen brains from cow and rat. The species specificities of available antibodies should be considered when choosing a tissue source. Frozen rodent tissues can be purchased commercially (Harlan) or fresh bovine tissues may be obtained from a local slaughterhouse. Certain proteins can lose activity during freezing, so we recommend that a first evaluation be made with fresh tissue. For frozen tissues, use samples flash frozen in liquid nitrogen to minimize damage from ice crystals. Later, one can test if a cycle of freezing–thawing changes a particular effect.
5. Electrophoresis and transfer conditions have to be optimized for each protein. For example, best separation and detection of kinesin light-chain isoforms is obtained by electrophoresing samples on gel gradients of 7.5–16% acrylamide in urea. After separation, we typically transfer proteins for 16–20 h at 4°C, at 25 V in 10 m*M* 3-(cylohexylamino)-1-propanesulfonic acid (CAPS) (Sigma) pH 11 onto ZetaProbe (Bio-Rad) membranes using a Transphor Electrophoresis unit

(Hoefer). Long transfer at constant low voltage is a much more reliable and sensitive method than shorter transfers at higher voltages for kinesin subunits (Stenoien and Brady, unpublished observations). The ZetaProbe membrane is a charged, cationic membrane that binds kinesin light chains with a greater affinity than other commonly used hydrophobic membranes such as polyvinylidene difluoride (PVDF) and nitrocellulose.

6. Vesicles should be resuspended with extreme care to avoid mechanical damage that can result in nonspecific protein release from membranes. First, the pellet is dislodged from the walls of the centrifuge tube with a 1-mL pipetman tip, breaking it into smaller pieces with several jets of HB. Then, the pellet pieces are transferred to an Eppendorf tube and passed very slowly (avoiding strong cavitation forces that could disrupt the membranes) through a 25-gage needle attached to a 1-mL syringe. Usually, two passages are enough to ensure a homogeneous stock of resuspended vesicles. To assess the integrity of membranes following this preparation, the partitioning of an integral membrane protein (e.g., synaptophysin) in pellet and supernatant can be evaluated by immunoblotting. Vesicles can be stored at –80°C. However, the effects of freezing on proteins of interest should be evaluated and compared to fresh preparations.
7. We recommend measuring the relative enrichment of each protein of interest in a given membrane fraction by quantitative immunoblots. This permits calculation of effective molar ratios for each effector and motor protein at which effects can be seen. For example, we found that conventional kinesin is approx 0.5% of the total protein in the microsomal fraction ***(2)***.
8. There are several good reviews describing the membrane solubilization properties of detergents ***(7,8)***. It is recommended that different classes of detergents be tried. Triton X-100 is a nonionic detergent that solubilizes membrane lipids. Even at low concentrations (0.05%), there is a release of soluble proteins, as a result of solubilization of the plasma membrane, whereas at higher concentrations (>0.5%), organelle contents can also be released. Nuclear and cytoskeletal structures are well preserved up to 1% of Triton X-100 (**Fig. 3**). Digitonin is a steroidal compound thought to solubilize membranes by complexing with plasma membrane cholesterol. At concentrations of 0.015%, soluble proteins, such as lactic dehydrogenase (LDH) and carbonic anhydrase, are effectively extracted. Even large proteins, such as myosin (220 kDa), desmoplakin II (>250 kDa) and calpastatin (300 kDa) are extracted, whereas the structure of endoplasmic reticulum and mitochondrial membranes remain intact. These organelles, however, start to be permeabilized at concentrations ≥ 0.1%.
9. Optimal extraction time should be experimentally determined for each motor protein and cell type, with each detergent. A compromise should be made among preservation of cell number, cell morphology, and efficient extraction of a monitored protein. The number of cells in control (unextracted) and experimental (extracted) cells can be compared by staining nuclei with standard nuclear markers (e.g., Hoechst, DAPI, To-Pro3, etc.). To assess changes in cell structure during detergent treatment, cells can be processed for immunohistochemistry to

visualize organelle and cytoskeletal markers (**Fig. 2** and **3**). In our experience, 4 min of extraction was optimal for the detergents tested.

10. We recommend the recently developed Alexa dye series OG488 and Texas Red (Molecular Probes) for immunofluorescence. These fluorophores are significantly brighter and more stable than fluorescein and rhodamine. Quenching of fluorescence, however, remains a problem. To avoid quenching, apply fluorophores in low light and keep slides in the dark. The last washes prior to adding an antifade-containing mounting medium should not contain detergents or phosphates, and the pH should be >7.8. We found Pro-Long antifade (Molecular Probes) the most effective agent to prevent fading during imaging. Independent of the fluorophore and antifade reagents used, slides should be imaged as soon as possible. Sealing the edges of cover slips with Permount (Fisher) prevents drying of samples. Avoid using nail polish, as these usually contain fluorescent compounds.

Acknowledgments

We thank Robin Wray for maintaining and purifying monoclonal antibodies, Zhao Min for generating the GFP-BHK21 subclone, and Harold Ross Payne for outstanding technical advice on imaging. Preparation of this manuscript was supported in part by grants from the National Institute of Neurological Disease and Stroke (NINDS) (NS23868 and NS23320), the National Institute of Aging (AG12646), NASA (NAG2–962), and the Welch Foundation (#1237) to STB and a Pew Fellowship to GM.

References

1. Elluru, R., Bloom, G. S., and Brady, S. T. (1995) Fast axonal transport of kinesin in the rat visual system: functionality of the kinesin heavy chain isoforms. *Mol. Biol. Cell* **6,** 21–40.
2. Stenoien, D. S. and Brady, S. T. (1997) Immunochemical analysis of kinesin light chain function. *Mol. Biol. Cell* **8,** 675–689.
3. Pfister, K. K., Wagner, M. C., Stenoien, D., Bloom, G. S., and Brady, S. T. (1989) Monoclonal antibodies to kinesin heavy and light chains stain vesicle-like structures, but not microtubules, in cultured cells. *J. Cell Biol.* **108,** 1453–1463.
4. Wagner, M. C., Pfister, K. K., Bloom, G. S., and Brady, S. T. (1989) Copurification of kinesin polypeptides with microtubule-stimulated Mg–ATPase activity and kinetic analysis of enzymatic processes. *Cell Motil. Cytoskeleton* **12,** 195–215.
5. Tsai, M.-Y., Morfini, G., Szebenyi, G., and Brady, S. T. (1999) Release of kinesin from vesicles by hsc70 and regulation of fast axonal transport. *Mol. Biol. Cell* **11,** 2161–2173.
6. Goslin, K. and Banker, G. (1991) Rat hippocampal neurons in low-density culture, in *Culturing Nerve Cells* (Banker, G. and K. Goslin, eds.), MIT Press, Cambridge, MA, pp. 252–281.
7. Ramsby, M. L. and Makowski, G. S. (1998) Differential detergent fractionation of eukaryotic cells. Analysis by two dimensional gel electrophoresis, in *2-D Proteome Analysis Protocols* (Link, A. J., ed.), Humana, Totowa, NJ, pp. 53–65.

8. Ramsby, M. L., Makowski, G. S., and Khairallah, E. A. (1994) Differential detergent fractionation of isolated hepatocytes: biochemical, immunochemical, and two dimensional gel electrophoresis characterization of cytoskeletal compartments. *Electrophoresis* **15,** 265–277.
9. Carter, N. (1997) Permeabilization strategies to study protein phosphorylation, in *Current Protocols in Protein Science* (Chanda, V. B., ed.), Wiley, New York.
10. Elluru, R., Bloom, G. S., and Brady, S. T. (1995) Fast axonal transport of kinesin in the rat visual system: functionality of the kinesin heavy chain isoforms. *Mol. Biol. Cell* **6,** 21–40.
11. Rodriguez, L., Stirling, C. J., and Woodman, P. G. (1994) Multiple N-ethylmaleimide-sensitive components are required for endosomal vesicle fusion. *Mol. Biol. Cell* **5,** 773–783.
12. Pfister, K. K., Wagner, M. C., Stenoien, D., Bloom, G. S., and Brady, S. T., (1989) Monoclonal antibodies to kinesin heavy and light chains stain vesicle-like structures, but not microtubules, in cultured cells. *J. Cell Biol.* **108,** 1453–1463.

14

Microinjection Methods for Analyzing the Functions of Kinesins in Early Embryos

Robert L. Morris, Heather M. Brown, Brent D. Wright, David J. Sharp, William Sullivan, and Jonathan M. Scholey

1. Introduction

Microinjection of kinesin-function-blocking antibodies into early embryos of echinoderms and *Drosophila melanogaster* has demonstrated the roles of kinesins in processes ranging from mitosis and spindle maintenance, to cell wound repair and to ciliogenesis ***(1–5)***. Echinoderm embryos have served as a model system in developmental and cell biology for more than a century because of their optical clarity and mechanical resilience. Early embryos of *Drosophila* serve as a favorite system for studies of kinesin function in mitosis because of the uniquely organized arrangement of spindles in the syncytial blastoderm. Microinjection of early echinoderm and *Drosophila* embryos provides a mean to directly test for functions of kinesins by inhibiting their actions at precise times during development. By microinjection, macromolecules such as rhodamine-conjugated tubulin can be introduced into embryos to allow visualization of spindle dynamics in living systems ***(3,6)***. Finally, blocking kinesin functions by microinjecting inhibitory antibodies frequently phenocopies corresponding mutants in genetically tractable organisms ***(7)***, attesting to the validity of this versatile approach to studying roles of kinesins in vivo.

A detailed treatment of microinjection in general has been presented elsewhere ***(8,9)*** and is beyond the scope of this chapter. Instead, we discuss the application of microinjection particularly to the study of kinesins. Techniques for preparing antibodies are followed by techniques for microinjecting echinoderm embryos and techniques for microinjecting *Drosophila* embryos. A final section on characterizing the effects of antikinesin antibody microinjection includes methods for individual embryo handling and analysis.

From: *Methods in Molecular Biology*, Vol. 164: *Kinesin Protocols*
Edited by: I. Vernos

2. Materials

2.1. To Study Kinesins By Microinjection

1. Necessary reagents include the following: purified experimental and control antibodies, other reagents to be injected (e.g., rhodamine-labeled tubulin) (*see* **Note 1**).
2. Necessary equipment include items for microinjection: pipet puller; microscope equipped with micromanipulator; injection apparatus, including syringe, hydraulic tubing, and microinstrument holder; diamond-tipped pencil; frames for Kiehart injection chamber; equipment for recording images of living systems such as time-lapse video and/or confocal microscope.
3. Necessary supplies include centrifugal concentrator devices for concentrating antibodies or exchanging antibody solutions, centrifugal 0.22-µm filters for filter sterilization of antibodies, double-stick tape, and a red wax pencil.

2.2. For Microinjection Into Echinoderm Embryos

1. Gravid echinoderms. Echinoderms with good optical clarity include the sea urchins *Lytechinus pictus* (cold-water species [i.e., 13°C], gravid June through at least September) and *Lytechinus variegatus* (warm-water species [i.e., 22°C], gravid January through May) (*see* **Note 2**). They can be maintained for weeks or months in well-conditioned, well-aerated marine aquaria if kept clean and under constant illumination and regularly fed dried kelp, egg whites, or carrot peelings.
2. Shedding and egg preparation equipment: 0.5 *M* KCl (pH 7.3); 27-gage needles and small syringes; 150-µm Nitex mesh; wide-mouth pipets.
3. Injection buffer. Aspartate injection buffer (AIB): 150 m*M* K·aspartate, 10 m*M* K·phosphate, monobasic, anhydrous, pH to 7.2 with KOH. Sterile filter with 0.22-µm filter. Make up fresh each week.
4. Filtered seawater (FSW). Natural or artificial seawater, filtered through a 0.22-µm filter, aerated for 1 h or more, and supplemented with penicillin to 10 U/mL and streptomycin to 10 µg/mL and maintained at correct temperature. Without antibiotics, FSW will keep indefinitely. Do not sterilize seawater by autoclaving.
5. Filtered seawater with *p*-aminobenzoic acid (FSW–PABA). FSW supplemented with 10 m*M* PABA. Add PABA dry to FSW. Make FSW–PABA up fresh, keep it in the dark, and use within 12 h.
6. Silane solution: 5% dimethyl-dichloro-silane in chloroform for siliconizing capillary tubes.
7. Wesson brand canola oil, 1 mo old or fresher, and filtered through a 0.22-µm filter.

2.3. For Microinjection into Drosophila Embryos

1. *Drosophila* animal stocks including experimental stocks and wild-type stocks.
2. Injection buffer. For *Drosophila*, phosphate-buffered saline (PBS): 137 m*M* NaCl, 2.7 m*M* KCl, 10 m*M* Na_2HPO_4, 1.8 m*M* KH_2PO_4 (pH 7.2).
3. Embryo collection and preparation equipment: grape-agar plates for laying and collection of embryos and halocarbon oil 700 (Sigma).

4. Heptane glue: Make by solubilizing adhesive off of double-stick tape with a heptane soak; consistency should be slightly thinner than rubber cement.

3. Methods

3.1. Preparation of Antibodies

1. Gather experimental and control antibodies (*see* **Note 1**). Monoclonal antibodies may be purified by protein-A affinity chromatography. Polyclonal antibodies must be affinity purified against their antigen. Prepare control antibodies to the same or higher concentration than experimentals. For monoclonal antibodies, use nonspecific antibody of identical isotype to the experimental as negative control. For polyclonal antibodies, use nonspecific antibodies from the same host species as negative control. For any antibody, an antikinesin antibody for which the phenotype of injection was previously characterized may be used as a positive control. Characterize all antibodies by Western blotting to confirm specificity of binding of experimental antibodies and lack of binding of negative control antibodies. *See* **Note 3** for caveats concerning specificity.
2. Transfer antibodies to a buffer suitable for microinjection. PBS is suitable for most injections. For echinoderm embryos, we have employed AIB (pH 7.2), as a more physiological buffer. Antibody can be exchanged into injection buffer by dialysis or by repeated concentration in centrifugal concentrator devices to remove existing buffer, followed by dilution in the desired injection buffer. Repeated rounds of concentration and redilution can exchange out detrimental buffer ingredients into which antibodies may have been purified or stored (e.g., azide-containing buffers).
3. Concentrate antibodies in injection buffer using centrifugal concentrators. The antibody concentration required to see an effect can only be determined empirically. Depending on the antibody, full effects have been achieved with in-the-needle antibody concentrations ranging from 0.6 ***(4)*** to 20 mg/mL ***(5)***. Many antibody solutions tend to become very sticky (tend to plug the needle tip frequently) above 5 mg/mL (*see* **Note 6**).
4. Filter-sterilize antibody solution by spinning through small-volume centrifugal 0.22-µm filter units. Store antibody on ice.

3.2. Microinjection into Echinoderm Embryos

1. Siliconize all capillary tubes from which needles are pulled to ensure protein does not adhere to the glass: Use Pyrex glass capillary pipets with an outer diameter of 1.0 mm. (e.g., Drummond "microcaps"). Soak capillary tubes in silane solution for 1 h. Drain silane. Dry tubes with jet of filtered air. If white crusty spots are present, rinse tubes briefly with acetone. Dry the tubes with jet of filtered air. Bake the capillary tubes at 180°C for 2 h in a dry oven. Keep cool tubes dust-free and handle them only at tips.
2. Pull needles to a gradual taper.
3. Assemble Kiehart injection chambers as illustrated in **Fig. 1** (after **ref. *8***, *see also* **ref. *9***). Clean all cover slips with boiling detergent solution prior to cutting or

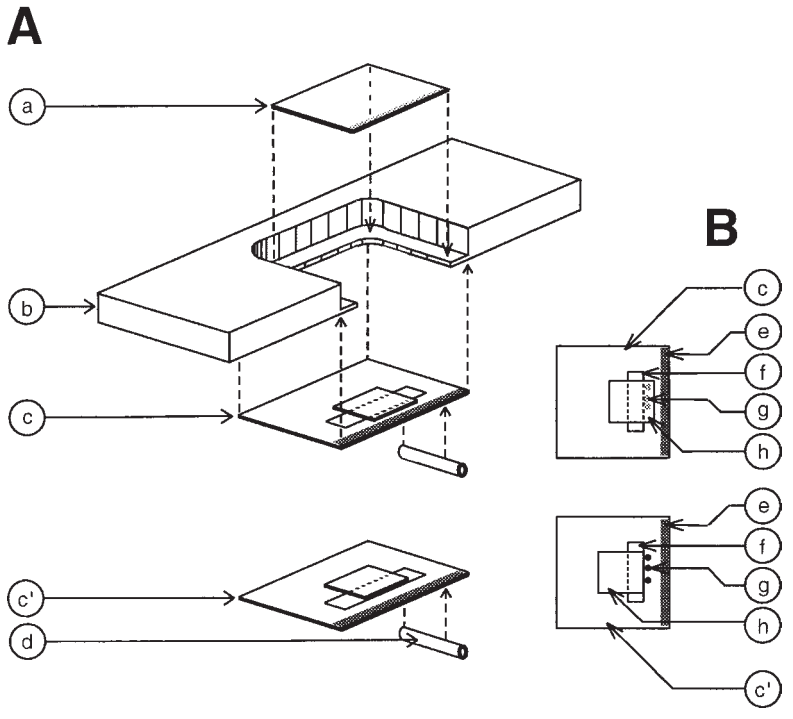

Fig. 1. Assembly of injection chambers for injecting echinoderm embryos (based on **ref. *8***; *see also* **ref. *9***). **(A)** Perspective drawing of exploded chamber, approximately to scale except for oversized embryos. Top cover slip (15 × 22 mm) (a) with wax-pencil line on underside of front edge is stuck down with silicone vacuum grease to a plastic or aluminum chamber frame (b). Also stuck to the frame with silicone grease is the cover slip (c) of the trapping chamber, which holds embryos for injection and subsequent observation, or cover slip (c') of the barrier chamber, which provides a barrier against which eggs are injected and offers easy access for removal of embryos from the chamber. To the bottom of (c) or (c'), a capillary tube (d) holding a droplet of injectable antibody in Wesson oil is attached with vacuum grease. A second capillary tube with control antibody (not shown) can be attached beside the first. **(B)** The trapping chamber is shown from the top down with the cover slip (c), wax-pencil line (e), and double-stick tape spacer (f) supporting the 11 × 11-mm fragment of the cover slip (h). The space under the ledge of the cover-slip fragment traps the embryos (g). The barrier chamber is also shown from the top down, including the cover slip (c') with the wax-pencil line (e) on its top surface. Here, embryos (g) sit against the double-stick tape (f) and 11 × 11-mm cover slip fragment (h), which are flush along their front edge. If the barrier chamber is kept flat, embryos remain in their original positions until they ciliate. Embryos are loaded into a dry trapping chamber, after which the top cover slip is rapidly positioned, the chamber is filled to pencil lines with FSW–PABA, and capped with oil. Embryos are loaded into the barrier chamber after it is assembled and filled with FSW–PABA but before it is capped with oil.

using them. Cut cover slips to appropriate sizes with a diamond-tipped etching pencil. Assemble antibody capillary from fresh antibody solution and filtered Wesson oil then store at 4°C (*see* **Note 4**).

4. Prepare needles for microinjection ahead of time (*see* **Note 5**). Back-load at least 25 needles per chamber with mercury and Wesson oil. Set back-loaded needles aside (*see* **Note 6**). Antibody will be front-loaded into needles later as injections take place — one needle per injection attempt (*see* **Note 4**).
5. Obtain gametes by "shedding" gravid sea urchins. Inject 0.5 *M* KCl equal to approx 5% of the animal's body volume into the peritoneal cavity through the membrane around the mouth. Gametes will be released through five gonopores at the apex of the animal's aboral (top) surface. Keep animals out of water while shedding is monitored. If female (releasing golden eggs), invert animal onto small-mouthed beaker of FSW so eggs always remain wet and at the correct temperature. Eggs will settle to bottom of beaker. If male (releasing milky white sperm), collect 10-µL aliquots of concentrated "dry" sperm (i.e., straight off the animal out of water), into capillary tubes. Store sperm aliquots on ice. Return animals to the holding tank of seawater while they finish shedding. Return shed animals to original tank only after shedding is complete, lest chemical cues from the shedding animals trigger others to shed in the tank.
6. Dejelly eggs by passing egg suspension through 150-µm Nitex mesh three to five times. Wash eggs with three changes of FSW, letting eggs settle out after each change. Separate dejellied washed eggs to several containers so that they are no deeper than a monolayer.
7. Transfer some eggs with a wide-mouth pipet to FSW–PABA.
8. Activate sperm by 1:1000 dilution of sperm aliquot into FSW. Use immediately. Sperm die within minutes of activation.
9. Fertilize eggs by adding one drop of activated sperm for each milliliter of egg suspension and gently rocking to mix. Fertilization should be complete within 5 min and can be monitored by observing the fertilization envelope lift off on a dissection scope. Wash zygotes free of sperm with three changes of FSW, letting zygotes settle out after each change.
10. Transfer zygotes to Kiehart chamber. Load zygotes under the ledge of the embryo trap in the trapping chamber kept dry or in front of embryo barrier in a barrier chamber preassembled and already filled with water. One or two rows of embryos in a monolayer should be back against the tape barrier in either chamber.
11. Mount Kiehart chamber on the microscope stage.
12. Inject zygotes using a mercury droplet force–transduction injection apparatus ***(8,9)***. Embryos can typically tolerate injections of 1–5% of cell volume (*see* **Notes 7** and **8**).
13. Monitor piercing, injection flow, and needle withdrawal. If any are too harsh, disregard that embryo. If, in the barrier chamber, the needle will not withdraw from the embryo, pull the impaled embryo back to Wesson oil that seals the water in Kiehart chamber; the embryo will come off when the needle is pulled out through the oil. It can then be gently pushed back to the barrier (*see* **Note 9**).

14. Make careful observations of the relative positions of the injected embryos so the effects of experimentals versus controls can be compared.
15. Inject the control antibody first, followed by experimentals, and finish with the control at the end. If injecting during mitosis, inject into the cytoplasm distant from the spindle and cease injections at the anaphase (*see* **Note 9**).

3.3. Microinjection into Drosophila Embryos

1. Pull the needles to a gradual taper. Use quick-filling borosilicate glass capillary tubes (e.g., World Precision Instruments' KWIK-Fil capillaries) unsiliconized.
2. Back-load ahead of time three needles per injection slide with the solutions to be injected. Set the loaded needles on ice (*see* **Notes 5** and **6**).
3. For injection apparatus, use air-pressure force–transduction system consisting of a 60-cc syringe of air connected by a three-way stopcock to a length of tubing connected to the microinstrument holder. The microinstrument holder holds a microneedle in one end and connects to the pressurized tubing at the other end.
4. Assemble the dechorionation slide as illustrated in **Fig. 2** in preparation for mounting embryos on the injection cover slip.
5. Obtain embryos by inverting laying *Drosophila* stock over the grape-agar plate, incubating at 25°C for 1 h, then removing the adult stock and incubating embryos an additional hour at room temperature.
6. Dechorionate embryos on a dechorionation slide (after **ref. *6***). With a fine paint brush, move intact embryos to the double-stick tape on the dechorionation slide. For each embryo, displace it from chorion adhering to the tape by gentle pressure on the embryo with the tip of sharp forceps. Gently transfer embryos with sharp forceps off of the ripped chorion onto line of heptane glue. Repeat this step until 12–15 embryos have been transferred. Remove the injection cover slip with its dechorionated embryos from the dechorionation slide.
7. Dehydrate the embryos (if they are not already dehydrated) by placing the cover slip in a Petri dish containing dessicant crystals. Allow embryos to remain in this dish for 1–5 min or until the plasma membrane can be seen to pull away slightly from the vitelline layer (*see* **Note 10**).
8. Submerge the embryos under a line of halocarbon oil for subsequent injection and monitoring steps.
9. Mount the injection cover slip on the microscope stage and mount the back-loaded needle in the injection apparatus.
10. Guide the needle tip to the edge of the cover slip, which can be seen by virtue of a wax pencil line on its surface. Break the needle tip against the leading edge of the cover slip so that the needle tip's outer diameter is 2–6 µm. Move the needle tip back over the top of the cover slip and into proximity of the embryos.
11. Begin the flow of antibody out of the needle tip by applying pressure with the injection apparatus syringe. Adjust pressure as needed to maintain flow.
12. As antibody is flowing, inject the embryos by gently piercing them with the needle tip. Allow antibody to flow into each embryo until the embryo regains its original volume within the vitelline layer. If there is leakage of the cytoplasm

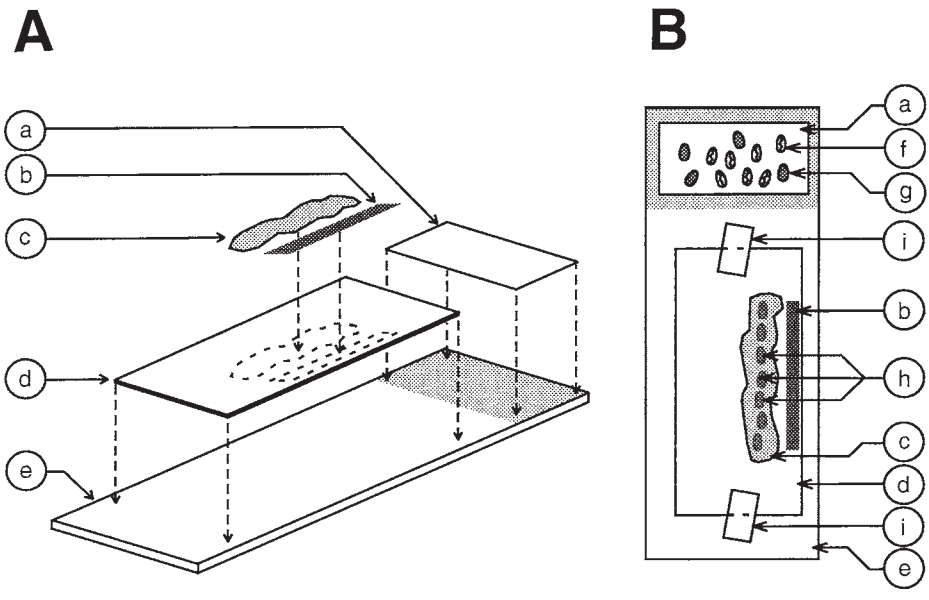

Fig. 2. Assembly of dechorionation slide and injection chamber for injecting *Drosophila melanogaster* embryos (after **ref. *6***). **(A)** Perspective drawing of an exploded chamber, approximately to scale except for oversized embryos. (a) A 20 × 25-mm piece of double-stick tape for dechorionating embryos is attached to the smoked end of the slide (e). A 22 × 50-mm #1 cover slip (d) on which injections will take place has a wax-pencil line (b) along the front edge, and behind this is a 20-mm line of heptane glue (c), which will hold embryos. **(B)** The assembled dechorionation slide is shown from the top down. Dechorionation begins with intact embryos (g) on double-stick tape (a). Embryos (h) are manually removed from chorion (f) and stuck down to the heptane glue stripe (c). The injection cover slip (d) is held down to the slide (e) with two pieces of single-sided tape (i). After dechorionation and alignment of embryos on heptane glue, the cover slip can be removed from the dechorionation slide. Embryos are then dehydrated as necessary and covered over with line of halocarbon oil for the duration of injections and monitoring of effects.

during injection or after needle withdrawal, that embryo has been overfilled and should be disregarded. Inject each embryo in turn with the same continuous stream of antibody from the same needle until all embryos for that condition have been injected or until the needle clogs, whichever comes first (*see* **Note 8**).

3.4. Characterization of Antikinesin Effects

1. Assess the effects of the antibody injection by multiple microscopic techniques. Effects on mitosis (e.g., on mitotic spindle structure) can be assessed immediately or within one cell cycle, depending on the timing of injection and the

antibody's diffusion rate. For *Drosophila* embryos containing fluorescently labeled proteins, take optical sections at the embryo surface at 5- to 15-s intervals from which to assemble time-lapse sequences of mitosis (*see* **Note 11**). In echinoderm embryos, use time-lapse video microscopy to assess effects on later developmental processes (e.g., ciliogenesis, cell fate specification, spindle positioning for macromere/micromere formation) (*see* **Note 12**).

2. For each effect observed, compare multiple experimental and control embryos, injected in side-by-side experiments using the same batches of embryos. Also, compare different batches of embryos, and repeat the experiments with different batches of the same antibodies (*see* **Notes 12** and **13**).
3. To observe effects of antikinesin injection on protein localization or cellular ultrastructure in microinjected echinoderm embryos, remove the injected embryos from barrier injection chamber for subsequent processing (*see* **Note 14**). The procedure is as follows:
   a. Clear uninjected embryos from around the injected embryo using a microinjection needle. Sweep embryos aside with the needle, or pull embryos away by "kissing" them with gentle suction from small needle tip placed against the embryo surface and backing away the needle.
   b. Break off a microinjection needle back-loaded only with Wesson oil so that its inner diameter is approx 150 µm.
   c. Bring large-diameter broken needle into proximity of injected embryo and gently suck the embryo into the needle with its surrounding seawater (*see* **Note 14**).
   d. Carefully back the needle out of the injection chamber, remove the microinstrument holder from the micromanipulator, and touch the needle tip to the surface of the water in another location. Heat from the fingertips will cause a droplet of solution at the very tip of the needle, containing the embryo, to be expelled.
   e. To observe the effects on protein localization, transfer the embryos to polylysine-treated slides or coverslips and process gently for immunofluorescence.
   f. To observe the effects on cellular ultrastructure by electron microscopy (EM), transfer the embryos to the well of the observation chamber. Monitor the development now without risk of losing the embryo in the chamber with many uninjected embryos. At appropriate developmental stage, transfer the embryo singly to EM fixative and process for EM (*see* **Note 14**). Single embryos can be removed from isolation in the observation chambers and discharged into the EM fixative by a mouth pipet.

4. Notes

1. The antibodies selected for injection are usually determined by availability. Try any and all purified antibodies available regardless of effectiveness at blocking motor activity in vitro.
2. In addition to the sea urchin species described, other echinoderms with transparent embryos amenable to microinjection include the sea star *Asterias forbesi* (cold

water, gravid May through July), and the sand dollar *Echinarachnius parma* (cold water, gravid March through August).

3. Because differences in antibody binding to denatured or renatured antigen on Western blots vs native protein inside a living cell cannot be tested, always be aware of potential differences between antibody behavior on a Western blot and in vivo. The best recourse is to test for similar effects on living cells by other antibodies or by complementary approaches such as using antisense oligonucleotides as probes or comparing antibody microinjection results with results of genetic knockouts of related molecules in other organisms.
4. Antibody solutions can act very "sticky" (i.e., plug the needle frequently or resist ejection entirely). Several recourses are possible: (1) Dilute the antibody. (2) Try another injection buffer. (3) Break a larger opening in the needle tip. Antibodies will often clog needles with tip diameters of 2 µm or less and embryos will often resist piercing by tip diameters of 5 µm or more. Embryos can be made "stiffer" to aid piercing with larger needle tips by osmotically swelling them with a small (1%) dilution of injection chamber seawater with distilled water.
5. Many parts of the injection apparatus, including all parts of the injection chamber and microneedles, can be assembled beforehand. Prepare an excess of needles before beginning a round of injections. Do not waste time on a plugged needle. If the needle clogs, immediately replace it with a new needle.
6. If injecting rhodamine–tubulin, take precautions to prevent tubulin polymerization in the needle: prechill the needles, back-load rhodamine–tubulin, then keep needles on ice until immediately before injection. If coinjecting rhodamine–tubulin and an antibody, do not mix the solutions. Inject each one separately. In *Drosophila*, inject rhodamine–tubulin first without inflating embryo completely to its overlying vitelline layer. Wait 5 min for tubulin dispersal, then inject antibody.
7. Preventing a rise in intracellular calcium upon injection can aid cell survivability. For this reason, many injection buffers are supplemented with 1 m*M* EGTA. The risk of interference with normal cellular calcium fluctuations can be addressed with control injections.
8. Use one needle per injection attempt with echinoderms. Use one needle for many *Drosophila* embryos by maintaining a continuous flow of antibody through the needle tip. It is possible to inject 10–16 *Drosophila* embryos per chamber for multiple chambers before the needle clogs and must be discarded.
9. Maintain the injection chamber at the appropriate temperature for embryos being injected. For cold-water echinoderm species, perform injections in cooled room or use thermally controlled injection chambers. After injection, maintain the embryos at the appropriate temperature throughout the development.
10. Do not over- or under-desiccate *Drosophila* embryos. Overdesiccation can lead to developmental abnormalities unrelated to injection, and underdesiccation can lead to difficulty with injection process. Overdesiccation is the most common source of artifacts in *Drosophila* injections ***(6)***. Daily fluctuations in ambient humidity necessitate different drying times from one day to the next. Use the first injections of the day to gauge the drying time required for that day.

11. For studies of antikinesin effects on spindle structure, the syncytial blastoderm stage of *Drosophila* offers the advantage of having many spindles affected by the same injection.
13. If the antibody microinjection experiments do not give a detectable effect on cell function, try one or all of the following options: (1) Concentrate the antibody further; (2) try a different antibody; (3) try a fresher antibody or antibody that has not been repeatedly frozen and thawed; (4) monitor other cell functions for unexpected effects.
12. Monitor as many cellular processes as possible because unexpected roles for the kinesin being studied may manifest as unexpected effects of antibody injection. Where possible, quantitate results. Quantitation can reveal subtle effects not visible with purely qualitative observation.
14. Outside of an injection chamber, echinoderm embryos can be transferred from location to location easily either singly or as a group using a capillary pipet flame-drawn to an inner diameter of 150 µm as a mouth pipet. Mouth pipet consists of rubber tubing connecting a mouthpiece to the pipet. Flame-drawn Pasteur pipets can be used similarly if airflow is attenuated by a constriction in the air path.

References

1. Bi, G.-Q., Morris, R. L., Liao, G., Alderton, J. M., Scholey, J. M., and Steinhardt, R. A. (1997) Kinesin- and myosin-driven steps of vesicle recruitment for Ca^{2+}-regulated exocytosis. *J. Cell Biol*. **138**, 999–1008.
2. Morris, R. L. and Scholey, J. M. (1997) Heterotrimeric kinesin-II is required for the assembly of motile 9+2 ciliary axonemes on sea urchin embryos. *J. Cell Biol*. **138**, 1009–1022.
3. Sharp D. J., Yu, K. R., Sisson, J. L., Sullivan, W., and Scholey, J. M. (1999) Antagonistic microtubule-sliding motors position mitotic centrosomes in *Drosophila* early embryos. *Nature Cell Biol*. **1**, 51–54.
4. Steinhardt, R. A., Bi, G.-Q., and Alderton, J. M. (1994) Cell membrane resealing by a vesicular mechanism similar to neurotransmitter release. *Science* **263**, 390–393.
5. Wright, B. D., Terasaki, M., and Scholey, J. M. (1993) Roles of kinesin and kinesin-like proteins in sea urchin embryonic cell division: evaluation using antibody microinjection. *J. Cell Biol*. **123**, 681–689.
6. Francis-Lang, H., Minden, J., Sullivan, W., and Oegema, K. (1995) Live confocal analysis with fluorescently labeled proteins. *Methods Mol. Biol*. **122**, 223–237.
7. Scholey, J. M. (1998) Functions of motor proteins in echinoderm embryos: an argument in support of antibody inhibition experiments. *Cell Motil. Cytoskeleton*. **39**, 257–260.
8. Kiehart, D. P. (1982) Microinjection of echinoderm eggs: apparatus and procedures. *Methods Cell Biol*. **25**, 13–31.
9. Jaffe, L. and Terasaki, M. (1999) *Microinjection Manual*. Online Resource. Available: http://egg.uchc.edu/injection/.

15

The Use of Dominant Negative Mutants to Study the Function of Mitotic Motors in the In Vitro Spindle Assembly Assay in *Xenopus* Egg Extracts

Haralabia Boleti, Eric Karsenti, and Isabelle Vernos

1. Introduction

The mitotic spindle is a transient cellular structure that distributes faithfully the chromosomes among the two daughter cells during mitosis. This highly dynamic bipolar structure assembles and disassembles periodically and its main structural components are microtubules (MTs) and chromosomes. Microtubule-dependent motors in particular members of the kinesin superfamily play an important role in directing the self-organization of microtubules into a bipolar spindle.

Although much can be learned using genetics, the analysis of the specific role of each motor in mitosis requires other kinds of approach. One such approach involves the use of low-speed (10,000*g*) *Xenopus* egg extracts in which spindles can be induced to form around sperm nuclei or chromatin beads ***(1–4)***. The functions of several kinesin-like proteins have been studied successfully in this system by interfering with their activity in any of the following ways: adding blocking antibodies, adding dominant negative mutants, or depleting the extract from the protein under study ***(5–10)***.

The first example of a well-defined dominant negative effect on spindle assembly in *Xenopus* egg extracts was observed during the experiments that we performed to characterize Xklp2, a plus-end directed *Xenopus* kinesin-like protein. Xklp2 was identified during a polymerase chain reaction (PCR) screen for MT motors belonging to the kinesin family ***(11)***. This MT motor localized at spindle poles in tissue culture cells throughout mitosis ***(5)***. We suspected that it could play a role in spindle assembly and set up a dominant negative approach using spindle assembly in egg extract and recombinant proteins to determine its function ***(5,12)***.

From: *Methods in Molecular Biology*, Vol. 164: *Kinesin Protocols*
Edited by: I. Vernos

In this chapter, we describe the methods used, including the preparation of *Xenopus* egg extracts, the formation of spindles in vitro, the selection of recombinant proteins, and their use to study Xklp2 function during spindle assembly.

2. Materials

2.1. Preparation of Mitotic (CSF-Arrested) Xenopus Egg Extracts

1. Five *Xenopus laevis* females.
2. Hormones: Pregnant mare serum gonadotropin (PMSG) at 200 U/mL in dH_2O (Intergonan purchased from Intervet). Human chorionic gonadotropin (HCG) at 2000 U/mL in dH_2O (Sigma cat. no. CG-10). This hormone can be stored at 4°C in solution for 1 wk.
3. MMR: 100 m*M* NaCl, 2 m*M* KCl, 1 m*M* $MgCl_2$, 2 m*M* $CaCl_2$, 0.1 m*M* EDTA, 5 m*M* HEPES (pH 7.8) with NaOH. Prepare as a 10X stock solution, autoclave, and store at room temperature.
4. 20X extract buffer (XB)-salts: 2 *M* KCl, 20 m*M* $MgCl_2$, 2 m*M* $CaCl_2$. Filter to sterilize and store at 4°C.
5. 2 *M* sucrose: Filter to sterilize and store at 4°C or frozen at –20°C.
6. 1 *M* K–HEPES (pH to 7.7) with KOH, filter to sterilize, and store at –20°C.
7. Cysteine, free base (Sigma C-7755).
8. Protease inhibitors: Leupeptin, pepstatin A, aprotinin or chymostatin at 10 mg/mL each in dimethyl sulfoxide (DMSO). Store at –20°C in aliquots. Use at 1:1000 dilution.
9. Cytochalasin D: 10 mg/mL cytochalasin D made up in DMSO and stored at –20°C. Use at 1:1000 dilution.
10. 20X energy mix: 15 m*M* creatine phosphate (5 m*M* stock, –20°C), 20 m*M* ATP (pH 7.4), 20 m*M* $MgCl_2$. Store at –20°C in aliquots.
11. Just before starting to collect the eggs, on the day of extract preparation, prepare the following solutions (the volumes are calculated for a standard preparation from four to five frogs).
    a. 1X MMR (1–2 L).
    b. Dejellying solution: 2% cysteine in 1X XB-salts (pH to 7.8) with NaOH. (500 mL).
    c. XB buffer: 1X XB-salts, 10 m*M* K–HEPES (pH 7.7), 50 m*M* sucrose. Prepare fresh from stocks (20X XB-salts, 2 *M* sucrose, 1 *M* K–HEPES) (500 mL) (*see* **Note 1**).
    d. CSF–XB buffer: 200 mL XB buffer with 2 m*M* $MgCl_2$ and 5 m*M* EGTA (pH 7.7) (*see* **Note 1**).
    e. 100 mL CSF–XB with protease inhibitors (*see* **Note 1**).

    Prepare also the following material:
    - Several 400-mL glass beakers rinsed twice with deionized water (*see* **Note 3**).
    - Pasteur pipets cut off to make a wide end and fire-polished.

- SW50.1 ultraclear tubes with 0.5 mL of CSF–XB with protease inhibitors and 1:1000 cytochalasin D and holder tubes to fit then into a centrifuge.

2.2. Spindle Formation in Xenopus Extracts

2.2.1. Preparation of Demembranated Sperm Nuclei

1. One *Xenopus laevis* male.
2. Sperm dilution buffer: 100 m*M* KCl, 1 m*M* $MgCl_2$, 150 m*M* sucrose.
3. 10 m*M* $CaCl_2$ in sperm dilution buffer.
4. HSP buffer: 250 m*M* sucrose, 15 m*M* HEPES (pH 7.4), 0.5 m*M* spermidine, and 0.2 m*M* spermine.
5. HSPP buffer: HSP containing 10 mg/mL leupeptin and 0.3 m*M* polymethylsulfonyl fluoride (PMSF).

2.2.2. In Vitro Spindle Assembly Assay

1. Fluorescently labeled tubulin (TMR tubulin) ***(13)***.
2. *Xenopus laevis* sperm cells at around 3×10^6/mL stored at –70°C in aliquots.
3. Hoechst 33342, 5 mg/mL in distilled water (Molecular Probes, H-1399). Store at 4°C in the dark.
4. 400 m*M* $CaCl_2$ stock solution in distilled water. Store in aliquots at –20°C.
5. 10X calcium solution: 4 m*M* $CaCl_2$, 100 m*M* KCl, 1 m*M* $MgCl_2$. Store in aliquots at –20°C.
6. Spindle fix: 48% glycerol (v/v), 11% formaldehyde, 1X MMR, 1 µg/mL Hoechst. Prepare on the day of use by combining 600 µL from 80% glycerol (v/v) in water, 300 µL 37% formaldehyde stock, 100 µL 1X MMR, and 1 µL Hoechst stock solution. Adjust to 1 mL.
7. Coverslips, square 22 × 22 mm.
8. Transparent nail varnish.

2.2.3. Spindle Pelleting onto Coverslips

1. BRB80: 80 m*M* K–PIPES (pH 6.8), 1 m*M* EGTA, 1 m*M* $MgCl_2$. Adjust the pH with KOH. Prepare a 5X stock, filter to sterilize, and store at 4°C.
2. Fix solution for pelleting spindles: 30% glycerol (v/v), 0.25% glutaraldehyde in BRB80.
3. Dilution buffer for pelleting spindles: 30% glycerol (v/v), 0.5% Triton X-100 in BRB80. Store at room temperature.
4. Cushion: 40% glycerol (v/v) in BRB80. Store at 4°C.
5. Corex tubes (15 mL) with Plexiglas adaptors (**Fig. 4**, Sawin and Mitchinson 1991).
5. Coverslips, round, 12 mm in diameter.
6. Methanol kept at –20°C.
7. TBS-TX 1X TBS (10 m*M* Tris-HCl [pH 7.4], 150 m*M* NaCl), 0.1% Triton X-100.
8. Mowiol mounting medium: 6 g glycerol, 2.4 g Mowiol 4-88 (Merck 4094), 12 mL 0.2 *M* Tris-HCl (pH 8.5), 6 mL distilled water. Place glycerol in 50-mL dispos-

able conical tube, add Mowiol, and stir thoroughly. Add water and leave for 2 h at room temperature. Add Tris-HCl and incubate at around 53°C until the Mowiol has dissolved and stir occasionally. Clarify by centrifugation at 3000*g* for 20 min. Aliquot the supernatant and keep at –20°C.

2.3. Interfering with Spindle Assembly to test Xklp2 Function

2.3.1. Expression and Purification of Xklp2 Recombinant Proteins

2.3.1.1. Cloning

1. cDNA coding for the kinesin-like protein.
2. Oligonucleotide primers with the sequences for appropriate restriction sites for cloning.
3. Amplitaq or Vent DNA polymerase.
4. pGEX-2T vectors (Stratagene).
5. Restriction enzymes.
6. TG1 or XL1Blue *Escherichia coli* cells.

2.3.1.2. Expression of Recombinant Proteins

1. LB. For 1 L, 10 g bactotryptone, 5 g yeast extract, 10 g NaCl (pH 7.0) with NaOH. Autoclave and keep at room temperature.
2. β-D-Thiogalactopyranoside (IPTG), 1 *M* solution (kept frozen at –20°C).
3. Phosphate buffered saline (PBS). For 1 L, 8 g NaCl, 0.2 g KCl, 1.44 g Na_2HPO_4, 0.24 g KH_2PO_4 (pH 7.4) with HCl. Autoclave and keep at room temperature.
4. Proteolytic inhibitors: PMSF (0.1 M), leupeptin (10 mg/mL), pepstatin (1 mg/mL) and aprotinin (10 mg/mL), frozen in liquid nitrogen and stored at –20°C. Use at 1:1000 dilution.
5. Triton X-100, 10% solution.
6. Glutathione Sepharose-4B resin (Pharmacia, 17-0756-01).
7. Reduced glutathione: 10 m*M*, in 50 m*M* Tris-HCl (pH 7.4) (Sigma, G-6013). Prepare fresh.

3. Methods

3.1. Preparation of Mitotic (CSF-arrested) Xenopus Egg Extracts

Unfertilized *Xenopus* eggs are naturally arrested in the second metaphase of meiosis ***(14)***. Crude cytoplasmic extracts arrested in a mitotic state ("mitotic extracts") are prepared from unfertilized eggs of *Xenopus laevis* by centrifugation at 10,000*g* (**Fig. 1**; ***[1,3,15]***). The protein concentration of the cytoplasmic fraction (>40 mg/mL) is close to the protein concentration in eggs in vivo. ATP and other nucleotides remain at levels close to the physiological levels even after incubation for several hours at room temperature without the addition of exogenous ATP-regenerating systems. These extracts are sort of "alive," although the integrity of the cell has been destroyed, and they reproduce the biochemical environment of the cytoplasm accurately.

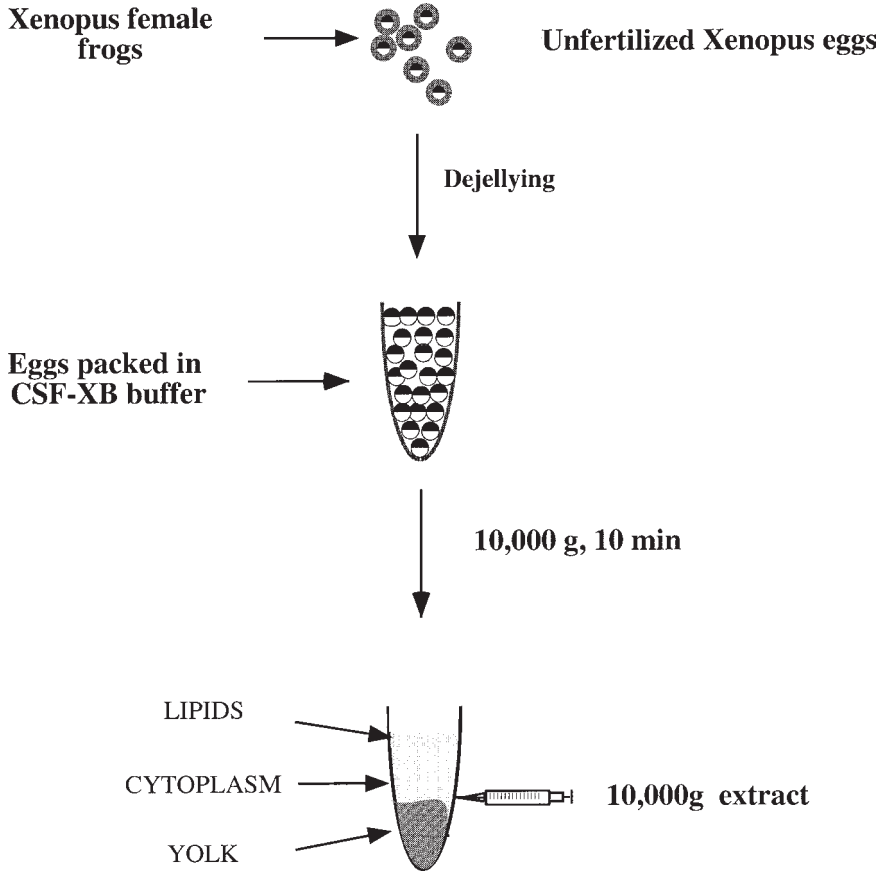

Fig. 1. Schematic representation of the main steps for the preparation of low-speed *Xenopus* egg extracts

The step by step preparation of egg extracts is as follows:

1. Unfertilized eggs are obtained in the following way. At least 4 d before extract preparation, *Xenopus laevis* females are induced to ovulate by one subcutaneous injection with 100 U of PMSG (500 µL per frog) performed with a 1-mL syringe and 27-gage needles. The day before extract preparation (16–18 h before), frogs are injected again with 1000 U of HCG (500 µL per frog). Frogs are placed in individual containers in MMR and placed in a 16°C incubator (*see* **Note 3**).
2. Eggs laid by each frog are collected in separate 400-mL rinsed beakers (*see* **Note 2**). The quality of the eggs is evaluated at this stage by their even pigmentation

and the lack of white eggs, lysed eggs, or stringy eggs. When there are more than 5% of such, the whole batch is discarded. Bad eggs are carefully removed with a pipet. Eggs of equivalent quality are pooled together and rinsed several times with MMR. To do this, pour some MMR on the side of the beaker, gently swirl the eggs around, and let them sediment before pouring out the buffer. Most or all of the debris will be removed during these washes.

3. To remove the jelly coat surrounding the eggs, the MMR is poured out and substituted by dejellying solution. Again, eggs are swirled around and allowed to sediment periodically. The presence of the jelly coat maintains a space between the eggs that can be clearly seen by looking at them from under the beaker. The dejellying solution can be changed two to three times. As soon as the eggs start to touch each other, pour out the dejellying solution and rinse the eggs two to three times with MMR. A prolonged incubation in the dejellying solution will result in egg lysis or activation. (*see* **Note 4**)
4. Eggs are then rinsed sequentially, four times with XB buffer, twice with CSF–XB buffer and once in CSF–XB with protease inhibitors. All damaged and abnormal eggs are removed with a pipet.
5. Eggs are transferred with a cut Pasteur pipet (*see* **Note 5**) into the SW 50.1 tubes containing CSF–XB with protease inhibitors and cytochalasin D. Bring the pipet opening in contact with the surface of the buffer and gently squeeze the eggs out, letting them sediment in the tube. Tubes are placed in the holder tubes to fit them into the rotor.
6. To pack the eggs, the tubes are centrifuged in a clinical centrifuge at 16°C for 60 s at 120 g, immediately followed by 30 s at 480*g*. All of the buffer on top of the eggs is removed (*see* **Note 6**).
7. Eggs are then crushed by centrifuging the tubes at 10,000*g* for 15 min at 16°C. At the end of the centrifugation, place the tubes on ice.
8. Three main layers are visible: a dark pellet containing the heavy yolk fraction, a gray–yellowish intermediate layer corresponding to the undiluted egg cytoplasm, and a bright yellow upper layer containing lipids. The cytoplasmic layer is collected by piercing the tube with an 18-gage needle on the side just above the yolk layer and aspirating slowly, taking care not to take lipids (**Fig. 1**).
9. The collected cytoplasm is transferred from the syringe (without the needle) into a new tube and put on ice. Proteolytic inhibitors, 10 µg/mL cytochalasin D, and energy mix at 1/20th of the extract volume are added and carefully mixed (*see* **Note 7**). After preparation, this extract can be kept on ice for several hours, during which time it remains competent to assemble spindles.

3.2. Spindle Formation in Xenopus Egg Extracts

The method for assembly of bipolar metaphase spindles in vitro provided here is based on the one described by Shamu and Murray ***(16)*** with some slight modifications. The steps of the assay are shown in **Fig. 2**.

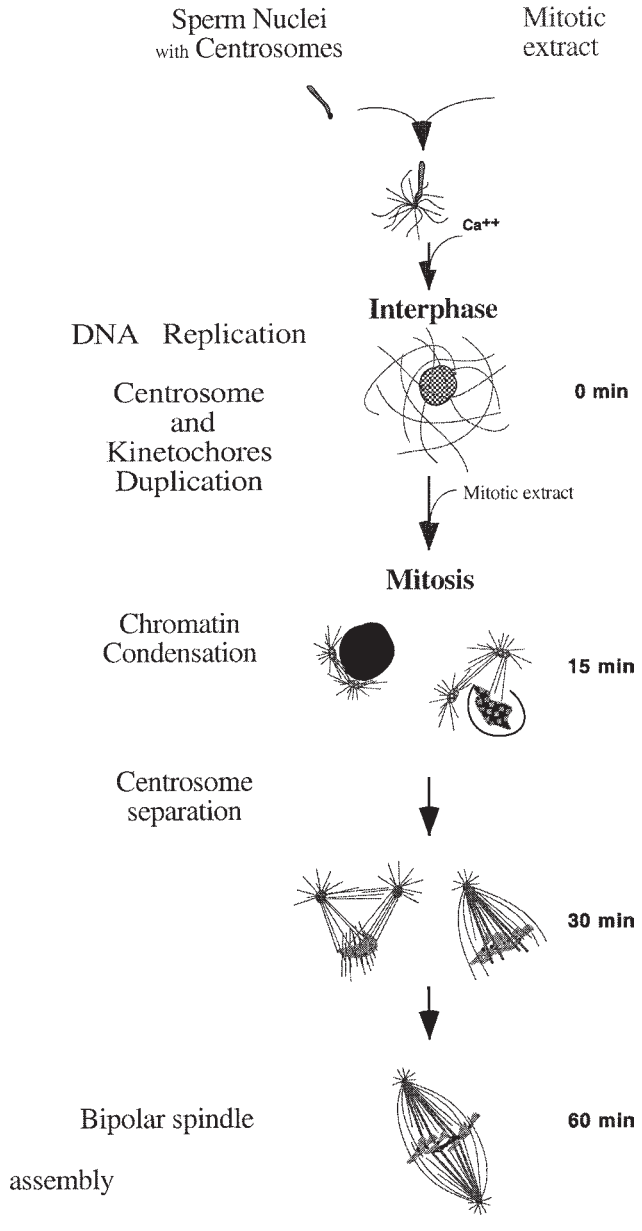

Fig. 2. Schematic representation of the steps of the in vitro spindle assembly assay in *Xenopus* egg extracts. Events taking place at the different steps are indicated on the left. Typical Figs. observed at each time-point in the assembly reaction are schematized. (Reproduced from Boleti et al. [1996] *Cell* **84,** 49–59, ©Cell Press, Cambridge, MA.)

3.2.1. Preparation of Demembranated Sperm Nuclei

Xenopus laevis sperm nuclei are prepared by a slight modification of the method described by Gurdon ***(17)***. A male frog is sacrificed and its testes are dissected into small pieces in HSP buffer. The homogenate is filtered through cheesecloth and the flowthrough is centrifuged at 750*g* for 10 min, to pellet sperm cells. The pellet is washed once with HSPP buffer and resuspended in 1 mL HSPP. Demembranation is performed by addition of 50 µL lysolecithin (10 mg/mL). After 5 min at room temperature, the reaction is stopped by the addition of 10 mL cold HSPP containing 3% bovine serum albumin and chilling (0°C). The demembranated sperm cells ("sperm nuclei") are pelleted by centrifugation (750 g, 10 min) and washed in 3 mL HSPP with 0.3% BSA. Finally, the nuclei pellet is resuspended in 2.5 mL HSPP containing 30% (w/v) glycerol and 0.3% (w/v) BSA. The nuclei are counted by staining them with Hoechst, and the suspension is diluted to about 3×10^6 cells/mL, frozen in liquid nitrogen, and stored at –70°C in aliquots.

3.2.2. In Vitro Spindle Assembly Assay

Before setting up a long experiment, we usually check that the extract is competent to assemble spindles. To this aim, a "half-spindle" reaction is set ***(2)*** and checked after 30–45 min. Take 20 µL of extract (*see* **Note 8**) and add on ice fluorescently labeled tubulin (100–150 µg/mL) and sperm nuclei (final concentration of 200–250/µL). Place the tube in a 20°C water bath and incubate for 30–45 min (*see* **Note 9**). To look at the structures formed, take 1.2 µL from the reaction with a tip (tip for a 20-µL pipet) cut at the end. Spot it onto a slide and overlay with 6 µL of spindle fix. Squash the drop gently under a cover slip (22 × 22 mm). Look under fluorescent illumination (*see* **Fig. 3**). The DNA should be condensed and microtubules should be organized into half-spindles connected to the DNA. Some bipolar spindles can also be formed by the association of two half-spindles ***(2)***. If the DNA is not condensed and there are long microtubules all over, the extract has turned into interphase and the experiment cannot be conducted.

The steps of the in vitro spindle assembly assay procedure are as follows. Spindles are usually assembled in a final reaction volume of 40–50 µL into 1.5-mL Eppendorf tubes.

1. Fluorescently labeled brain tubulin (100–150 µg/mL) is added to 40–50 µL of CSF extract on ice, carefully mixed by pipetting up and down a few times; the mixture is divided into two equivalent aliquots (*see* **Note 10**).
2. Sperm nuclei (at a final concentration of 200–250/µL) are added into one aliquot. The second aliquot is kept on ice for later use.
3. The extract containing nuclei is placed into a 20°C water bath for 10 min.

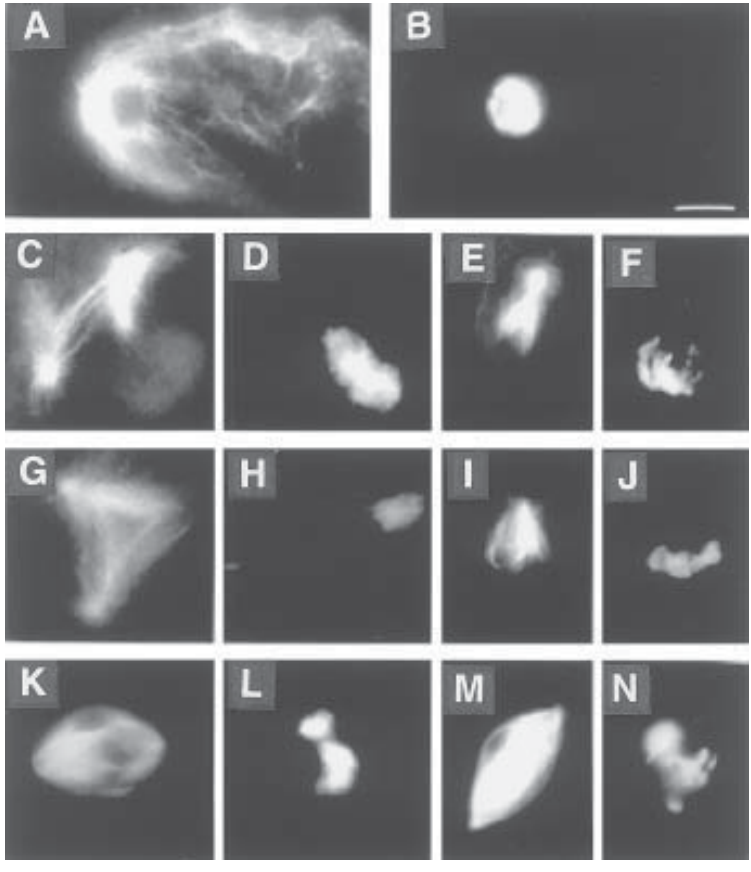

Fig. 3. Mitotic spindle assembly in *Xenopus* egg extracts. Representative structures observed by taking squashes at different time points: At 65 min after calcium addition (–15 min), the extract is in interphase **(A,B)**; after addition of CSF extract, the extract goes back into mitosis and spindle assembly occurs. Figures observed at 15 **(C-F)**, 30 **(G-J)**, and 60 min **(K-N)** after re-entry into mitosis are shown. Two examples are shown for each time-point. Microtubules are shown in panels A, C, E, G, I, K, and M. DNA is shown in panels B, D, F, H, J, L, and N. Scale bar: 20 μ*M*.

4. The extract is then driven into the interphase block by the addition of calcium, releasing the metaphase block (1× calcium solution, final concentration of 0.4 m*M* $CaCl_2$) (*see* **Note 11**).
5. At 65 min after calcium addition, a sample is taken as described above, to check for the formation of interphase nuclei and long interphase microtubules.
6. The reaction is incubated at 20°C for 80 min after calcium addition in total.
7. To drive back the extract into mitosis, an equal volume of CSF extract (the aliquot that was kept on ice and contained tetra methylrhodamine [TMR]-labeled

tubulin) is added and carefully mixed by pipetting up and down a few times with a cut tip (tip for a 20-µL or 200-µL pipet).
8. The reaction is incubated at 20°C. Samples can be taken at several time-points to monitor spindle assembly (**Fig. 3**; *see* **Note 12**). Metaphase spindles will form by 45–60 min of incubation (**Fig. 3**).
9. To keep the samples for a few days (4°C), cover slips are sealed with nail varnish.

3.2.3. Spindle Pelleting onto Coverslips

For data quantification and localization studies, spindles can be pelleted onto coverslips and processed for immunofluorescence microscopy.

1. Prepare one 15-mL Corex tube holding plexiglas adaptors and a round cover slip (11 mm) for each sample to be spun down (**Fig. 4**). Pour 5 mL of cushion solution equilibrated at room temperature into each tube.
2. Place 20 µL of spindle assembly reaction into a 1.5-mL Eppendorf tube and dilute them by adding quickly 1 mL of spindle fix. Close the tube and invert it once or twice. Alternatively, the sample can be diluted with spindle dilution buffer (equilibrated at room temperature) without fixation. Prepare all the samples first and then layer them onto the cushion in the Corex tubes, using a plastic pipet.
3. Tubes are centrifuged at 6000*g* for 15 min at 20°C, selecting a rotor according to the number of tubes (*see* **Note 13**).
4. Aspirate the sample and half of the cushion. Wash once with BRB80 and aspirate out everything. Retrieve the cover slips one by one and place them in a holder.
5. Fix or postfix (for the spindle already fixed in glutaraldehyde) the cover slips by immersing the holder into –20°C methanol for 5 min.
6. Rehydrate the samples in TBS–Tx for 5 min.
7. Glutaraldehyde (when used) is quenched with two consecutive incubations in 0.1% $NaHB_4$ in PBS for 5 min at room temperature.
8. Incubations with primary and secondary antibodies diluted in TBS–TX can be done at this point. DNA is labeled by incubation in TBS–TX containing 1 µg/mL Hoechst for 1 min.
9. Coverslips are mounted with Mowiol or mounting medium and sealed with nail varnish.

3.3. Use of Dominant Negative Mutants to Study the Function of Xklp2 in the In Vitro Spindle Assembly Assay

3.3.1. Selection of Possible Dominant Negative Proteins

Possible dominant negative mutants for a KLP include truncated pieces of the protein containing the targeting information for its localization but not the motor domain. We prepared different recombinant GST–Xklp2 deletion polypeptides and tested their localization on spindles assembled in *Xenopus* egg extracts. The purified recombinant proteins were added to the egg extract at the beginning of the experiment and their localization was analyzed by

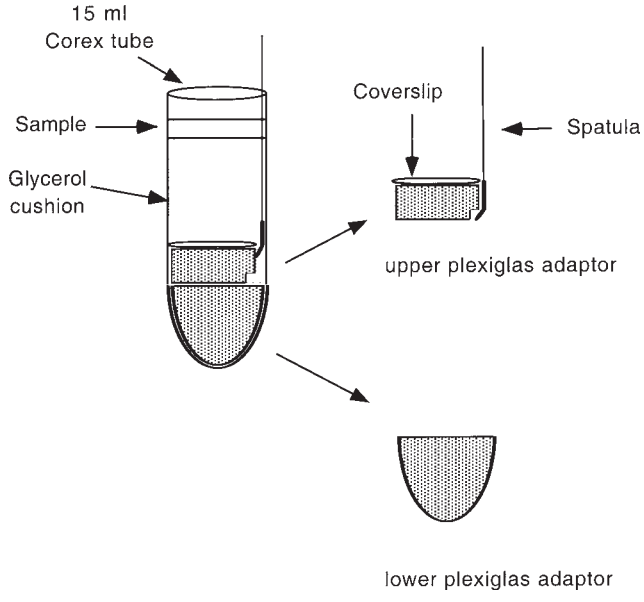

Fig. 4. Drawings showing the setup for spinning down spindle reactions on cover slips. Corex tubes (15 mL) are fitted with a lower Plexiglas adaptor and an upper one with an indentation used for retrieval with a small bent spatula. The upper adaptor holds a round cover slip on which the spindles will be centrifuged.

immunofluorescence on metaphase spindles spun onto cover slips using a polyclonal antibody against the GST protein. We found that Xklp2 was targeted to spindle poles through its C-terminal domain ***(5,12)***. We anticipated that constructs containing the C-terminal tail domain of Xklp2 but not the motor domain would block the function of the endogenous protein by competition, thus acting as dominant negative mutants.

3.3.2. Expression and Purification of Xklp2 Recombinant Proteins

For localization and functional studies, recombinant fragments of Xklp2 were expressed in bacteria as fusion proteins with the glutathione-*S*-transferase (GST) using the pGEX vectors (Stratagene). The following constructs were made: GST–Xklp2-S1: aa 363–720, a truncated stalk, GST–Xklp2-S2: aa 363–1136, the full-length stalk, GST–Xklp2-T: aa 1137–1387, the tail of Xklp2; and GST–Xklp2-ST: aa 363–1387, the Xklp2 full-length stalk plus tail (**Fig. 5**). The Xklp2 subfragments with the appropriate restriction sites for cloning were produced by PCR.

Recombinant plasmids were transformed into TG1 cells for protein expression. Cells were grown at 37°C to A_{600} = 0.6–0.7 and protein expression was

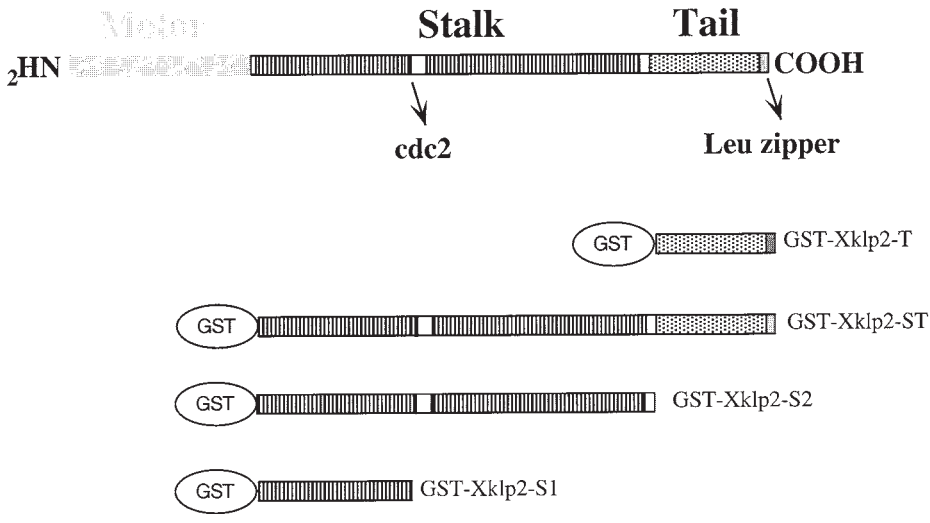

Fig. 5. GST–Xklp2 recombinant constructs used for functional analysis of Xklp2 in the spindle assembly reaction in egg extracts.

induced by addition of IPTG to 0.1–0.3 m*M* and rapid shaking for 5–9 h at room temperature or at 15–20°C overnight.

The GST fusion proteins were purified according to a protocol based on the instructions provided by Pharmacia and on the method described by Smith and Johnson ***(18)***. Pellets of induced cells were resuspended in PBS (1/50th of the original culture volume) containing proteolytic inhibitors (PMSF, 0.1 m*M*; leupeptin, 10 µg/mL; pepstatin, 1 µg/mL and aprotinin, 10 µg/mL), frozen in liquid nitrogen and stored at –70°C. After thawing under running water, lysozyme was added (1 mg/mL) and the cell suspension incubated at 4°C for 0.5–1 h. Cells were broken by sonication (three times for 30 s, interrupted by 30-s intervals; tip sonicator, 60 kHz) and Triton-X 100 was added (1% final concentration). The lysate was centrifuged at 10,000*g* (Sorvall SS34) for 5 min to remove the cell debris. The supernatant was added to preswollen glutathione Sepharose-4B resin (volume of resin 1/10th of the lysate volume) and incubated by end to end mixing at room temperature for 30 min. The resin was sedimented by centrifugation (450 g, 5 min) and the purification step was repeated with fresh resin. The glutathione resin was washed three times with 10 vol of PBS with proteolytic inhibitors and the GST fusion protein was eluted with 1 vol/vol swollen resin of reduced glutathione. The protein concentration of the eluate was measured and the peak fractions were extensively dialyzed against CSF–XB and concentrated to around 2–5 mg/mL. Proteins were frozen in aliquots in liquid nitrogen and kept frozen at –70°C.

3.3.2. Testing the Effect of the Dominant Negative Constructs

To test the effect of the different recombinant proteins on spindle assembly, different amounts (*see* **Note 14**) of the purified recombinant proteins are added to a freshly prepared *Xenopus* egg extract and incubated on ice for 30 min before the addition of fluorescently labeled tubulin and sperm nuclei (*see* **Note 15**). To quantify the relative proportion of added protein, take a small aliquot for Western blot analysis with a specific antibody that recognizes both the endogenous protein and the recombinant protein (**Fig. 6A**). The effect of the recombinant GST–Xklp2 polypeptides on spindle assembly is monitored by fluorescence microscopy. The percentage of abnormal spindles (**Fig. 6B**) gives the estimate of the dominant negative effect. The following control samples are always run in parallel, one with the equivalent volume of CSF–XB added and another with the same amount of GST protein (*see* **Note 16**).

The role of Xklp2 in metaphase can be examined by adding the recombinant fragment (at 1/10th of the extract volume), 60 min after entry into mitosis when bipolar spindles have already assembled. Samples can be observed 20 min later.

4. Notes

1. Check again the pH of all the solutions and adjust if required.
2. Eggs can stick onto the dry glass surface and activate as a consequence.
3. After PMSG injection, the frogs can be used for up to 2 wk. The number of frogs to be injected depends on the quantity and quality of the eggs. In our hands, a standard experiment requires three to five frogs. The time from HCG injection to the beginning of egg laying is variable, on average 12–14 h. Arrange the injection time to harvest the eggs not later than 16–18 h after the time of injection.
4. Handle *Xenopus* eggs very carefully during the dejellying procedure as they become very sensitive when the jelly coat is removed and they can be activated and exit the mitotic state by simple mechanical force. After dejellying, all the eggs will orient with the heavy vegetal pole down.
5. Wet the pipet before pipetting the eggs to again avoid sticking to the dry surface.
6. This step ensures that a minimum amount of buffer remains in the tube and the cytoplasmic fraction obtained after centrifugation will be undiluted having a protein concentration close to that found in the egg.
7. The addition of cytochalasin D inhibits actin polymerization and reduces the contraction of the extract that results in the formation of a clump in the tube.
8. Always cut the end of tips (for 20- or 200-µL pipets) to be used for pipetting extract.
9. An easy way to set up a 20°C water bath is to fill a bucket with water and adjust the temperature by adding some crushed ice if required. The temperature has to be checked from time to time, but it is usually quite stable when the environment is not too hot.
10. When several reactions are to be run in parallel, take the total amount of extract required plus 20% to account for losses during pipetting and add the fluorescently

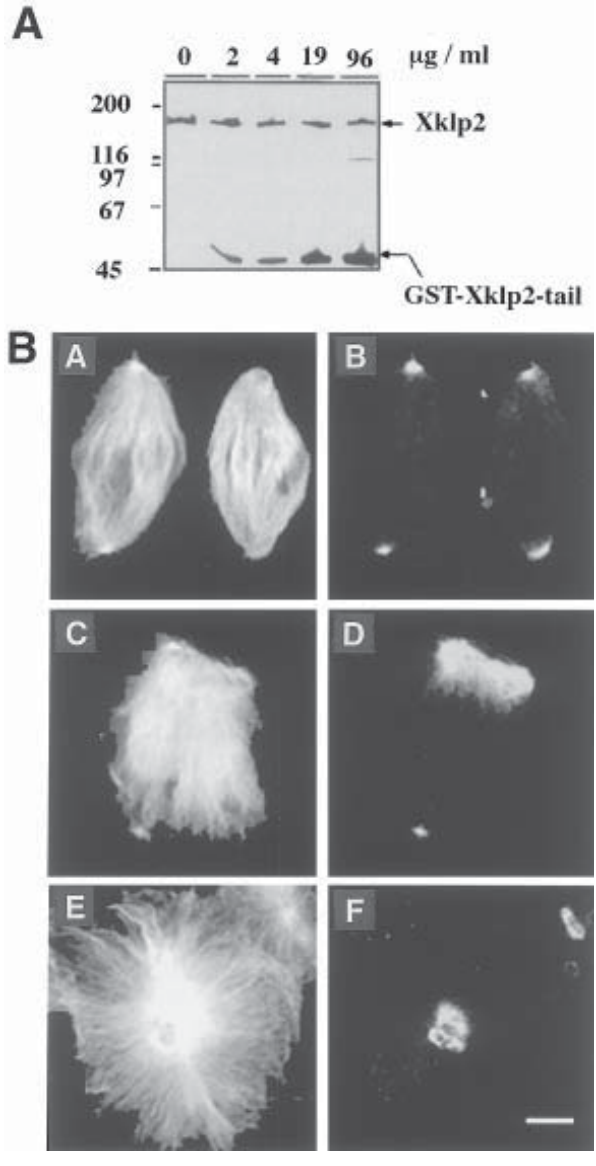

Fig. 6. **(A)** Western blot of egg extracts containing increasing amounts of GST–Xklp2-tail and developed with an anti-Xklp2 antibody. The amount of GST–Xklp2–tail protein added is shown above each lane. The band corresponding to endogenous Xklp2 and GST–Xklp2–tail are shown. Molecular-weight markers are indicated on the left. This type of blot allows a direct estimation of the relative proportion of the added recombinant protein versus the endogenous one. (Reproduced from Boleti et al. [1996] *Cell* **84,** 49–59, ©Cell Press, Cambridge, MA.)

labeled tubulin. Split this volume in two and add nuclei to half of the reaction, then split into the required number of tubes.

11. Calcium addition mimics the natural release of calcium that occurs after fertilization and triggers the destruction of the CSF factor responsible for the metaphase arrest.
12. At early stages of assembly (15–30 min after entry into mitosis), mitotic figures resembling intermediate structures in the assembly pathway are observed (**Fig. 3**). After 15 min, the predominant "prometaphaselike" structures are monopolar spindles in which either MTs are just beginning to make contact with the condensed chromatin or separated centrosome asters are starting to make connection with the chromatin (15 min). These structures correspond to figures where the centrosomes start to separate before or after the nuclear envelope breakdown (**Fig. 4**). Similar structures are observed in cultured cells at the onset of mitosis (prometaphase). After 30 min, the predominant structures are either monopolar spindles in which centrosome-nucleated MTs have made good connection with the condensed chromatin (**Fig. 4**) or paired half-spindles have connected with the same DNA mass (typical prometaphase-like structure) on their way to establishing bipolar spindles. At 60 min, 70–90% of the counted structures are bipolar spindles. The size of the spindles or the "prometaphaselike" structures varies even in the same sample. Sometimes, especially when the assay is prolonged longer than 60 min, spindles appear to fuse laterally or through their poles to form clusters.
13. For an HB4 rotor, spin at 10 K for 12 min. For an HS4, spin at 6 K for 25 min. For an HB6, spin at 5.5 K rpm for 30 min. The rotor is selected according to the numbers of tubes to be spun down.
14. The concentration of recombinant polypeptides necessary to inhibit the function of the protein under study has to be determined by titration. In our studies, the function of Xklp2 was blocked by 50% when the CSF-arrested extracts were preincubated with a concentration of GST–Xklp2–T protein equimolar to the endogenous Xklp2 concentration ***(5)***. Almost complete inhibition was obtained with a 15-fold excess of GST–Xklp2–T. This indicated that the recombinant protein competed efficiently with the endogenous Xklp2 protein for binding to specific targets.
15. One important consideration is to avoid adding to the reaction more than 10% volumewise of reagents in order to maintain a good competence to assemble spindles.

Fig. 6. **(B)** Spindles assembled in egg extracts. (a, b) Spindles assembled in control reactions, spun onto cover slips and stained with an anti-Xklp2 antibody. (c-f) Spindles assembled in an egg extract containing GST–Xklp2–tail. Two main structures are observed: half-spindles (c, d) and rosettes (e, f) that we interpret as the result of a defect in centrosome separation. (a, c, e) microtubules; (b, d, f) anti-GST antibody staining revealing the localization of GST–Xklp2–tail recombinant protein. Scale bar: 10 μ*M*.

16. Equimolar amounts of GST protein should be used in the control reactions. In control samples where spindle assembly was done in the presence of equivalent concentrations of GST, only 2–7% of the mitotic figures observed looked abnormal.

References

1. Felix, M. A., Clarke, P. R., Coleman, J., Verde, F., and Karsenti, E. (1993) Frog Egg Extract as a System to Study Mitosis in: *The Cell Cycle: a practical approach* (Fantes, P., ed.), IRL, Oxford, pp. 253–283.
2. Sawin, K. E. and Mitchison, T. J. (1991) Mitotic spindle assembly by two different pathways in vitro. *J. Cell Biol.* **112**, 925–940.
3. Murray, A. (1991) Cell cycle extracts, in *Xenopus Laevis: Practical Uses in Cell and Molecular Biology*, vol. 36 (Kay, B. K. and Peng, H. B., eds.), Academic, San Diego New York, pp. 581–605.
4. Heald, R., Tournebize, R., Blank, T., Sandaltzopoulos, R., Becker, P., Hyman, A., and Karsenti, E. (1996) Self organization of microtubules into bipolar spindles around artificial chromosomes in Xenopus egg extracts. *Nature* **382**, 420–425.
5. Boleti, H., Karsenti, E., and Vernos, I. (1996) Xklp2, a novel Xenopus centrosomal kinesin-like protein required for centrosome separation during mitosis. *Cell*. **84**, 49–59.
6. Walczak, C., Mitchison, T. J., and Desai, A. B. (1996) XKCM1: A Xenopus kinesin-related protein that regulates microtubule dynamics during mitotic spindle assembly. *Cell* **84**, 37–47.
7. Walczak, C. E., Verma, S., and Mitchison, T. J. (1997) XCTK2: a kinesin-related protein that promotes mitotic spindle assembly in Xenopus laevis egg extracts. *J. Cell Biol*. **136**, 859–870.
8. Wood, K. W., Sakowicz, R., Goldstein, L. S., and Cleveland, D. W. (1997) CENP-E is a plus end-directed kinetochore motor required for metaphase chromosome alignment. *Cell* **91**, 357–366.
9. Sawin, K. E., LeGuellec, K., Philippe, M., and Mitchison, T. J. (1992) Mitotic spindle organization by plus-end-directed microtubule motor. *Nature* **359**, 540–543.
10. Vernos, I., Raats, J., Hirano, T., Heasman, J., Karsenti, E., and Wylie, C. (1995) Xklp1, a chromosomal Xenopus kinesin-like protein essential for spindle organization and chromosome positioning. *Cell* **81**, 117–127.
11. Vernos, I., Heasman, J., and Wylie, C. (1993) Multiple kinesin-like transcripts in Xenopus oocytes. *Dev. Biol.* **157**, 232–239.
12. Wittmann, T., Boleti, H., Antony, C., Karsenti, E., and Vernos, I. (1998) Localization of the kinesin-like protein Xklp2 to spindle poles requires a leucine zipper, a microtubule-associated protein, and dynein. *J. Cell Biol*. **143**, 673–685.
13. Hyman, A., Drechsel, D., Kellogg, D., Salser, S., Sawin, K., Steffen, P., et al. (1991) Preparation of modified tubulins. *Methods Enzymol*. **196**, 478–485.
14. Kirschner, M. W., Newport, J., and Gerhart, J. C. (1985) The timing of early developmental events in *Xenopus*. *Trends Genet.* **1**, 41–47.

15. Lohka, M. and Maller, J. (1985) Induction of nuclear envelope breakdown chromosome condensation, and spindle formation in cell-free extracts. *J. Cell Biol.* **101**, 518–523.
16. Shamu, C. E. and Murray, A. W. (1992) Sister chromatid separation in frog egg extracts requires DNA topoisomerase II activity during anaphase. *J. Cell Biol.* **117**, 921–934.
17. Gurdon, J. B. (1976) Injected nuclei in frog oocytes: fate, enlargement, and chromatin dispersal. *J. Embryol. Exp. Morphol.* **36**, 523–540.
18. Smith, D. B. and Johnson, K. S. (1988). Single step purification of polypeptides expressed in *Escherichia coli* as fusions with glutathione S-transferase. *Gene* **67**, 31–40.

16

A Dominant Negative Approach for Functional Studies of the Kinesin II Complex

Vladimir I. Gelfand, Nathalie Le Bot, M. Carolina Tuma, and Isabelle Vernos*

1. Introduction

There are a few ways to generate a dominant negative mutant. Specifically for the study of functions of motor proteins, two approaches have been successfully used. The first approach consists of the deletion of the motor domain. In this case the mutant protein is not able to hydrolyze ATP or/and bind to the cytoskeleton, and consequently, unable to promote movement. This is often referred to as a "headless" mutant, as the motor domain is commonly referred as the "head" of a motor protein. This strategy has been used previously for the study of motor protein functions for both microtubule and actin-based motors ***(1–3)***. The second type of dominant negative mutant is a rigor mutant, generated by a point mutation in the ATP-binding site; as a result, the motor binds to the cytoskeletal filament (actin or microtubules) but cannot hydrolyze ATP; this ATP-bound form of the motor is irreversibly locked to its cytoskeleton partner, a state defined as a rigor complex. Rigor mutants have been first identified, sequenced, and characterized for the yeast kinesin-like motor Kar3p ***(4)*** and *Drosophila melanogaster* nod ***(5)***. In both cases, the mutant protein was shown to bind irreversibly to microtubules. These observations suggested the use of rigor mutants as a tool for investigating the function of kinesin-like motors, and this approach has been successfully used for conventional kinesin ***(6)***.

In order to generate a dominant negative mutant of kinesin II, we chose to use the "headless" approach for two reasons. First, it is known that kinesin II forms a heterotrimeric complex containing two different motor subunits ***(7)***. Therefore, deletion of the motor head on one of the subunits would result in the for-

*Note: All authors have contributed equally to this chapter

From: *Methods in Molecular Biology*, Vol. 164: *Kinesin Protocols*
Edited by: I. Vernos

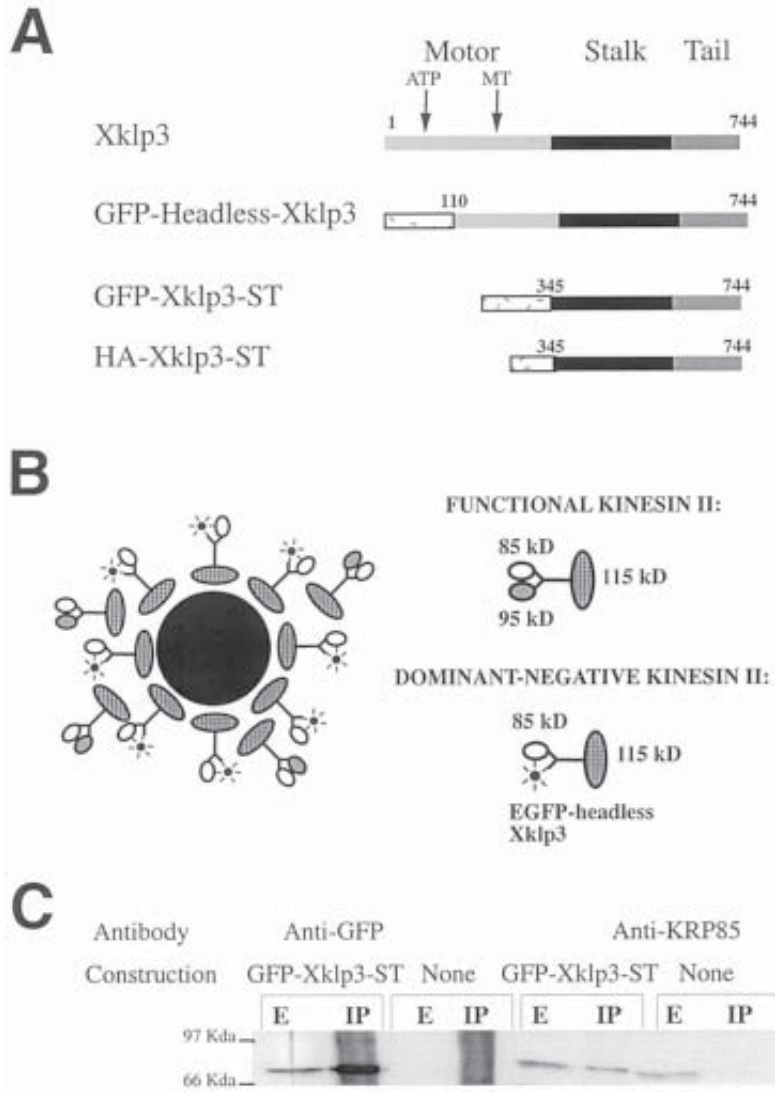

Fig. 1. **(A)** Schematic representation of the mutants prepared and used for these studies. The light gray box corresponds to the motor domain of Xklp3, the black to the stalk, and the dark gray to the tail. The region corresponding to the ATP-binding site or to the microtubule-binding sites are indicated with an arrow. The tag used, either GFP or HA, is represented by a white box with dots. **(B)** Illustration depicting a possible model for the dominant negative mechanism of action. The overexpressed headless form of Xklp3 forms complexes with the endogenous kinesin II subunits. Single-headed complexes compete with endogenous ones for binding sites on the organelles (melanosomes or Golgi vesicles). Alternatively, the headless form could sequester in

mation of single-headed complexes. As the functional significance of dimerization of motor subunits may be to allow the complex to move processively along microtubules in a "hand-over-hand" fashion, as proposed for conventional kinesin ***(8–10)*** and for kinesin II ***(11)***, the single-headed complex would probably be less processive. Still, this complex could bind to the organelles and prevent the binding of the functional endogenous kinesin II. The second reason to choose the headless approach as opposed to the rigor-type mutant approach is that we do not know which mutation in the Xenopus kinesin-like protein 3 (Xklp3) ATP-binding domain would generate a rigor mutant. Therefore, such an approach could involve multiple trials before finding an effective point mutation, being thus more time-consuming.

To facilitate the identification of cells expressing the mutant protein, we tagged it with a label, either the enhanced green fluorescent protein (EGFP) or the hemaglutinin epitope (HA). Two different types of constructs have been generated in a similar way (**Fig. 1**). To obtain a form called "GFP–headless–Xklp3," the N-terminal 110 amino acids of the protein were replaced by the EGFP. We have also prepared a slightly shorter version of the protein by replacing the whole motor domain (345 amino acids) either with the EGFP (GFP–Xklp3–ST), or the HA (HA–Xklp3–ST) tag. All constructs were obtained using polymerase chain reaction (PCR)-directed mutagenesis, and we present here in detail the method to prepare "GFP–headless–Xklp3." We also describe the methods followed to study the function of kinesin II using this dominant negative approach in two types of *Xenopus* cultured cells: melanophores and A6 cells. This includes the methods of transfection and analysis of the effect of the mutant protein on the movement of melanosomes, by video microscopy, and on the transport of membranes along the secretory pathway, using immunofluorescence techniques. In addition, we analyze the possible mechanism of action of the dominant negative protein by immunoprecipitation.

2. Materials

2.1. PCR-Directed Mutagenesis and Cloning into Expression Vector

1. 40 ng linearized DNA template (i.e., PBluescript with Xklp3 cDNA).

---

the cytoplasm the other partners and prevent the formation of a complex able to bind to the organelles. **(C)** Testing the mechanism of action of the dominant negative protein. The cytosol prepared from A6 cells transfected with the mutant GFP–Xklp3–ST was used for immunoprecipitation with the anti–GFP antibody (lanes GFP–Xklp3–ST). The extract (E) and the immunoprecipitate (IP, loaded five times more than E) were probed with the anti–GFP antibody and with the anti-KRP85 antibody. As a control, the experiment is performed as well with nontransfected cells (lanes: none). (Reproduced from *The Journal of Cell Biology*, 1998, vol. 143, p. 1568, **Fig. 8A**, by copyright permission of the Rockefeller University Press.)

Table 1
Oligonucleotides Used to Generate the Mutant Proteins

Mutant construct	Forward primer	Reverse primer	Vector
GFP–Headless Xklp3	GCGCG**GGTACC-**AAGAGAGGGG TAATACC	CGCGC**GGATCC** TTATTTGGGTACGA GGCTGTGACTG	pEGFP–C1 in *Kpn*I/*Bam*HI sites
GFP–Xklp3–ST	GGC**CTCGAG**AAT-GAAGACCCCAAGG	GGT**GGATCC**AG AGGGCTGGGA	pEGFP–C3 in *Xho*I/*Bam*HI sites
HA–Xklp3–ST	GGC**CTCGAG**AAT-GAAGACCCCAAGG	GGT**GGATCC**AG AGGGCTGGGA	pH A–C3 in *Xho*I/*Bam*HI sites

Note: The bases corresponding to the restriction sites used for the cloning are in bold.

2. Primers at 50 μ*M* in water. We designed the primers so that unique restriction sites would be added at the ends of the amplified fragments, for easy insertion into an eukaryotic expression vector (pEGFP–C1, or pEGFP-C3 [Clontech, Palo Alto, CA], or pH A-C3). The sequences of the oligos with their restriction sites and the plasmids used are presented in **Table 1**.
3. Deoxynucleotides (dATP, dCTP, dTTP, and dGTP) mixed in stock solution at 10 m*M* each in water.
4. PCR buffer containing Mg^{2+} (Gibco-BRL Life Technologies, Gaithersburg, MD).
5. *Taq* polymerase (Gibco-BRL Life Technologies, Gaithersburg, MD).

2.2. Testing the Mechanism of Action of the Dominant Negative Protein

2.2.1. Transfection of Xenopus A6 Cells

1. Superfect reagent from Qiagen (Santa Clara, CA), kept at 4°C.
2. Plasmid DNA carrying the mutant form of Xklp3 (pEGFP–Xklp3–ST or pH A–Xklp3–ST) of Qiagen Maxiprep quality, around 1 mg/mL, kept sterile and stored at –20°C.
3. Complete medium: Leibovitz–15 (Sigma Chemical Co., St. Louis, MO) completed with 15% fetal calf serum (FCS) and diluted to 70% with water.
4. FCS-free medium for *Xenopus* cells: dilute L-15 medium to 70% with water.
5. Complete medium: L-15 supplemented with 15% FCS and diluted to 70% with water.

2.2.2. Immunoprecipitation of the Transfected Protein

1. Protein A–Sepharose beads from Pharmacia (Uppsala, Sweden); 3 g of beads are swollen in 10 mL of phosphate-buffered saline (PBS) and kept at 4°C, with 20 m*M* sodium azide.
2. Rabbit polyclonal anti–GFP antibody, affinity purified.
3. 2% bovine serum albumin (BSA) solution in PBS, filtered and kept at 4°C.

4. Cell lysis buffer: 200 m*M* NaCl, 25 m*M* Tris-Cl (pH 7.6), 1% Triton X-100. Make it fresh from stock solutions of 5 *M* NaCl, 1.5 m*M* Tris-HCl (pH 7.6), 10% Triton X-100, and add dithiothreitol (DTT) to 1 m*M* and protease inhibitors (leupeptin, pepstatin, aprotinin; final concentration: 10 µg/mL each).
5. Washing buffer: lysis buffer with 0.1% Triton X-100.
6. 1X sodium dodecyl sulfate-polyacrylamide gel electrophoresis (SDS-PAGE) reducing sample buffer.

2.3 Analyzing the Effects of the Mutant Protein in the Movement of Membrane-bound Cargoes

2.3.1. Melanophores

2.3.1.1. Transfection

1. PBS at 70% strength, pH 7.4, ice cold.
2. PBS at 70% strength, pH 7.0, ice cold.
3. L-15 medium at 70% strength with 5% fetal calf serum.
4. Poly-lysine-coated cover slips (22 × 22 mm). Glass cover slips are washed in chromic acid for at least 1 h, extensively rinsed with distilled water, incubated in 1 mg/mL poly-lysine in 0.1 *M* borate buffer (pH 8.5), for 1 h at room temperature, then extensively rinsed in distilled water and allowed to air-dry.
5. 35-mm tissue culture chambers: The bottom surface of tissue culture plates is perforated to make a 1.5-cm-diameter hole, and a 22 × 22-mm poly-lysine-coated cover slip is attached to that hole with the Sylgard 184 silicone elastomer kit (Dow Corning, Midland, MI).
6. Electroporation cuvets, 2 mm wide (Invitrogen, Carlsbad, CA).
7. Electroporator (Gene Pulser II, Bio-Rad Laboratories, Hercules, CA).

2.3.1.2. Microinjection

1. Microinjection buffer: 90 m*M* KCl and 10 m*M* NaH_2PO_4, pH adjusted to 7.2 with KOH.
2. Plasmid DNA purified by centrifugation in CsCl density gradient (GFP–headless–Xklp3 or pEGFP–C1 for controls or coinjection).

2.3.1.3. Fluorescence Microscopy of Fixed *Xenopus* Melanophores

1. Fixation in formaldehyde at 4%, diluted in PBS at 70% strength (pH 7.4).
2. ProLong mounting medium (Molecular Probes, Eugene, OR).

2.3.1.4. Assay of Pigment Movement in *Xenopus* Melanophores

1. Melatonin (Sigma, St. Louis, MO) stock solution at 10 µ*M* in ethanol. Prepare fresh, protect from light, use at a final concentration of 10 n*M*.
2. α-Melanocyte stimulating hormone (MSH) (Sigma, St. Louis, MO, stock solution at 100 m*M* in water, store at –20°C), to use at a final concentration of 100 n*M*.
3. Serum-free L-15 medium at 70% strength.

2.3.2. Xenopus A6 Cells

1. All reagents needed for transfection as detailed in **Subheading 2.2.1**.
2. 11-mm cover slips washed with ethanol.
3. Fixation: 70% PBS, cold methanol, kept at –20°C.
4. Antibodies are diluted in the following buffer: 2% BSA solution in TBS–Triton X-100, 0.1%, filtered and kept at 4°C.
5. First antibodies: rabbit polyclonal anti-HA (gift from T. Nilsson), mouse monoclonal antitubulin (Amersham, Buckinghamshire, England), used at 1:200, rabbit polyclonal anti-γ-tubulin (gift from T. Ashford, EMBL) used at 1:100.
6. Second antibodies: Cy3 coupled donkey anti-rabbit, Cy3 coupled donkey anti-mouse, Cy5 coupled anti-mouse, AMCA coupled donkey anti-rabbit (Dianova, Hamburg, Germany).
7. Rhodamine-coupled *Helix pomatia* lectin (Sigma).
8. Mowiol 4-88 purchased from Hoechst (Frankfurt, Germany) and prepared as follows: 2.4 g of Mowiol added to 6 g of glycerol, and stirred. After addition of 6 mL of water, the mix is left for several hours at room temperature. Add 12 mL of 0.2 *M* Tris-HCl (pH 8.5), and heat at 50°C for 10 min. Clarify by centrifugation at 5000*g* for 10 min, add 2.5% DABCO, and aliquot for storage at –20°C.

3. Methods

3.1. PCR-Directed Mutagenesis and Cloning into Expression Vector

1. PCR reactions were set in volumes of 100 µL as follows: 10 µL 10X PCR buffer, 5 µL dNTP stock solution (at 10 m*M*), 1 µL of each primer (stock solutions at 50 µ*M*), 40 ng linearized template DNA, remainder of volume completed with sterile double distilled water. Tubes containing reaction mixtures are put into thermal cycler, heated up to 94°C for 5 min, 1 µL *Taq* is added to each tube, then subjected to 30 cycles of 94°C for 1 min, 50°C for 1 min, 72°C for 10 min, followed by 72°C for 10 min, and kept at 4°C.
2. The PCR-amplified fragment was digested with the appropriate restriction enzymes (i.e., *Kpn*I and *Bam*HI) run on a 1% agarose gel and the band containing the fragment was cut (standard protocols as described in **ref. *12***, and purified with the use of a QIAquick gel extraction kit (Qiagen, Valencia, CA).
3. To insert the PCR product into an expression vector, the purified PCR product was ligated to pEGFP–C1 plasmid (Clontech Laboratories, Palo Alto, CA) that had been previously cut with *Kpn*I and *Bam*HI and purified by electrophoresis on a 1% agarose gel as described in **step 2** for the insert. The resulting headless construct (GFP–headless–Xklp3) encodes a fusion protein between EGFP and the Xklp3 stalk.

3.2. Testing the Mechanism of Action of the Dominant Negative Protein

To identify the interacting partners of the mutant protein GFP–Xklp3–ST, we transfected a large number of A6 cells and let the protein to be expressed for 24 h, before preparing the cell extract. The complex was immunoprecipitated

from the extract with an antibody directed against the GFP tag (*see* **Note 1**), and the presence in the immunoprecipitate (IP) of other subunits of the *Xenopus* kinesin II were tested by Western blot.

1. Day 1: *Xenopus* A6 cells are plated in a Petri dish of 15 cm diameter, using a cell dilution such that they will reach 50–70% confluence on the next day (*see* **Note 2**).
2. Day 2: Fifty micrograms of plasmid are mixed together with 600 µL of FCS-free medium. One hundred microliters of Superfect reagent are added and the transfection mix vortexed briefly before incubation at room temperature for 10 min. Six milliliters of conditioned complete medium is added and the DNA–Superfect complex is incubated on the cells at 23°C, for 2.5 h. The cells are washed twice with 70% PBS and once with complete medium and returned to the incubator for 16–20 h (*see* **Note 3**).
4. Day 3: Preparation of the protein A-Sepharose beads coupled to the anti–GFP antibody. Two hundred microliters of slurry of protein A beads are washed a couple of times with 2% BSA in PBS by spinning them gently at 700*g* for 3 min. They are resuspended in 1 mL of 2% BSA in PBS and incubated at 4°C on a rotating wheel for 30 min. Fifteen micrograms of anti–GFP antibody are added and the beads are incubated on the wheel at 4°C for 1–2 h. The beads are finally washed twice with PBS and once with lysis buffer.
5. Lysis of the transfected cells: The cells are washed once with 70% PBS and incubated on ice for 5 min with 1 mL of lysis buffer. The cells are then scraped and left in a tube on ice for an additional 5 min. The extract is centrifuged at 4°C for 10 min, and the supernatant is saved.
6. Immunoprecipitation of the transfected protein: An aliquot of the extract is kept for Western blot analysis. The supernatant is incubated with the protein A beads coupled with the anti–GFP antibody, for 1 h on the rotating wheel at 4°C. The beads are washed twice with the washing buffer and resuspended in 100 µL of SDS-PAGE sample buffer. The IP is analyzed by Western blot, using the anti–GFP antibody to verify the presence of the mutant form of Xklp3, an antibody directed against Xklp3 or an antibody directed against an endogenous interacting partner, such as the sea urchin KRP85 homolog (**Fig. 1C**).

3.3. Analyzing the Effects of the Mutant Protein in the Movement of Membrane-Bound Cargoes

3.3.1. Melanophores

Immortalized *Xenopus* melanophores were cultured as previously described ***(13,14)***. Melanophores were transfected by electroporation ***(13)*** or by nuclear microinjection ***(14)*** with the GFP–headless–Xklp3 construct or the pEGFP–C1 vector, as a control.

3.3.1.1. Transfection/Microinjection of Melanophores

1. Day 1: Introduction of DNA into melanophores (*see* **Note 4**). For electroporation, cells are detached with trypsin/EDTA, rinsed once with serum-containing L-15

medium to quench trypsin, then once in 70% PBS pH 7.4, and once in 70% PBS pH 7.0. Cells were resuspended in 70% PBS pH 7.0 and 200 µL of suspension containing about 10^6 cells was mixed with 10 µg of DNA. After 20 min incubation on ice, the cell suspension was transferred into a cuvet and electroporated (450 V, 200 Ω, 250 µF). This suspension was immediately diluted to 10 mL with full-growth medium and plated onto polylysine-coated cover slips. For microinjection, cells were plated onto poly-L-lysine-coated cover slips that were sealed to holes at the bottom of 35-mm tissue culture plates. Individual cells were microinjected with a solution of 0.2 mg/mL of DNA in microinjection buffer. DNA solution used for microinjection was clarified by centrifugation at 265,000*g* at 4°C immediately prior to injection.

2. Day 2: Replacement of FCS-containing medium with serum-free medium.
3. Day 3: After 48 h of expression of the exogenous protein, cells are ready to be tested for pigment movement, by either fixed-time-point assay or real-time live observations (*see* **Note 5**).

3.3.1.2. Fixed Time-Point Assay

Cells are treated with melatonin (10 n*M*) or MSH (100 n*M*) for 60 min, then rinsed in 70% PBS, fixed in 4% formaldehyde in 70% PBS for 10 min, rinsed in 70% PBS three times, 10 min each, then mounted in ProLong mounting medium (Molecular Probes, Eugene, OR).

Transfected cells are identified by fluorescence microscopy and pigment distribution determined by phase-contrast microscopy, using a 10 × 0.3 N. A. lens in an upright fluorescent microscope (Microphot-SA, Nikon, Inc., Melville, NY). We choose to use small numerical aperture lens to register only cells expressing high levels of exogenous proteins, thus excluding cells with low levels of expression that could be confused with cells having only background fluorescence. Pigment distribution in the transfected cells is scored into three categories: aggregated, partially dispersed, and dispersed. Cells are considered to have aggregated pigment if the pigment granules are packed into a tight spherical mass at the cell center. If melanosomes are evenly distributed in the cytoplasm, filling all processes, the pigment is considered dispersed. All other cells are scored as having partially dispersed pigment (**Fig. 2**).

3.3.1.3. Video Microscopy of Living Cells

For real-time analysis of pigment movement, injected cells are identified by epifluorescence microscopy and pigment movement is observed by bright-field microscopy on a Nikon Diaphot 300 inverted microscope equipped with a ×40 1.0 N.A. oil-immersion lens. As *Xenopus* melanophores are known to react to visible light of wavelength less than 650 nm by dispersing pigment ***(15)***, the light source is equipped with a red filter with a cutoff of 695 nm (Chroma Technology, Brattleboro, VT) to minimize the effect of light on pigment move-

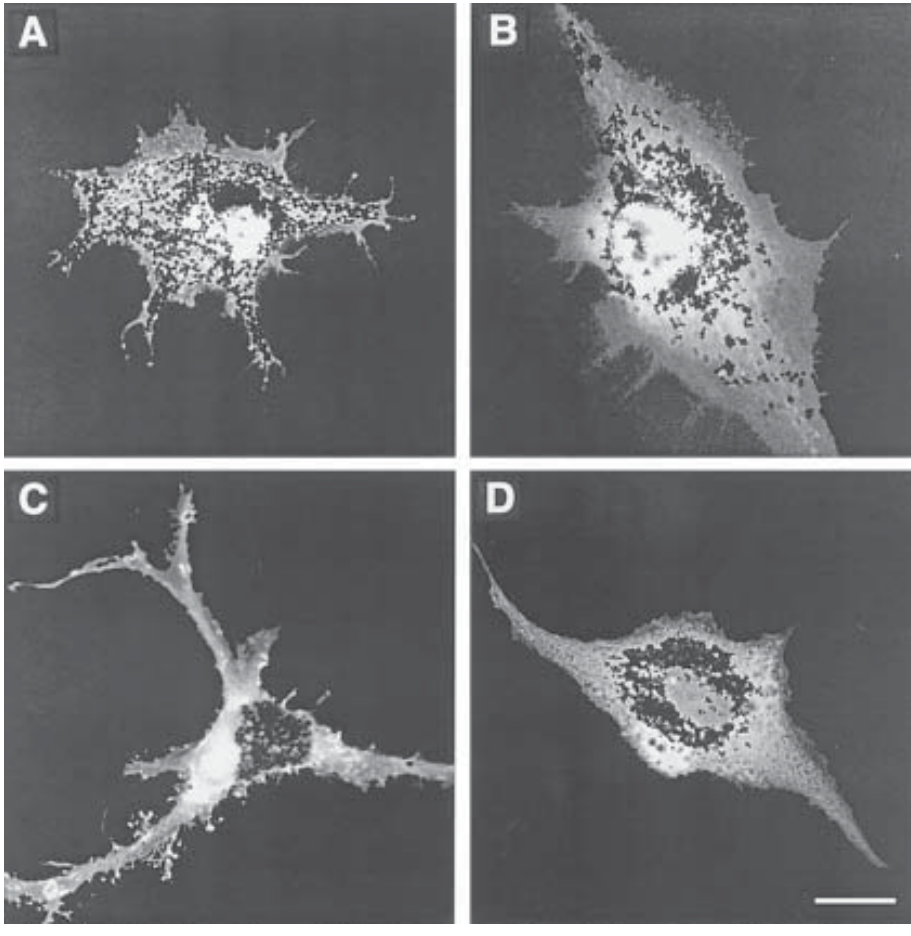

Fig. 2. Overexpression of headless Xklp3 inhibits pigment dispersion but not aggregation. Nuclei of melanophores were injected with plasmids pEGFP–C1 **(A,C)** or pEGFP–headless Xklp3 **(B,D)**. Cells were allowed to recover and express exogenous protein for 48 h, then treated either with melatonin followed by 1 h in MSH to induce pigment dispersion **(A,B)** or with melatonin for 1 h to induce pigment aggregation **(C,D)**. A cell expressing EGFP **(A)** dispersed its pigment normally, whereas a cell expressing the EGFP–headless Xklp3 fusion protein **(B)** dispersed melanosomes only partially. Bright-field and fluorescence images of cells were overlaid to show pigment distribution in cells expressing EGFP-tagged proteins (bar: 20 μm).

ment. Images are captured with a Newvicon camera (C2400-07) and processed for background subtraction and contrast enhancement using an Argus–10 video processor (Hamamatsu Photonics, Hamamatsu City, Japan).

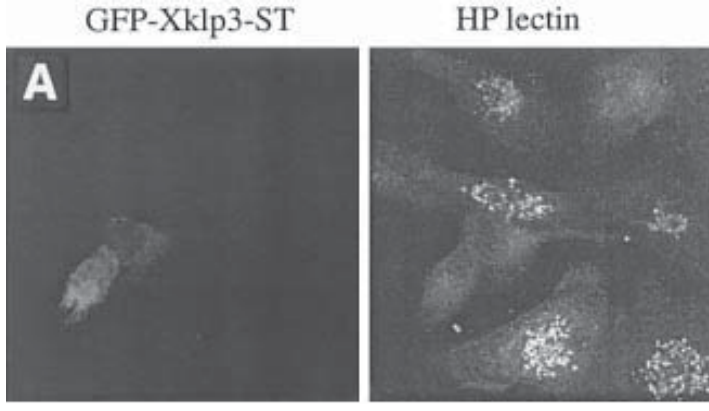

Fig. 3. Effect of Xklp3-ST overexpression in *Xenopus* A6 cells. **(A)** A6 cells transfected with GFP–Xklp3–ST are stained with the lectin helix pomatia coupled to rhodamine. This lectin normally binds to *N*-acetyl galactosamine residues on cargo proteins in the Golgi apparatus. It does not recognize anything in the transfected cells (bar: 10 μm).

For analysis of aggregation, cells are initially dispersed with MSH, and for the analysis of dispersion, they are initially aggregated with melatonin. Then, cells expressing GFP-tagged proteins are identified using epifluorescence, the medium is changed to medium with melatonin for aggregation or with MSH for dispersion, and pigment migration is recorded using a time-lapse S-VHS recorder (Panasonic) at a 12-fold compression. Thirty frames (one frame every 2 min) were digitized for each cell and then analyzed using the NIH Image software (NIH, Bethesda, MD).

For a quantitative description of pigment distribution, we used the ratio of the area occupied by the pigment to the area occupied by the cell. The pigment mass and the cell outline are manually traced and their areas are calculated using NIH Image. With pigment dispersion, the pigment area increases, thus the ratio of pigment area to the cell area approaches 1. The resulting ratios are plotted versus time, and from these curves, the time-points corresponding to 50% dispersion or 50% aggregation are calculated.

3.3.2. Xenopus A6 cells: Effect of the Mutant on the Movement of Membranes Between the Golgi and the ER

In *Xenopus* fibroblast cells, like A6 and XL177, the Xklp3 unit of the heterotrimeric kinesin is associated with tubulo-vesicular structures, around the Golgi apparatus (more precisely between the endoplasmic reticulum and the Golgi), as it has been shown by immunofluorescence, electron microscopy

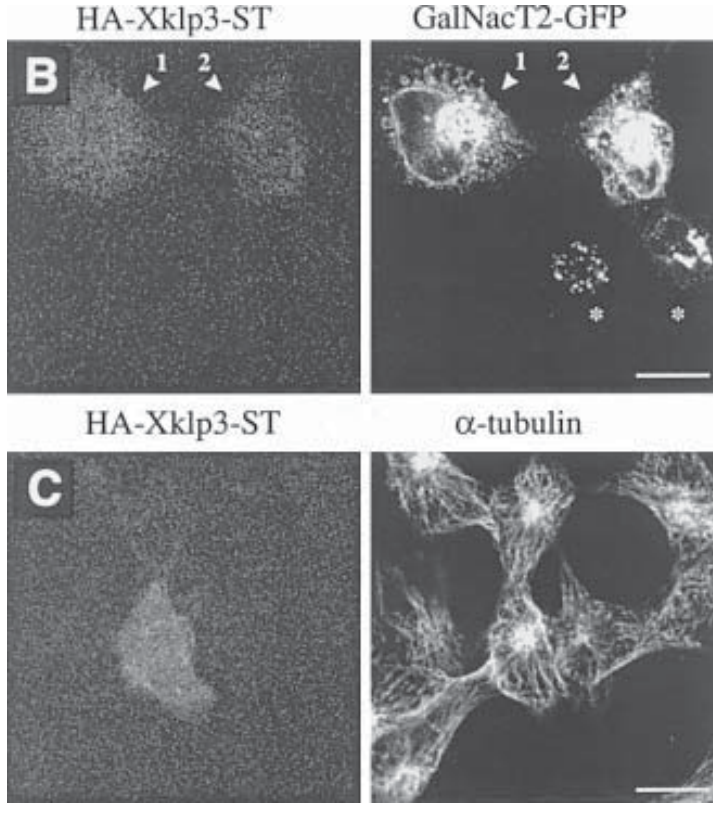

Fig. 3. **(B)** A6 cells cotransfected with HA–Xklp3–ST and the Golgi marker GalNacT2GFP. In cells expressing GalNacT2–GFP alone (asterisks) the marker localizes to the Golgi apparatus. In cells expressing both the marker and the mutant form of Xklp3, the newly synthesized GalNacT2–GFP does not reach the Golgi apparatus properly and is found instead in the ER and large aggregates in the cytoplasm (bar: 10 μm) (Reproduced from *The Journal of Cell Biology*, 1998, vol. 143, p. 1570, **Fig. 9C**, by copyright permission of the Rockefeller University Press). (**C**) The tubulin staining of cells transfected with Xklp3-ST shows that microtubule organization is not disturbed by expression of the mutant protein (bar: 10 μm).

and biochemical fractionation studies ***(16)***. The mutant proteins GFP–Xklp3–ST and HA–Xklp3–ST have been expressed in A6 cells to study the role of the heterotrimeric kinesin between the ER and the Golgi.

3.3.2.1. Transfection of A6 Cells

A6 cells are plated on 15-mm cover slips, using a dilution such that they will be at 60% confluence on the next day. On the day of transfection, the cover slips

are placed in 24-well plates, and transfected with the Superfect reagent as described in **Subheading 3.2.**, using the following quantities of the different reagents: 5 µg of DNA, 5 µL of Superfect, 60 µL of serum-free medium. After formation of the complex, 350 µL of conditioned complete medium is added. After incubation on the cells for 2.5 h, the mix is washed away as described in **Subheading 3.2**. Cells are incubated for 15–20 h for expression of the constructs.

3.3.2.2. Analysis

The cover slips are washed once with 70% PBS and fixed with methanol at –20°C for 10 min. They are then processed for immunofluorescence analysis as described by Boleti et al. ***(17)***. Briefly, cells are incubated for 15 min with the first antibodies diluted in 2% BSA and TBS–Triton X-100 (0.1%); the cover slips are washed for 5 min, two times, with PBS, and then incubated 15 min with the second antibodies, diluted as earlier. They are finally washed twice with PBS and mounted in 3 µL of Mowiol (*see* **Notes 6** and **7**).

The distribution of different elements of the secretory pathway can be observed in the transfected cells (**Fig. 3**).

4. Notes

1. The rabbit polyclonal anti–GFP antibody was raised by injecting the animal with a His-tagged bacterially produced GFP, and the antibodies were purified from the sera on a column coupled with a GST–GFP following the standard ***(18)***. The fractions eluted from the column were first dialyzed against PBS, before being kept at –20°C with 50% glycerol.
2. It is important to plate the A6 cells at 60% confluence, prior to transfection, as they do not like to be sparse. The transfection efficiency is much higher if the complex DNA–Superfect is prepared with conditioned complete medium.
3. When conducting the immunoprecipitation experiment, the efficiency of transfection should be around 15–20%, in order to see the transfected protein. Should this efficiency be lower, it is worth transfecting two or three 15-cm-diameter Petri dishes.
4. Electroporation of melanophores was used when a large number of cells was to be scored; microinjection was used for single-cell analysis. Electroporation usually results in significant cell death and the cultures of transfected cells usually contain a large number of melanosomes released from lysed cells. Microinjection of DNA into the nucleus results in better preservation of cell morphology and, therefore, was the method of choice for live imaging.
5. When deciding on how long after transfection we should perform the analysis of pigment in melanophores expressing mutant proteins, we did a time-course of the expression. Even though at 24 h some cells are expressing the GFP-tagged proteins, the number of expressing cells is very low. For experiments in which a large number of cells will be scored, it is better to wait for 48 h after expression.

6. If one needs to stain for DNA when making transfection using the A6 cells and the Superfect reagent, one should be aware that much of the Superfect–DNA complexes will be stuck on the cover slips, even after the three washes advised here and will be revealed with the DNA dye.
7. It can be difficult to find A6 transfected cells in mitosis, and one needs to be patient to find them. One might consider using the microinjection method in the need of scoring phenotypes in mitotic A6 cells.

References

1. Burns, C. G., Larochelle, D. A., Erickson, H., Reedy, M., and De Lozanne, A. (1995) Single-headed myosin II acts as a dominant negative mutation in *Dictyostelium*. *Proc. Natl. Acad. Sci. USA* **92**, 8244–8248.
2. Bi, G. Q., Morris, R. L., Liao, G., Alderton, J. M., Scholey, J. M., and Steinhardt, R. A. (1997) Kinesin- and myosin-driven steps of vesicle recruitment for Ca^{2+}-regulated exocytosis. *J. Cell Biol.* **138**, 999–1008.
3. Arhets, P., Olivo, J.-C., Gounon, P., Sansonetti, P., and Guillen, N. (1998) Virulence and functions of myosin II are inhibited by overexpression of light meromyosin in *Entamoeba histolytica*. *Mol. Biol. Cell*. **9**, 1537–1547.
4. Meluh, P. B. and Rose, M. D. (1990) Kar3, a kinesin-related gene required for yeast nuclear fusion. *Cell* **60**, 1029–1041.
5. Rasooly, R. S., New, C. M., Zhang, P., Hawley, R. S., and Baker, B. S. (1991) The lethal (1) TW-6cs mutation of *Drosophila melanogaster* is a dominant antimorphic allele of nod and is associated with a single base change in the putative ATP-binding domain. *Genetics* **129**, 409–422.
6. Nakata, T. and Hirokawa, N. (1995) Point mutation of adenosine triphosphate-binding motif generated rigor kinesin that selectively blocks anterograde lysosome membrane transport. *J. Cell Biol.* **131**, 1039–1053.
7. Rashid, D. J., Wedaman, K. P., and Scholey, J. M. (1995) Heterodimerization of the two motor subunits of the heterotrimeric kinesin, KRP (85/95). *J. Mol. Biol*. **252**, 157–162.
8. Hackney, D. D. (1994) Evidence for alternating head catalysis by kinesin during microtubule-stimulated ATP hydrolysis. *Proc. Natl. Acad. Sci. USA* **91**, 6865–6869.
9. Gilbert, S. P., Webb, M. R., Brune, M., and Johnson, K. A. (1995) Pathway of processive ATP hydrolysis by kinesin [see comments]. *Nature* **373**, 671–676.
10. Vale, R. D., Funatsu, T., Pierce, D. W., Romberg, L., Harada, Y., and Yanagida, T. (1996) Direct observation of single kinesin molecules moving along microtubules. *Nature*. **380**, 451–453.
11. Cole, D. G. and Scholey, J. M. (1995) Structural variations among the kinesins. *Trends Cell Biol.* **5**, 259–262.
12. Sambrook, J., Fritsch, E. F., and Maniatis, T. (1989) *Molecular Cloning: a Laboratory Manual*. Cold Spring Harbor Laboratory, Cold Spring Harbor, New York.
13. Reilein, A. R., Tint, I. S., Peunova, N. I., Enikolopov, G. N., and Gelfand, V. I. (1998) Regulation of organelle movement in melanophores by protein kinase A

(PKA), protein kinase C (PKC), and protein phosphatase 2A (PP2A). *J. Cell Biol*. **142**, 803–813.
14. Tuma, M. C., Zill, A., Le Bot, N., Vernos, I., and Gelfand, V. (1998) Heterotrimeric kinesin II is the microtubule motor protein responsible for pigment dispersion in *Xenopus* melanophores. *J. Cell Biol*. **143**, 1547–1558.
15. Daniolos, A., Lerner, A. B., and Lerner, M. R. (1990) Action of light on frog pigment cells in culture. *Pigment Cell Res.* **3**, 38–43.
16. Le Bot, N., Antony, C., White, J., Karsenti, E., and Vernos, I. (1998) Role of xklp3, a subunit of the *Xenopus* kinesin II heterotrimeric complex, in membrane transport between the endoplasmic reticulum and the Golgi apparatus. *J. Cell Biol*. **143**, 1559–1573.
17. Boleti, H., Karsenti, E., and Vernos, I. (1996) Xklp2, a novel *Xenopus* centrosomal kinesin-like protein required for centrosome separation during mitosis. *Cell*. **84**, 49–59.
18. Harlow, E. and Lane, D. (1988) Storing and purifying antibodies, in *Antibodies. A Laboratory Manual*. Cold Spring Harbor Laboratory, Cold Spring Harbor, New York.

17

Identification of Kinesin-Associated Proteins

Lisa C. Lindesmith, Janardan Kumar, and Michael P. Sheetz

1. Introduction

Kinesin can be found in both the soluble and vesicular fractions of cytosol. In both fractions, kinesin exists as a complex with other proteins that are hypothesized to provide regulation of the vesicle-binding and the ATPase activities of the kinesin heavy chain, effectively regulating kinesin-mediated vesicle motility. Thus, the identification of these kinesin-associated proteins would greatly increase our understanding of how kinesin function is regulated in vivo.

The kinesin light chains are the best-characterized kinesin accessory proteins. Each conventional kinesin has two light-chain molecules interacting with two heavy-chain molecules. Although the heavy chains contain the vesicle-binding, microtubule-binding, and ATPase domains, the light chains appear to provide regulation of these functions. Kinesin light-chain mutants in axons result in large membrane aggregates, with neither kinesin nor cytoplasmic dynein able to function ***(1)***, emphasizing the importance of the light chains in vesicle motility. Isoforms of kinesin light chain generated by alternative splicing of the gene ***(2)*** may mediate kinesin cargo selection. In support of this theory, evidence for specific isoform localization to specific cargo is accumulating ***(3–5)***. Additionally, an antibody to a conserved region of a kinesin light chain has been shown to cause the release of a kinesin heavy chain from the vesicle surface ***(6)***. The above observations coupled with those indicating that kinesin light chain may keep kinesin in an inactive conformation in the absence of a cargo ***(7)*** support a critical role for kinesin light chains in the regulation of kinesin activity.

Our laboratory has devised two experimental approaches to successfully identify additional novel proteins that interact with kinesin. The first experimental approach allows us to study the vesicle-bound kinesin-associated pro-

From: *Methods in Molecular Biology*, Vol. 164: *Kinesin Protocols*
Edited by: I. Vernos

teins by utilizing the monoclonal antikinesin heavy-chain antibody SUK4. SUK4 binds kinesin near the motor domain, at the N-terminal, microtubule-binding end of kinesin ***(8)***. This localization of the antibody to the kinesin head group allows the extended rod of kinesin to remain available for binding to accessory proteins on the vesicle surface. Immunoprecipitation of detergent-solubilized high-density vesicles with SUK4 identified a vesicle-bound kinesin complex. The major components of this complex were kinesin and kinectin, a previously unidentified 160-kDa transmembrane protein, which appears to provide a membrane-attachment site for kinesin on endoplasmic reticulum membranes ***(9–11)***. The second approach allows us to study the soluble kinesin complex. This protocol is based on the principle that in the absence of ATP and the presence of the nonhydrolyzable ATP analog AMP–PNP, the kinesin heavy chain binds microtubules in a rigor state, allowing for easy separation of the kinesin complex from the cytosol by centrifugation. Once separated, the kinesin complex can then be released from the microtubules by the addition of ATP. Utilizing this method, we have identified two kinesin-associated proteins. These two proteins are the functional kinesin light-chain kinase and phosphatase, which balance the phosphorylation state of the light chain and effect kinesin motility in vitro ***(12,13)***.

There are potentially many more kinesin-associated proteins that govern kinesin interaction with cargo and regulate kinesin enzymatic activity. By applying the techniques we have developed, many of these unknown partners can be identified and their role in intracellular motility characterized.

2. Materials

2.1. Purification of the Vesicle-Bound Kinesin Complex

2.1.1. Isolation of High-Density Vesicles

1. PMEE buffer: 35 m*M* 1,4 piperazinediethane sulphonic acid (PIPES) (pH 7.4), 5 m*M* $MgSO_4$ (*see* **Note 1**), 5 m*M* EGTA, 0.5 m*M* EDTA, 1 m*M* dithiothreitol (DTT). The buffer can be filtered and stored at 4°C for months. It is convenient to prepare 0.5L of a 5X stock of PMEE. The other stock solutions are needed in microliter volumes per experiment. Therefore, the amount of stock prepared should be dependent on the ease of measuring and pH adjustment.
2. 100 m*M* PMSF (phenylmethylsulfonyl fluoride) stock prepared in isopropanol. PMSF is stable in isopropanol but degrades very quickly upon addition to the buffer. Therefore, it is necessary to add fresh PMSF stock to the buffer at each buffer change through out the purification procedure.
3. 400X EtOH-soluble protease inhibitor cocktail: 0.2 mg/mL pepstatin A, 2 mg/mL TAME (*N*α-*p*-tosyl-L-arginine methyl ester), 2 mg/mL TPCK [L-1-chloro-3-(4-tosylamido)-4-phenyl-2-butanone]. Protease inhibitor stocks can be aliquotted and stored at –80°C for up to 6 mo.

4. 400X H_2O-soluble protease inhibitor cocktail: 0.2 mg/mL leupeptin, 2 mg/mL soybean trypsin inhibitor. Protease inhibitor stocks can be aliquotted and stored at –80°C for up to 6 mo.
5. Chick embryo brains (*see* **Note 2**).
6. 50% and 20% Nycodenz (5-(*N*-2,3-dihydroxypropylacetamido)-2,4,6-triiodo-*N*,*N*'-*bis*(2,3-dihydroxypropyl)-isophthalamide) solutions prepared in PMEE plus protease inhibitors. Stock solutions of Nycodenz can be stored at –20°C and fresh protease inhibitors added at the time of use. Nycodenz is marketed through Sigma Chemical.

2.1.2. Solubilization of the High-Density Vesicles

1. 10% CHAPS (3-[(3-cholamidopropyl) dimethyl-ammonio]-1-propanesulfonate) freshly prepared in water
2. 5 *M* NaCl freshly prepared in water

2.1.3. Immunoprecipitation of the High Density Vesicle-Bound Kinesin Complex

1. Antikinesin heavy-chain antibody SUK4.
2. Protein A-coated agarose beads.
3. NET buffer : 50 m*M* Tris-HCl (pH 8.0), 150 m*M* NaCl, 5 m*M* EDTA.
4. 2× sodium dodecyl sulfate-polyacrylamide gel electrophoresis (SDS-PAGE) sample buffer.

2.2. Purification of the Soluble-Kinesin Complex

2.2.1. Fractionation of the Cytoplasm

Refer to **Subheading 2.1.1.** for details.

1. PMEE buffer.
2. 100 m*M* PMSF.
3. 400X EtOH-soluble protease inhibitor cocktail.
4. 400X H_2O-soluble protease inhibitor cocktail.
5. Chick embryo brains (*see* **Note 2**).

2.2.2. Polymerization of the Endogenous Microtubules

1. 200 m*M* GTP prepared in PMEE (pH 7.0). Nucleotide stock solutions should be prepared in PMEE, the final pH adjusted to 7.0 with NaOH, aliquotted, and stored at –80°C for up to 6 mo.
2. 4 m*M* taxol prepared in dimethyl sulfoxide (DMSO). Taxol is toxic, handle with gloves. Taxol stocks can be stored at –20°C for 6 mo. Taxol is marketed through CalBiochem as Paclitaxel.

2.2.3. Removal of Microtubule-Associated Proteins from Polymerized Microtubules

1. 1 *M* KCl prepared in PMEE.
2. 4 m*M* taxol in DMSO.

2.2.4. Isolation of the Motor Complex-Decorated Microtubules

1. Glucose.
2. Hexokinase.
3. AMP–PNP (5'-adenylylimidodiphosphate).
4. 25% Sucrose (ultrapure) prepared in PMEE plus protease inhibitors.

2.2.5. Release of the Motor Complex from the Microtubules

1. 100 m*M* ATP in PMEE (pH 7.0). Nucleotide stock solutions should be prepared in PMEE and the final pH adjusted to 7.0 with NaOH, aliquotted, and stored at –80°C for up to 6 mo.
2. 200 m*M* $MgSO_4$ (*see* **Note 1**).
3. 4 m*M* taxol in DMSO.
4. 1 *M* KCl in PMEE.

2.2.6. Separation of the Cytoplasmic Dynein Complex from the Kinesin Complex

Five percent and 20% sucrose (ultrapure) solutions prepared in PMEE plus protease inhibitors and 0.1 m*M* ATP.

3. Methods

3.1. Purification of the Vesicle-Bound Kinesin Complex

3.1.1. Isolation of High-Density Vesicles

1. Harvest 10 g of chick embryo brain from 12-d-old chick embryos. This amount corresponds roughly to the amount recovered from five dozen eggs.
2. Wash the brains in cold PMEE until the wash is colorless.
3. Homogenize the brains in an equal volume of complete PMEE (PMEE supplemented with 1 m*M* PMSF, 1× EtOH-soluble and 1× H_2O-soluble protease inhibitors) with a Dounce homogenizer (10 strokes up and down) on ice.
4. Leave the homogenate on ice for 5 min, then repeat the 10 strokes.
5. Centrifuge the homogenate at 10,000*g* for 15 min at 4°C to pellet the cellular debris, nuclei, and nonvesicular organelles.
6. Remove the low-speed spin supernatant from the loose pellet and centrifuge at 171,000*g* for 30 min at 4°C to pellet the vesicular fraction.
7. While the sample is in the centrifuge, prepare a Nycodenz step gradient by layering 2 mL of 50% Nycodenz topped by 1 mL of 20% Nycodenz.
8. Remove and discard the high-speed spin supernatant.
9. Suspend the vesicle pellet in an equal volume of complete PMEE.
10. Layer the vesicle suspension on top of the Nycodenz step gradient and centrifuge at 100,000*g* for 45 min at 4°C (*see* **Note 3**).
11. The high-density vesicles will form a tight, white band at the 20–50% Nycodenz interface. Using a pipet, remove and discard everything above this interface before gently aspirating off the vesicles with a 1-mL pipet.

3.1.2. Solubilization of the High-Density Vesicles

1. Adjust the high-density vesicle fraction to a final concentration of 2% CHAPS and gently suspend on ice. The suspension will clear. After clearing, adjust the suspension to a final concentration of 0.5 *M* NaCl and mix on ice.
2. Dilute the solubilized vesicles with 2 vol of complete PMEE.
3. Pellet any detergent-insoluble material by centrifuging at 100,000*g*, for 30 min at 4°C.
4. Remove supernatant with the detergent-soluble vesicle proteins.

3.1.3. Immunoprecipitation of the High Density Vesicle-Bound Kinesin Complex

1. Add the antikinesin heavy-chain antibody SUK4 to the solubilized vesicle proteins at a final concentration of approx 5 µg/mL (*see* **Note 4**).
2. Incubate overnight at 4°C with slow rotation.
3. Wash the needed amount (*see* manufacture's recommendation) of protein A-coupled agarose beads three times in PMEE by gently suspending the beads and then letting them gravity-settle on ice (*see* **Note 5**).
4. Add the washed protein A beads to the sample and incubate for 3–4 h at 4°C, with gentle rotation.
5. Settle the beads on ice, remove the supernatant, suspend the beads in 10 vol of NET buffer, transfer them to a new tube, and centrifuge at 900*g* for 5 s. Discard the wash. Repeat the suspension in fresh NET buffer two more times, transferring the beads to a new tube before the final wash.
6. Release the immune complex from the protein A beads by suspending the beads in an equal volume of either 2× SDS-PAGE sample buffer or 0.2 *M* glycine (pH 2.8). If the acid elution method is used, the eluate should be neutralized immediately by adding 0.1 vol of 1 *M* Tris-HCl (pH 8.0) (*see* **Note 6**).

3.2. Purification of the Soluble-Kinesin Complex

3.2.1. Fractionation of the Cytoplasm

1. Harvest 10 g of chick embryo brain from 12-d-old chick embryos. This amount corresponds roughly to the amount recovered from five dozen eggs.
2. Wash the brains in cold PMEE until the wash is colorless.
3. Homogenize the brains in an equal volume of complete PMEE (PMEE supplemented with 1 m*M* PMSF, 1× EtOH-soluble, and 1× H_2O-soluble protease inhibitors) with a Dounce homogenizer (10 strokes up and down) on ice.
4. Leave the homogenate on ice for 5 min, then repeat the 10 strokes.
5. Centrifuge the homogenate at 10,000*g* for 15 min at 4°C to pellet the cellular debris, nuclei, and nonvesicular organelles.
6. Remove the low-speed spin supernatant from the loose pellet and centrifuge at 171,000*g* for 30 min at 4°C to pellet the vesicular fraction.
7. Remove the supernatant and discard the pellet.

3.2.2. Polymerization of Endogenous Microtubules

1. Adjust the high-speed spin supernatant to a final concentration of 0.5 m*M* GTP and 20 μ*M* taxol and incubate for 15 min at 37°C with occasional gentle mixing. As the tubulin polymerizes into microtubules, the solution will begin to appear gelatinous.
2. Pellet the microtubules at 100,000*g* for 10 min at 30°C. The resulting supernatant is the microtubule-depleted cytosol and can be used further for purification of kinesin by either immunoprecipitation (*see* above) or ATP-dependant microtubule affinity. To purify kinesin by ATP-dependant microtubule affinity, place the supernatant on ice and do not discard the microtubule pellet.

3.2.3. Removal of Microtubule- Associated Proteins from Polymerized Microtubules

1. Suspend the microtubule pellet in 2 vol of 1 *M* KCl/20 μ*M* taxol prepared in PMEE. Avoid making air bubbles.
2. Add an equal volume of complete PMEE supplemented with 20 μ*M* taxol to the wash and incubate for 5 min at room temperature.
3. Pellet the salt-washed microtubules at 174,000*g*, for 10 min at 30°C. Discard the microtubule-associated protein (MAP)-containing supernatant.

3.2.4. Isolation of the Motor Complex-Decorated Microtubules

1. Suspend the salt-washed microtubules in the microtubule-depleted cytosol prepared in **Subheading 3.2.2.**
2. Add 10 mg of glucose and 2 U of hexokinase per milliliter of microtubule-depleted cytosol to the suspension to deplete the endogenous ATP.
3. Add 0.51 mg AMP–PNP per milliliter to the suspension. The microtubule motors will bind the microtubules in the presence of the nonhydrolyzable ATP analog and remain bound in a rigor state.
4. Incubate for 15 min at room temperature with occasional gentle mixing.
5. Prepare an equal volume of 25% sucrose in complete PMEE supplemented with 0.1 m*M* AMP–PNP and 20 μ*M* taxol.
6. Layer the microtubule suspension on top of the cushion.
7. Pellet the microtubules through the sucrose at 100,000*g* for 30 min at 24°C.
8. Wash the microtubule pellet with 2 vol of complete PMEE supplemented with 0.1 m*M* AMP–PNP and 20 μ*M* taxol. Centrifuge at 100,000*g* for 10 min at 24°C.
9. Remove and discard the supernatant.

3.2.5. Release of the Motor Complex from the Microtubules

1. Gently suspend the microtubule pellet in 1 mL of ATP-release buffer (10 m*M* ATP, 10 m*M* $MgSO_4$, 50 m*M* KCl, 20 μ*M* taxol in complete PMEE) and incubate for 10 min at room temperature.
2. Centrifuge at 100,000*g* for 10 min at 24°C.
3. Remove the ATP-released microtubule-binding proteins and store on ice until further use.

3.2.6. Separation of the Cytoplasmic Dynein Complex from the Kinesin Complex

1. Prepare a 12-mL 5–20% linear sucrose gradient in complete PMEE supplemented with 0.1 m*M* ATP.
2. Layer the ATP-released microtubule-binding proteins on top of the gradient and centrifuge at 100,000*g* for 16–18 h at 4°C.
3. Rinse the bottom of the gradient tube and puncture it with a 25-gage needle.
4. Collect 1-mL fractions from the bottom. Kinesin is usually found in fractions 5–7, reflecting the various conformations of kinesin and association of accessory proteins (*see* **Note 7**).

4. Notes

1. In the preparation of the needed solutions, do not substitute $MgCl_2$ for $MgSO_4$, as Cl ion concentrations above 35 m*M* inhibit kinesin motility.
2. The richest source for kinesin is fresh brain. Kinesin can be purified from frozen tissues, but it has been reported that the kinesin–kinectin complex is not preserved in frozen samples ***(9)***, suggesting that the complexes may be temperature sensitive.
3. Kinectin is a linear molecule and does not provide a tight association with the motor. The complex is stabilized by Nycodenz and remains intact during solubilization with CHAPS. NaCl should be added after the detergent solubilization. Under conditions of incomplete solubilization, as indicated by a turbid solution following suspension in detergent, the complex is not immunoprecipitated. Following solubilization, the sample should not be diluted more than threefold to maintain the necessary concentration of Nycodenz.
4. Most of the antikinesin heavy-chain antibodies available bind to the rod of kinesin. However, it is essential that the antibody used to immunoprecipitate the kinesin complex bind to the head of kinesin. SUK4 is a well-characterized monoclonal antibody that binds to the head, inhibits kinesin motility, and is commercially available from Babco (Berkley, CA).
5. It is important to let the protein A-coated agarose beads gravity-settle during the initial wash steps. This allows an effective separation of intact beads and the "bead fines" that result from damaged beads and contribute to background binding. After the immune complex has bound to the beads, the number of washes should be limited to three. Excessive washing leads to a loss of bound kinesin accessory proteins.
6. An additional component of the immune complex, an isoform of kinectin, was identified using N-terminal sequencing. To use this technique, blockage of the N-terminus must be avoided. This can be done by curing the gel at 4°C for 24 h before use and including the scavenger molecule thioglycolate at 11.4 mg/L in the gel running buffer. Acid-eluted proteins should be denatured in SDS-PAGE sample buffer at 100°C for 2 min before electrophoresis. Following electrophoresis, the proteins should be transferred overnight to polyvinylidene difluoride

membrane, briefly stained with Ponceau S, and the band of interest excised immediately and stored at –20°C in a sealed tube.

7. Motile activity of microtubule motor complexes is inhibited by sucrose, requiring a buffer exchange before motility assays can be performed on sucrose gradient-purified motors. Alternatively, a Nycodenz gradient can be used to separate the dynein and kinesin complexes.

References

1. Gindhart, J. G., Jr. and Goldstein, L. S. (1998) Kinesin light chains are essential for axonal transport in Drosophila. *J. Cell. Biol*. **141**, 443–454.
2. Cyr, J. L., Pfister, K. K., Bloom, G. S., Slaughter, C. A., and Brady, S. T. (1991) Molecular genetics of kinesin light chains: generation of isoforms by alternative splicing. *Proc. Natl. Acad. Sci. USA* **88**, 10,114–10,118.
3. Khodjakov, A., Lizunova, E. M., Minin, A. A., Koonce, M. P., and Gyoeva, F. K. (1998) A specific light chain of kinesin associates with mitochondria in cultured cells. *Mol. Biol. Cell* **9**, 333–343.
4. Lizunova, E. M., Khodiakov, A. L., Gioeva, F. K., and Minin, A. A. (1998) One of the kinesin light chains is selectively associated with mitochondria. *Mol. Biol. (Mosk.)*, **32**, 154–161.
5. Rahman, A., Friedman, D. S., and Goldstein, L. S. (1998) Two kinesin light chain genes in mice. Identification and characterization of the encoded proteins. *J. Biol. Chem*. **273**, 153,95–15,403; erratum: *J. Biol. Chem.* **273**, 24,280.
6. Stenoien, D. L. and Brady, S. T. (1997) Immunochemical analysis of kinesin light chain function. *Mol. Biol. Cell* **8**, 675–689.
7. Verhey, K. J., Lizotte, D. L., Abramson, T., Barenboim, L., Schnapp, B. J., and Rapoport, T. A. (1998) Light chain-dependent regulation of Kinesin's interaction with microtubules. *J. Cell Biol*. **143**, 1053–1066.
8. Ingold, A., Cohn, S., and Scholey, J. (1988) Inhibition of kinesin-driven microtubule motility by monoclonal antibodies to kinesin heavy chains. *J. Cell Biol.* **107**, 2657–2667.
9. Toyoshima, I., Yu, H., Steuer, E. R., and Sheetz, M. P. (1992) Kinectin, a major kinesin-binding protein on ER. *J. Cell Biol.* **118**, 1121–1131.
10. Kumar, J., Erickson, H. P., and Sheetz, M. P. (1998) Ultrastructural and biochemical properties of the 120-kDa form of chick kinectin. *J. Biol. Chem.* **273**, 31,738–31,743.
11. Kumar, J., Toyoshima, I., and Sheetz, M. P. (1998) Isolation and characterization of kinectin. *Methods Enzymol.* **298**, 185–97.
12. Lindesmith, L., McIlvain, J. M., Jr., Argon, Y., and Sheetz, M. P. (1997) Phosphotransferases associated with the regulation of kinesin motor activity. *J. Biol. Chem.* **272**, 22,929–22,933.
13. McIlvain, J. M., Jr., Burkhardt, J. K., Hamm-Alvarez S., Argon, Y., and Sheetz, M. P. (1994) Regulation of kinesin activity by phosphorylation of kinesin-associated proteins. *J. Biol. Chem.* **269**, 19,176–19,182.

18

Assaying Spatial Organization of Microtubules by Kinesin Motors

François Nédélec and Thomas Surrey

1. Introduction

A fundamental property of some motor proteins is their ability to organize filaments in space ***(1)***. This property is a consequence of their oligomeric state, which makes them able to simultaneously bind two microtubules. Here, we describe an in vitro assay for the direct observation of the organization of microtubules by these motors. With this assay, patterns of microtubules are formed that reflect the morphogenetic abilities of the motors. The assay relies on the collective behavior of motors and microtubules in solution. It is, therefore, qualitatively different from methods based on immobilization of motor proteins, as, for example, in motility assays ***(2,3)***.

1.1. Proteins Used To Form Oligomeric Motor Complexes

We construct multiheaded kinesin and non-claret disjunctional (NCD) complexes artificially by biotin–streptavidin or GST antibody links. These artificial oligomers serve as models for naturally occurring oligomeric motor proteins like the members of the BimC family of kinesins ***(4)*** or oligomers generated by regulated assembly (e.g., cytoplasmic dynein–Numa complexes) ***(5)***. We chose kinesin and NCD as the best characterized examples for kinesin-like motors of opposite directionality ***(6)***. We describe bacterial expression, purification, and storage of these proteins.

1.2. Glass Treatment and Handling

Kinesin-related proteins have a tendency to stick nonspecifically to glass, without loosing their ability to bind to microtubules. In the thin samples needed for microscopy, this stickiness would hinder analysis of reactions occurring in

From: *Methods in Molecular Biology*, Vol. 164: *Kinesin Protocols*
Edited by: I. Vernos

solution. Adsorption of motor proteins onto the glass surface would cause microtubule gliding as in "motility assays" and deplete the motors from the solution. Therefore, we describe a glass-coating procedure to prevent motors from binding nonspecifically to the surface: We coat cleaned glass cover slips with a thin agarose film ***(7)*** and then block it with bovine serum albumin (BSA). The motors and microtubules are then free to interact in solution.

1.3. Sample Preparation and Microscopic Assay

In this section, we describe the microscopic assay for real-time observation of spatial organization of microtubules by the artificial multiheaded kinesin and NCD complexes. In principle, any oligomeric motor can be studied using this organization assay. Self-organization is initiated from a homogeneous mixture of these motors, tubulin, and nucleotides by starting microtubule polymerization with a temperature increase. The dynamics of the process are observed by dark-field and fluorescence microscopy in a standard video microscopy setup ***(8)***.

2. Materials

2.1. Purification of Proteins Needed To Form Oligomeric Motor Complexes

1. Plasmids
   a. pEY5 ***(9)*** for expression of the N-terminal 401 amino acids of *Drosophila* kinesin heavy chain (motor domain and stalk) fused to the C-terminal 87 amino acids of the biotin carboxyl carrier protein of *Escherichia coli* (= K401-Bio).
   b. pGEX–NCD ***(10)*** for expression of glutathione-*S*-transferase fused to the C-terminal 590 amino acids of *Drosophila* NCD (= GST–NCD).
2. Bacterial strain BL21(E-3)pLysS ***(11)***.
3. Monoclonal anti-GST antibody, GST-2 (sold as mouse ascites, Sigma G1160).

2.2. Glass Treatment and Handling

1. No. 1 cover slips, size 24 × 60 mm (VWR cover slips yield the best results in our hands).
2. A modified pot for cleaning the coverslips in ethanol vapor (*see* **Fig. 1**): It is assembled from a commercially available stainless-steel vapor cooker. Four parallel metal springs are attached horizontally close to the bottom of the perforated inset of the cooker (only two are shown in **Fig. 1**). They can hold up to 100 separate coverslips in two parallel rows.
3. Teflon silicon wafer holders with 24 positions (Metron Technology, Burlingame, CA) for holding coverslips.
4. Agarose, ultrapure, electrophoresis grade (Gibco BRL No. 15510-027).
5. BSA stock solution: 100 mg/mL BSA in 80 m*M* piperazine-*N*,*N*-*bis*(2-ethanesulfonic acid) (PIPES)/KOH pH 6.8, dissolved overnight.

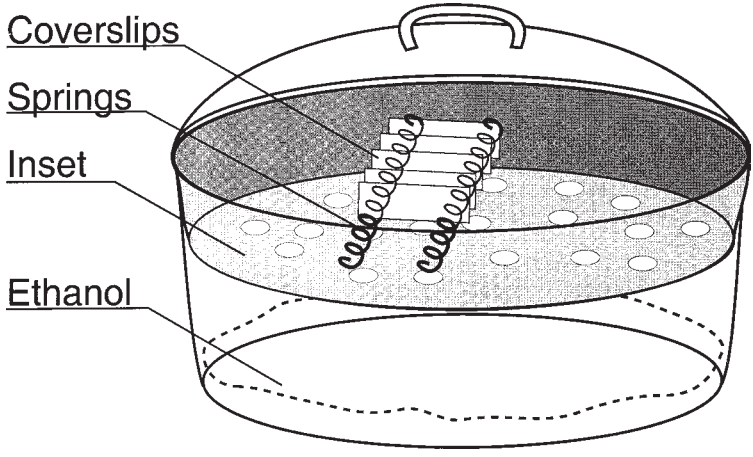

Fig. 1. Schematic drawing of the pot used for cleaning glass cover slips in ethanol vapor.

2.3. Sample Preparation and Microscopic Assay

1. Chemicals: All solutions are filtered through 0.1-µm filters, aliquoted, and stored at –20°C.
   a. Glutamate buffer (GB): 500 m*M* glutamate, 20 m*M* PIPES, 0.5 m*M* $MgCl_2$, 0.25 m*M* EGTA (pH 6.9).
   b. 100 m*M* MgATP (pH 7.0).
   c. 100 m*M* GTP (pH 7.0).
   d. 500 m*M* phosphenolpyruvate ph not adjusted (PEP); do not keep longer than 1 mo.
   e. 10 m*M* Paclitaxel (Molecular Probes, P-3456) in dimethyl sulfoxide (DMSO), thawed, and diluted just before the experiment.
   f. VALAP. 1:1:1 mixture of vaselin, lanolin, paraffin that is kept melted at 90°C in a heat block.
2. Proteins
   a. 1 mg/mL purified biotinylated kinesin and 2 mg/mL purified GST–NCD frozen in liquid ethane and stored in liquid nitrogen (as described in **Subheading 3.1.3.**).
   b. 4 mg/mL purified anti-GST antibody stored at –20°C (as described in **Subheading 3.1.4.**).
   c. Fluorescein-labelled streptavidin (Molecular Probes, S-869) dissolved in ddH_2O to a final concentration of 5 mg/mL, filtered through 0.1-µm filters, aliquoted, and stored at –20°C. Thaw just before the experiment and dilute to 0.25 mg/mL in GB.
   d. Pyruvate kinase (SIGMA, P-7768), stored at 4°C, and diluted to 70 µg/mL in GB just before the experiment.

e. 14 mg/mL tubulin in 80 m*M* PIPES, 1 m*M* $MgCl_2$, 0.5 m*M* EGTA (pH 6.8) purified from cow brain and cycled once as described ***(12)***. After cycling, filter through a 0.1-µm filter, aliquot, freeze, and store in liquid nitrogen.

3. Methods

3.1. Purification and Storage of Proteins Needed To Form Oligomeric Motor Complexes

3.1.1. Purification of Biotinylated Kinesin

Expression of biotinylated kinesin in *E. coli* is performed essentially as described ***(13)***. We obtain best yields when inducing the cells at 27°C. After lysing the cells using a French press, the biotinylated kinesin is purified by affinity chromatography on a monomeric avidin column essentially as described ***(9)***. The fast dialysis is replaced by a desalting column (Bio-Rad, 10DG), and the final eluate from the HitrapQ column is dialyzed twice against storage buffer (50 m*M* imidazole/HCl [pH 6.8], 50 m*M* KCl, 4 m*M* $MgCl_2$, 2 m*M* EGTA, and 20% [w/v] glycerol) containing 10 m*M* of 2-mercaptoethanol. This dialysis also concentrates the protein. If necessary, the purified kinesin can be further concentrated to 1 mg/mL using centrifugal concentrators (Millipore UFC4LTK25, and Amicon 42409). Higher concentrations result in protein aggregation (the solubility of kinesin is significantly lower in buffers containing PIPES). Finally, the solution is filtered through 0.1-µm centrifugal filters (Millipore UFC0VVNB).

3.1.2. Purification of GST–NCD

Expression of the GST–NCD fusion protein and its purification by affinity chromatography using glutathione–agarose is performed essentially as described ***(10)***. A few modifications are introduced: (1) To facilitate lysis, the protein is expressed in bacteria carrying the lysozyme-producing plasmid pLys; lysis is then carried out using a French press. (2) To improve the protein's solubility, we replace PIPES by imidazole in all buffers and add 10% glycerol. (3) We remove insoluble material after elution from the glutathione–agarose column by brief ultracentrifugation. (4) Glutathione is then removed by two dialysis steps against storage buffer containing 1 m*M* DTT. (5) The protein is concentrated with centrifugal filters to 1–2 mg/mL and filtered through a 0.1-µm filter (Millipore UFC0VVNB).

3.1.3. Storage of Purified Kinesin Fusion Proteins

The best preservation of kinesin and NCD activity is obtained by flash-freezing in liquid ethane and storage in liquid nitrogen (*see* **Note 1**). Ethane gas is liquefied by condensation in a small metal container cooled by liquid nitrogen

(14) (liquid ethane is used as a standard cryogen in cryo-electron microscopy laboratories). Kinesin aliquots of several microliters in thin-wall polymerase chain reaction (PCR) tubes are dipped into liquid ethane, and then transferred into liquid nitrogen for final storage. **Note:** Extreme care has to be taken when handling liquid ethane: (1) Contact with skin or eyes has to be absolutely avoided because it instantly "burns" the affected area. (2) Open fire or electrical sparks can ignite ethane and lead to explosions. Always handle ethane in a fume hood.

3.1.4. Purification of an Anti-GST Antibody

The monoclonal anti-GST antibody is purified from commercially available ascites by protein A affinity chromatography using a high-salt protocol ***(15)***. It is then dialyzed into 50 m*M* K–PIPES (pH 7.3), 50 m*M* NaCl, 50% (v/v) glycerol resulting in a final protein concentration of 4 mg/mL. After filtering through a 0.1-µm filter, the antibody is stored at –20°C (freezing of this monoclonal antibody resulted in protein aggregation).

3.2. Glass Treatment and Handling

3.2.1. Cleaning in Ethanol Vapor

Place cover slips in the two rows of springs attached to the perforated metal inset of the pot (*see* **Fig. 1**). Fill the bottom of the pot halfway to the inset with absolute ethanol and cover it with the lid. "Cook" on a hot plate, in a fume hood, for about 4 h. (The lid is not airtight, and no pressure is built up. **Caution:** Hot ethanol vapor is highly flammable). The temperature should be sufficiently high to produce ethanol vapor that condenses on the cover slips and drips back into the reservoir (which should never be fully evaporated). The cleaned cover slips can be stored for months. Whenever possible, perform the handling of the glass cover slips in a laminar-flow hood, to avoid dust on the slides (*see* **Note 2**). The glass surface of vapor cleaned glass is usually not hydrophilic and cannot be evenly coated with agarose.

*3.2.2. Sonication in Alkaline Ethanol (similar to **ref.** 16)*

To 200 mL of 25% (w/v) NaOH in deionized water in a glass beaker, add 95% ethanol to a final volume of 800 mL. Immerse ethanol-vapor-cleaned coverslips placed in a round teflon holder. Sonicate the beaker for 10 min in a water-bath sonicator. Rinse thoroughly, by immersing five times in deionized water. After drying, the glass surface should be very hydrophilic and can be used for a few days.

3.2.3. Agarose Coating

To coat coverslips with a thin layer of agarose, dip single coverslips into a warm solution of 0.1% agarose (in a 50-mL plastic tube, 5 mL of boiling 1%

agarose are added to 45 mL warm water (~70°C); *see* **Note 3**). Even agarose films can only be obtained if the glass surface is hydrophilic. Avoid dipping the tweezers that are used to hold the coverslip into the solution. Wait until the agarose-coated coverslips look dry (1–2 h) and use them immediately for the next step. The agarose layer is most homogeneous in the central region of the coverslip, which is used in the self-organization assays (*see also* **Note 4**).

3.2.4. BSA Coating

Finally, the agarose layer is treated with BSA to further reduce nonspecific protein adsorption. Agarose-coated coverslips are dipped into a solution of 10 mg/mL BSA in a 50-mL plastic tube (a stock solution of 100 mg/mL BSA in 80 m*M* PIPES/KOH [pH 6.8], dissolved overnight, is diluted 1:10 and filtered through a 0.22-µm filter). Immediately after BSA coating, each coverslip is rinsed by dipping it sequentially into five tubes of deionized water. The coverslips are then kept in a teflon holder inside a humid chamber (a glass beaker with water at the bottom, covered with parafilm), preferably in the refridgerator. These coverslips should be used within a couple of hours of BSA coating (*see* **Note 5**).

3.2.5. Breaking of Coverslips

We also need small coverslips with exactly the same coating (*see* **Subheading 3.3., step 4**). These are made simply by breaking a 12 × 12-mm piece from the central region of an 24 × 60-mm coverslip already coated with agarose/BSA. Breaking can easily be achieved by laying the glass coverslip onto parafilm supported by a pad of tissue papers and by gently pressing tweezers and a razor blade against the glass edges.

3.3. Sample Preparation and Microscopic Assay

Aliquots of stock solutions are thawed just before the experiment. All solutions are then kept on ice.

1. "Kinesin complexes" are formed by mixing 2 µL GB, 0.7 µL 0.25 mg/mL fluorescein-labelled streptavidin (*see* **Note 6**), and 2.5 µL biotinylated kinesin stock solution (*see* **Note 7**); these complexes can be kept on ice for several hours.
2. "NCD complexes" are formed by mixing 2.5 mL GST–NCD stock solution with 0.5 mL purified anti-GST antibody 10 min before the experiment (*see* **Note 7**). These complexes can be kept on ice for 1 h.
3. Self-organization buffer (SB) is prepared by adding 5 µL Mg–ATP, 2.3 µL GTP, 2.3 µL pyruvate kinase, and 0.8 µL PEP to 45 µL GB (*see* **Note 8**).
4. The self-organization experiment: The pattern of microtubules generated in the experiment depends on the concentration of tubulin dimers and motor complexes and on the type of motor. Among the variety of structures that can be organized, we present two examples.

Asters organized by kinesin (**Fig. 2A**). One milliliter of SB, 0.7 µL H_2O (sometimes containing Paclitaxel; *see* **Note 9**), 0.5 µL "Kinesin complexes," and 0.5 µL tubulin are mixed on ice, vortexed, and a drop of 1.0–1.3 µL of this mixture is then pipetted onto an 24 × 60-mm agarose/BSA-coated cover slip, and covered with a 12 × 12-mm agarose/BSA cover slip (prepared as described in **Subheading 3.2.5.**). The sample is sealed with VALAP (applied using a small paint brush). The sample is immediately transferred to the microscope and brought into oil contact with the heated dark-field condenser. The resulting sample temperature of 30°C promotes microtubule polymerization and subsequent motor-mediated organization.

Asters organized by NCD (**Fig. 2B**): One microliter of SB, 0.5 µL H_2O, 0.8 µL "NCD complexes," and 0.5 µL tubulin are mixed (*see* **Note 8**). The sample was then prepared and observed as described in the paragraph above.

4. Notes

1. The self-organization experiments require highly active kinesin and NCD preparations. Flash-freezing the motors in liquid ethane is superior to freezing them in liquid nitrogen, probably because the sample cools down more rapidly in liquid ethane. This method may also prove useful for freezing other purified proteins.
2. If fluorescence microscopy is used instead of dark-field microscopy, the ethanol cleaning step can be omitted.
3. The thickness of the agarose layer can be varied by using different concentrations of agarose in the dipping solution (*see* **Subheading 3.2.3.**). Below approx 0.06% of agarose, the layer becomes uneven and patchy.
4. Agarose-coated glass without subsequent BSA treatment may already be suitable for studies in cell extracts like *Xenopus* extracts. The agarose coat may prevent microtubule gliding on the surface that is often observed when using uncoated glass for such samples.
5. The first person who significantly improves the glass preparation, particularly with respect to the long-term storage of treated cover slips, before 2002 will receive a bottle of fine red wine from the authors ***(2)***.
6. Using fluorescein-labeled (instead of unlabeled) streptavidin for the formation of oligomeric kinesin complexes improves the solubility of the complexes and allows their detection by fluorescent microscopy.
7. The optimal ratio between biotinylated kinesin and streptavidin and between GST-NCD and anti-GST antibody for the construction of oligomeric motor complexes is obtained empirically by optimizing the velocity of aster formation.
8. To avoid protein aggregation in experiments with NCD complexes, we found it necessary to have glutamate in the buffer, to keep PIPES concentrations low, and to perform the experiment at temperatures not higher than 30°C. For self-organization experiments with kinesin complexes, buffers of simpler composition can be used and the sample can be brought to higher temperatures ***(1)***.
9. The self-organization process depends critically on microtubule nucleation. Because different tubulin preparations have quite different nucleation properties,

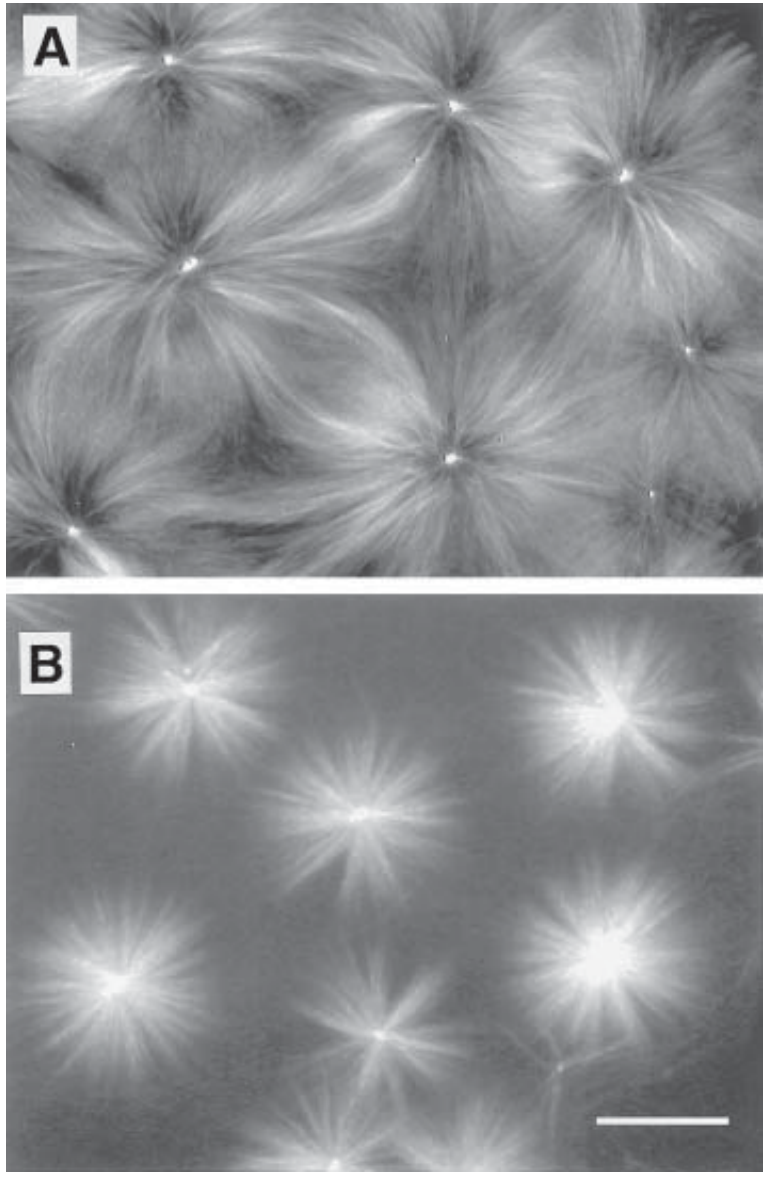

Fig. 2. Microtubule asters organized by kinesin complexes **(A)** and by NCD complexes **(B)**. In these two cases, self-organization of microtubules and motors produce asters. However, because the two motor proteins have opposite directionality the asters formed have opposite polarity (manuscript in preparation). In asters organized by kinesin complexes, the plus end of the microtubules is in the center, whereas organization of microtubules by NCD complexes produces asters with minus ends in the center. The images are taken in dark field. Scale bar: 50 μm.

we found it necessary for some tubulin preparations to stimulate nucleation by adding the taxol-derivative Paclitaxel to the mixture (up to a final concentration of 4 μ*M*) to start self-organization. Microtubules should become visible after 10–20 sec.

Acknowledgments

We thank J. Gelles for the gift of plasmid pEYS, L. B. Goldstein for the gift of plasmid pGEX-NCD, M. B. Elowitz for help with the glass cleaning procedure, and A. Desai for critically reading the manuscript. We also thank S. Leibler and E. Karsenti for continuous support.

References

1. Nedelec, F. J., Surrey, T., Maggs, A. C., and Leibler, S. (1997) Self-organization of microtubules and motors. *Nature* **389,** 305–308.
2. J. Howard, Hunt, A. J., Back., S. (1993) Assay for microtubule movement driven by single kinesin molecules, in *Methods in Cell Biology*, vol. 39: *Motility Assays For Motor Proteins* (Scholey, J.M., ed.), Academic, Sand Diego, CA, pp. 138–147.
3. Svoboda, K. and Block, S. M. (1994) Force and velocity measured for single kinesin molecules. *Cell* **77,** 773–784.
4. Kashina, A. S., Rogers, G. C., and Scholey, J. M. (1997) The bimC family of kinesins: essential bipolar mitotic motors driving centrosome separation. *Biochim. Biophys. Acta* **1357,** 257–271.
5. Merdes, A., Ramyar, K., Vechio, J. D., and Cleveland, D. W. (1996) A complex of NuMA and cytoplasmic dynein is essential for mitotic spindle assembly. *Cell* **87,** 447–458.
6. Amos L. A. and Cross, R. A. (1997) Structure and dynamics of molecular motors. *Curr. Opin. Struct. Biol.* **7,** 239–246.
7. Holy T. E., Dogterom, M., Yurke, B., and Leibler, S. (1997) Assembly and positioning of microtubule asters in microfabricated chambers. *Proc. Natl. Acad. Sci. USA* **94,** 6228–6231.
8. Jnoue, S. (ed.) (1989) *Video Microscopy*. Plenum, New York.
9. Young, E. C., Berliner, E., Mahtani, H. K., Perez-Ramirez, B., and Gelles, J. (1995) Subunit interaction in dimeric kinesin heavy chain derivatives that lack the kinesin rod. *J. Biol. Chem.* **270,** 3926–3931.
10. Stewart, R. J., Thaler, J. P., and Goldstein., L. B. (1993) Direction of microtubule movement is an intrinsic property of the motor domains of kinesin heavy chain and Drosophila NCD protein. *Proc. Natl. Acad. Sci. USA* **90,** 5209–5213.
11. Studier, F. W. (1991) Use of bacteriophage T7 lysozyme to improve an inducible T7 expression system. *J. Mol. Biol.* **219,** 37–44.
12. Ashford, A. J., Andersen, S. S. L., and Hyman, A. A. (1998) Preparation of tubulin from bovine brain, in *Cell Biology: A Laboratory Handbook*, vol. 2 (Celis, J. E., ed.), Academic, San Diego, CA, pp. 205–212.

13. Berliner, E., Mahtani, H. K., Karki, S., Chu, L. F., Cronan, J. E., Jr., and Gelles, J. (1994) Microtubule movement by a biotinated kinesin bound to a streptavidin-coated surface. *J. Biol. Chem.* **269,** 8610–8615.
14. Lepault, J. and Dubochet, J. (1986) Electron microscopy of frozen hydrated specimens: preparation and characteristics. *Methods Enzymol.* **127,** 719–730.
15. Harlow, E., and Lane, D. (eds.) (1988) *Antibodies: A Laboratory Manual*. Cold Spring Harbor Laboratory, Cold Spring Harbor, NY.
16. Brown, P. O., Stanford University, Experimental Protocols http://cmgm.stanford.edu/pbrown/protocols.

19

Crystallization of Kinesin

Manfred Thormählen, Jens Müller, and Eckhard Mandelkow

1. Introduction

Kinesin is the founding member of a family of motor proteins. It translocates along microtubules in the direction of the plus or fast-growing end. Conventional kinesin consists of two identical heavy chains carrying the motor activity, and two light chains. Based on its amino acid sequence, the heavy chain can be divided into three separate domains: (1) an N-terminal head, or motor domain, (2) an elongated α-helical stretch forming a coiled coil with a second kinesin heavy-chain polypeptide, (3) a C-terminal globular domain responsible for cargo binding and regulation of the motor's activity (for reviews, *see* **refs. *1–4***).

Kinesin-like proteins may be classified, according to the position of the motor domain in the polypeptide chain: N, I, or C type (motor domain N-terminal, as in conventional kinesin, internal, or at the C-terminal end, as in nonclaret disjunctional [NCD]). So far, all C-type kinesins were found to move to the microtubule minus end (i.e., in the opposite direction compared to kinesin). Examples of C-type kinesins are the NCD protein from *Drosophila* or the KAR3 protein from yeast.

To date, six different kinesin crystal structures have been solved and published: monomeric human kinesin ***(5)*** (protein data bank [PDB] code:1bg2), monomeric rat kinesin ***(6)*** (PDB code: 2kin), dimeric rat kinesin ***(7)*** (PDB code: 3kin), monomeric NCD ***(8)*** (not deposited in the PDB), dimeric NCD ***(9)*** (PDB code: 2 ncd), and monomeric KAR3 ***(10)*** (PDB code:3kar). All proteins were truncated and consisted only of the motor domain, or of the motor domain and a short additional stretch of the coiled-coil region called the neck. Two of these structures showed the dimeric form of conventional kinesin ***(7)*** and NCD ***(9)***, respectively. The other four constructs were monomeric, consisting of the con-

From: *Methods in Molecular Biology*, Vol. 164: *Kinesin Protocols*
Edited by: I. Vernos

served motor domain and a stretch of the neck too short to allow the formation of a stable dimer (human and rat kinesin, NCD and KAR3).

As expected from the high level of sequence conservation between motor domains, the structural similarity of the different monomeric molecules is high, both for plus-end and minus-end directed motors. The core is well conserved and most differences can be observed in loops connecting the structural elements. Larger differences that might be related to their different directionalities can only be observed in the dimeric kinesin and NCD structures, because, in these cases, the sequences outside the conserved motor domain are visible for both types of motors. A comparison of the different structures can be found in **ref. *11***.

The crystal structure analysis of a protein is a complex task, but a number of technical developments have moved crystallography out of an area reserved for a few specialists (for recent reviews, *see* **refs. *12*** and ***13***). The requirement of high protein concentrations makes it essential to obtain pure protein in sufficient quantities. This has been greatly simplified by the use of recombinant expression systems in combination with tagged proteins. A major step is to obtain crystals that diffract well enough to be suitable for analysis. Although this is still far from trivial, it has been accelerated by the advent of kit technology based on sparse matrix or grid screening methods. The damage to protein crystals exposed to X-ray beams can be minimized by flash-freezing and keeping the crystals at liquid-nitrogen temperatures throughout the data collection.

A problem that was often almost as difficult as the initial crystallization itself was the need to obtain heavy-atom derivatives of the crystals to determine the phases required to calculate the electron density. These derivatives had to be isomorphous to the native crystals. Traditionally, heavy atoms have been incorporated by soaking native crystals in solutions of heavy metal salts or by cocrystallization in the presence of these salts. This often required considerable effort and was not always successful. However, the recent past has seen an increase in structures obtained by use of MAD (multiple wavelength anomalous diffraction) phasing. MAD depends on incorporation of anomalous scatterers, such as selenium, which can replace sulfur in methionine residues (Se-Met) after expression in *E. coli,* and on the use of synchrotron beam lines to generate a tunable X-ray beam. In principle, both the native dataset and the derivative dataset can then be obtained from one single crystal. With the advance of fast detector systems (e.g., CCD [charge coupled device] detectors), combined with the high intensity of a synchrotron beam line and cryo technology, the high-resolution data can now be obtained within a few hours (in favorable instances). This instrumentation is available at synchrotron laboratories such as DESY (Hamburg, Germany), ESRF (Grenoble, France), BNL (Brookhaven, NY), APS (Chicago, IL), SSRL (Stanford, CA), KEK (Tsukuba,

Japan), and others. However, much of the necessary initial work can still be done using a rotating anode to generate X-rays (e.g., screening to find high-quality crystals or heavy-atom derivatives).

If a protein is known to conform to a certain fold, as is the case for kinesin, phases can also be obtained from the available structures by "molecular replacement" without the necessity to generate heavy-atom derivatives. Once a native dataset together with the respective phases is present, it is amenable to interpretation and the corresponding structure can be built using a computer graphics interface.

2. Materials

Even though the number of proteins that are being crystallized is increasing rapidly, the market for crystallization equipment is still small in comparison. Equipment can be obtained from companies such as Hampton Research (http://www.hamptonresearch.com), Douglas Instruments (http://www.douglas.co.uk), or Emerald BioStructures (http://www.emeraldbiostructures.com). Some material is also available from other companies (e.g., ICN, Nunc). Chemicals should be obtained in the best quality.

Basic materials include the following:

1. Crystallization plates (e.g., Linbro™ plates can be obtained from ICN or Hampton Research; Hampton Research also offers several types of plates for sitting drop methods (e.g., VDX plates™ for hanging drop crystallography, Chryschem plates™ or CrystalClear™ strips for sitting drop crystallography); MicroWell™ is available from Nunc; CombiClover™ is available from Emerald BioStructures).
2. Crystallization solutions (crystallization kits are available from the companies named in **item 1**): Buffer stock solutions should be standardized (e.g., 0.5 *M* or 1 *M*) to simplify the preparation of reservoir solutions. Stock solutions of precipitants should be at concentrations near their maximum solubilities. Pass all stock solutions through a 0.22-µm filter and store in sterile containers (*see* **Notes 1** and **2**).
3. Siliconized cover slips (can be prepared in the laboratory; *see* **Subheading 3.1.**; also available from Hampton Research).
4. Silicon vacuum grease (Baysilone™ is available from Roth, Karlsruhe, Germany; Dow Cornell™ grease is available from Hampton Research) or clear sealing tape (available from Hampton Research or Emerald BioStructures).
5. Controlled environment with regard to temperature and absence of vibration.

Because the solubility of the protein under crystallization conditions depends on the temperature of the sample, it is essential to have a temperature-stable environment. This can be either a separate room equipped with a stable air-conditioning system or an incubator that can be both heated or cooled to reach a desired temperature.

Sometimes, more sophisticated equipment has to be employed; for example, in cases where microheterogeneity of the sample is caused by aggregation of the protein particles. In general, a homogeneous particle size (homodispersity) will be advantageous. A method to determine if a sample has a uniform particle size is dynamic light scattering. Instruments from several manufacturers are available for this purpose (e.g., Protein Solutions, Charlottesville, VA; Precision Detectors, Franklin MA).

3. Methods

To obtain protein crystals from a concentrated solution of protein, it is necessary to bring the system to a metastable state of reduced solubility and at the same time allow the molecules to self-assemble into a crystalline lattice. This can be done by gradually increasing the level of saturation of salt, such as ammonium sulfate, thereby increasing the ionic strength, or of a polymeric precipitating agent, such as polyethylene glycol (PEG), but also by variations of pH or temperature. The use of high-ionic-strength solutions relies on a phenomenon known as "salting out," where protein and salt ions compete for the water from the solvent. Its effect relies mainly on anions, and because it is a function of the valency of the ion, multiply charged ions such as sulfate or phosphate are considerably more effective than monovalent ions such as chloride, nitrate, or acetate. PEGs also compete for water molecules, but they have another important property. PEG molecules are long and flexible, and they continuously twist and gyrate in solution, monopolizing far more space than their molecular mass alone would suggest. Thus, they push protein molecules together and deprive them of solvent, thereby excluding them from the solution.

The range of conditions at which different proteins can be crystallized varies considerably. They may be drastically different even for homologous proteins and no general method can be expected to be applicable for every protein, not even for closely related ones, such as kinesin homologs. However, the technical setup used in crystallization will be briefly described here and reasonings on similarities between conditions for crystallization of kinesin based on our own experience and the available literature will be given (*see* **Note 4**). For a more general description of the principles that govern crystallization, the reader is referred to **ref.** ***14***.

One of the basic rules in crystallography is to use protein samples that are as pure as possible. Even small impurities (e.g., protein fragments or aggregates) may result in lattice defects or prevent the formation of crystals entirely. Although in some cases crystallization has been employed as a purification procedure, the vast majority of proteins is quite sensitive to contaminants.

As should be expected from the high level of genetic conservation between motor domains, the structural similarity of the different monomeric molecules

is high. However, the conditions under which crystals were obtained varied considerably, but fall into two broad classes: (1) crystallization in the presence of high salt, and (2) crystallization in the presence of polyethylene glycols.

The conditions together with the respective references are given in **Table 1**. So far, all successful attempts of kinesin crystallization have been done with genetically engineered fragments that possessed only the motor domain or, at most, a short additional stretch of the otherwise long coiled-coil fragment and were expressed in *E. coli*. Crystals were grown either by vapor diffusion, both by the hanging drop or the sitting drop method, or in a microbatch experiment, either at room temperature or at 4°C.

3.1. Growing Crystals by the Hanging Drop Method

The method relies on the slow formation of an equilibrium between the mother liquor containing the protein and a larger reservoir containing an elevated concentration of the precipitant. Vapor diffusion will allow supersaturation to occur slowly so that contacts between protein molecules will form gradually. This avoids quick, amorphous aggregation and precipitation and favors the formation of ordered nuclei that may grow into crystals.

1. Siliconize a number of cover slips to which a drop of protein and precipitant will finally be applied. Siliconization is performed by stacking the cover slips into a holder that will allow each to come in contact with the reagent (we use one built from plastic in our lab for this purpose) and to expose them for 5 min in a tetraethoxysilane atmosphere generated in an desiccator under moderate vacuum. Presiliconized cover slips are also commercially available from Hampton Research.
2. The experiment is set up in a 24-well Linbro tissue culture plate (*see also* **Note 3**). Use the one that provides wells with elevated rims. The wells can be sealed by 20 × 20-mm siliconized glass cover slips. Similarly, a VDX plate can be used.
3. The wells will hold the reservoir of buffer and precipitant that is used in the experiment. Typically, the reservoir volume will range from 500–1000 µL per well, but can also be higher.
4. The chamber that is formed by the well and the cover slip is sealed by vacuum grease of moderate viscosity, such as Baysilone or Dow Cornell high-vacuum grease. First, fill the grease from its tube into a 10- or 20-mL syringe. Then, use the syringe to apply the grease onto the elevated rim so that it will form a complete ring when the cover slip is pressed gently on it afterward.
5. Mix the required reservoir solutions. This can be done in a separate tube or directly in the well. Mixing may require special attention when working with highly viscous solutions such as PEGs (*see* **Note 6**).
6. The protein and the precipitant are mixed in one drop on the cover slip. The volume of the drop may range from 2 to 20 µL (*see* **Note 5**).
7. The cover slip is then turned so that the drop faces the reservoir and carefully pressed on the grease so that a tight seal will form.

Table 1
Published Conditions for Kinesin Crystallization

Construct	Method	Conditions	Ref.
Human kinesin hK349	Sitting drop, 4°C	5 mg/mL protein in 50 m*M* Na-acetate (pH 4.6), 75 m*M* KCl, 3.5% (w/v) PEG4000, 2.5 m*M* ATP, 10 m*M* $MgCl_2$ Reservoir: 100 m*M* Na–acetate (pH 4.6), 150 m*M* KCl, 7% PEG4000, 5 m*M* ATP, 20 m*M* $MgCl_2$	***(5)***
Rat kinesin rK354	Hanging drop, room temperature	9–14 mg/mL protein 20 m*M* PIPES (pH 7.5), 50 m*M* KCl, 1 m*M* EGTA, 1 m*M* DTT, 0.9 *M* Li_2SO_4 Reservoir: 1.8 *M* Li_2SO_4 equally buffered, **or** 15 mg/mL protein in 10 m*M* PIPES (pH 7.5), 50 m*M* NaCl, 1 m*M* EGTA, 1 m*M* DTT, 0.5 m*M* NaN_3, 0.9 *M* $(NH_4)_2SO_4$ Reservoir: 1.8 *M* $(NH_4)_2SO_4$,50 m*M* NaCl	***(6,15)***
Rat kinesin rK379	Hanging drop, room temperature	15 mg/mL protein 10 m*M* PIPES (pH 7.5), 200 m*M* NaCl, 1 m*M* EGTA, 1 m*M* DTT, 0.5 m*M* NaN_3, 0.8 *M* $(NH_4)_2SO_4$ Reservoir: 1.6 *M* $(NH_4)_2SO_4$, 200 m*M* NaCl	***(7,15)***
Drosophila NCD 335–700	Sitting drop, room temperature	7 mg/mL protein in 10 m*M* PIPES, (pH 7.2), 100 m*M* NaCl, 1 m*M* EGTA, 1 m*M* DTT, 7% (w/v) PEG4000, 0.3% octyl-β-D-glucoside; 2 m*M* ATP, 10 m*M* $MgCl_2$ Reservoir: 15% (w/v) PEG4000, 60 m*M* NaCl equally buffered	***(8,16)***
Drosophila NCD 296–700	Sitting drops, 4°C	20 mg/mL protein in 20 m*M* HEPES (pH 7.5), 100 m*M* NaCl, 1 m*M* EGTA, 1 m*M* EGTA, 0.7 *M* Li_2SO_4, 2 m*M* ADP, 10 m*M* $MgCl_2$ Reservoir: 20 m*M* HEPES (pH 7.5), 1.4 *M* Li_2SO_4, 1 m*M* EGTA, 1 m*M* DTT, 10 m*M* $MgCl_2$	***(9)***
Yeast KAR3 383–729	Microbatch, room temperature	11 mg/mL protein 10 m*M* HEPES (pH 7.5), 150 m*M* NaCl, 1 m*M* DTT, 1 m*M* $MgCl_2$, 0.2 m*M* NaN_3, 2 m*M* ADP combined equally with 22% methyl ether PEG2000, 100 m*M* NaCl, 2% ethylene glycol, 50 m*M* HEPES (pH 7.0)	***(10)***

8. Store the plates in a quiet place at constant temperature. Watch for the formation of crystals under a light microscope. Crystals can be more easily visualized using polarized light (*see* **Notes 7** and **8**).

3.2. Growing Crystals by the Sitting Drop Method

This method is also based on vapor diffusion. However, the surface geometries of the protein droplets and of the reservoirs can be more variable and different from those of a hanging drop experiment. Thus, conditions that will not work in a hanging drop assembly might do so in a sitting drop experiment, and vice versa.

1. Several types and sizes of sitting drop arrays are commercially available (e.g., Chryschem plates or CrystalClear strips from Hampton Research or CombiClover from Emerald BioStructures). In general, they consist of a sort of tissue culture plate possessing an elevated tray above the level of the reservoir that holds a small depression of several microliters in which the protein and precipitant are mixed. The surrounding larger well will hold the reservoir.
2. The reservoir may contain up to 1 mL in a multiwell plate down to 100 µL when CrystalClear Strips (Hampton Research) are used.
3. Mix the required reservoir solutions. This can be done in a separate tube or directly in the well. Mixing may require special attention when working with highly viscous solutions such as PEGs (*see* **Note 6**).
4. The protein and the precipitant are mixed in one drop on the tray. The volume of the drop may range from 2 to 20 µL (*see* **Note 5**).
5. Sealing is done with clear sealing tape.
6. Store the plates in a quiet place at constant temperature. Watch for the formation of crystals under a light microscope using polarized light (*see* **Notes 7** and **8**).

3.3. Growing Crystals in a Microbatch Experiment

1. Batch crystallization relies on the direct mixing of an undersaturated protein solution with a precipitant solution. This causes the solution to become oversaturated with respect to protein and, under favorable conditions, crystals may form.
2. Batch crystallization can be performed in the microscale range using microliter amounts in glass capillaries or in microdroplets under oil.
3. To set up a microbatch experiment in a MicroBatch (Hampton Research) or MicroWell (Nunc) plate mix the protein solution and the reservoir and pipet it under a layer of paraffin oil. In this setup, all the reagents will be present at their final concentration and no significant concentration of either the protein or the reagents will occur in the drop.
4. Alternatively, a mixture of silicon oil and paraffin oil can be used that will allow water to diffuse to the surface of the oil layer, so that a gradual increase of the concentrations in the drop will occur.

3.4. Examples: Crystallization of Rat Kinesin

The rat kinesin crystals we obtained in our laboratory were crystallized with the hanging drop method using ammonium or lithium sulfate as precipitant (*see* **Notes 9** and **10**).

3.4.1. Crystallization of Rat Kinesin Dimer rK379

1. Prepare a Linbro plate and siliconized cover slips as described in **Subheading 3.1**.
2. Mix 1000 µL of reservoir solution containing 1.6 *M* ammonium sulfate, 200 m*M* sodium chloride, and 20 m*M* piperazine-*N*,*N*-*bis*(2-ethanesulfonic acid) (PIPES) (pH 7.5) and fill into the well (*see* **Note 11**).
3. Mix 6 µL of protein solution at 30 mg/mL (*see* Table1 for buffer) with 6 µL of reservoir solution.
4. Crystals grow from the clear solution at room temperature within 48 h. Growth may continue until the fourth day, at which time it should be stopped by the addition of 20 µL of reservoir solution to the mother liquor. Crystals are of an oblong teardrop-shape and generally reach a length of 0.75 to 1 mm and a diameter of 0.25 mm (*see* **Note 12**).

3.4.2. Crystallization of Rat Kinesin Monomer rK354

1. Prepare a Linbro plate and siliconized cover slips as described in **Subheading 3.1**.
2. Mix a reservoir solution of 1.8 *M* lithium sulfate and 20 m*M* PIPES (pH 7.5) and fill into the reservoir well (*see* **Note 13**).
3. Mix 5 µL of the protein solution at 20–25 mg/mL in 20 m*M* PIPES (pH 7.5), 100 m*M* KCl, 1 m*M* EGTA, 1 m*M* DTT with 5 µL of the reservoir and place the cover slip over the reservoir.
4. Crystals grow from the solution within 2 d at room temperature. They reach their final size within a week but remain smaller than the crystals from the rat kinesin dimer.

4. Notes

1. Filter all buffers and stock solutions through a 0.22-µm filter and store them in sterile bottles or vials. In most cases, this abolishes the need to use antimicrobial agents such as sodium azide. PEG solutions should be stored in the dark or in dark containers.
2. Centrifuge the protein sample at 10,000*g* for 5–10 min immediately before use to remove aggregates and amorphous precipitate.
3. Other tissue culture plates can also be used (e.g., Costar). However, here the wells are more closely spaced and the elevated rim may be missing, which makes handling more difficult. Also, smaller cover slips may be required. The advantage of these would be a lower price for the plates.

4. Most crystallization experiments with kinesins have been successful at pH values between 7.2 and 7.5 (except hK349; *see* **Table 1**). This might be an incentive to begin the screening procedure around neutral pH. However, a general screening protocol varying the concentration of precipitants against different pH values might also be employed.
5. Screening will generally be performed with smaller drop sizes. After setting up the experiment observe the drop under a light microscope, possibly in a dark-field mode. Does a precipitate form? If a precipitate does form, what does it look like? Is it amorphous, or does it look microcrystalline? Consider the effect of temperature. If possible, set up your experiment at 4°C and at room temperature.
6. When mixing the protein and the precipitant, in most cases the ratio of protein solution and reservoir solution will probably be 1:1. However, this is no necessity. In fact, especially when using a screening kit employing a sparse matrix protocol, like the Crystal Screen kits from Hampton Research, a 1:1 ratio of protein and reservoir may already lead to supersaturation, so that the experiment will be a microbatch experiment rather than being governed by vapor diffusion. A higher protein to reservoir ratio may be advisable in such cases.
7. Once crystals have formed, increase the drop size to grow larger crystals.
8. As a rule, crystals will grow larger and be of better quality if the growth rate is slow. If microcrystals are formed, their growth rate may be reduced by more gradual equilibration with the reservoir in order to obtain larger sized crystals. This can be done by setting up a shallower gradient between the drop and the reservoir or by covering the reservoir with paraffin oil. A mixture of silicon oil and paraffin oil can be used that will allow water to diffuse, but it will reduce the rate of diffusion.
9. If you are not able to obtain crystals from a protein, even after trying different variants by mutagenesis, consider changing the protein source. For example, we have been able to obtain crystals of rat kinesin, but not of squid kinesin, despite numerous attempts.
10. Get your protein as pure as possible. In the case of rat kinesin rK379, only a few contaminating bands were visible after the MonoQ ion-exchange chromatography step. One of these was responsible for a yellow tint of the protein solution. Removal of this contamination by gel filtration was essential to get crystals.
11. The RK379 protein was initially crystallized in the presence of 2 m*M* EGTA. However, crystals grown in the absence of the chelator showed no difference to the original crystals, neither in morphology nor in resolution. Correspondingly, although RK354 crystals were initially formed in the absence of Mg^{2+} and the Mg^{2+} was not found in the first crystal structure, the addition of the ion to the buffer yielded crystals that had Mg^{2+}present, but were otherwise similar to the original crystals. This has been interpreted by the assumption that the "empty space" created by the absence of Mg^{2+} was occupied by a Li^{+} ion.
12. Growth of rK379 crystals for more than 4 d led to deterioration of crystal shape and/or to new nucleation on the surface of existing crystals and formation of twin crystals.

13. It was also possible to crystallize the monomeric construct RK354 with ammonium sulfate. Drops of 8 µL protein (30 mg/mL) in 20 m*M* PIPES (pH 7.5), 50 m*M* NaCl, 2 m*M* DTT, 1 m*M* NaN_3 and 8 µL of 1.8 *M* ammonium sulfate were equilibrated over a reservoir of 1.8 *M* ammonium sulfate and 50 m*M* NaCl. However, the crystals obtained with lithium sulfate diffracted significantly better. This was possibly caused by the fact that the crystals had to be frozen in order to yield a complete dataset from the X-ray beam, and that the crystals grown in ammonium sulfate became very fragile when suspended in cryo protection buffer. In contrast, crystals grown in lithium sulfate were more stable.

Acknowledgment

We thank Stefanie Freitag for critical reading of the manuscript and suggestions.

References

1. Vale, R. D. and Fletterick, R. J. (1997) The design plan of kinesin motors. *Annu. Rev. Cell Dev. Biol.* **13**, 745–777.
2. Mandelkow, E. and Johnson, K. A. (1998) The structural and mechanochemical cycle of kinesin. *TIBS* **23**, 429–433.
3. Goldstein, L. S. B. and Philp, A. V. (1999) The road less traveled: emerging principles on kinesin motor utilization. *Annu. Rev. Cell. Dev. Biol.* **15**, 141–183.
4. Endow, S. A. (1999) Determinants of molecular motor directionality. *Nature Cell Biol.* **1**, E163–E167.
5. Kull, F. J., Sablin, E. P., Lau, R., Fletterick, R. J. and Vale, R. D. (1996) Crystal structure of the kinesin motor domain reveals a structural similarity to myosin. *Nature* **380**, 550–555.
6. Sack, S., Müller, J., Marx, A., Thormählen, M., Mandelkow, E.-M., Brady, S. T. and Mandelkow, E. (1997) X-ray structure of motor and neck domains from rat brain kinesin. *Biochemistry* **36**, 16155–16165.
7. Kozielski, F., Sack, S., Marx, A., Thormählen, M., Schönbrunn, E., Biou, V., et al. (1997) The crystal structure of dimeric kinesin and implications for microtubule-dependent motility. *Cell* **91**, 985–994.
8. Sablin, E. P., Kull, F. J., Cooke, R., Vale, R. D., and Fletterick, R. J. (1996) Crystal structure of the motor domain of the kinesin-related motor NCD. *Nature* **380**, 555–559.
9. Sablin, E. P., Case, R. B., Dai, S. C., Hart, C. L., Ruby, A., Vale, R. D., Fletterick, R., J. 1998. Direction determination in the minus-end-directed kinesin motor Ncd. *Nature* **395**, 813–816.
10. Gulick, A. M., Song, H., Endow, S. A., and Rayment, I. (1998) X-ray crystal structure of the yeast KAR3 motor domain complexed with Mg. ADP to 2. 3 Å resolution. *Biochemistry* **37**, 1769–1776.
11. Sack S., Kull, F. J., and Mandelkow, E. (1999) Motor proteins of the kinesin family. Structures, variations, and nucleotide binding sites. *Eur. J. Biochem.* **262**, 1–11.
12. Carter, C. W., Jr. and Sweet, R. M. (eds.) (1997) *Macromolecular Crystallography Part A*. *Methods in Enzymology* **276**.

13. Carter, C. W., Jr. and Sweet, R. M. (eds.) (1997) *Macromolecular Crystallography Part B*. *Methods in Enzymology* **277**.
14. McPherson, A. (1999) *Crystallization of Biological Macromolecules*. Cold Spring Harbor Laboratory, Cold Spring Harbor, NY.
15. Kozielski, F., Schönbrunn, E., Sack, S., Müller, J., Brady, S. T., and Mandelkow, E. (1997a) Crystallization and preliminary X-ray analysis of the single-headed and double-headed motor protein kinesin. *J. Struct. Biol.* **119**, 28–34.
16. Sablin, E. P. and Fletterick, R. J. (1995) Crystallization and preliminary structural studies of the NCD motor domain. *Proteins* **21**, 68–69.

20

Structural Analysis of the Microtubule–Kinesin Complex by Cryo-Electron Microscopy

Fabienne Beuron and Andreas Hoenger

1. Introduction

The structures of microtubule–kinesin complexes have been intensely studied within the last few years by using negative stain or cryo-electron microscopy (cryo-EM; for a review, *see* **ref. *1***) and digital three-dimensional (3D) image reconstruction ***(2–4)***. On a working system, these methods constitute a straightforward approach to generate 3D data at around 20 Å resolution within a few weeks. Such maps all ow the interpretation the 3D configuration of protein domains such as the binding geometry of kinesin motor heads to tubulin protofilaments ***(5)*** or the configuration of dimeric kinesin motor domains when bound to microtubules under different nucleotide conditions ***(6–8)***. More recently, the availability of near-atomic-resolution data of the components of microtubule–kinesin complexes, namely the αβ-tubulin dimer ***(9)*** and several monomeric and dimeric kinesin motor constructs (for a review, *see* **ref. *10***), made it possible to interpret the structure of an intact microtubule ***(11)*** and the motor-tubulin interactions at near-atomic detail ***(8,12)***.

This chapter describes the preparation of frozen specimens for cryo-EM (**Fig. 1**) and how to record them in the microscope (**Fig. 2**). We will outline the essential steps to obtain microtubule–kinesin complexes. An introduction is given to the methods and software used today to obtain 3D reconstructions from cryo-micrographs of microtubule–kinesin complexes. However, a comprehensive description of digital image processing is beyond the possibilities of this chapter. Here, we will introduce helical 3D reconstruction, which is now commonly used to analyze electron microscopy data of microtubule–kinesin complexes (**Figs. 4** and **5**). The method is discussed here qualitatively and should provide a general guide to helical processing. Because the most

From: *Methods in Molecular Biology*, Vol. 164: *Kinesin Protocols*
Edited by: I. Vernos

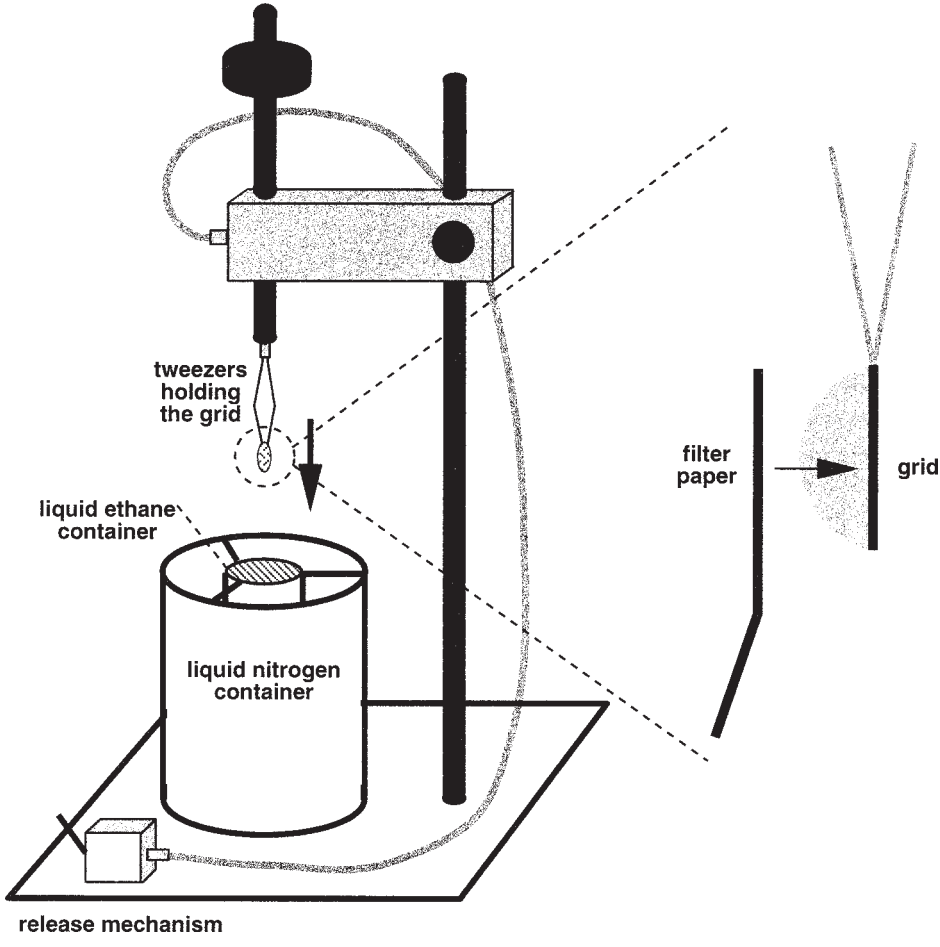

Fig. 1. Schematic drawing of a plunger setup for the quick freezing of EM grids. This setup can be relatively quickly copied by a workshop. The idea is to hold the grid with a drop of solution a few centimeters above a little (metal) bin filled with liquid ethane and cooled from a bath of liquid nitrogen. The parts that are holding the grid have to be constructed such that they be released and stopped again before the grid hits the bottom of the ethane container. Then, the grid will be blotted as shown on the right and quickly injected into the liquid ethane by releasing the entire grid-holding unit.

common types of microtubules are not showing a true helical symmetry ***(13–15)***, this chapter also describes how to obtain and identify helical microtubules (**Fig. 3**).

More recently, docking of atomic resolution data of individual components into the 3D scaffolds of large macromolecular assemblies (**Fig. 6**) has been

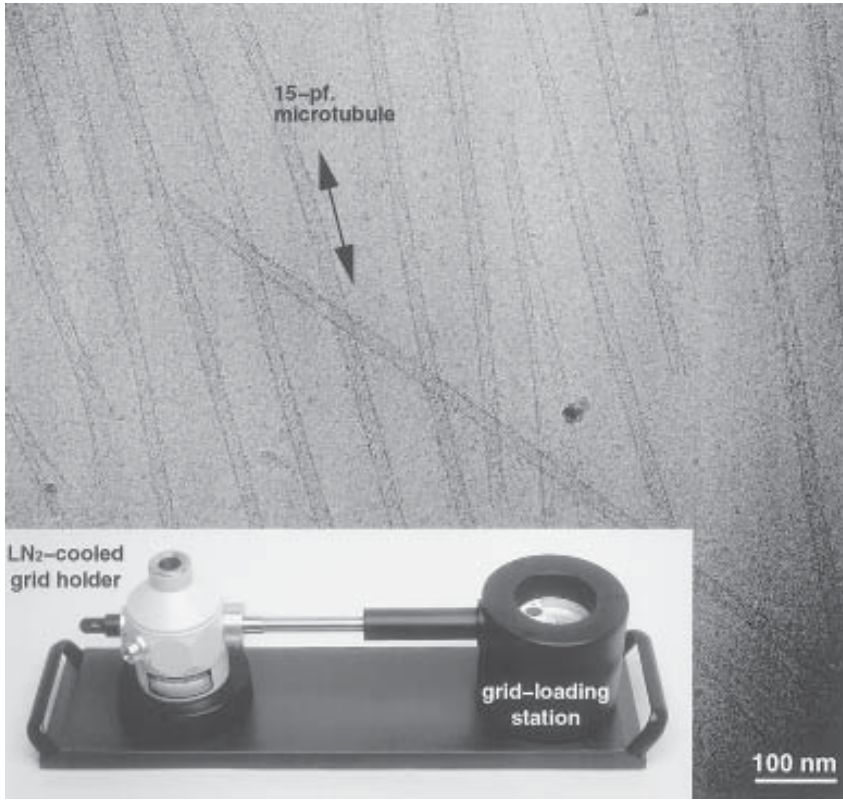

Fig. 2. Cryo-electron micrograph of microtubules decorated with kinesin motor domains. The kinesin decoration can be seen as little protrusions along the tubule edges. A helical 15-protofilament microtubule is indicated. The inset shows a cryo-holder (Gatan) and the grid-mounting station that is required for cryo-electron microscopy. The dewar on the left maintains the grid at LN2 temperature in the microscope.

shown to be very useful for studying protein–protein interactions in atomic detail ***(16)***. Several attempts to improve these docking procedures and to make them more reliable and reproducible are currently under development ***(17,18)***.

2. Materials

The requirements to chemicals and wet-lab equipment used here do not exceed the possibilities of standard biochemical laboratories. There is, however, some technical equipment that goes beyond that what is used by standard electron microscopy facilities. This special equipment used for cryo-microscopy is listed and discussed at the end of this section.

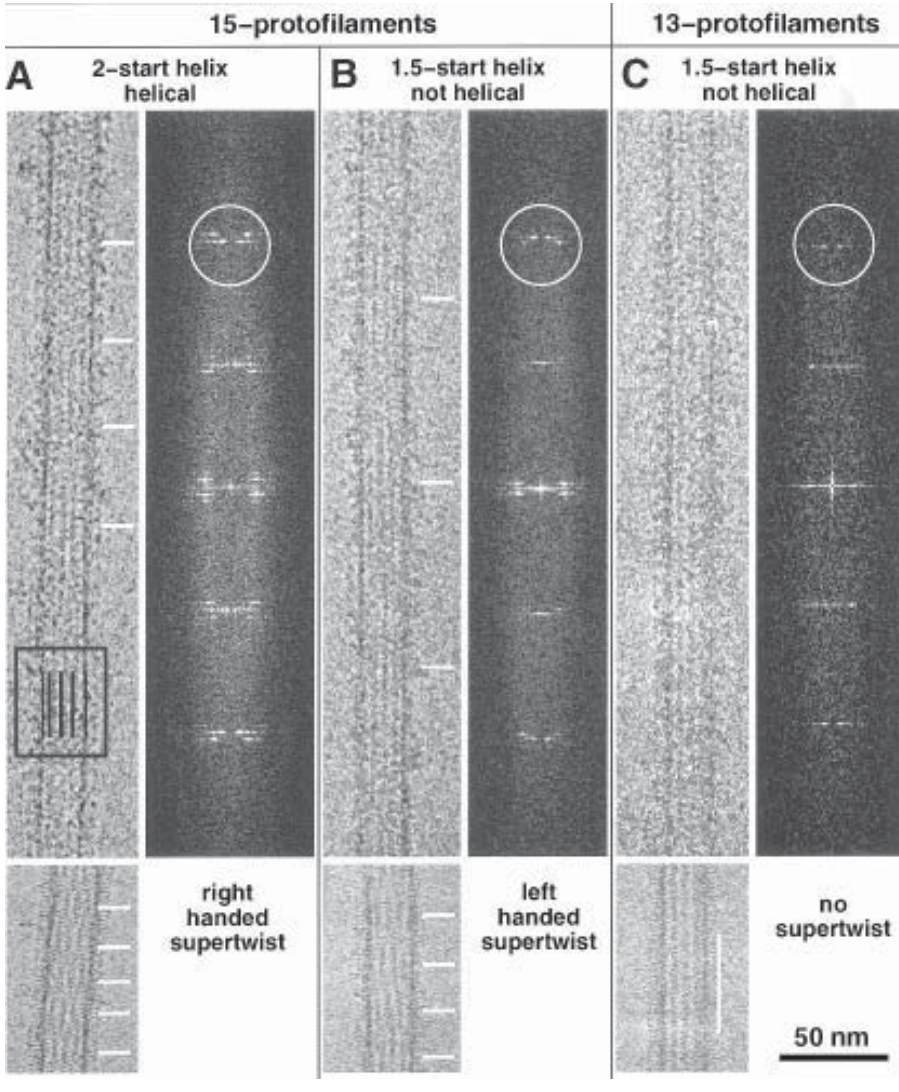

Fig. 3. Identification of helical 15-protofilament microtubules is crucial for a successful reconstruction. Column **(A)** shows a truly helical IS-protofilament microtubule with a right-handed supertwist. The tubule in **(B)** is also composed of 15 protofilaments, but has a left-handed and slightly longer, supertwist. These tubes contain a seam. As a comparison, 13-protofilament microtubules do not show any supertwist (C). The so-called Moiré repeats are a very sensitive measure for protofilament number and supertwist, forming alternating fuzzy and striated regions. Sharp lines appear where the projection of protofilaments from top and bottom halves overlay each other (white bars); fuzzy areas occur where they are shifted by a half-

2.1. Proteins

For a successful start, the reader should have a reliable source of bovine or pig brain tubulin. Several protocols on how to purify tubulin are available in the literature (e.g., *see* **ref. *19***). The procedure is relatively straightforward. The reader needs access to a slaughterhouse, which allows him to obtain very fresh (!!) brain tissue. Tubulin at a quality suitable for electron microscopy is now also commercially available (e.g., CYTOSKELETON, Denver CO). All the tubulin used here should be free of glycerol! Store tubulin at –80°C or in liquid nitrogen (LN2). Consult the other chapters of this volume on how to obtain motor proteins (*see also* **Note 1**).

2.2. Chemicals and buffers

The chemicals used here that need special attention are as follows:

1. Taxol to stabilize microtubules.
2. Nucleotides (GTP, ATP, ADP).
3. Nonhydrolyzable nucleotide analogs such as 5'-adenylyl imidophosphate (AMP–PNP) (the best source to our personal knowledge is ICN, Costa Mesa, CA).
4. Apyrase (2 U/mL) is used to maintain a ATP-free environment to obtain motor conformations in a nucleotide-free state.
5. Water-free dimethylsulfoxide (DMSO) is required during tubulin polymerization to enhance the amount of helical (15 protofilament) microtubules or flat tubulin sheets where desired.

   The sheets described here should not be confused with Zinc-induced tubulin sheets which show a different (antiparallel) protofilament arrangement. Zinc-induced sheets were mostly used for high-resolution electron crystallography ***(8)*** and do not appear to interact very well with molecular motors ***(20)***.
6. The standard buffer used is known in the literature as BRB80 (80 m*M* piperazine-*N*,*N*-*bis*[2-ethanesulfonic acid] [PIPES] [pH 6.8], 1 m*M* $MgCl_2$, 1 m*M* EGTA, 0.01 m*M* GTP). For tubulin polymerization, this buffer is supplemented with 2 m*M* GTP, 2 m*M* $MgCl_2$, and DMSO (5% final concentration to obtain 15-protofilament microtubules, and up to 15% to obtain tubulin sheets).

---

width. The position of the sharp lines have to be slightly off center, which is typical for odd numbers of protofilaments (box in A; compare also to the 13-protofilament microtubule on the right). The Moiré repeats are easier to observe on images that are axially compressed (insets below). Once some potential candidates are selected by optical inspection, one should check the diffraction patterns of these tubes, preferentially *after* the tubules were computationally straightened. The pattern of the layerlines at 1/4-nm (rings) identify the right-handed (left) from the left-handed supertwisted tubes (center). The layerlines at this position fall into one with tubes without supertwist (right). The distance from the equator to the 1/4 nm layerline should be about ×34 the spacing of the first layering (*see also* **Fig. 4**).

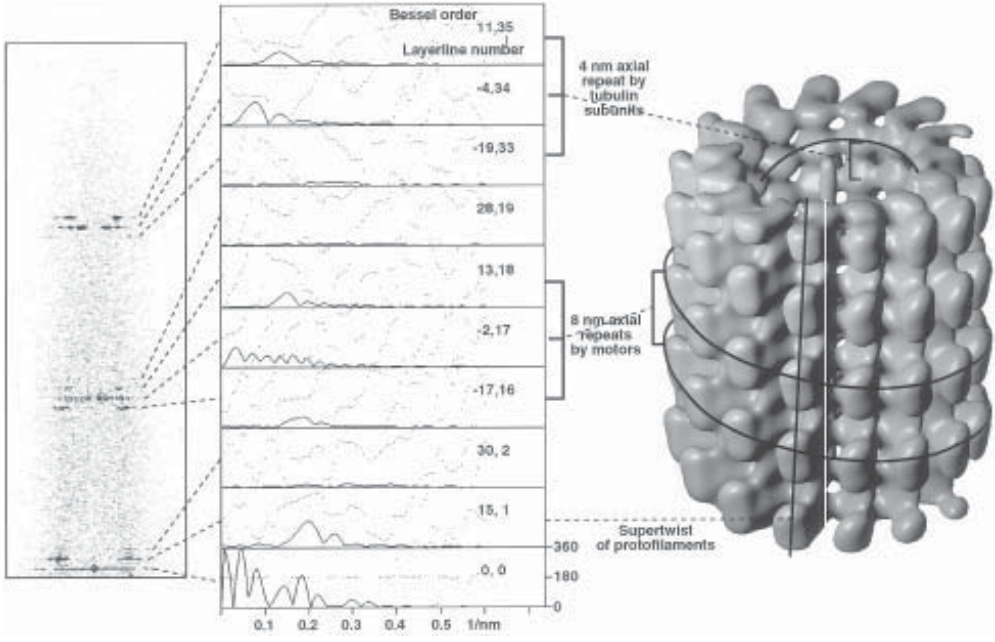

Fig. 4. Correlation of layerlines, layerline numbers, Bessel order, and the real-space features of a helical microtubule. The phase (dotted lines) and amplitude values (continuous lines) of layerlines as they appear on a diffraction pattern can be plotted as shown here. The resolution along the x-axis increases from the meridian on the left towards the right. The scale is nm^{-1}. The position of the first layerline in such a pattern is given by the helix with the longest helical pitch, which, in this case, is the protofilament supertwist. Because there are 15 protofilaments in the microtubule they form 15 parallel, right-handed supertwisted helices. Accordingly, the corresponding Bessel order of the first layerline is +15 (+ for right handed). There are two parallel left-handed helices with a pitch of 16 nm connecting motors laterally which form an axial 8-nm repeat. Accordingly, the bessel order of this hayerline is –2. Its layerline number is given by the sampling determined by the first layerline spacing and comes to 17 here. Four left-handed parallel helices create a 4-nm repeating pattern on the microtubule. The corresponding layerline is twice as far from the equator than the 1/8-nm layerline and has a Bessel order of –4 (four parallel left-handed helices) and the layerline number is 34. The convolution of the supertwist with the shorter pitched helices is creating a set of three strong layerlines clustered around the layerlines from the 8-nm and 4-nm repeats. These three hayerlines merge to one in a microtubule without supertwist since there the layerline spacing is given by the (noncontinuous !) 12-nm helix instead (*see* **Fig. 3C**).

7. No special chemicals are required for cryo-EM except gaseous ethane or propane to quick-freeze the specimens (*see* **Subheading 3.**).

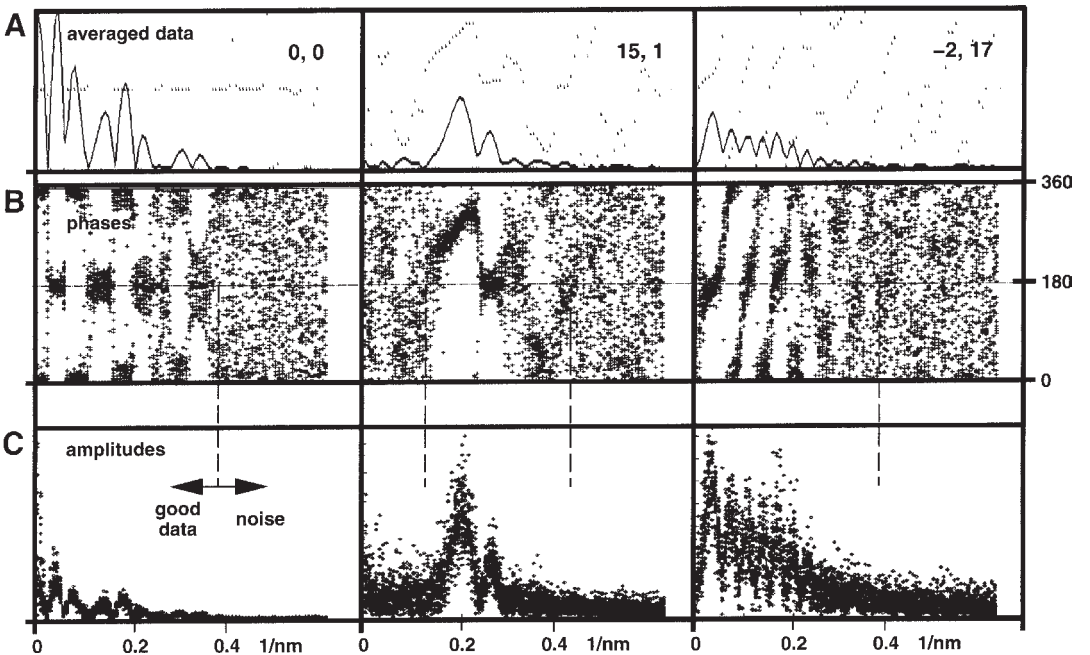

Fig. 5. The overlay of phase/amplitude plots from several individual datasets give you a measure for the quality in the data. Prior to this, all datasets have to be shifted to the same phase origin. A Averaging of a reasonable amount of datasets will automatically reduce the noise contribution in the resulting 3D map. The plots in row **(A)** show the phase (dotted line) and the amplitude values (solid line) along three selected layerlines as they emerge from averaging the data shown in **(B)** (phases) and **(C)** (amplitudes). These values were finally taken to create a 3D map as shown in **Fig. 4** (right) and **Fig. 6**. The amplitude values allow one to assess the contribution of the particular layerline, and the scattering of the phases shows the extent of reliable image data. Data are useful only in areas where the phases of the individual dataset are clustering roughly at the same position. Each dot on the plot at the bottom correspond to one phase or amplitude value. Areas with a random distribution of phases can only be considered as noise.

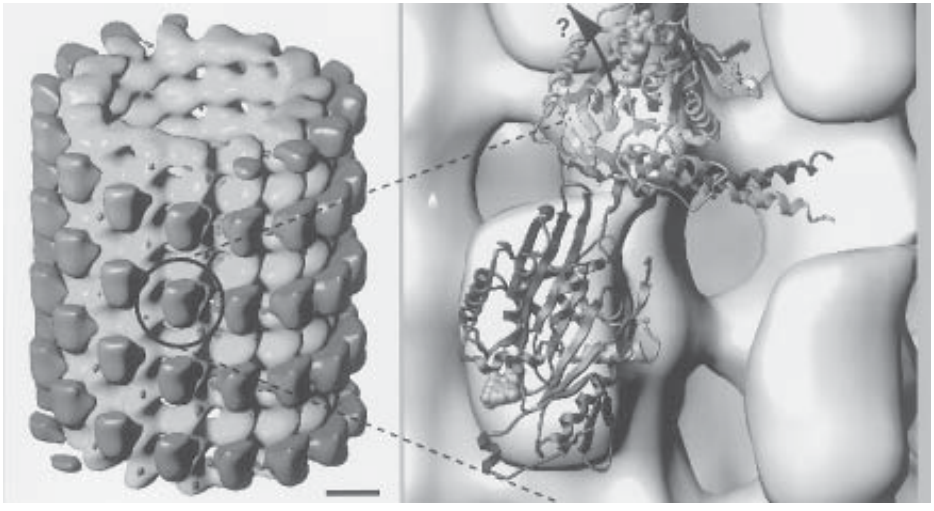

Fig. 6. Electron microscopy 3D data of macromolecular assemblies at a resolution shown here can be supplemented with the atomic resolution EM, X-ray, or NMR structures of the individual components if available. Shown here is the docking of the high-resolution X-ray map of dimeric rat kinesin into an intermediate resolution EM map of a microtubule–kinesin complex. This will allow one to interpret the interaction of tubulin and motor domain at atomic detail. These docking experiments may also reveal strong conformational changes between the state of a molecule in a 3D crystal and the situation in a more native environment. The example shown here demonstrates that the second head in the kinesin dimer (light gray) changes position upon binding to the microtubule surface. It may be bound to the next adjacent binding site (arrow), or it may be completely separated from the first head through a melting of the coiled-coil interaction and simply diffused away (see **ref.** ***10***).

8. A 2% solution of uranyl acetate or a 0.8% solution of uranyl formate is typically used for negative-stain microscopy ***(21)***.

2.3. Nonstandard Technical Equipment Related to cryo-EM

Cryo-EM requires access to some equipment not regularly available in standard electron microscopy labs. Special attention should also be given to the microscope that will be used.

1. The microscope should be designed to obtain high-resolution images and has to be equipped with a low-dose setup (e.g., FEU-Philips Tecnai-12 and up, JEOL-1200, Hitachi H7000, or LEO EM910/912). This allows one to focus the image next to the actual area of interest to avoid electron radiation damage ***(22)***.
2. The vacuum system should be in excellent condition to minimize contamination (which could build up onto the cold specimen and, hence, reduce the contrast).

3. Cryo-microscopy requires access to a special cryo-holder to keep the specimen at liquid nitrogen temperature. The most widely used cryo-holders are produced by Gatan (Pleasanton CA; *see* **Fig. 2**).
4. The microscope should be equipped with built-in (e.g., as on a Phillips CM120- or Teenz-12-Biotwin) or an added LN2-cooled anti-contamination blades (e.g., Gatan). The items listed under 3 and 4 might be quite expensive! (Cryo-holder with pump stand, approx $40,000–50,000 US.
5. On the lower-cost side, preparation of frozen samples requires a plunger for quick-freezing of samples (*see* **Fig. 1**), and LN_2 storage dewars.
6. With samples as the ones presented here it is recommended to use electron microscopy grids (e.g., 300-mesh copper grids) coated with a holey film to image the specimen embedded in amorphous ice (vitrified buffer) without carbon/formvar support. This increases the signal-to-noise ratio and reduces flattening artifacts of a cylindrical structure such as a microtubule.
7. Holey films can either be prepared by the reader himself (requires access to an evaporator to coat the grids with a thin carbon film, 100 Å thick at most, under high vacuum) or are now commercially available as well (e.g., Plano, Wetzlar, Germany).
8. The reader should have access to some computer-related equipment such a high-precision negative scanner (e.g., Zeiss SCAI scanner, Perkin Elmer, Hi-Scan), which allows one to scan a micrograph at step sizes in the range of 10–20 µm (on the negative).
9. Another relatively expensive item is a UNIX-based workstation such as a Silicon Graphics (SGI), SUN, or DEC-Alpha workstation. Unfortunately, most of the software used today for digital 3D reconstructions of electron microscopy data still does not run on PC platforms.
10. There are several software packages available for digital 3D reconstructions. Some are commercially available (e.g., IMAGIC; ***[23]***), others are public domain for nonprofit institutions or may be purchased with a small license fee (e.g., SPIDER). Here, we are using a public-domain package called PHOELIX ***(24)*** which combines two different packages for an optimal performance with helical reconstructions of actin-based macromolecular assemblies (SUPRIM ***[25]*** and MRC ***[26]***).

3. Methods

3.1. Microtubule Polymerization

One of the first steps to obtain microtubule–kinesin complexes is the generation of microtubules or tubulin sheets (i.e., opened-up microtubule walls with parallel protofilaments). If the microtubules are used for subsequent helical 3D reconstruction one has to take special care in the preparation of tubules that are composed of 15 protofilaments. Most common types of microtubules are carrying a so-called seam that interrupts the helical symmetry ***(13–15)*** and, therefore, cannot be used for helical analysis (*see* **Notes 7** and **8**).

1. Prepare fresh BRB8O buffer (*see* **Subheading 2.2.**; or use aliquots stored at –20°C). PIPES will dissolve only at close to neutral pH.
2. Prepare a 2X polymerization mixture: GTP 4 m*M*, MgCI, 8 m*M*, taxol 40 µ*M* in 100% DMSO, 10 µ*M* phenylmethylsulfonyl fluoride (PMSF), 10% DMSO to (or 30% for sheets) complete to, for example, 100 µL with BRB8O buffer. Do not mix GTP and $MgCl_2$ concomitantly (risk of precipitation).
3. Tubulin is polymerized at a final concentration of 5 mg/mL by adding an equal volume of the tubulin solution and the polymerization mixture for 20 min at 37°C, followed by an incubation at room temperature for 1 h. When polymerization is achieved, the solution should show tiny bubbles that are trapped by the increased viscosity.
4. Wash the microtubules by centrifugation in a microcentrifuge at 10,000*g* for 3 min. DMSO forms a turbid cushion in which the microtubules set. Discard the supernatant down to the cushion. Add fresh BRB8O buffer supplemented with 20 µ*M* taxol and resuspend the pellet (usually invisible) carefully (*see* **Note 4**).

Microtubules polymerized in the presence of taxol are stable for several hours at room temperature and should not be stored on ice. Nonstabilized microtubules are extremely cold-sensitive! In our experience 5% DMSO was sufficient to yield a reasonable amount of 15-protofilament tubes. 15% of DMSO was added to prepare tubulin sheets (*see* **Note 5**).

3.2. Decoration of Microtubules with Motor Head Domains

The decoration of microtubules with motor head domains can either be performed in the test tube or directly on an electron microscopy grid. It is recommended to clarify all protein solutions from aggregates by a short spin (3–5 min) at 100,000*g* (*see* **Note 4**).

3.2.1. Decoration in Solution

1. Decoration in solution is done by diluting the microtubules with BRB8O to obtain a final concentration of approx 0.5 mg/min (after the addition of motor solution).
2. Motor head domains are added in a two- to threefold molar excess over tubulin dimers and incubated at room temperature for about 3–5 min.
3. Depending on the nucleotide state desired, one may add the appropriate amount of ATP, ADP, AMP–PNP, or other analogues (usually in the range of 1–2 m*M*).
4. To obtain a nucleotide-free binding state, it is recommended to incubate all solutions briefly with a small amount of apyrase to digest residual nucleotides.
5. The final solution should then be used immediately to prepare stained or frozen grids (*see* **Subheading 3.3.**).

3.2.2. Decoration on the Grids

Some motor domains, and particularly double-headed constructs, may have a tendency to bundle microtubules. In these cases, it may be better to perform

the actual decoration of microtubules directly on the grid. In our experience, bundling of microtubules may occur with both, single-headed as well as double headed motor constructs (*see also* **Note 7**).

1. Adsorb 5 µL of a 0.5-mg/mL solution of polymerized microtubules for approx 1 min to a plasma glow-discharged carbon-coated grid (for cryo-EM: a holey carbon film). Glowdischarging reduces the hydrophobicity of carbon films and promotes the adsorption.
2. Wash the grid briefly in 20 µ*M* BRB8O-taxol supplemented with the desired nucleotide and then add the motor solution at a two- to threefold molar excess over tubulin dimers.
3. Incubate for 3–5 min at room temperature, wash again onto 1–2 drops of BRB8O-taxol 5 µ*M* supplemented with the desired nucleotide. After a short wash on distilled water, the grid is ready to be stained or frozen (go to **Subheading 3.3.**, **step 2**).

3.3. Quick-Freezing of Specimens

The preparation of frozen samples is a slightly tricky step that needs a bit of experience. It requires a so-called plunger (**Fig. 1**) which allows to quick-freeze samples in such a way that the embedding ice remains in a vitreous (amorphous) state. This is achieved by injecting them in a slush of liquid ethane (or propane). Vitrification is crucial for the structure preservation keeping the sample in a most native state; this is one of the major advantages of cryomicroscopy over any other sample preparation method. It is recommended to monitor the room's temperature and humidity and keep it as stable as possible. The humidity should not be too low (preferably above 30%) to avoid cooling of the specimen by evaporation (*see* **Notes 5–7**).

1. Prepare the plunger setup as suggested in **Fig. 1**. Mount a small metal container (5–10 mL) into a liquid-nitrogen bath. Condense the ethane gas in that container by flowing a stream of gas along the metal walls. This can be done by mounting a Pasteur pipet at the end of a tube that comes from the ethane bottle and holding its tip to the lower edges. The ethane will then condense and slowly fill up the container.
2. If the decoration has been performed in solution, adsorb 5 µL of the solution to the grid for approx 1 min. If the decoration has been done on the grid following the procedure in **Subheading 3.2.2.** go straight to **step 2**. Try to avoid to high concentrations of DMSO, glycerol and so forth because these solvents act as cryogens (*see* **Note 8**).
3. Blot excess protein solution from the grid and wash it briefly in buffer supplemented with the required nucleotides.
4. Dip the grid to the surface of a drop of wash solution and mount the tweezers with the grid to the plunger and keep the wash drop still hanging on. Use a rubber band to keep the tweezers closed.

5. Blot the grid with a small stripe of filter paper (e.g., Whatman No. 1) so that it does not dry out completely (*see* **Fig. 1**). This step may need some training and experience. It is best not to become discouraged too early by initial failures. In our own experience, it works better when the filter paper is held flat against the grid by using the capillary force to keep it in place while liquid flows into the paper. Once enough liquid is pulled from the grid, it releases spontaneously from the filter paper. This is the moment when it should immediately be plunged into the liquid ethane (*see* **Note 6**).
6. The grid should be kept under LN_2 during all transfers. Mounting grids on a cryo-holder requires a special cryo-transfer stage (**Fig. 2** inset). Once frozen, the grids should be exposed as short as possible to humid air!
7. Frozen specimens can be stored indefinitely under LN_2 (*see* **Note 7**).

3.4. Imaging of Frozen Specimen

Recording cryo-micrographs requires access to special equipment as described in **Subheading 2.3**. Images may be recorded on film or by using a slow-scan CCD camera where available. For regular cryo; samples it is common to generate contrast by defocusing between 1–3 µm (the measure of defocus given by the readout of the microscope is somewhat arbitrary. For accurate defocus value determination *see* **ref.** ***27***. We normally use a defocus range between 1.2 and 1.8 µm for motor-microtubule complexes. If film is used, then the micrographs have to be digitized by a scanner for further processing. In the case of an application as shown here the expected resolution is typically in the range of 25 Å. Therefore, the images should be scanned at least with a step size that brings one pixel to about 20–30 $Å^2$. We normally record our images at a magnification of ×37,000. Accordingly, the scanner step size has then to be about 20 µm on the negative (= 5.3 Å on the sample; *see also* **Notes 9** and **10**).

3.5. Identification of Helical Microtubule–Kinesin Complexes

To obtain accurate 3D maps by helical reconstruction methods it is absolutely crucial to verify the helical symmetry of the microtubule under investigation. In a good experiment, there are between 3% and 5% useable helical 15-protofilament tubes (*see also* **Note 3**). Identification and verification should be done as outlined below and in **Fig. 3**:

1. Examine the Moiré pattems created by the projection of the supertwisted protofilaments.
2. Check the lateral asymmetry of axially running line patterns caused by the projection of superimposed protofilaments (box in **Fig. 3A**).
3. Carefully analyze the diffraction pattern and measure the observed layerline spacing.

The Moiré pattem is typical for supertwisted microtubules and alternates between striated and fuzzy regions with a spacing of about 130–150 nm in the case of helical 15-protofilament microtubules (*see* **Fig. 3A**). The striated regions on 15-protofilament microtubules (and on all other tubules composed of an odd number of protofilaments) are asymmetric with respect to the tubule axis (box in **Fig. 3A**). This is a reliable feature that allows one to separate 15-protofilament tubes from the similarly looking 16-protofilament microtubules that sometimes copolymerize under the conditions described here. The 16-protofilament microtubules are usually helical as well, but occur at an even lower rate than the 15-protofilament ones. Any microtubule with an even number of protofilaments shows a symmetrical pattern.

3.6. Digital Image Analysis

Digital image analysis as discussed here serves two main purposes: (1) separation of the image signal from random image noise and (2) the reconstruction of a 3D macromolecular assembly from a set of 2D projections recorded at different angles.

3.6.1. Averaging

Improvement of the signal-to-noise ratio is essential for any type of electron-microscopy-related 2D and 3D image reconstruction, especially when done from cryo-micrographs. The low contrast of ice-embedded specimen and the low-dose imaging conditions are leading to extremely noisy images (*see* **Fig. 2**). Signal enhancement is generally achieved by averaging as many identical image elements as possible. Under ideal conditions, the signal-to-noise ratio increases by the square root of element numbers ***(28)***. This procedure works because the image signal in identical elements is constant, whereas the image noise (caused by inelastic scattering, quantum noise, etc.) from one element to another is randomly distributed. This is only successful, however, when identical image elements are properly aligned prior to averaging (i.e., refinement for an identical phase origin in Fourier space), otherwise detailed image features will be lost. Accurate alignment and variabilities within the image elements are key factors for the final resolution of a reconstruction. Nature can be quite helpful sometimes as it may directly align individual particles for us in the forms of 2D or 3D crystals, icosahedral virus capsids or helices. In the case of microtubule–kinesin complexes, we are taking advantage of helical microtubules. Similarly, tubulin sheets are a prealigned set of tubulin–motor complexes in a 2D crystalline array. In both cases, we can use the prealigned image elements to improve the signal-to-noise ratio. In the case of a helix, our number of identical image elements is determined by the number of helical repeats

along the tubule axis. For assemblies are shown here, there are typically 8–10 repeats per micrograph. In the case of a (perfect) 2D crystalline array, we have as many aligned identical elements as unit cells in the crystal, which can be several hundreds per picture. Consequently, 2D crystalline arrays reveal a much larger number of identical image elements than helices, but helices directly reveal identical image elements with a complete set of helical building blocks (has αβ-tubilin-kinesin complexes) at all angular projections required for a 3D reconstruction.

3.6.2. 3D Reconstruction

Here, we will describe qualitatively the essential steps that should be understood to assess the quality of helical 3D reconstructions such as the ones shown here. It will not be possible to give a comprehensive introduction to digital 3D reconstruction methods within the limits of this chapter (for more detailed information, *see* **refs. *2–4***; an overview about the most common methods is given in **ref. *29***). We will also not go into the aspects of correcting images for the contrast-transfer function of an electron microscope. At the resolutions discussed here, this is not yet an absolute necessity. However, keep in mind that at typical defocus ranges used for cryomicroscopy, all data that exceeds a resolution of approx 25 Å may be contrast inverted.

1. As mentioned in **Subheading 3.5.** the first step to a successful reconstruction is the verification of the assumed helical symmetry. How this can be done with microtubules is shown in **Fig. 3**. Generally, a helix can be described as a one-dimensional crystal with regular repeats along the helix axis. Accordingly, the corresponding diffraction pattern (showing the amplitude distribution after a Fourier analysis in reciprocal space) reveals sampling along the tubule axis, caused by repetitive, equally spaced features, but continuous information laterally. Therefore, diffraction of helical assemblies reveals so-called layer lines rather than distinct spots such as found in the diffraction image of 2D crystals (*see* **Figs. 3** and **4**).
2. The next step is the correct determination of all the parameters describing the symmetry of a helical assembly. These are the helical selection rule (lowest number of asymmetric units and helical turns, which are necessary to describe one full repeat; here we used 257/137, but this may vary slightly), handedness, layerline numbering, and assignment of bessel orders in Fourier space. **Figure 4** shows a correctly indexed layerline pattern of a 15-protofilament microtubule and points out the relationship of the different helical paths within a microtubule with the observed layerlines on a diffraction image. Once the helical parameters are known, we can assign the correct angles to the different projections of the asymmetric units (i.e., individual tubulin–motor complexes in this case) along a helical turn.
3. Processing of tubular assemblies usually requires computational straightening. Check the diffraction of a microtubule before and after unbending.

4. Now, individual datasets may be averaged. A single projection of a full helical repeat contains two complete helical datasets, one from the so-called near side (upper half of the tube), and one from the far side (lower half). This is theoretically sufficient to yield a 3D reconstruction with isotropic resolution. However, as pointed out in **Subheading 3.6.1.**, in reality this will result in a rather noisy unreliable reconstruction because not much averaging has been applied so far. A reliable reconstruction with a significantly improved signal is obtained by averaging at least 10–20 good microtubules (i.e., tubules with good diffraction such as shown in **Figs. 3** and **4**) consisting of approx 6–10 repeats each. Overlaying individual origin-refined phase/amplitude plots of selected strong layerlines allows one to assess the quality of the data in the manner demonstrated in **Fig. 5**. The clustering of individual phase values along these layerlines clearly reveal the resolution limits in the resulting 3D map. The data are considered noisy where phases are scattered randomly. Data averaging can, in principle, be done in both real or Fourier space. Which manner to choose depends largely on the software available. Averaging in Fourier space is essentially an addition of vectors with amplitudes and phases at every sample point along a layerline and eliminates automatically irrelevant information.
5. Once all helical parameters are determined and an averaged dataset is obtained, the 3D Fourier space can be calculated. This reveals a complete set of angular projections from the individual helical building blocks (i.e., tubulin–motor complexes). Back-transformation then creates the real-space 3D volume.

3.6.3. Interpretation of 3D Maps

There are of several ways to interpret EM-derived 3D maps at intermediate resolution. Individual domains can be identified (e.g., by calculating maps with and without a specific domain and subsequent calculation of difference maps), which allows one to identify the additional densities. Two separate sets of maps can be tested against each other using a Student's *t*-test. This test allows determine the significance of density differences between two averaged data sets, that is, this can be very useful if undecagold labels have been used to identify a certain site of interest and the map is tested against a nonlabeled one.

Very powerful interpretations can be done by supplementing EM-derived 3D data of macromolecular complexes with X-ray, EM, or nuclear magnetic resonance (NMR)-derived high-resolution maps of individual components (**Fig. 6**). If done carefully, this will allow one to identify protein interactions within a complex at near-atomic detail ***(16)***. The methods, however, to perform such docking experiments in a quantitative way are still developing (***17,18***; N. Volkmann and D. Hanein, personal communication) and do not yet seem to work very satisfactory. It is highly recommended to consider additional aides such as site-directed gold labels ***(30)***, site-specific mutagenesis (on kinesin

[31]) or footprinting data (on kinesin *[32]*) to confirm the correct position of a high-resolution structure within an intermediate resolution EM map of an entire complex. A manual docking of X-ray structures into 3D EM maps can be done by using the software package '0' *(33)*.

4. Notes

1. Both unpolymerized tubulin and most kinesin like motor domains are relatively unstable proteins and have to be kept frozen or on ice as long as possible. However, when decorating nonstabilized microtubules, one should warm the motor solution briefly before it is added to the tubes to avoid their depolymerization resulting from a temperature shock. This is particularly important when the decoration is done directly on the EM grid.
2. Make sure your microtubules are regularly decorated. Most image reconstruction methods rely on some sort of symmetry in a macromolecular assembly that is used to collect a large number of identical image elements to be averaged together. In the case of microtubule–kinesin complexes, these image elements are the individual αβ-tubulin dimer–motor complexes arranged in a helical assembly (in the case of 15-protofilament microtubules) or 2D crystalline array. A reliable and reproducible reconstruction of a tubulin–motor complex depends on a complete decoration with motor head domains. Anything that is significantly below a stoichiometric ratio of motor domains to tubulin dimers will result in a reduced representation of the actual motor mass andlor a wrong representation of certain image features. It is therefore crucial to know the percentage of active motor heads in your solution to calculate a reasonable ratio of active motors to microtubule binding sites. In our experience, a two- to threefold molar excess is sufficient for most motor domains to achieve complete decoration. Just keep in mind that double-headed motor constructs (i.e., the ones that dimerize through a portion of their stalk), may decorate with a stoichiometry of two motor domains per tubulin dimer. Constructs with long stalks tend to decorate incompletely probably because of sterical hindrance of the adjacent binding site by the stalk.
3. Microtubules are quite polymorphic structures. Not only do they vary their number of protofilaments from one tube to the next, but they may change even within a tube. Other symmetry-disrupting events such as missing or wrongly inserted dimers and even sudden changes in supertwist are occasionally observed as well. Check the microtubules carefully and compare whenever possible to a well-known tube that has been confirmed to be a true helical 15-protofilament microtubule. The Moiré repeats are a very sensitive measure for the microtubule structure and should be determined carefully. They are best observed either in a computer by compassing a digitized micrograph along the microtubule axis, as shown in **Fig. 3**, or simply by using prints of micrographs and looking down along a microtubule axis under a steep angle (close one eye). With some experience, one will *see* the repeats directly on a micrograph. It is always a very good idea to check micrographs quickly at an optical bench. This allows one to pre-

select potential candidates and, as a plus, shows the overall quality (resolution, focus, astigmatism) of a micrograph.

4. It is highly recommended for electron microscopy to clarify all protein solutions used by a 3- to 5-min spin at approx 100,000*g* in a micro-ultracentrifuge. Small aggregates are usually visible in the microscope and may severely obstruct a reconstruction.
5. To reproducibly freeze samples, it is important to monitor, and if possible stabilize, the air temperature and humidity in order to avoid evaporation of the specimen ***(34)***. Some people freeze their samples in a cold room where the humidity is generally very high, others mount their plunger in a humidity controlled chamber (e.g., *see* **ref. *35***). In our experience, a cold room can be quite useful, but one has to be careful about cooling the sample prior to blotting and freezing, that is, this is particularly important if one works with nonstabilized microtubules that are very cold sensitive. Any preparation prior to freezing should then be done outside the cold room.
6. Liquid ethane freezes at liquid-nitrogen temperature. The ethane ice builds up slowly from the border of the little container and can either be removed by bubbling fresh ethane gas through the slush or by scratching it off the walls with a warm scalpel blade. The freezing of grids works best if the ethane is a slush of liquid and frozen parts. When adjusting the stopping height of the plunger keep in mind that frozen ethane builds up relatively rapidly from the bottom. Keep frozen grids as best as possible away from humid air (e.g., control your own breath when mounting them on the EM holder and whenever they are handled elsewhere!). Be careful when handling liquid ethane! In its liquid state it behaves like oil and causes burn marks on the skin. Protect your eyes!
7. Grids can be stored in a LN_2 dewar for an extended period of time. We keep our grids in a small plastic storage box that takes four grids at a time and which can be closed with a lid.
8. Washing the microtubules with DMSO-free buffer is necessary to avoid the cryoprotection effect of DMSO, which may cause bubbling of the ice once the specimen is exposed to the electron beam. A last wash in distilled water may then be needed if problems with high-salt solutions are encountered. We found this to be unproblematic for microtubules, but a sudden change in buffer conditions may cause damage to other specimens. Excess GTP should be washed out prior to motor decoration to avoid any interference with the preferred nucleotide state of the motor head domains.
9. During the initial phase of an experiment, it is usually sufficient to check the motor-decoration of microtubules by negative-stain microscopy. This is much easier and faster than cryo-EM. Do not waste your holey grids for negative staining!
10. Image formation in the microscope is a complex process. In essence, image contrast is based on a combination of amplitude and phase contrast and is modulated by the so-called envelope function of the microscope and the contrast-transfer function (CTF) of the lenses. The latter is a focus-dependent function that reverses

the contrast of image elements at a certain resolution intervals. In order to record the most faithful representation of the object in the image, it is important to be aware of the defocus dependence of the contrast-transfer function in particular. As a rule of thumb, if you want to achieve a resolution of better than approx. 25A from cryo-micrographs, you should seriously consider correcting images for contrast modulations by the CTF.

11. If one experiences difficulties in getting 15-protofilament microtubules, one can increase the amount of DMSO to about 10%. Keep in mind, however, that too much DMSO shows a destabilizing effects on the tubes. In any case, be prepared to record a large number of micrographs, of which only a few percent will be usable later.
12. If buffers with high-salt concentrations are used, it may be necessary to briefly wash an adsorbed specimen prior to freezing with distilled water to avoid uneven ice.

References

1. Dubochet, J., Adrian, M., Chang, J.-J., Homo, J.-C., Lepault, J., MeDowall, A. W., and Schultz, P. (1988) Cryo-electron microscopy of vitrified specimens. *Quart. Rev. Biophys.* **21,** 129–228.
2. DeRosier, D. and Moore, P. B. (1970) Reconstruction of three-dimensional images from electron micrographs of structures with helical symmetry. *J. Mol. Biol.* **52,** 355–369.
3. Amos, L. A., Henderson, R., and Unwin, P. N. T. (1982) Three-dimensional structure determination by electron microscopy of two-dimensional crystals. *Prog. Biophys. Mol. Biol.* **39,** 183–231.
4. Frank, J. (1996) *Three-Dimensional Electron Microscopy of Macromolecular Assemblies* (Frank., J., ed.), Academic, San Diego, CA.
5. Hoenger, A. and Milligan, R. A. (1997) Motor domains of kinesin and Ncd interact with microtubule protofilaments with the same binding geometry. *J. Mol. Biol.* **265,** 553–564.
6. Hirose, K., Lockhart, A., Cross, R. A., and Amos, L. A. (1996) Three-dimensional cryoelectron microscopy of dimeric kinesin and ncd motor domains on microtubules. *Proc. Natl. Acad. Sci. USA* **93,** 9539–9544.
7. Arnal, I. and Wade, R. H. (1998) Nucleotide-dependent conformations of the kinesin dimer interacting with microtubules. *Structure* **6,** 33–38.
8. Hoenger, A., Sack, S., Thormaehlen, M., Marx, A., Mueller, J., Gross, H., and Mandelkow, E. (1998) Image reconstruction of microtubules decorated with monomeric and dimeric kinesins: comparison with X-ray structure and implications for motility. *J. Cell Biol.* **141,** 419–430.
9. Nogales, E., Wolf, S. G., and Downing, K. H. (1998) Structure of the u13 tubulin dimer by electron crystallography. *Nature* **391,** 199–203.
10. Mandelkow, E. and Hoenger, A. (1999) Structures of kinesin and kinesin-microtubule interactions. *Curr. Opin. Cell Biol.* **11,** 34–44.

11. Nogales, E., Whittaker, M., Milligan, R. A., and Downing, K. H. (1999) High-resolution model of the microtubule. *Cell* **96,** 79–88.
12. Sosa, H., Dias, D. P., Hoenger, A., Whittaker, M., Wilson-Kubalek, E., Sablin, E., et al. (1997) A model for the microtubule-Ned motor protein complex obtained by cryo-electron microscopy and image analysis. *Cell* **90,** 217–224.
13. Wade, R. H., Chrétien, D., and Job, D. (1990) Characterization of microtubule protofilament numbers; how does the surface lattice accommodate? *J. Mol. Biol.* **212,** 775–786.
14. Song, Y. H. and Mandelkow, E. (1995) The anatomy of flagellar microtubules: polarity, seam, junctions, and lattice. *J. Cell Biol.* **128,** 81–94.
15. Sosa, H. and Milligan R. A. (1996) Three-dimensional structure of ncd decorated microtubules obtained by a back-projection method. *J. Mol. Biol.* **260,** 743–755.
16. Baker, T. S. and Johnson, J. E. (1996) Low resolution meets high: towards a resolution continuum from cells to atoms. *Curr. Opin. Struct. Biol.* **6,** 585–594.
17. Wriggers, W., Milligan, R. A., Schulten, K., and McGammon, J. A. (1998) Self-organizing neural networks bridge the biomolecular resolution gap. *J. Mol. Biol.* **284,** 1247–1254.
18. Wriggers, W., Milligan, R. A., and MeGammon, J. A. (2000?) Situs: a package for docking crystal structures into low-resolution maps from electron microscopy. *J. Struct. Biol.* **125,** 185–195.
19. Hyman, A., Drechsel, D., Kellog, D., Salser, S., Sawin, K., Steffen, P., et al. (1991) Preparation of modified tubulins. *Methods Enzymol.* 196, 478–485.
20. Ray, S., Wolf, S. G., Howard, J., and Downing, K. H. (1995) Kinesin does not support the motility of Zn-macrotubes. *Cell Motil. Cytoskel.* **30,** 146–152.
21. Leberman, R. (1965) Use of uranyl formate as a negative stain. *J. Mol. Biol.* **13,** 606–611.
22. Glaeser, R. M. and Taylor, K. A. (1978) Radiation damage relative to transmission electron microscopy of biological specimens at low temperature. *J. Microsc.* **112,** 127–138.
23. Van Heel, M., Harauz, G., and Orlova, E. (1996) A new generation of the IMAGIC image processing system. *J. Struct. Biol.* **116,** 17–24.
24. Whittaker, M., Carragher, B. O., and Milligan, R. A. (1995) PHOELIX: a package for semi-automated helical reconstruction. *Ultramicroscopy* **58,** 245–259.
25. Schroeter, J. P. and Bretaudiere, J.-P. (1996) SUPRIM: Easily modified image processing software. *J. Struct. Biol.* **116,** 131–137.
26. Henderson, R., Baldwin, J. M., Ceska, T. A., Zemlin, F., Beckmann, E., and Downing, K. H. (1990) Model for the structure of bacteriorhodopsin based on high-resolution electron cryo-microscopy. *J. Mol. Biol.* **213,** 899–929.
27. Lepault, J. and Leonard, K. (1985) Three-dimensional visualization of unstained, frozen-hydrated extended tails of bacteriophage T4. *J. Mol. Biol.* **182,** 431–441.
28. Aebi U., Fowler W. E., Buhle E. L., and Smith, P. R. (1984) Microscopy and image processing applied to the study of protein structure and protein-protein interaction. *J. Ultrastruct. Res.* **88,** 143–176.

29. Hoenger, A. and Aebi, U. (1996) 3-D reconstruction from ice-embedded and negatively stained biomacromolecular assemblies: a critical comparison. *J. Struct. Biol.* **117,** 99–116.
30. Safer, D. Bolinger, L., and Leigh, J. S. (1986) Undeca-gold clusters for site specific labeling of biological macromolecules. *J. Inorg. Biochem.* **26,** 77–91.
31. Woehlke, G., Ruby, A. K., Hart, C. L., Ly, B., Hom-Booher, N., and Vale, R. D. (1997) Microtubule interaction site of the kinesin motor. *Cell* **90,** 207–216.
32. Alonso, M. C., Vandamme, J., Vandekerckhove, J., and Cross, R. (1998) Proteolytic mapping of kinesinlNcd-microtubule interface: nucleotide-dependent conformational-changes in the hoops L8 and L12. *EMBO J.* **17,** 945–951.
33. Jones, T. A., Zou, J. Y., Cowan, S. W., and Kjeldgaard, M. (1991) Improved methods for building protein models in electron density maps and the location of errors in these models. *Acta Crystallogr.* **A47,** 110–119.
34. Cyrklaff, M., Adrian M., and Dubochet, J. (1990) Evaporation during preparation of unsupported thin vitrified aqueous layers for cryo-electron microscopy. *J. Electron Microsc. Technol.* **16,** 351–355.
35. Trachtenberg, S. (1998) A fast-freezing device with a retractable environmental chamber suitable for kinetic cryo-electron microscopy studies. *J. Struct. Biol.* **123,** 45–55.

Index

METHODS IN MOLECULAR BIOLOGY™ • 164
Series Editor: *John M. Walker*

Kinesin Protocols

Edited by

Isabelle Vernos
European Molecular Biology Laboratory, Heidelberg, Germany

It is now clear that kinesin-like-proteins (KLP), generally thought to be responsible for the transport of cellular cargoes, are involved in many different cellular processes now being widely investigated. In *Kinesin Protocols,* Isabelle Vernos and a panel of hands-on experts present their most productive and reproducible techniques for the identification, purification, and characterization of the kinesin superfamily of microtubule-dependent motors. The methods range from the most basic to the most sophisticated and include step-by-step instructions and extensive cautionary notes to ensure experimental success. Among the approaches discussed are methods to express and purify kinesins in different systems, to characterize microtubule-enhanced ATPase activity and motility properties, and to test microtubule destabilizing activity. Detailed examples of how to address functional studies are also presented, along with some very new methods for studying the role of KLP in the organization of microtubules in three dimensions. There are also advanced methods for the study of kinesins at the structural level.

Comprehensive and highly practical, *Kinesin Protocols* makes available all the key basic and cutting-edge methods needed successfully to study the multifaceted world of kinesin-like proteins and to explore their many functions.

FEATURES

- **Includes methods for determining microtubule-enhanced ATPase activity, motility, and microtubule destabilizing activity**
- **Details protocols to crystallize kinesin motor domains and study the structure of the kinesin–microtubule complex**
- **Studies kinesin motor proteins from the molecule to its cellular function**
- **Provides a wide range of protocols to study kinesin protein at different levels**

CONTENTS

ISBN 0-89603-766-5

Methods in Molecular Biology™ • 164
KINESIN PROTOCOLS
ISBN: 0-89603-766-5
http://humanapress.com